

A simple technique for N-end  
rule-controlled conditional protein  
accumulation *in vivo*

DISSERTATION

ZUR ERLANGUNG DES  
DOKTORGRADES DER NATURWISSENSCHAFTEN (DR. RER. NAT.)

DER

NATURWISSENSCHAFTLICHEN FAKULTÄT I  
– BIOWISSENSCHAFTEN –

DER MARTIN-LUTHER-UNIVERSITÄT HALLE-WITTENBERG,

VORGELEGT VON

HERRN FREDERIK FADEN  
GEB. AM 15.07.1986 IN SIEGBURG

**REVIEWERS**

PROF. DIERK SCHEEL, LEIBNIZ INSTITUTE OF PLANT BIOCHEMISTRY  
PROF. SACHA BAGINSKY, MARTIN-LUTHER-UNIVERSITÄT  
HALLE-WITTENBERG  
PROF. R. JÜRGEN DOHMEN, UNIVERSITÄT ZU KÖLN

**DEFENSE**

11<sup>TH</sup> OF JULY 2017



# Contents

<b>List of Figures</b>	<b>IV</b>
<b>List of Tables</b>	<b>VI</b>
<b>List of Abbreviations</b>	<b>VII</b>
<b>1 Introduction</b>	<b>1</b>
1.1 Conditional protein accumulation as a tool in molecular biology	1
1.2 The Ubiquitin System	3
1.2.1 Recognition of ubiquitin chains and initiation of degradation at the proteasome	8
1.3 The N-end rule pathway of protein degradation	10
1.3.1 Structure of the eukaryotic N-end rule	11
1.3.2 The canonical N-degron of the Arg/N-end rule, its structure and recognition by N-recognins	16
1.3.3 The temperature-sensitive N-degron	19
1.4 Aim of the work	22
<b>2 Material and Methods</b>	<b>23</b>
2.1 Cloning	23
2.1.1 Assembly of degron reporter constructs for plants	25
2.2 Bacteria work	29
2.3 Yeast work	31
2.4 Drosophila work	32
2.5 Plant work	32
2.6 Expression, purification, and <i>in vitro</i> stability of recombinant proteins	35
2.7 Degron stability assays <i>in vivo</i>	36
2.8 Protein Techniques	38
2.9 SPOT assays	41
<b>3 Results</b>	<b>43</b>
3.1 The degron cassette mediates temperature dependent control over protein abundance over a wide variety of proteins of interest	43

3.1.1	Generation of a K2:GUS expressing reporter line	43
3.1.1.1	Characterization of the <i>ProUBQ10:K2:GUS</i> reporter line	44
3.1.2	Cloning and expression of Tobacco Etch Virus protease as a degron fusion protein	49
3.1.3	Cloning and expression of the BASTA resistance protein PAT as a degron fusion protein	49
3.1.4	Addressing different N-recognins of the plant N-end rule through Phe- and Arg-starting K2:GFP constructs	51
3.1.5	The K2 cassette mediates efficient protein degradation in <i>D.melanogaster</i> embryonic Kc cells	52
3.1.6	Transcript analysis confirms regulation of degron levels on protein level	53
3.1.7	Cytotoxic barnase expressed in <i>Arabidopsis</i> trichomes as a degron fusion is able to stir organ formation	53
3.2	Using a peptide array to determine N-terminal sequences with improved binding to PRT1	58
3.2.1	SPOT membrane design	58
3.2.2	SPOT assay - detection, optimization, and data analysis	62
3.2.3	<i>In depth</i> analysis of binding of PRT1 to membrane 1 comparing direct and blot-based detection as well as different temperatures	65
3.2.4	Membrane 2 - direct on SPOT detection and binding of PRT1 at different temperatures	69
3.3	Influence of altered N-terminal sequences on degron/E3 interaction and stability <i>in vitro</i> and <i>in vivo</i>	73
3.4	Using a newly cloned vector for easy degron tagging	80
<b>4</b>	<b>Discussion</b>	<b>85</b>
4.1	The degron is an efficient tool to mediate phenotypes <i>on demand in vivo</i>	85
4.1.1	Different POIs expressed as degron fusions show plasticity and responsiveness of the degron approach	85
4.1.2	A degron-barnase fusion protein is able to control trichome formation in <i>A.thaliana</i>	89
4.2	Reporter that do not support the degron fusion	92
4.2.1	The degron is unable to confer conditional BASTA-resistance when fused to the resistance protein PAT	92
4.2.2	The degron disrupts the function of the homeotic proteins LEAFY and AGAMOUS	93
4.3	An improved and completely quantifiable SPOT assay design offers tremendous advantages over existing methods	97

---

4.4	SPOT assay based degron optimization suggests limited importance of the N-terminal degron sequence on recognition by PRT1 <i>in vitro</i>	98
4.4.1	Membrane 1	98
4.4.2	Membrane 2	101
4.4.3	Conclusions	104
4.5	<i>In vitro</i> stability assays and heterologous expression do not confirm SPOT assay results	105
4.6	<i>In vivo</i> testing of different N-terminal sequences reveals altered interaction and stability patterns	106
4.7	Conclusions from the degron optimization approach	110
4.8	The degron's mode of action is most likely a predominant mix of conditional ubiquitination and conditional degradation	111
4.9	The degron system compared to other conditional degron techniques	116
4.10	Outlook - How to map degron kinetics, mode of action, and the influence of the POI	121
<b>5</b>	<b>Supplementary information</b>	<b>125</b>
5.1	Supplementary Tables	125
5.2	Supplementary Figures	133
<b>6</b>	<b>Bibliography</b>	<b>151</b>
<b>7</b>	<b>Acknowledgments</b>	<b>173</b>
<b>8</b>	<b>Personal data and information on education / Angaben zur Person und zum Bildungsgang</b>	<b>175</b>
8.1	Personal data / Angaben zur Person	175
8.2	Information on education / Angaben zum Bildungsgang	175
8.3	Publications	176
<b>9</b>	<b>Statement / Eidesstattliche Erklärung</b>	<b>177</b>

# List of Figures

1.1	Scheme of the ubiquitination process	5
1.2	Structure of the plant N-end rule	15
1.3	Schematics of the temperature-sensitive N-degron system	20
3.1	The degron cassette stirs K2:GUS accumulation in a highly responsive, temperature dependent manner	46
3.2	Inhibitor treatments, enrichment, and mass spectrometric analysis suggest potential distinct ubiquitinated species of K2:GUS and its degradation via the UPS	48
3.3	Analysis of Tobacco Etch Virus (TEV) and phosphinothricin-N-acetyltransferase (PAT) as degron fusions	51
3.4	K2:GFP with different N-termini addresses both known N-recognins in plants as well as the N-end rule in <i>D.melanogaster</i> . The phenotype is a true protein one and not the result of transcriptional regulation	53
3.5	A K2:BAR fusion protein expressed in <i>A.thaliana</i> trichomes controls organ formation in a temperature dependent manner	55
3.6	The K2:BAR fusion protein is degraded by the E3 ubiquitin ligase PRT1 and the phenotype is organ specific	56
3.7	Optimizing synthetic peptide binding assays from a purely qualitative to a fully streamlined quantitative experiment identifying optimized N-terminal sequences for PRT1 binding	64
3.8	In-depth analysis of different experimental setups synthesized on membrane one	67
3.9	In-depth analysis of different experimental setups synthesized on membrane two	73
3.10	Recombinant degron protein is readily degraded in a proteasomal dependent albeit N-terminal independent manner in crude plant extract	76
3.11	PRT1 dependent instability of K2:GFP variants in yeast	76
3.12	Different N-termini alter interaction with PRT1 as well as PRT1 dependent stability of a degron luciferase fusion <i>in vivo</i>	79
3.13	Cloning and expression of two degron-tagged transcription factors involved in flowering in their respective mutant backgrounds	83

---

4.1	Model of degron degradation	114
5.1	Superimposition of human and yeast UBR1 structures	133
5.2	First generation K2-reporter	134
5.3	Supplementary information for the <i>ProUBQ10:K2:GUS</i> expressing lines	135
5.4	Col-0 BASTA control	136
5.5	Confirmation of the K2:GFP fluorescence signal	136
5.6	TRYPTICHON expression data as obtained from the eFP browser	136
5.7	Electrostatic surface potential of <i>Escherichia coli</i> ( <i>E. coli</i> ) ClpS	137
5.8	Design of the first SPOT membrane	138
5.9	Design of the second SPOT membrane	139
5.10	Comparative quantification of binding efficiency of labeled 8xHis:MBP:PRT1 to the SPOT membrane 1 at different temperatures comparing blot-based and direct detection approaches.	140
5.11	SPOT assay using recombinant PRT1 <sub>C29A</sub> on membrane 1.	141
5.12	Comparative quantification of binding efficiency of labeled 8xHis:MBP:PRT1 to the SPOT membrane 2 at different temperatures.	142
5.13	SPOT assay using recombinant PRT1 <sub>C29A</sub> on membrane 2.	143
5.14	Schematic overview over the cloning strategy yielding new <i>pENTR:K2</i> versions	144
5.15	Quantification of ImmunoBlue based fluorescent detection of 8xHis:MP:PRT1 protein.	144
5.16	Cloning strategy of an improved destination vector for easy degron tagging	145
5.17	Crystal structure of the GUS enzyme	147
5.18	Crystal structure of barnase	147
5.19	Possible modes of degron stabilization/destabilization kinetics	148
5.20	Crystal structure of PAT from <i>Brucella ovis</i>	148
5.21	Structure of murine DHFR and position of K2 mutations	149
5.22	Fluorescence of <i>in vitro</i> generated GFP in a diluted plant extract	150

# List of Tables

5.1	Statistical analysis of shifted K2:GUS plants	125
5.2	List of primary antibodies	125
5.3	List of secondary antibodies	125
5.4	Primers used in this work	126
5.5	Newly synthesized N-terminal sequences	128
5.6	All sequences of membrane 1	130
5.7	All sequences of membrane 2	131



# List of Abbreviations

4-MUG	4-methylumbelliferyl- $\beta$ -D-glucuronide
4-MU	4-methylumbelliferone
aa	amino acid
<i>A. thaliana</i>	<i>Arabidopsis thaliana</i>
<i>A. tumefaciens</i>	<i>Agrobacterium tumefaciens</i>
Ala	Alanine
ATP	Adenosine triphosphate
BAR	bacterial ribonucleas
<i>bla</i>	<i>beta</i> -lactamase
bp	basepairs
<i>C. elegans</i>	<i>Caenorhabditis elegans</i>
CBB	Coomassie Brilliant Blue
CHX	cycloheximide
Col-0	Columbia-0
CRL	Cullin RING Ligase
Cys	cysteine
<i>D. melanogaster</i>	<i>Drosophila melanogaster</i>
Da	dalton
DAPI	4',6-diamidino-2-phenylindole
DHFR	Dihydrofolate Reductase
DMSO	Dimethyl sulfoxide
dNTP	deoxynucleotide
DTT	dithiothreitol
DUB	De-Ubiquitinating Enzyme
<i>E. coli</i>	<i>Escherichia coli</i>
EDTA	Ethylenediaminetetraacetic acid
EGFP	Enhanced Green Fluorescent Protein
eK	extension containing Lysines
EMS	Ethyl methanesulfonate
FBS	fetal bovine serum
GFP	green fluorescent protein
GAGA	Glycine-Alanine

<b>Gln</b>	glutamine
<b>GUS</b>	$\beta$ -glucuronidase
<b>HECT</b>	Homologous to E6AP C-terminus
<b>His</b>	histidine
<b>Ile</b>	Isoleucine
<b>IP</b>	Immunoprecipitation
<b>IPTG</b>	Isopropyl- $\beta$ -D-thiogalactopyranosid
<b>kDa</b>	kilo dalton
<b>LB</b>	Luria Miller broth
<b>Leu</b>	Leucine
<b>LUC</b>	Luciferase
<b>m</b>	mega
<b>MCS</b>	multiple cloning site
<b>MES</b>	2-(N-morpholino)ethanesulfonic acid
<b>Met</b>	Methionine
<i>M. musculus</i>	<i>Mus musculus</i>
<b>MS</b>	Murashige & Skoog
<i>N. benthamiana</i>	<i>Nicotiana benthamiana</i>
<b>ORF</b>	open reading frame
<b>PABA</b>	4-Aminobenzoic acid
<b>PAT</b>	phosphinothricin-N-acetyltransferase
<b>PBS</b>	phosphate buffered saline
<b>PCR</b>	polymerase chain reaction
<b>PEG</b>	Poly(ethylene glycol)
<b>Phe</b>	Phenylalanine
<b>PI</b>	proteasome inhibitor
<b>POI</b>	protein of interest
<b>PPT</b>	phosphinothricine
<b>PVDF</b>	polyvinylidene fluoride
<b>RBR</b>	Ring Between Ring
<b>RING</b>	Really Interesting New Gene
<b>RIPA</b>	radioimmunoprecipitation assay
<b>rpm</b>	rounds per minute
<b>RT</b>	reverse transcriptase
<i>S. cerevisiae</i>	<i>Saccharomyces cerevisiae</i>
<b>SDM</b>	site-directed mutagenesis
<b>SDS</b>	sodium dodecyl sulfate
<b>Ser</b>	Serine
<b>SPOT</b>	Synthetic Peptide On membrane support Technique

<b>TBS</b>	tris buffered saline
<b>TBST</b>	tween + tris buffered saline
<b>TEV</b>	Tobacco Etch Virus
<b>Thr</b>	Threonine
<i>ts</i>	temperature-sensitive
<b>TUBE</b>	Tandem Ubiquitin Binding Entities
<b>U</b>	unit
<b>UBD</b>	Ubiquitin-Binding Domain
<b>UB</b>	ubiquitin
<b>UPS</b>	Ubiquitin Proteasome System
<b>(v/v)</b>	volume percent
<b>Val</b>	Valine
<b>(w/v)</b>	weight percent
<b>X-Gluc</b>	X-glucuronide sodium salt
<b>YEB</b>	Yeast Extract Broth
<b>YPD</b>	Yeast Extract Peptone Dextrose



# 1 Introduction

## 1.1 Conditional protein accumulation as a tool in molecular biology

The control of protein abundance *in vivo* under, ideally physiological, conditions, has always been an important tool in basic and applied research as well as in biotechnology. A plethora of different approaches now enables researchers to influence amount and functionality of a given protein of interest in a temporal and spatial manner (reviewed in Faden *et al.* 2014). Still, most approaches have limitations such as reaction velocity, off-target effects due to possible inducer toxicity, poor reversibility or leakiness in their "off"-state. The simplest way to influence a protein of interest's abundance is still the disruption of the corresponding gene, leading to reduction or removal of a functional form of the protein.

This has long been used for the determination of the function of a given gene and protein of interest (POI) respectively. Deletion libraries for many essential and non-essential genes for most important biological model organisms such as e.g. the yeast *Saccharomyces cerevisiae* (*S. cerevisiae*), the nematode *Caenorhabditis elegans* (*C. elegans*), the fruit fly *Drosophila melanogaster* (*D. melanogaster*), the mouse *Mus musculus* (*M. musculus*), or the mouse ear cress *Arabidopsis thaliana* (*A. thaliana*) are readily available. However, gene disruption does not always represent the ideal approach for studying the complete function of a protein in its physiological context, for example due to negative effects resulting from the reduction of amounts of functional protein at early developmental stages or because mostly the generation of alternative alleles originally required untargeted mutagenesis or random insertion of nonsense DNA fragments, potentially introducing undesired background mutations masking the physiological influence of the altered allele itself. These considerations make the implementation of fully conditional systems to control protein abundance as well as functionality, and to therefore generate *phenotypes on demand*, all the more important.

Control over protein abundance in eukaryotic systems has been achieved on the level of transcription, translation, or directly through impinging on the protein of interest itself. Commonly applied techniques include the use of inducible promoters, temperature-sensitive (*ts*)-alleles, and protein tags conferring degradation or stabilization dependent on different stimuli.

Inducible promoters have been utilized extensively in a vast variety of different organisms.

Similarly to the *lac*-operon in *E. coli*<sup>1</sup>, many of these promoters in yeast, the simplest eukaryotic system commonly used, rely on the presence of different carbohydrates such as the sugar galactose (reviewed in Weinhandl *et al.* 2014). Lately, work has been undertaken to develop more efficient, fully synthetic promoters for yeast that can also be used in the context of synthetic biology (Redden & Alper, 2015). In higher eukaryotic systems, one can generally distinguish between two approaches, namely inducible promoters that directly regulate the abundance of a given POI, or inducible promoters that regulate expression of a factor that interacts with the protein of interest on DNA, RNA, or protein level leading to its destruction, therefore generating a situation of conditionally altered protein abundance.

Examples of the former in animals are e.g. the ecdysone and tetracycline-inducible systems (Gossen & Bujard, 1992, No *et al.* , 1996, Saez *et al.* , 1997, Stebbins *et al.* , 2001), or the copper-, tetracycline-, and ethanol-induced systems in *A. thaliana* and *Nicotiana benthamiana* (*N. benthamiana*) (reviewed in Faden *et al.* 2014). RNA interference, based on the interaction of small fragments of RNA with complementary strands of messenger RNA (mRNA) leading to their destruction, thereby efficiently down-regulating the active pool of a protein of interest (Fire *et al.* , 1998), as an example of the latter has been used extensively in almost all higher organisms (reviewed in Cerutti & Casas-Mollano 2006)<sup>2</sup>.

Besides altering the transcription/translation status of a protein of interest, impinging directly on the level of the protein has been proven a powerful way, mainly due to a shorter reaction time of the system and the avoidance or reduction of a "phenotypic lag", since upon disruption of a protein's transcription/translation its removal from the cell is determined by its intrinsic half-life *in vivo* (reviewed in Varshavsky 2005, Faden *et al.* 2014).

One of the simplest ways to affect the active pool of a given protein of interest is the use of *ts*-alleles. A *ts*-allele is a version of a protein of interest that carries (a) point mutation(s) rendering it unstable, mainly at higher temperatures, but usually allowing endogenous function at lower temperatures. A temperature, where a given *ts*-protein is degraded, is called the restrictive temperature, whereas the opposite situation, when the temperature allows the functional protein to accumulate, is called the permissive temperature. In yeast, *ts*-alleles have been adopted widely and successfully applied to elucidate the function of proteins at different developmental stages (e.g. Hartwell *et al.* 1970, Shortle *et al.* 1984, Jäntti *et al.* 2002, Ben-Aroya *et al.* 2010) but also in *C. elegans* (O'Rourke *et al.* , 2011), in *M. musculus* (Mason *et al.* , 1992), and *A. thaliana* (e.g. Pickett *et al.* 1996, Sablowski & Meyerowitz 1998, Lane *et al.* 2001, Whittington *et al.* 2001, Quint *et al.* 2005, Hoeberichts *et al.* 2008, Howles *et al.* 2016) temperature sensitive alleles have been described and exploited.

---

<sup>1</sup>The use of inducible promoters in bacteria will not be discussed, since they are commonly used for mass production of proteins rather than for elucidation of biological questions (e.g. Beckwith & Zipser 1970, de Boer *et al.* 1983, Amann *et al.* 1988, Bass & Yansura 2000).

<sup>2</sup>Even though RNAi is an evolutionary conserved system, it has been lost in *S. cerevisiae* but has been identified in other yeast species (Drinnenberg *et al.* , 2009).

Nevertheless, due to the fact that these alleles are not straightforward and easy to identify and usually require large mutational screens for a targeted approach, their use is mainly restricted to unicellular organisms and large libraries of *ts*-alleles of different essential genes have only been constructed for yeast (Li *et al.* , 2011b, Kofoed *et al.* , 2015)<sup>3</sup>.

An alternative strategy has been described through generation of a library of temperature sensitive intein<sup>4</sup> switches to be introduced in any organism that supports their splicing (Zeidler *et al.* , 2004, Tan *et al.* , 2009). Another possibility of generating conditional temperature sensitive alleles is the N-degron approach that will be discussed in-depth in section 1.3.3. In cases where generating temperature sensitive alleles is not possible the fusion of a protein of interest to a variety of different tags mediating conditional degradation is possible.

Some, like the AUX or JAZ1 degron, rely on the plant hormones auxin and jasmonate (Nishimura *et al.* , 2009, Chini *et al.* , 2007, Thines *et al.* , 2007) and are therefore not usable in plants due to off-target effects. Similar approaches such as SHIELD (Banaszynski *et al.* , 2006), LOV2 (Renicke *et al.* , 2013a), or the approach by engineered F-box proteins, the substrate recognition particles of Cullin RING Ligase (CRL) based SCF E3 complexes, hijack the endogenous degradation machinery for the removal of proteins from the cell (reviewed in Faden *et al.* 2014). Even though many of these systems show improved reaction velocity over the use of inducible promoters, they still have limitations such as poor conditionality or potential toxicity and off-target effects of the inducing substances, hormones, or peptides (reviewed in Faden *et al.* 2014).

## 1.2 The Ubiquitin System

The Ubiquitin System has emerged as one of the key players in many different cellular processes. Its overall importance is highlighted by the fact that about 6% of the plant genome code for different components of the Ubiquitin System (Downes & Vierstra, 2005). As one of the most important systems for protein degradation in all eukaryotic organisms, it has always been a primary target for various approaches aiming at targeted protein degradation.

Ubiquitin is a small protein modifier ubiquitously found in all eukaryotic cells. It was discovered in 1975 as "ubiquitous immunopoietic (immune system activating) polypeptide (UBIP)", shown to induce lymphocyte differentiation *in vitro* (Goldstein *et al.* , 1975). Its discoverers quickly realized that ubiquitin, as it was renamed in a later publication by the same authors (Schlesinger & Goldstein, 1975), was found almost in every tissue they analyzed.

---

<sup>3</sup>A screening strategy for the discovery of *ts*-alleles in plants has been proposed (Vidali *et al.* , 2009).

However, the approach involves the knowledge of structural data for targeted mutation of the protein of interest as well as a functionality screening in a heterologous organism, the moss *Physcomitrell pathens*.

<sup>4</sup>An intein represents the protein version of the DNA intron (reviewed in Liu 2000).

Due to its remarkably high evolutionary conservation, sequence differences between species are minor with the human ubiquitin only differing from the plant ubiquitin in three and from the yeast ubiquitin in only two amino acids (Gausling & Barkardottir, 1986).

Even though ubiquitin is not present in prokaryotes, an evolutionary origin of the Ubiquitin System in prokaryotes is discussed. Bacteria, namely *Mycobacterium tuberculosis*, were found to possess ubiquitin-like proteins involved in similar cellular processes as ubiquitin (Pearce *et al.* , 2008, Delley *et al.* , 2012), hinting towards this hypothesis. Also, it was found that the bacterial proteins ThiS and Moad share remarkable structure similarities with ubiquitin, with ThiS even possessing a ubiquitin fold, a structural element typical for ubiquitin and ubiquitin-like proteins. Furthermore, the activity of these proteins *in vivo* with their respective co-factors highly resembles distinct steps in the ubiquitination cascade found in eukaryotes (Wang *et al.* , 2001, Rudolph *et al.* , 2001, Pickart & Eddins, 2004).

Ubiquitination (= ubiquitylation), the process of covalently attaching a ubiquitin moiety to a specific amino acid residue of a target protein, is a highly flexible and dynamic process. It was discovered by Ciechanover and colleagues who demonstrated that a substrate protein is degraded in an ATP-dependent manner in a rabbit reticulocyte extract (Ciechanover *et al.* , 1978, 1980a, 1981). Later, the peptide responsible for a size increase followed by degradation of the substrate protein, was indeed identified as the small heat-stable polypeptide identified previously (Goldstein *et al.* , 1975, Wilkinson *et al.* , 1980). As a side note, highlighting the overall importance of the Ubiquitin System, the three researchers Aaron Ciechanover, Avram Hershko, and Irwin Rose were awarded the 2004 Nobel Prize in chemistry for their discovery. However, also Alexander Varshavsky's contribution has been discussed by his colleagues to be of significant importance (Baumeister *et al.* , 2004). It was also Alexander Varshavsky and his colleagues who discovered and established the N-end rule of protein degradation as an independent field of research within the greater context of the Ubiquitin Proteasome System (see section 1.3), the pathway the N-degron system addresses.

The process of ubiquitination is carried out through a three-step enzymatic cascade that involves the consecutive action of three different families of enzymes. (fig. 1.1). The cascade starts with the E1 ubiquitin activating enzyme, which was first identified through its binding to a ubiquitin loaded column supplemented with ATP (Ciechanover *et al.* , 1982). This enzyme catalyzes the activation of the ubiquitin through adenylation and subsequent formation of a thioester bond between the C-terminal of ubiquitin and the active site Cysteine of the E1. The reaction consumes ATP. When ubiquitin is bound to the E1 the reaction starts again resulting in an *in vivo* state, in which the E1 exists as a complex of E1-ubiquitin, ubiquitin, and ATP (Lee & Schindelin 2008). Two E1 enzymes have been described in *A. thaliana* to be integrated into the Ubiquitin System (Hatfield *et al.* , 1997). However, there is a range of other E1 enzymes catalyzing the activation of



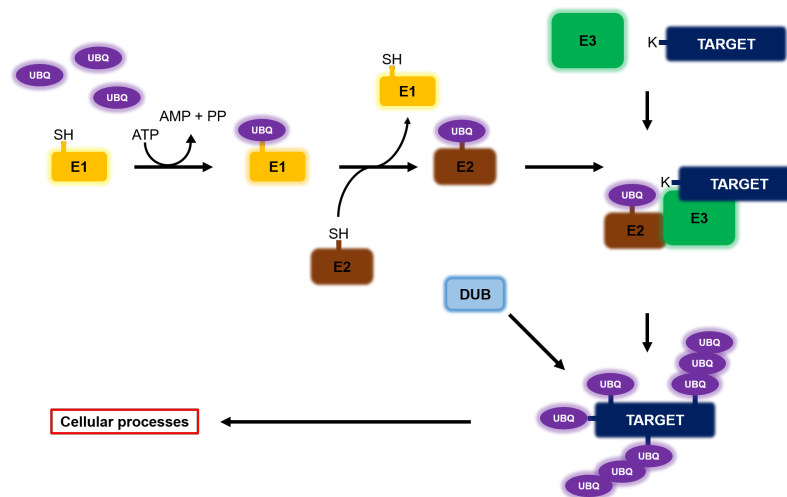


**Figure 1.1 – Scheme of the ubiquitination process.** Ubiquitin (UB) is activated through an ATP-dependent reaction with the ubiquitin activating enzyme (E1). It is then transferred onto the active cysteine residue of the ubiquitin conjugating enzyme (E2), before forming a complex together with the ubiquitin ligase (E3) transferring the ubiquitin moiety onto a Lysine (or other amino acid) residue of the target (T). Here depicted is a situation where the E3 is a monomeric RING (or U-box) E3 ligase (for explanation see text). Depending on the type of E2/E3 recruited, different kinds of ubiquitin chains can be synthesized on the target such as e.g. poly-monoubiquitination, or different chains adopting different conformations. Deubiquitinating enzymes (DUBs) can edit the chains or even reverse ubiquitination adding an additional layer of regulation. For detailed references see text.

ubiquitin-like proteins (reviewed in Schulman & Harper 2009).

The next step of the ubiquitination cascade is the transfer of the ubiquitin moiety to the active Cysteine of an E2 ubiquitin-conjugating enzyme (UBC). While there are 48 UBCs in *A. thaliana* showing the conserved UBC domain, only 37 of them are believed to possess E2 activity through their active site Cysteine, indicated by their ability to form a thioester bond with a ubiquitin moiety transferred from an E1 enzyme. The remaining proteins might serve other roles as e.g. co-factors (reviewed in Vierstra 2009, Callis 2014). The last step in the transfer of ubiquitin onto a target protein is finally catalyzed by a diverse enzyme class called E3 ubiquitin ligases. They usually confer substrate specificity also indicated by their high numbers, even though processes of E3 independent ubiquitination have been described (Hoeller *et al.*, 2007, Kao *et al.*, 2012). In *A. thaliana* more than 1400 E3 ubiquitin ligases are predicted (compared to only two E1s and 37 E2s) (reviewed in Vierstra 2009) as opposed to only 60-100 predicted E3s in *S. cerevisiae* (reviewed in Finley *et al.* 2012) and about 1000 E3s hpredicted in mammals (reviewed in Schwartz & Ciechanover 2009).

The E3 enzyme, in concert with the ubiquitin-loaded E2 enzyme, catalyzes the formation of an isopeptide bond between the C-terminal of the ubiquitin and the  $\epsilon$ -amino group of a Lysine residue. Also so-called non-canonical ubiquitination, where the ubiquitin is not conjugated to a Lysine but rather to a Serine, Tyrosine, Cysteine, or even the N-terminal of a protein, has emerged in animals as early as 1998 (Breitschopf *et al.* 1998, reviewed

in Kravtsova-Ivantsiv & Ciechanover 2012) and has recently also been described in plants (Gilkerson *et al.* , 2015). The Ubiquitin System, in its hierarchical organization, allows the regulation and influence on every level of the enzymatic cascade. While the E3 ligases mainly confer target recognition, the interaction of the different components plays a central role in the regulation of the system. For example, interaction of the E2 with the E3 enzyme is an important regulatory point and not only can the interaction strength of these two enzymes be influenced, for example through co-factors, as it has been described for the mammalian E3 Smurf2 (Ogunjimi *et al.* , 2005), but also can one E3 interact with different E2s resulting in diverse chain topologies and different cellular processes as described e.g for the mammalian E3 TRIM21 (Fletcher *et al.* , 2015).

Additionally, the E3 ligases themselves undergo regulation through post-translational modifications such as phosphorylation (Barbash *et al.* 2011, Cheng *et al.* 2011), through other enzymes such as De-Ubiquitinating Enzyme (DUB)s (Wu *et al.* , 2004), or also regulation through oligomerization (Fletcher *et al.* , 2015, Koliopoulos *et al.* , 2016) and autoubiquitination (Varfolomeev *et al.* , 2007, Amemiya *et al.* , 2008, Bourgeois-Daigneault & Thibodeau, 2012). Due to its extremely high degree of conservation and overall systemic importance, the Ubiquitin System has been a well characterized entry point for pathogens hijacking and modulating the ubiquitination machinery (reviewed in Steele-Mortimer 2011, Ashida *et al.* 2014, Maculins *et al.* 2016).

Since E3 ligases catalyze the final step of ubiquitin attachment to the target, confer substrate specificity, and linked to their enormous number, their importance is reflected in a variety of different types that exhibit high flexibility and diverse modes of action. They can be broadly divided into four distinct sub-classes: The Homologous to E6AP C-terminus (HECT), Really Interesting New Gene (RING)/U-BOX, Ring Between Ring (RBR), and the Cullin RING Ligase (CRL) type E3 ligases according to their general structure and activity. The former three represent monomeric E3 ligases, whereas the latter one represents a class of complex multimeric enzymes.

HECT E3 ligases (Huibregtse *et al.* , 1995) are a family of monomeric E3 ligases. In contrast to most other E3 ligases, that function as a scaffold to bring the E2 and a target protein in close proximity, they take up the ubiquitin itself from the charged E2 enzyme onto an active site Cysteine within their conserved HECT domain before transferring it onto the target residue. In *A. thaliana* there are eight potential HECT E3 ligases (Vierstra, 2009).

RING and U-box E3 ligases are another family of monomeric E3 ligases with 477 and 64 members respectively (Vierstra, 2009). They contain a conserved RING or U-box domain that mediates E2 interaction bringing charged E2 and the acceptor residues on the target protein into the appropriate proximity for transfer of ubiquitin. The RING domain is a specialized Zinc-finger domain of 40-60 amino acid length containing an octet of Histidine and Cysteine residues. This spatially conserved motif conjugates two zinc ions. In U-box E3

ligases this spatial arrangement of Cysteine and Histidine residues is replaced by a network of hydrogen bonds that chelates zinc through the combined action of Cysteine, Serine, and Glutamate side chains. The structure of the 70 amino acid U-box was first determined in plants in the PLANT U-BOX 14 (PUB14) protein (Andersen *et al.*, 2004). Since neither RING nor U-box E3 ligases bind ubiquitin but rather only destabilize the ubiquitin-E2 binding through attack of the thioester bond, therefore facilitating the attack by an amino group (Das *et al.*, 2009, 2013), they act as scaffolds/catalysts for the ubiquitination reaction.

A newly emerging type of E3 ligases are the RBR proteins (reviewed in Spratt *et al.* 2014). They possess unique features of both HECT and RING E3 ligases namely the fact that they recruit the ubiquitin charged E2 via a RING domain but instead of transferring the ubiquitin directly onto the target protein, like RING or U-box E3s would do, they transfer the ubiquitin onto an active center Cysteine much like the formerly described HECT enzymes.

The last and probably most complex type of E3 ligases, in regard to their structure, are the multi-subunit CRL E3 ligases. They contain a RING-box 1 (RBX1) motif for interaction with the E2 and variable target recognition modules called F-box proteins. Cullin proteins (Cul) provide the scaffolding backbone for both, RBX1 and the target adapter. Much like the the formerly described RING and U-box E3s they do not directly interact with the ubiquitin but catalyze its reaction with the target protein (reviewed in Petroski & Deshaies 2005, Hua & Vierstra 2011).

Additionally to initial chain synthesis by the E3 ubiquitin ligases, another class of enzymes, termed the E4 ubiquitin chain elongation factors, is described. However, since they, additionally when working in concert with the E3 ligases, also possess ubiquitination activity their identity as a separate class of enzymes is still a reason for debate (reviewed in Hoppe 2005).

One of the main reasons for the high plasticity of the Ubiquitin System, besides the high diversity of its components, is the possibility to encode for a plethora of information through the topology of the formed ubiquitin chains. Ubiquitin possesses a total of seven Lysine (K) residues (K6, K11, K27, K29, K33, K83) that are theoretically available for ubiquitin chain formation<sup>5</sup>. Additionally to the seven Lysine residues, ubiquitin chains can also be linked in a linear fashion via their respective C-and N-terminals (reviewed in Walczak *et al.* 2012). This activity by e.g. the RBR E3 Ligase complex LUBAC has only been identified so far in mammalian systems (Kirisako *et al.*, 2006, Stieglitz *et al.*, 2012). The most abundant linkage types in *A. thaliana* are, in decreasing order of abundance, K48, K63, K11, K33, K6, and K29 (Maor *et al.* 2007, Kim *et al.* 2013, reviewed in Callis 2014).

---

<sup>5</sup>The non-surface exposed K27 residue has not yet been shown to be involved in such processes in *A. thaliana* (Kim *et al.*, 2013), even though this linkage type has been found in yeast (Peng *et al.*, 2003) and in mammals but requires conformational changes within the ubiquitin (Meierhofer *et al.*, 2008, Xu *et al.*, 2009).

Additionally to homogeneous chains of one type of linkage, also mixed chains are discussed as carriers of even more information (Nakasone *et al.* , 2013, Walsh & Sadanandom, 2014, Shibata *et al.* , 2017).

Due to this high number of regulatory layers the Ubiquitin System represents a highly versatile and flexible system for regulation of a wide variety of cellular processes efficiently controlling cellular homeostasis. With its high plasticity, it is able to code for a much higher amount of information than other, binary post-translational modifications such as phosphorylation or acetylation, where the information content can only be stored via the presence or absence of the respective modification.

### 1.2.1 Recognition of ubiquitin chains and initiation of degradation at the proteasome

The 26S proteasome is a large, about 2.5 mDa sized, protein complex in the cytosol and nucleus of eukaryotic cells. It consists of a barrel-shaped 20S core particle (CP) and two 19S regulatory subunits. The 20S CP, a structure that, as simpler versions, is also conserved in prokaryotic organisms, contains seven different  $\alpha$ - and  $\beta$ -subunits. The  $\beta$ -subunits 1/2 and 5 possess caspase, trypsin, and chymotrypsin-like activities and are therefore responsible for the destruction of target proteins (Groll *et al.* 1997, reviewed in Kish-Trier & Hill 2013). The spatial arrangement within the barrel is a ring of  $\alpha$ -subunits on the top and on the bottom of the core particle, with two rings of  $\beta$ -subunits in the middle that their active sites facing the hollow inside of the barrel (Groll *et al.* 1997, reviewed in Kish-Trier & Hill 2013). The  $\alpha$ -subunits build a gate that ensures that only unfolded target proteins can enter the central catalytic chamber. Additionally, the CP is able to keep proteins in an unfolded state, efficiently inhibiting refolding within the central barrel, thus ensuring access of the active proteases to the primary structure of the target protein (Ruschak *et al.* , 2010). The 19S proteasome activator subunits include the lid on top of the barrel-shaped core particle. They are called activators because they induce an open conformation of the otherwise closed gate build by the  $\alpha$ -subunits of the core particle (reviewed in Kish-Trier & Hill 2013).

Poly-ubiquitin chains decorating a target protein are associated with proteasomal degradation depending on their chain topology. The proteasome contains a number of ubiquitin receptors, some of them being part of the proteasome itself, some of them being shuttle proteins that carry ubiquitin and proteasome interacting domains.

At the proteasome itself, Rpn10 and Rpn13 represent the main ubiquitin receptors. Rpn10 recognizes ubiquitin chains through two ubiquitin-interacting motifs (UIM) situated towards its C-terminal. The two UIMs bind ubiquitin with different affinities but function in a cooperative manner if more than one ubiquitin is bound to the target (Finley, 2009). Rpn13 binds ubiquitin through a structurally diverse mechanism, which interacts with the

same surface of ubiquitin as in Rpn10<sup>6</sup>.

The different shuttle proteins exhibit ubiquitin- and proteasome-binding properties, delivering ubiquitinated protein substrates to the proteasome. Radiation Sensitive 23 (Rad23) from yeast has been shown to interact with poly-ubiquitin, especially K48-linked chains, through its UBA domain whereas its N-terminal UBL domain confers interaction with the proteasome, namely the Rpn10 19S subunit (Schauber *et al.*, 1998, Chen & Madura, 2002, Elsasser *et al.*, 2004). Mammalian hHR23a molecules are proposed to interact with each other through their UBL domain which becomes accessible for proteasome binding upon interaction of the UBA domain with ubiquitin (Wang *et al.*, 2003). However, also contradictory findings have been published namely that binding of Rad23, especially to K48 linked ubiquitin chains on ubiquitinated target proteins, leads to their stabilization rather than to their degradation through a mechanism of competitive binding of Rad23 outcompeting proteasomal ubiquitin receptors such as Rpn10 (Raasi & Pickart, 2003). In plants, it has been shown that two RAD23 isoforms from carrot are able to complement the yeast *rad23-Δ* mutant phenotype (Sturm & Lienhard, 1998) and that the family of RAD23 proteins is involved in cell cycle regulation, fertility and morphology, through their action as shuttles of polyubiquitinated target proteins in *A. thaliana* (Farmer *et al.*, 2010).

The shuttle protein Dsk2, being present as two orthologs in *A. thaliana* (DSK2a and DSK2b), also contains ubiquitin and proteasome interacting domains suggesting a similar role as RAD23 family proteins (Farmer *et al.*, 2010). In yeast, it was shown that overexpression of Dsk2 leads to over-accumulation of K48-linked ubiquitin chains probably disturbing the entire ubiquitin System resulting in decreased vitality of cells. The interaction of Dsk2 and Rpn10 acts as a ubiquitin chain length sensor due to the different affinities of both proteins for different types and length of ubiquitin chains (Zhang *et al.*, 2009). Also, a mechanism has been reported where Rad23 and Dsk2 interact directly with an E4 ubiquitin ligase/chain elongation enzyme, suggesting that the shuttle proteins are able to acquire proteins directly at the place of ubiquitin tagging (Hänzelmann *et al.*, 2010).

Another ubiquitin shuttle protein in yeast, Ddi1 has been shown to adopt a retroviral-like protein fold (Sirkis *et al.*, 2006). It also interacts with the proteasomal subunit Rpn1 (Gomez *et al.*, 2011) and is involved in the turnover of the SCF<sup>UFO1</sup> complex, a CRL type E3 ligase (Ivantsiv *et al.*, 2006).

Besides the ubiquitination signal present on the target protein, even though there is reported cases of ubiquitin-independent proteasomal degradation (reviewed in Erales & Coffino 2014), a degradation initiation site is crucial for degradation. This initiation site can be site of local structural flexibility or disordered region within the protein and does not have to be necessarily directly in the vicinity of the degradation signal even though the position of the degradation signal determines the direction of proteasomal degradation

---

<sup>6</sup>This so called Pleckstrin-like receptor for ubiquitin (Pru) domain is the only domain exclusively relying on loop-build surface for ubiquitin interaction (Schreiner *et al.*, 2008).

from either C-to N-terminal or vice versa. The structure of a protein, besides the initiation region, highly influences stability and degradation efficiency with some secondary structures like  $\alpha$ -helices being degraded significantly easier than buried  $\beta$ -strands (Prakash *et al.* , 2004, 2009, Inobe *et al.* , 2011, Guharoy *et al.* , 2016). Hereby, instability is a function of the length of the flexible region (the longer the more instable), with the length-requirements for terminal extensions being significantly shorter than for internal regions (Verhoef *et al.* , 2009, Fishbain *et al.* , 2011, Yu *et al.* , 2016). Structural rigidity can even lead to a complete stabilization and escape from degradation of a protein despite it being heavily ubiquitinated, as observed for example in the case of the ubiquitin receptor protein Rad23 (Fishbain *et al.* , 2011).

### 1.3 The N-end rule pathway of protein degradation

The N-end rule pathway of protein degradation represents a special subset of the Ubiquitin System. It links the identity of an N-terminal amino acid to protein stability and was discovered as early as 1986 when it was shown that a  $\beta$ -galactose reporter exhibited stability as a function of its N-terminal amino acid in yeast (Bachmair *et al.* , 1986). The canonical N-degron, which, in addition to the appropriate N-terminal amino acid, also contains a certain number of Lysine residues for ubiquitination, was defined in later work through the investigation of the behavior of an elongated linker (= extension) sequence derived from the *E. coli lacZ* gene fused to a Dihydrofolate Reductase (DHFR) protein as a reporter, again in yeast, where it was confirmed, that not only that certain amino acids act in a destabilizing manner but also that the presence of Lysine residues in a defined distance to the N-terminus are crucial for the degradation of the reporter (Bachmair & Varshavsky, 1989, Suzuki & Varshavsky, 1999). The so-called eK sequence (extension containing Lysines) derived from these initial constructs was the first described sequence to follow the N-end rule and has been used ever since in reporter probes addressing the N-end rule pathway of protein degradation (e.g. Bachmair & Varshavsky 1989, Bachmair *et al.* 1993, Potuschak *et al.* 1998).

Since protein translation usually starts with a Methionine<sup>7</sup>, it became necessary to implement a new technique for exposure of a desired N-terminal amino acid. The approach, termed the Ubiquitin-Fusion-Technique (UFT), functions via fusion of a ubiquitin moiety directly upstream of the N-terminal amino acid of the target protein. The expression of the ubiquitin-POI fusion occurs from the same open reading frame. Co-translationally the ubiquitin is cleaved off through endogenous DUBs. Since DUBs only recognize the C-terminal di-glycine motif of the ubiquitin, with no regard for any following amino acid, this technique allows for efficient cleavage of ubiquitin *in vivo* in eukaryotes (reviewed in

---

<sup>7</sup>Non-canonical initiation at non-methionine coding codons has been identified but remains a special case (e.g. Schmitz *et al.* 1996, Simpson *et al.* 2010).

Varshavsky 2005).

More recent work also shows that processing of ubiquitin-fusions using DUBs is also possible through co-expression in bacteria (Piatkov *et al.*, 2013) or *in vitro* using purified DUBs (Sriram *et al.*, 2013). Instead of ubiquitin, an almost identical approach has been used, exploiting the ubiquitin-like protein SUMO and its corresponding SUMO-hydrolase to generate N-end rule substrates (Schmidt *et al.*, 2009). An alternative to using DUBs *in vitro* is the use of recombinant Tobacco Etch Virus (TEV) protease (Naumann *et al.*, 2016) or the co-expression of TEV and substrate in *E. coli* as a possibility to generate recombinant N-degron probes (Shih *et al.*, 2005).

### 1.3.1 Structure of the eukaryotic N-end rule

The N-end rule has been mapped to date to be a hierarchical system distributed over three branches. Some of the branches include additional upstream layers of processing before the substrate can be recognized by an E3 ligase. In general, it is divided in so-called primary, secondary, and tertiary destabilizing residues, where the former can be recognized immediately by a specialized subset of E3 ligases of the N-end rule whereas the latter two have to be processed in order to become primary destabilizing residues<sup>8</sup>.

The longest known branch is the Arg/N-end rule. It includes two sub-branches with unique primary destabilizing residues. Type 1 primary destabilizing include basic residues such as Arginine (R), Lysine (K), and Histidine (H), whereas type 2 primary destabilizing residues include aromatic and aliphatic amino acids such as Tyrosine (Y), Phenylalanine (F), Tryptophane (W), Isoleucine (I), and Leucine (L).

The secondary destabilizing residues Aspartic acid (D) and Glutamic acid (E) can be arginylated through the action of an arginyltransferase that attaches an Arginine moiety to the N-terminal which then acts as a primary destabilizing residue. This R-transferase (Ate1) has been described, before even the N-end rule was known (Savage *et al.*, 1983), and later associated with functioning within this pathway (Balzi *et al.*, 1990). Like the entire pathway, also the arginylation step of the N-end rule pathway is conserved in eukaryotes.

In plants, two homologs of the yeast Ate1, termed ATE1 and ATE2, which show functional redundancy, have been described (Graciet *et al.*, 2009). In mammals, only one *ate* gene has been identified but transcription/translation of the gene results in a total of four splicing variants with partial functional redundancy and distinct, partially overlapping, cellular localization (Kwon *et al.*, 1999, Rai & Kashina, 2005)<sup>9</sup>.

Upstream of the secondary destabilizing residues one has identified de-amidases that are able to convert Asparagine (N) and Glutamine (Q) to either Aspartic acid (D) and

<sup>8</sup>The bacterial N-end rule, which also forwards protein toward degradation via the Clp proteases, dependent on their N-terminal amino acid (reviewed in Dougan *et al.* 2010, 2012), will not be discussed here.

<sup>9</sup>In bacteria also Phe/Leu-transferases have been found (Shrader *et al.*, 1993, Graciet *et al.*, 2006, Ninnin *et al.*, 2009).

Glutamic acid (E), and therefore secondary destabilizing residues, respectively. In yeast, this is carried out by the enzyme Nta1 (Baker & Varshavsky, 1995) whose precise mode of action on a molecular level has only recently been described (Kim *et al.* , 2016). In mammals and plants, the action of the single yeast enzyme is thought to be split into two distinct enzymes termed NTAN1 and NTAQ1 respectively (Grigoryeva *et al.* , 1996, Kwon *et al.* , 2000, Wang *et al.* , 2009). Additionally, in plants and mammals, an N-terminal Cysteine can act as tertiary destabilizing residue, which upon oxidation by NO, O<sub>2</sub> (Hu *et al.* , 2005), or, in the case of *A. thaliana*, through the action of a specialized class of enzymes termed Plant Cysteine Oxidases (PCOs, Weits *et al.* 2014, White *et al.* 2017), can be converted into a secondary destabilizing residue potentially being recognizable by ATE1/2 (White *et al.* , 2017).

Besides the Arg-branch of the N-end rule<sup>10</sup>, more recent work showed that additional branches of the N-end rule include the recognition of acetylated N-termini, defining a new branch of the N-end rule called the Ac (acetylation)-branch (Hwang *et al.* , 2010a). Later it was shown that even N-terminal Methionine (Met) can act as a degradation signal when it is either followed by a hydrophobic residue at position two, forwarding a substrate to the Arg/N-end rule or, through acetylation, regardless of the identity of the amino acid residue at position two, forwarding it to degradation through the Ac/N-end rule (Kim *et al.* , 2014). Met as an N-terminal, with the following amino acid, signal for degradation represents a type 2 degradation signal, which in yeast would be recognized through the ClpS homology domain of Ubr1 (Kim *et al.* , 2014).

Recently, even Proline at the N-terminal has been identified as a real primary in yeast (Chen *et al.* , 2017), after first observations about N-terminal Proline being important for protein degradation had been made as early as 1998 (Hämmerle *et al.* , 1998). Interestingly, the authors could demonstrate that also the structural context of the Proline N-degron is extremely important for its recognition. Strikingly, also Proline at position two of one of the identified substrates has been found to confer instability in the appropriate structural context (Chen *et al.* , 2017). This is very similar to non-acetylated Methionine as a primary destabilizing residue that can only be recognized when followed by a "classical" type 2 primary destabilizing residue of the Arg/N-end rule (Kim *et al.* , 2014), rule suggesting also some influence of the structural context in the identification of these type 2 residues by Ubr1. All identified substrates of this new Proline-branch of the N-end rule are enzymes important for neoglucogenesis and expressed by yeast in glucose starving conditions. The Proline-N-end rule plays an important role in degrading these enzymes upon availability of glucose (Chen *et al.* , 2017).

---

<sup>10</sup>Even though in many organisms the recognition of different primary destabilizing residues is distributed onto a multitude of E3s this branch of the N-end rule is still called the Arg/N-end rule, probably historically being connected to the fact that R was the amino acid initially shown to be the most unstable (Bachmair *et al.* , 1986) as well as the fact that in yeast, where all the branches were initially discovered, only one E3, albeit having different recognition sites, is responsible for the degradation of all primary destabilizing residues of the Arg/N-end rule.



Now all proteinogenic amino acids have been shown to confer degradation, however depending on modifications, as well as their structural context. While the "classical" Arg/N-end rule has been shown conclusively to act in plants, the functionality of the Ac/N-end-rule, the extended Arg/N-end rule including Methionine, as well as the newly discovered Pro/N-end rule has yet to be demonstrated.

The N-end rule relies on a subset of specialized E3 ligases in eukaryotes that mediate the degradation of target proteins. These E3 ligases, termed N-recognins<sup>11</sup>, are responsible for the recognition of the N-terminal amino acids in accordance with the N-end rule. At the point of discovery of the N-end rule no "N-end-recognizing factor" was identified *in vivo*. First experiments in rabbit reticulocyte extract suggested this particle to be an E3 ubiquitin ligase (Reiss *et al.*, 1988, Gonda *et al.*, 1989) which was identified as Ubr1 in yeast (Bartel *et al.*, 1990).

Ubr1 is a large, about 220 kilo dalton (kDa) sized, protein. Interestingly, the yeast Ubr1 possesses binding sites for both types of canonical N-degrons (type 1 and type 2) and is therefore regarded to be the main determinant of Arg/N-end rule specific degradation in yeast (Xia *et al.*, 2008b). The yeast RING E3 Ubr1 interacts with the HECT E3 Ufd4, an E3 ligase of the ubiquitin-fusion degradation (UFD) pathway (Johnson *et al.*, 1995, Hwang *et al.*, 2010b). Fascinatingly, Ubr1 even possesses a third recognition site targeting the transcriptional repressor, of the peptide transporter Ptr2, Cup9. Degradation activity towards Cup9 is enhanced by binding of peptides simultaneously to both, type 1 and type 2 recognition sites (Du *et al.*, 2002, Xia *et al.*, 2008a). Additionally, activity of Ubr1 is regulated by phosphorylation *in vivo* (Hwang & Varshavsky, 2008). This unprecedented versatility of Ubr1 highlights the interaction and cross-talk of the yeast Arg/N-end rule with diverse cellular processes.

Through the discovery of the Ac/N-end rule, a second set of yeast E3 ligase of the N-end rule pathway was identified. The first one, Doa10, had previously been shown to be involved in K11 linked ubiquitin chain formation (Xu *et al.*, 2009, Hwang *et al.*, 2010a), a rather uncommon chain topology in the context of degradation, as opposed to K48 type chains synthesized by Ubr1 (Chau *et al.*, 1989). It is linked to Endoplasmatic Reticulum-Associated Degradation (ERAD) in yeast, mediating degradation of misfolded proteins exported from the ER-lumen (reviewed in Ruggiano *et al.* 2014, Zattas & Hochstrasser 2015). Later a second E3 of the Ac/N-end rule was identified. Not4 targets a distinct subset of acetylated targets in yeast (Shemorry *et al.*, 2013). The degron sequence of a substrate of Not4, Cog1, has been proposed only to be shielded by steric means proposing a mechanism of degron exposure through conformational reconfiguration (Shemorry *et al.*, 2013).

The E3 ligase Gid4 has been found to be the N-recognin of the Pro/N-end rule (Chen

---

<sup>11</sup>The term was introduced as name for "proteins that are functionally equivalent to the N-end-recognizing yeast Ubr1 protein." (Bartel *et al.*, 1990).

*et al.*, 2017). Since it was found to recognize not only the N-terminal of a degron but that it "senses" up to six amino acids in their structural context, its relation to peptide-binding grooves of antigen-presenting MHC proteins is discussed (Chen *et al.*, 2017).

In animals, a number of N-recognins have been identified as well. So far, using sequence homologies and peptide-based pull-downs, a total of seven mammalian N-recognins of the Arg/N-end rule, called UBR1-7, have been proposed (reviewed in (Tasaki & Kwon, 2007)). Of these seven enzymes, four (UBR1/2/4/5) have been accounted with N-end rule specific binding (Tasaki *et al.*, 2005). Interestingly the different enzymes seem to belong to different types of E3 ligases with UBR1-3 being proposed to function as RING, UBR5 as a HECT, and UBR6 believed to be a part of a CLR (through an F-box) E3 ligase complex. UBR7 is thought to work through a PHD domain <sup>12</sup>) and finally, UBR4, even though it has been shown to have activity towards type 1 and type 2 N-degrons is not yet accounted any type of E3 ligase (reviewed in Tasaki & Kwon 2007). Also, an N-recognin of the Ac/N-end rule has been identified in mammals. Teb4, similarly to Doa10, is associated with the ER and forwards its targets to degradation via their acetylated N-terminals (Park *et al.*, 2015). In *D. melanogaster* also at least Ubr1, Ubr4, and Ubr5 homologs have been proposed (Tasaki *et al.*, 2005). Interestingly, the mammalian UBR4 protein has been discussed to be a sequelog of the *A. thaliana* protein BIG and the *D. melanogaster* protein PUSHOVER, with whom it shares its exceptionally huge size (UBR4 = 570 kDa, BIG = 540kDa, PUSHOVER = 560 kDa) (Tasaki *et al.*, 2005).

The N-end rule has been connected to a wide variety of processes in yeast, *D. melanogaster*, and mouse such as chromosome stability, negatively regulating apoptosis, positively regulating apoptosis, as a nitric oxide (NO) sensor, or even behavior and memory (e.g Kwon *et al.* 2000, Rao *et al.* 2001, Varshavsky 2003, Ditzel *et al.* 2003, Hu *et al.* 2005, Piatkov *et al.* 2012, reviewed in Tasaki & Kwon 2007, Varshavsky 2011, Sriram *et al.* 2011, Tasaki *et al.* 2012).

In plants, to date, only two potential N-recognins have been identified. PLANT PROTEOLYSIS 1 (PRT1) has been described first by Bachmair and colleagues using an artificial reporter (Bachmair *et al.*, 1993). It's activity, as crucial part of degradation of type 2 primary destabilizing residues, has been shown later, also based on heterologous expression in yeast (Potuschak *et al.*, 1998, Stary *et al.*, 2003). Interestingly, PRT1 seems to be a plant pioneer enzyme. It does only share functional homology to the yeast Ubr1 but is otherwise not conserved on an amino acid level neither in yeast nor mammals. Its crystal structure is unknown, but based on sequence analysis it is believed to consist of two RING domains and a ZZ domain which is a domain closely related to a RING domain (Potuschak *et al.*, 1998). It does not contain a ClpS homology domain (reviewed in Tasaki *et al.* 2012). To date a proven interaction of PRT1 with an endogenous substrate *in vivo* still remains

---

<sup>12</sup>PHD domains are structurally closely related to RING domains and proposed to confer E3 activity (Coscoy & Ganem, 2003).

elusive.

The other proposed *A. thaliana* N-recognin is PLANT PROTEOLYSIS 6 (PRT6) (Garzón *et al.*, 2007). It shows the conserved UBR domain, also known to be responsible for type 1 N-degron recognition in yeast, however, it misses the ClpS homology domain responsible for type 2 N-degron recognition. PRT6 is, so far, the only proposed N-recognin of the Arg/N-end rule in *A. thaliana*.

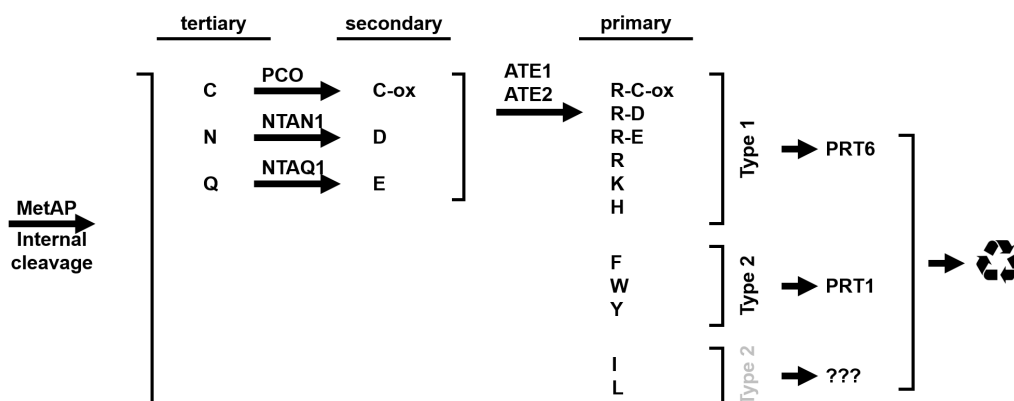


**Figure 1.2 – Structure of the plant N-end rule.** The Arg/N-end rule, as shown to be active *in planta*, consists of a hierarchical, multi step system of primary, secondary and tertiary destabilizing residues. Primary destabilizing residues can be recognized directly by the potential N-recognins PRT1 and PRT6, type 1 and type 2, respectively. While Leucine (L) and Isoleucine (I) have been shown to be instable in yeast and bacteria, they show only moderate instability in plants and are not recognized by PRT1, implying the existence of potentially more N-recognins. Secondary and tertiary destabilizing residues have to be processed in order to be recognizable (PCO = Plant Cysteine Oxidase, ATE = Arginyl-Transferase). Exposure through processing of new N-terminals by Methionine-Aminopeptidases (MetAP), or through internal cleavage can theoretically generate every kind of destabilizing residue (tertiary, secondary, primary). Modified and combined from (Graciet *et al.*, 2010, Weits *et al.*, 2014, White *et al.*, 2017)

Even though the existence of the N-end rule in plants is known since 1993 (Bachmair *et al.*, 1993), little is known about its overall functions and endogenous substrates *in planta*. It has been connected to some biological processes in *A. thaliana* such as leaf senescence, shoot, and leaf development, seed germination, and pathogen defense (Yoshida *et al.*, 2002, Graciet *et al.*, 2009, Holman *et al.*, 2009, de Marchi *et al.*, 2016).

So far, direct interaction of PRT1 with a probe has been the only demonstrated target binding for this E3, albeit *in vitro* (Mot *et al.*, 2017). One endogenous substrate has been suggested recently in *A. thaliana* (Dong *et al.*, 2017). While genetic evidence is very strong, direct interaction of the E3 and the substrate *in vivo* was not demonstrated but only shown through *in vitro* peptide-based binding assays as well as stability assays in *A. thaliana* protoplasts.

In barley the N-end rule has also been linked to developmental processes as well as stress response potentially through the action of PRT6 (Mendiondo *et al.*, 2016). However, the only accepted substrate proteins for PRT6 identified so far are a class of ETHYLENE RESPONSE FACTORS (ERF) of the subgroup VII. The ERF RAP2.12 is degraded under

normoxic conditions through a proposed O<sub>2</sub> dependent oxidation of its N-terminal Cysteine and subsequent degradation via the Arg/N-end rule. Under hypoxia, through the lack of available oxygen, the N-terminal Cysteine can not be oxidized and RAP2.12 is stabilized eliciting downstream responses (Licausi *et al.* , 2011, Gibbs *et al.* , 2011). While the genetic evidence presented in these publications is extremely strong, no direct interaction of RAP2.12 with ATEs or PRT6 has been shown on protein level. Later work showed that the initial oxidation process was actually carried out by the newly discovered enzyme class of Plant Cysteine Oxidases (PCOs) (Weits *et al.* , 2014). A recent work demonstrated that oxidation through the action of a PCO is a crucial prerequisite for subsequent arginylation of peptides by ATE1 *in vitro* (White *et al.* , 2017).

### 1.3.2 The canonical N-degron of the Arg/N-end rule, its structure and recognition by N-recognins

A degron is defined as a peptide sequence within a protein conferring its instability and therefore its degradation (Varshavsky, 1991). Degrons are usually hidden within a protein and are exposed through passive or active processes. An example for a passive process would be the Endoplasmatic-Reticulum Associated Degradation (ERAD), where misfolded proteins in the lumen of the Endoplasmatic Reticulum (ER) are recognized via hydrophobic patches that would be hidden in a "normal" conformation. Proteins are then shuffled into the cytosol and degraded by the ubiquitin-proteasome machinery (reviewed in Meusser *et al.* 2005).

An N-degron is a typical example for a degron that is generated through an active process. Since all proteins, except for some exceptions, start with a Methionine as the amino acid of the translation initiation codon ATG normally all N-degrons are hidden. This means that exposure of an N-degron requires proteolytic processing of the protein either directly at the N-terminal or somewhere within the primary sequence exposing a new N-terminal which can serve as a destabilizing residue of the N-end rule (primary, secondary, or tertiary). Interestingly, in *A. thaliana* (primary) destabilizing residues at position one after the initial Methionine are strongly underrepresented and cleavage by Met-aminopeptidases is altered when such a destabilizing residue is found at that position. Recently increased work has been undertaken in deciphering the N-terminal peptidome for the elucidation and identification of potential new substrates of the N-end rule using mass spectrometry based methods (Staes *et al.* , 2008, Majovsky *et al.* , 2014, Venne *et al.* , 2015).

Since there are different kinds of N-degrons starting with different kinds of primary destabilizing residues there is also a certain diversity in the identity of the N-degron binding/recognition domains of the N-end rule pathway. The type 1 binding pocket was early on identified as the so-called UBR domain named after the first N-recognin, the yeast Ubr1. The structure of this domain, which is a conserved feature of most N-recognins of

the Arg/N-end rule in eukaryotes, has been solved for yeast Ubr1 and human UBR1 and UBR2 (Choi *et al.* , 2010, Matta-Camacho *et al.* , 2010). Human UBR1 and UBR2 domains were found to contain two antiparallel  $\beta$ -sheets with additional small  $\alpha$ -helices in between. The structure coordinates a total of three zinc ions. Loss of one of these zinc ions leads to a collapse of the domain *in vitro*, an observation that also has biological significance as the loss of one of the zinc ions through a mutation in UBR1 leads to a severe disease in humans called Johanson-Blizzard syndrome (Zenker *et al.* , 2005, Matta-Camacho *et al.* , 2010, Hwang *et al.* , 2011). The residues mediating zinc coordination are conserved through UBR1 to UBR3 but are missing in UBR4 to UBR7 indicating that either they can assure proper domain folding only through two zinc ions, something that seems unlikely in the light of the fact that loss of a zinc ion leads to the collapse of the tertiary structure of UBR1 and UBR2, but rather hints towards other mechanisms for tertiary structure stability and maintenance (Matta-Camacho *et al.* , 2010).

Binding studies with different peptides suggested that mainly the first two amino acids of the peptide play an important role in N-terminal mediated binding to the negatively charged binding pocket of the UBR domain. The domain showed the highest affinity towards an RD starting peptide mimicking the state of N-terminal arginylation. Binding is mediated through the positively charged side chain of the N-terminal arginine with the negative binding pocket. An important residue in the human UBR domain is Phe148 which coordinates the position of the N-terminal amino group forming an aromatic hydrogen bond additional to two more hydrogen bonds with Asp150 and the carbonyl backbone of Phe148 thus ensuring specificity and rigid binding only to N-terminal substrates (Matta-Camacho *et al.* , 2010).

Structure of the yeast UBR domain does not show significant differences in the structural arrangement when compared to human UBR1. Also here, the secondary structure is maintained through three coordinated zinc ions. Additionally, the secondary structure does not contain small  $\alpha$ -helices but small  $\beta$ -sheets instead (Choi *et al.* , 2010). Superimpositions of the two UBR1 structures shows an almost complete structural conservation between the two protein domains. Substrate coordination is almost indistinguishable (fig. S 5.1), however, the authors of the yeast UBR domain publication focus more on the importance of the second residue in a given N-end rule type 1 substrate showing that mainly hydrophobic residues at position two show the most efficient binding to the yeast UBR domain (Choi *et al.* , 2010).

Unfortunately, there is no structure of the eukaryotic type 2 binding domain available to date. Even though it is known that yeast Ubr1 carries a ClpS homology domain responsible for type 2 degron recognition, its structure has not been solved. In mammals, UBR1 and UBR2 have been shown to bind Phe-starting peptides in a pull-down assay from mouse embryonic fibroblasts (Tasaki *et al.* , 2005), suggesting the existence of, an at least functionally, ClpS homology domain in these proteins similar to the yeast Ubr1 (discussed

in Dougan *et al.* 2010). To date, the structures of the bacterial ClpS proteins from different bacterial species together with different N-degrons and during interaction with ClpA have been solved and characterized (Zeth *et al.* , 2002, Erbse *et al.* , 2006, Román-Hernández *et al.* , 2009, Schuenemann *et al.* , 2009, Román-Hernández *et al.* , 2011, Stein *et al.* , 2016). Due to the similarity between the ClpS and the ClpS-homology domain, it is tempting to extrapolate from the binding mode of the prokaryotic to the eukaryotic system. ClpS has a large C-terminal domain consisting of three antiparallel  $\beta$ -strands and three  $\alpha$ -helices forming a highly hydrophobic binding pocket. Five residues, conserved between *E.coli* and *C.crescentus* (D36/D49, T38/T51, D35/D48, N34/47, H66/79), coordinate binding of the hydrophobic type 2 N-degron (reviewed in Dougan *et al.* 2010).

The C-terminal domain also mediates interaction with the bacterial protease ClpA, responsible for N-degron degradation. It is believed to undergo structural rearrangements upon N-degron binding influencing binding to ClpA (reviewed in Dougan *et al.* 2010). Opposed to UBR-mediated N-degron binding the secondary structure of ClpS is not stabilized by zinc-coordination but rather through hydrogen bonds and salt bridges. Additionally, it has been shown that some bacteria, such as *Agrobacterium tumefaciens* (*A. tumefaciens*), express two isoforms of ClpS with different affinities for different type 2 destabilizing residues (Stein *et al.* , 2016). Opposed to the ubiquitin ligase activity mediating degradation of PRT1 targets, ClpS merely acts as a recognition and shuttle particle directly recruiting targets for degradation to the ClpA protease without actually modifying said target (Schmidt *et al.* , 2009).

Contrarily to UBR domain-mediated N-degron binding, the structural analysis of the ClpS domain indicates a much lesser importance of the secondary amino acid in the N-degron chain, but rather that the N-degron sequence, after coordination into the binding pocket, retains a high degree of flexibility indicated by the spatial arrangement away from the binding site. Some peptides showed re-folding onto the surface of the ClpS domain, which might be a pure *in vitro* effect without any *in vivo* significance (Schuenemann *et al.* , 2009) but could as well play a role in type-2 N-degron binding. A so-called gatekeeper residue ensures specificity to type 2 N-degrons (reviewed in Lucas & Ciulli 2017) and previous findings discuss that recognition of the type 2 substrate peptide is improved by a net positive charge (Erbse *et al.* , 2006).

Alltogether, the UBR-domain as well as the ClpS domain both retain a sturdy secondary and tertiary structure without significant structural rearrangement upon N-degron binding. Binding to the UBR1 domain seems, to a certain extent, to be dependent on the identity of the second amino acid of the degron sequence, an effect that might not play a role in type 2 binding to the ClpS domain. However, even though the potential plant N-recognin PRT1 does complement a yeast *ubr1-Δ* mutant allele in regard to degradation of type 2 N-degrons (Stary *et al.* , 2003) it does not carry a ClpS homology domain.

In the end, all the work done so far by different groups fails to finally define an N-degron

consensus sequence which could be used to model new, optimized, N-terminal degradation cues for the N-end rule. The only exceptions with *in vivo* significance are findings that elucidate N-degron stability in the structural context of the N-terminal primary destabilizing residues for N-terminal Methionine, which can be degraded if it's followed by a hydrophobic residue (Kim *et al.* , 2014), and the newly described Pro/N-end rule, where it was demonstrated that binding by the responsive N-recognin is influenced by the first six amino acids and that different amino acids at different positions allow or disrupt binding (Chen *et al.* , 2017).

Even though different peptides with different length were used in co-crystallization studies the rest of the proteins probably plays a significant role in binding due to its influence on the mobility of the N-terminal, since also a mechanism of sterical shielding of an N-degron, however by another protein, has been reported (Shemorry *et al.* , 2013). Additionally, recognition of an N-degron is only half the deal since degradation via the 26S-proteasome also requires some molecular prerequisites such as ubiquitination and flexible regions for degradation (see section 1.2.1) and also the availability of Lysine residues on the target protein that are available for ubiquitination can significantly influence degron stability (Bachmair & Varshavsky, 1989, Suzuki & Varshavsky, 1999).

### 1.3.3 The temperature-sensitive N-degron

Temperature-sensitive N-degrons are a specialized type of inducible degrons. Besides the exposure of endogenous N-degrons leading to the degradation of N-end rule substrates, artificial N-degrons have been a long-established tool for conditional protein abundance and for the generation of *phenotypes on demand* in a variety of organisms, namely in different yeast species, chicken cell culture, as well as drosophila (reviewed in Faden *et al.* 2014) and recently also in plants, tobacco, and adult *D. melanogaster* (Faden *et al.* , 2016b).

An artificial N-degron is a protein sequence fused to the N-terminal of a POI that can be processed in a way that the mature degron leads to the destruction of the fused POI. Two systems exist that offer some level of reversibility and plasticity. The so-called TEV protease induced protein inactivation (TIPI) (Taxis *et al.* , 2009), where a protein of interest is expressed with an N-terminal tag containing a dormant N-degron within a TEV protease cleavage site. Since TEV protease does exhibit low specificity for the amino acid at position one after the cleavage site it can be used to generate N-terminals of desired identity (applied and discussed in Naumann *et al.* 2016).

In this case, the protease is expressed under the control of an inducible promoter. Induction of TEV expression leads to processing and exposure of the mature N-degron leading to the removal of the POI from the cell. To improve velocity and efficiency of the system the N-degron contains also a sequence stretch of the SF3b protein which interacts with a p23 sequence fused to the TEV protease. The system offers poor conditionality. Even after

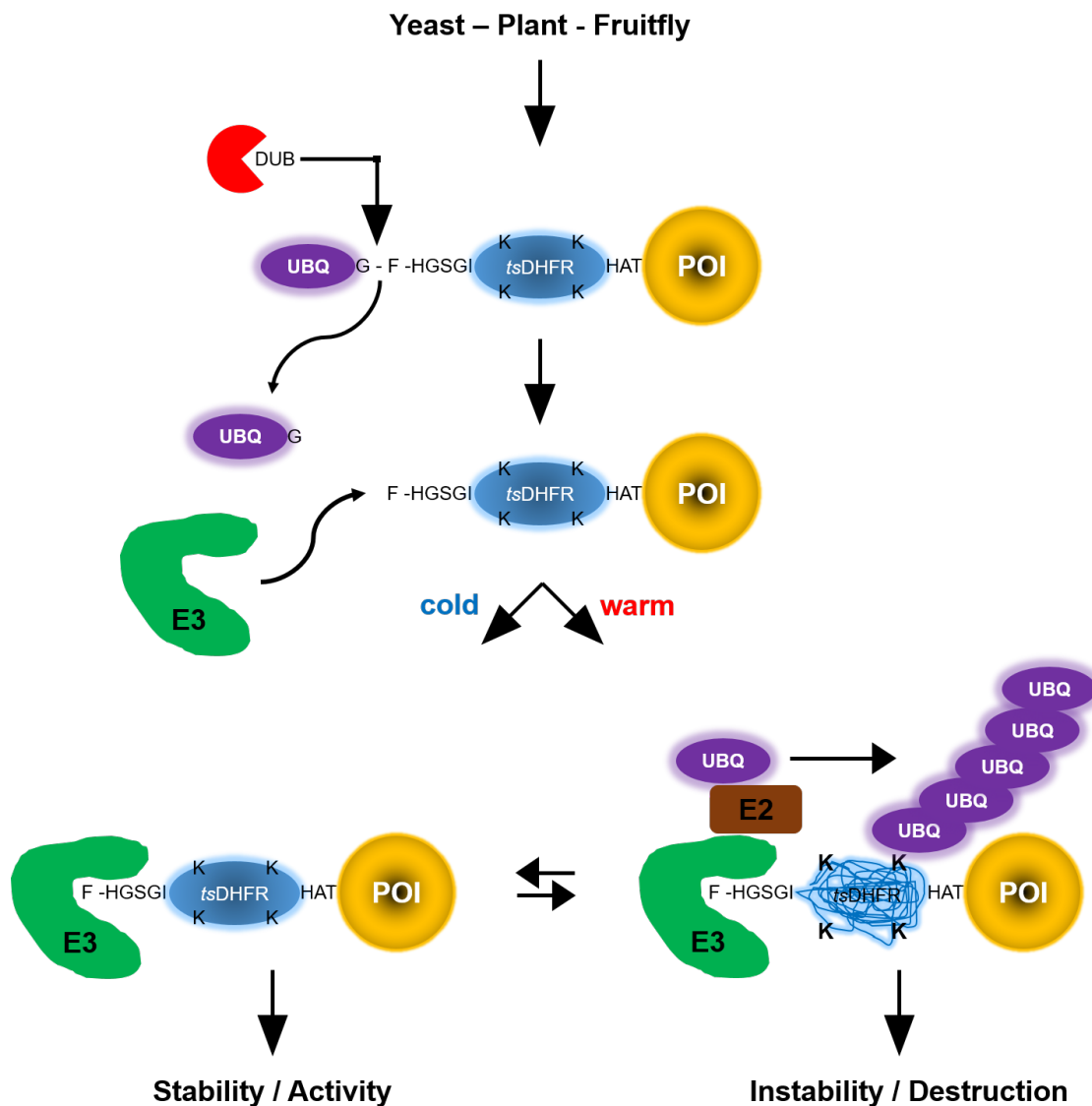


**Figure 1.3 – Schematics of the temperature-sensitive N-degron system according to the literature (Dohmen *et al.*, 1994, Faden *et al.*, 2016b).** Co-translationally the N-terminal moiety is cleaved of by endogenous DUBs exposing the destabilizing N-terminal F or R (not shown). After a temperature shift to either permissive or restrictive temperature the protein is either stabilized or ubiquitinated and degraded via the N-end rule pathway.



promoter shut-off, TEV is still present in the cell mediating the degradation of the POI. Therefore this system is mainly being used for removal of a POI as a one-time event. It has so far only been used in yeast (Taxis *et al.* 2009, Jungbluth *et al.* 2010, McIsaac *et al.* 2011, reviewed in Faden *et al.* 2014).

Another, well-established system, mainly in yeast, for fully conditional control over protein abundance via a temperature stimulus is the heat-inducible N-degron cassette (Dohmen *et al.* , 1994). It was demonstrated that a protein cassette, based on a point-mutated DHFR, is able to efficiently mediate protein degradation via the N-end rule (Dohmen *et al.* , 1994). This degron cassette generates an artificial *ts*-allele of any fused protein. The approach of this system is slightly different since it does not rely on a conditional exposure of the destabilizing N-terminal but rather on a hypothesized temperature induced (partial) unfolding of the point mutated DHFR leading to its ubiquitination and degradation. The N-terminal is always co-translationally exposed through the use of the Ubiquitin-Fusion-Technique (Varshavsky 2005).

This so-called *ts*-degron cassette was shown to operate in a temperature range of 28°C (permissive temperature) to 37°C (restrictive temperature), a range to extreme for most higher eukaryotic organisms. This is the reason why its application is mainly restricted to yeast or cell cultures<sup>13</sup> (e.g. Hardy 1996, Gregan *et al.* 2003, Ben-Aroya *et al.* 2008 in *S.cerevisiae*, Rajagopalan *et al.* 2004, Champion *et al.* 2010, Piazzon *et al.* 2012 in *S.pombe*, and in chicken cell culture Su *et al.* 2008, Bernal & Venkitaraman 2011) with one example of the system being applied in *D. melanogaster* (Speese *et al.* 2003, for a full review of all applications so far see Faden *et al.* 2014).

Recently the degron was adapted for the use in multicellular organisms at a significantly lowered temperature range of 14°C to 28°C (Faden *et al.* , 2016b). This degron consists of the following parts: An N-terminal ubiquitin moiety for N-terminal processing according to the ubiquitin fusion technique (UFT), a short linker sequence (F-HGSGI) with the primary destabilizing residue phenylalanine (F), a point-mutated temperature sensitive (*ts*) DHFR (T39A, E173D, Gowda *et al.* 2013, Faden *et al.* 2016b), and a triple HAT tag in the linker to the POI for easy immunological detection via western blot (figs. 1.3 and 5.2).

This degron cassette now represents a truly modular approach to generate artificial temperature sensitive alleles of a given protein of interest efficiently bypassing the tedious screening procedure usually linked to the identification of temperature sensitive alleles.

---

<sup>13</sup>Chicken cell cultures even require a higher restrictive temperature of up to 42°C (see references in text).

## 1.4 Aim of the work

The aim of the work was to transfer the well-established temperature-sensitive degron from the yeast system to multicellular organisms, especially plants. Initial work in the identification of the temperature-sensitive degron cassette had already been done previously by Nico Dissmeyer. I was able to significantly deepen the understanding of the degron technique by showing its applicability with different proteins of interest in different organisms. Through analysis of degron behavior and (de)stabilization kinetics the applicability was demonstrated.

In the end the obtained data resulted in a new and revised model about the degron's mode of action, being in accordance with previously published work. Additionally, a peptide-based screen was established and performed, gaining further insight into the mechanisms of N-degron binding by PRT1.

Finally a new vector, based on the widely used gateway cloning technique, was generated that will allow researchers to easily apply the degron technique in their own research.

## 2 Material and Methods

### 2.1 Cloning

**Cloning:** For classical cloning standard methods were applied. In brief: Vector and insert were digested using the appropriate compatible enzymes. Enzymes were purchased from either New England Biolabs (NEB) or Thermo Scientific. Plasmid DNA was purified from *E. coli* using the GeneJet Plasmid Miniprep Kit (Thermo Scientific). Ligation was performed using T4 DNA ligase (Thermo Scientific) according to the manufacturers instructions. For blunt-end cloning the Quick Blunting and Quick Ligation Kit (NEB, Cat.No. E0542S) was used according to the manufactureur's instructions. 4  $\mu$ l of the reaction mixture was used for heat shock transformation of 50  $\mu$ l chemo-competent *E. coli*. Gateway Cloning (Hartley *et al.* , 2000) was performed according to the manufacturer's instructions (Invitrogen/Thermo Scientific). The BP or LR clonase II Enzyme Mix was used respectively as a  $1/4$  reaction. The entire reaction was used for heat shock transformation of *E. coli*. A PCR product carrying the appropriate *att*-overhangs, together with *pDONR201*, yielded an entry-vector (*pENTR*) in a BP reaction. This *pENTR* was then used together with a suitable destination vector (*pDEST*) to yield the different expression vectors (*pEXPR*) in an LR-reaction.

PCR products and fragments resulting from DNA digestion were purified from an agarose gel using the GeneJet Gel Extraction Kit (Thermo Scientific). DNA concentrations were measured using a photospectrometer (Tecan; M200 pro). For *in silico* planing of cloning strategies the Vector NTI 10 software package (Invitrogen/Thermo Scientific) was used.

**PCR:** All polymerase chain reaction (PCR) reactions were carried out in Labcycler gradient machines (SensoQuest) using homemade *pfuX7* polymerase (Nørholm, 2010) for cloning and homemade *taq* polymerase (Desai & Pfaffle, 1995) (GenBank accession No. J04639) for genotyping purposes. For PCR reactions using *pfuX7* a commercially available 5x buffer (Thermo Scientific; Phusion Green HF Buffer, Cat.No. F-538L) was used. For GC-rich templates betaine (Sigma Aldrich; Cat.No. B2754) was added to a final concentration of 1 M. For PCR reactions using *taq*, a homemade buffer (10x, 100 mM pH 8.3, KCl 500 mM, MgCl<sub>2</sub> 15 mM) was used. A 100 mM dNTP stock (25 mM each) was mixed and stored at -20°C (Thermo Scientific; dNTP Set, Cat.No. 10297-117). A standard 20  $\mu$ l PCR reaction consisted of following components: 1x Phusion HF buffer, 10 mM dNTPs,

10 pmol each primer, ca. 100 ng of template DNA, 0.2  $\mu$ l of *pfuX7*<sup>1</sup>, and H<sub>2</sub>O to 20  $\mu$ l. Primer melting temperature  $t_M$  was calculated using the Vector NTI 10 software. The used annealing temperature was always  $t_M - 2^\circ\text{C}$ . Elongation time was set at a rate of 15s/kb for *pfuX7* and 30s/kb for *taq* polymerase.

To fuse two pieces of DNA, both were amplified individually with eight base pairs (bp) overhangs, complementary to the respective other fragment. PCR fragments were purified and mixed in an equimolar concentration. 100 ng of DNA were used for a PCR using spanning 5'-and 3'-primers optionally already containing either *att* overhangs for gateway cloning or restriction sites for classical cloning<sup>2</sup>. Due to the decreased efficiency of very long primers it was sometime necessary to use short primers for the fusion PCR and re-amplify the fusion product subsequently with primers carrying the desired overhangs for downstream application.

An adapter PCR was used if overhangs were to long to be contained within one primer. In this case, a first PCR was performed with a primer carrying only a part of the desired overhang. After purification of the fragment a second PCR was performed on the fragment with a primer that anneals to the previously attached part of the overhang. This was used to attach a TEV-protease cleavage site to a DNA fragment followed by attachment of *att* sites for gateway cloning as described previously (Naumann *et al.* , 2016).

**Plant cDNA synthesis:** Plant RNA for reverse transcriptase (RT)-PCR analysis was purified from two week old *A. thaliana* seedlings using the RNeasy Plant Mini Kit (Quiagen; Cat.No. 74904) according to the manufacturer's instruction. Quality and yield of the purified RNA were determined using a photospectrometer (Tecan; M200 pro). RNA was stored at  $-80^\circ\text{C}$  or used directly for cDNA synthesis. In brief: 200 U of RevertAid Reverse Transcriptase (Thermo Scientific; Cat.No. EP0442) were used in a 20  $\mu$ l total reaction volume together with the supplied reaction buffer, dNTPS (2  $\mu$ l of a 10 mM stock), 20 U RiboLock RNase inhibitor (Thermo Scientific; Cat.No. EO0381), and 100 pmol of Oligo-dT primer. The amount of template was chosen according to the application: For semi-quantitative analysis of transcript abundance 1  $\mu$ g of RNA was used. For cloning purposes 3  $\mu$ g of RNA were used. A standard transcription protocol used was: Mix RNA, Oligo-dT primer, and water. Incubate in the PCR cycler at  $65^\circ\text{C}$  for 5min. Chill on ice and add all the other leftover components. Run the reaction in a pcr cycler for 1h at  $42^\circ\text{C}$  followed by a 10 min incubation step at  $70^\circ\text{C}$ . After the reaction cDNA was either stored at  $-20^\circ\text{C}$  or directly used in downstream applications.

**Side Directed Mutagenesis:** Primers were designed by the QuickChange Primer Design Tool<sup>3</sup>. A PCR reaction with modified annealing/elongation steps was used. In

---

<sup>1</sup>Because the polymerases were homemade no exact determination of active U/ $\mu$ l could be determined.

<sup>2</sup>Because many restriction enzymes cut inefficiently if their recognition site is too close to the end of the DNA strand, a list published by NEB ([www.neb.com/tools-and-resources/usage-guidelines/cleavage-close-to-the-end-of-dna-fragments](http://www.neb.com/tools-and-resources/usage-guidelines/cleavage-close-to-the-end-of-dna-fragments)) was used to optimize primers in that regards.

<sup>3</sup>Agilent: [www.genomics.agilent.com/primerDesignProgram.jsp](http://www.genomics.agilent.com/primerDesignProgram.jsp)

brief: Annealing temperature was set to 55°C. Elongation time was set to 30 s/kb. 18 cycles were run. Subsequently, the PCR reaction was digested using one µl of FastDigest DpnI (Thermo Scientific; Cat.No. FD1703) for at least two hours to overnight at 37°C, to eliminate non-mutated (methylated) template DNA. Five µl of the reaction were used for transformation of 50µl of chemocompetent *E. coli* of the appropriate strain. In case of difficult or inefficient mutagenesis betaine was added to a final concentration of 1 M. If this did not yield satisfactory results, a modified protocol according to the SPRINP protocol (Edelheit *et al.*, 2009) was applied. This protocol efficiently increases site-directed mutagenesis (SDM) performance by running an individual reaction for each primer which then are annealed in a second step.

**Sequence verification:** Sequence identity of plasmids was achieved via sequencing, following at least three independent restriction analyzes using different restriction enzymes. Sequencing was done in both directions for every sequence (forward/reverse) by either MWG (Eurofins Genomics GmbH, Ebersberg, Germany) or GATC (GATC Biotech, Konstanz, Germany). Primers SelA and SelB were used as standard sequencing primer for gateway pENTR vectors (tab. 5.4).

### 2.1.1 Assembly of degon reporter constructs for plants

In most cases, K2 was fused to the protein of interest using a fusion PCR approach, sub-cloned into *pDONR201* yielding an *pENTR*, and used to assemble an *pEXPR* clone in the *pAM-PAT* backbone carrying different promoters. These vectors are all derivatives of the vector *pAM-PAT-MCS* (multiple cloning site; GenBank accession number AY436765; Lipka, V., Rademacher, T. and Panstruga, R., unpublished), which by itself is a derivate of the *pPAM* vector (GenBank accession number AY027531) (Rademacher *et al.*, 2002). All these vectors have in common that they carry the *beta*-lactamase (*bla*) gene that confers carbenicillin (Carb)/ampicillin (Amp) resistance in bacteria as well as the *bar* gene that codes for the phosphinothricin-N-acetyltransferase (PAT) protein which confers resistance to phosphinothricin (glufosinate ammonium, BASTA<sup>4</sup>; Bayer CropScience) *in planta*.

GFP constructs are based on a *pAM-PAT* derivate called *pAM-KAN* carrying the GFP-gene downstream of the gateway site and also using the *nptII* gene conferring kanamycine (Kan) resistance *in planta*. The *pEXPR* construct based on this vector was generated through an LR reaction with *pENTR:K2* (addgene ID 80684), containing a degon cassette without stop after the last Glycine-Alanine (GAGA) linker.

**Cloning of K2:GUS expression constructs:** *PENTR:K2:GUS* was generated through amplification of the K2:GUS coding sequence from *pLEELA:K2:GUS* (kind gift from Nico Dissmeyer, Leibniz Institute of Plant Biochemistry, Halle), using primers K2(P2)\_frw and

<sup>4</sup>BASTA (glufosinate, phosphinothricin) is a widely used herbicide. Resistance to BASTA or its active components is conferred by the *bar* gene coding for the PAT enzyme. Two homologues have been initially isolated from *Streptomyces hygroscopicus* (Thompson *et al.*, 1987) and *Streptomyces viridochromogenes* (Wohlleben *et al.*, 1988). Since then it has been used in a wide variety of plants as a selection marker.

att\_GUS\_rev followed by recombination into *pDONR201* through a gateway BP reaction. The resulting *pENTR:K2:GUS*, after sequence verification, was used to generate *pEXPR-Pro35S/ProUBQ10/ProCDKA;1:K2:GUS* through LR reactions with the respective *pAM-PAT* vectors.

**Cloning of K2:TEV expression constructs:** The expression clone *pAM-PAT:K2:TEV*<sup>5</sup> was kindly provided by Nico Dissmeyer (Faden *et al.* , 2016b).

**Cloning of K2:PAT expression constructs:** The clone *pENTR:K2:PAT* was recovered from *pLEELA:K2:PAT* (kind gift from Nico Dissmeyer, Leibniz Institute of Plant Biochemistry, Halle) through a reverse BP reaction. This *pENTR* vector was recombined in a LR reaction with *pJAN33* (double CaMV35S promoter fused to the first intron of WRYKY33, selectable marker NPTII (Kan)) (Weigel *et al.* , 2003) to yield *pJAN33:K2:PAT*.

Since the *pAM-PAT* vectors used already contain a BASTA selection marker (PAT), it was necessary to modify the vectors *pAM-PAT-ProUBQ10/CDKA;1* to express K2:PAT. For that, both vectors were modified using site-directed mutagenesis to ablate the BASTA selection marker by mutating the start codon as well as introducing an additional stop codon into the ORF of the PAT gene. These vectors were termed *pAM-NOP-ProUBQ10* and *pAM-NOP-ProCDKA;1*<sup>6</sup> respectively. Different version of *pENTR:K2:PAT*, namely F-, R-, and L-starting, were now recombined with these vectors. The latter two were generated through site directed mutagenesis with *pENTR:K2:PAT* as a template using primer pairs K2\_Phe-Leu\_frw/K2\_Phe-Leu\_rev and K2\_Phe-Arg\_frw/K2\_Phe-Arg\_rev respectively. Identity of the mutations was verified via sequencing. Subsequently, *pEXPR* clones were generated through an LR reaction.

**Cloning of K2:GFP expression constructs:** Expression clones were created through recombination of *pENTR:K2/R-K2* with the destination vector *pAM-KAN-Pro35S:GW:GFP*. The K2 cassette was amplified from *pLEELA:K2:GUS* (kind gift from Nico Dissmeyer, Leibniz Institute of Plant Biochemistry, Halle) using primers K2(P2)\_frw and K2(P2)\_rev and recombined into *pDONR201* through a BP reaction yielding *pENTR:K2* (addgene ID 80684). R-K2 was generated through site-directed mutagenesis using *pENTR:K2* as a template and primers previously used to generate *pENTR:R-K2:PAT*.

For generation of suitable expression clones for the transfection of *D. melanogaster* Kc cells, *pENTR:K2* was recombined with the *pAWG* vector (Murphy, 2003). This vector carries a gateway site followed by a EGFP for C-terminal tagging of target proteins. Expression of the ORF is driven by the strong constitutive Actin5c promoter.

**Exchanging the N-terminal sequences in *pENTR:K2* to generate *pENTR* clones with altered N-terminals:** To test various sequences identified in SPOT assays *in vivo* the vector *pENTR:K2* was opened using the restriction enzymes SalI and EcoRI. The sequence containing the new N-terminal peptide was synthesized, already carrying

---

<sup>5</sup>In this work TEV protease refers to the 27 kDa C-terminal fragment of the full length protein that is used in biology and biotechnology, reviewed in Waugh 2011.

<sup>6</sup>NOP = no PAT

the appropriate overhangs (complete list of all new N-terminal sequences can be found in supplementary table 5.5). All sequences were optimized for *A. thaliana* codon usage using the JCat engine<sup>7</sup>. After annealing of the single stranded fragments through slow cool down after denaturing conditions, the new double stranded insert was ligated into the opened *pENTR:K2* vector, using the Quick Ligation Kit (NEB; Cat.No. M2200S), yielding a new vector *pENTR:X-K2* (X = N-terminal sequence) (fig. 5.14).

The introduction of the new N-terminal sequence was monitored by standard restriction analysis through a newly introduced BamHI site which is a result of the N-terminal exchange and yields an additional digestion fragment (3151 bp and 63 bp vs. 2611 bp, **540 bp**, and 63 bp). Following, the sequence identity of all new *pENTRs* was verified through sequencing.

**Cloning expression clones for recombinant production of four K2 variants:** K2 variants F/M-K2 and F/M-W-GUS-K2 were cloned as described previously (Naumann *et al.*, 2016). In brief: The degon cassettes with either the W-GUS or wild type N-terminal were amplified from their respective *pENTR* vectors (see above) using primers K2(WT)\_tev\_frw/K2(WORL)\_tev\_frw and K2-TEV\_BP\_rev. To change the Phenylalanine at the N-terminal to Methionine, primers K2(WT)\_M\_tev\_frw/K2(WORL)\_M\_tev\_frw were used. The fragments were purified and again amplified using primers adapter\_tev/K2-TEV\_BP\_rev. After another round of fragment purification, the pieces were amplified again using primers K2-TEV\_BP\_frw and K2-TEV\_BP\_rev to yield a PCR product suitable for BP gateway cloning. These fragments were recombined with *pDONR201*, yielding four different *pENTR* vectors which were recombined with *pVP16* (Invitrogen) for expression of the fusion protein 8xHis:MBP<sub>TEV-rec</sub>-F/M-K2-WORL/WT.

**Cloning an expression clone for simultaneous expression of the E3 PRT1 with different K2-versions form the same ORF in yeast:** In a first step the ubiquitin (UB) in *pENTR:K2* was mutated to UBQ<sub>K29/48/63</sub> using site directed mutagenesis and primer pairs K29R\_frw/K29R\_rev, K48R\_frw/K48R\_rev, and K63R\_frw/K63R\_rev). All mutations were traceable via restriction digestion (abolished Psp1406I site for K29R, abolished XhoI site for K48R, abolished XmiI site for K63R) and were confirmed via sequencing.

To prepare *pENTR:K2* for insertion of the 3xHA:PRT1 fragment, an XhoI site within the ubiquitin moiety had to be eliminated using site-directed mutagenesis and the primer pair KillXhoI\_frw and KillXhoI\_rev (template *pENTR:3xHA:PRT1*, kind gift from Maria Klecker). This vector was then opened using BglII and XhoI. 3xHA:PRT1 was amplified from *pENTR:3xHA:PRT1* using primers HA\_XhoI\_frw/PRT1\_Bgl\_rev. These primers carried the respective restriction site in their overhangs. Importantly, PRT1\_Bgl\_rev also

<sup>7</sup><http://www.jcat.de> (Grote *et al.*, 2005)

carries some additional basepairs to keep the frame since the BglII site in the Ub moiety of K2 is some basepairs after the initial ATG. The PCR fragment was digested using XhoI and BglII and ligated into the opened K2 backbone yielding *pENTR:3xHA:PRT1:K2* which was renamed to *pENTR:Ref:K2*. Success of cloning was verified through digestion analysis and sequencing.

The vector was modified further to allow the exchange of the N-terminal sequence as described before. Because introduction of the K63R mutation accidentally eliminated the Sall restriction site important for N-terminal exchange, it was reconstituted using site-directed mutagenesis and the primer pair Sall\_re\_frw/Sall\_re\_rev. Also, since Eco31I, the other enzyme crucial for the exchange of the N-terminal sequence, has two recognition sites within the PRT1 coding sequence, these two restriction sites were eliminated via site-directed mutagenesis as well, using the two primer pairs prt\_kill\_ec1\_frw/prt\_kill\_ec1\_rev and prt\_kill\_ec2\_frw/prt\_kill\_ec2\_rev introducing silent mutations. Success was again verified via restriction and sequencing.

Two *pENTR:Ref:K2*-based *pEXPR* vectors were generated through exchanging the N-terminal amino acids with a yeast codon-optimized version of the K2 wildtype and W-GUS sequence generating *pENTR:Ref:K2-WT* and *pENTR:Ref:K2-W-GUS*. Codon optimization was again achieved through the formerly described JCAT tool<sup>8</sup>. After another verification through sequencing, both *pENTR* vectors were recombined into *pAG426GAL-EGFP* (Alberti *et al.*, 2007) yielding yeast transformable *pEXPR* clones. For control purposes also *pENTR:K2-WT* and *pENTR:K2-W-GUS* were generated as yeast codon-optimized versions and recombined into the same *pDEST* vector.

**Cloning constructs for split luciferase and luciferase stability assays:** The vectors *pENTR:F-WT/W-GUS/W-GUS-E/W-LUC/W-LUC-D/W-LUC-K/nsP4/nsP4-K/eK/G-GUS/poly-G/poly-GS/M/G-K2* were ligated into *pDEST-GW-nLUC*. This vector carries the C-terminal fragment of luciferase downstream of a gateway site. Expression is driven by the strong viral ProCaMV35S. The K2-versions need a C-terminal fusion because of the necessary exposure of their N-terminal through co-translational cleavage of the N-terminal UB moiety. The interacting partner PRT1 was ligated into *pDEST-cLUC-GW* using *pENTR:3xHA:PRT1*.

For a luciferase-based stability assay, the different K2 versions were recombined into the *pAM-PAT-Pro35S:LUC pDEST* vector carrying a firefly luciferase for C-terminal POI tagging.

**Cloning *pAM-PAT*-based expression vectors for easy degron-tagging of a POI:** The K2 cassette was amplified from *pENTR:K2* using the primer pair K2\_XhoI\_frw and K2\_XhoI\_rev. The reverse primer contains an additional two basepairs to maintain the reading frame in the *pEXPR* vector. The K2 pcr fragment was digested and ligated into *pAM-PAT-ProUBQ* and *pAM-PAT-ProCDKA;1*, using the restriction enzyme XhoI,

---

<sup>8</sup><http://www.jcat.de> (Grote *et al.*, 2005)



yielding the gateway destination vectors *pLTDK2-ProUBQ10* and *pLTDK2-ProCDKA;1*. Proper insertion of K2 was verified via sequencing using primers *pLTDK2\_seq1/2*.

**Using the *pLTDK2* vectors for degron-tagging of the transcription factors AGAMOUS and LEAFY:** CDNA was generated from *A. thaliana* flower buds and used to amplify the full coding sequence of LEAFY (LFY) and AGAMOUS (AGA) containing gateway compatible BP recombination overhangs using primer pairs *AG.1\_att\_frw/AG\_att\_rev* and *LFY\_att\_frw/LFY\_att\_rev* respectively. The primer *AG.1\_att\_frw* contains an ATG start codon to eliminate the non-canonical translation initiation codon ACG as a precaution to ensure translation over the whole fusion construct. Both PCR fragments were used in a BP reaction to generate *pENTR:LFY* and *pENTR:AGA*. After sequence verification through specific restriction/digestion and sequencing, these vectors were recombined with *pLTDK2-ProUBQ10* and *pLTDK2-ProCDKA;1* to yield the four expression vectors *pLTDK2-ProUBQ10/ProCDKA;1:LFY/AG*.

**Using *pLTDK2-ProCDKA;1* to generate a new versatile vector for simplified promoter exchange and POI-degron-tagging :** In a first step the C-terminal XhoI restriction site, previously used to introduce the degron cassette in the *pAM-PAT* backbone for generation of *pLTDK2*, was eliminated using the primer pair *Kill\_XhoI\_ref\_frw / Kill\_XhoI\_ref\_rev* (fig. 5.16 1/2). After elimination of the XhoI site, the vector was opened using the enzymes AscI and XhoI to insert a multiple cloning site (MCS) for easy promoter insertion (fig. 5.16 3). The MCS was synthesized as a whole and offers 13 different unique restriction sites. Additionally, a new NdeI site was inserted between the TMV omega leader sequence and the ATG of the UB by opening the vector with XhoI and BglII and inserting a TMV-NdeI fragment that, as the MCS, was also synthesized (fig. 5.16 4). The NdeI/BglII sites offer the possibility to insert a stable reference upstream of the degron cassette (e.g. DHFR, GUS, or a fluorophore such as GFP). This Ubiquitin-Fusion/Reference-Technique has been used extensively for stability normalization *in vivo* (Varshavsky, 2005). However, it should be taken into account that the UB within the degron cassette is a wild type ubiquitin. If a reference construct is to be used, after cleavage of the fusion protein, the UB remains on the reference protein where it might influence its stability, even though this has not been reported when using a DHFR as a stable reference (Varshavsky, 2005). However, using the vector with a stabilized UB\_K29/48/63R without a reference would result in an unwanted stabilization of ubiquitinated proteins because the free, overexpressed, and mutated UB would lead to chain disruption when incorporated in polyubiquitin chains of the K29/48/63R type.

## 2.2 Bacteria work

### Strains:

- *E.coli* Dh5 $\alpha$  - standard plasmid propagation and cloning strain

F<sup>-</sup> *endA1 glnV44 thi-1 recA1 relA1 gyrA96 deoR nupG purb20 φ80/ lacZΔM15 4Δ*  
(*lacZYA-argF*) U169, *hsdR17*(r<sub>K</sub><sup>-</sup>, m<sub>K</sub><sup>+</sup>), λ<sup>-</sup>

- ***E. coli* DB3.1** - *ccdB* resistant strain for propagation of empty gateway vectors  
F<sup>-</sup> *gyrA462 endA1 glnV44 Δ(sr1-recA) mcrB mrr hsdS20*(r<sub>B</sub><sup>-</sup>, m<sub>B</sub><sup>-</sup>) *ara14 galK2*  
*lacY1 proA2 rpsL20*(Sm<sup>r</sup>) *xyl5 δleu mtl1*
- ***E. coli* BL21(DE3)** - standard strain for expression of recombinant proteins. Carries  
DE3 for T7 promoter expression  
F<sup>-</sup> *ompT gal dcm lon hsdS<sub>B</sub>*(r<sub>B</sub><sup>-</sup>m<sub>B</sub><sup>-</sup>) λ(DE3 [*lacI lacUV5-T7 gene 1 ind1 sam7*  
*nin5*])
- ***A. tumefaciens* GV310::pMP90** - Rif<sup>r</sup>, Gent<sup>r</sup>, Kan<sup>r</sup> (Koncz & Schell, 1986)

**Growth conditions:** *E. coli* were grown overnight in LB media (Carl Roth; Cat.No. X968.3) supplemented with antibiotics, if applicable, at 37°C/120 rpm. *A. tumefaciens* were grown overnight in YEB media (Carl Roth; 5 g/l saccharose, 5 g/l bakto-pepton, 5 g/l beef extract, 1 g/l yeast extract, 2 mM MgSO<sub>4</sub> pH 7.0) at 28°C/120 rpm also supplemented with the appropriate antibiotics.

**Transformation protocols:** Chemically competent *E. coli* were used throughout this work<sup>9</sup> and transformed using a standard heat-shock protocol. In brief: 0.5 µl of plasmid DNA or a gateway reaction were incubated with 50 µl of competent bacteria on ice for 15 min. After a heat shock (55 s, 42°C) cells were regenerated with 250 µl LB media on a thermoshaker (Eppendorf; 37°C, 800 rpm) for one hour and streaked out on MacConkey-Agar plates containing the appropriate antibiotics for selection. For verification, single colonies were inoculated in 4 ml LB containing the appropriate antibiotics for selection and grown overnight. The next day plasmid DNA was extracted using the GeneJet Plasmid MiniPrep Kit (Thermo scientific) and analyzed via restriction/digestion of DNA using three different enzymes.

*A. tumefaciens* were transformed using a standard electroporation protocol. In brief: 1 µl of plasmid DNA were mixed with 50 µl of competent cells in a pre-cooled electroporation cuvette (VWR; 2 mm width). Electroporation was carried out using a Gene Pulser (BioRad; capacity 25 µF; voltage 2.5 kV; resistance 400 Ω). Cells were regenerated in 1 ml YEB for 3 h and streaked out on MacConkey-Agar plates containing the appropriate antibiotics. To verify positive colonies single colonies were inoculated in 4 ml YEB containing the appropriate antibiotics for selection and grown overnight. Plasmid DNA was extracted as described above and used for re-transformation of *E. coli*. Plasmid identity was then verified as described above.

---

<sup>9</sup>For a protocol using rubidium chloride compare: [www.cryst.bioc.cam.ac.uk/hyvonnen/methods/competent\\_cells](http://www.cryst.bioc.cam.ac.uk/hyvonnen/methods/competent_cells)

## 2.3 Yeast work

### Strains:

- *S.cerevisiae* **JD47-13C** - Wild type strain  
MAT a leu2- $\Delta$ 1 trp1- $\Delta$ 63 his3- $\Delta$ 200 ura3-52 lys2-801 ade2-101
- *S.cerevisiae* **JD55** - Ubr1 knock out strain (in the JD52 background)  
Mat a trp1- $\Delta$ 63 ura3-52 his3- $\Delta$ 200 leu2-3112 lys2-801 ubr1 $\Delta$ :HIS3

**Cultivation conditions:** Untransformed cells were cultivated in YPD media (Carl Rot; Cat.No. X970.2) or on YPD plates (Carl Roth; Cat.No. X971.2). After transformation, cells were grown on selective minimal media (0.67% yeast nitrogen base (Carl Roth; Cat.No. HP26.1); 2% glucose; 0.07% amino acid drop-out mix (stock consists of: 0.5 g Adenine, 2.0 g Histidine, 4.0 g Leucine, 2.0 g Lysine, 2.0 g Methionine, 2.0 g Tryptophane, 2.0 g Tyrosine; mixed/ground and stored in the fridge); 2% agar). Since the used strains cannot synthesize Uracil, this was used as a marker for selection of transformed cells. Therefore, no uracil was added to the selective media or plates. For galactose dependent induction of the GAL1 promoter in transformed yeast the glucose in the selective media was replaced with galactose. For direct fluorescence measurements in transformed yeast an alternative yeast nitrogen base (5 g/l  $(\text{NH}_4)_2\text{SO}_4$ , 1 g/l  $\text{KH}_2\text{PO}_4$ , 0.5 g/l  $\text{MgSO}_4$ , 0.1 g/l NaCl, 0.1 g/l  $\text{Ca}_2\text{Cl}$ , 0.5 mg/l  $\text{H}_3\text{BO}_4$ , 0.04 mg/l  $\text{CuSO}_4$ , 0.1 mg/l KI, 0.2 mg/l  $\text{FeCl}_3$ , 0.4 mg/l  $\text{MnSO}_4$ , 0.2 mg/l  $\text{Na}_2\text{MoO}_4$ , 0.4 mg/l  $\text{ZnSO}_4$ , 2  $\mu\text{g}$ /l biotin, 0.4 mg/l calcium pantothenate, 2 mg/l inositol, 0.4 mg/l niacin, 0.2 mg/l PABA, 0.4 mg/l pyridoxine HCl, and 0.4 mg/l thiamine) was used. This nitrogen base did not contain riboflavin and folic acid, which, due to their strong autofluorescence, would mask any GFP signal (Sheff & Thorn, 2004). The nitrogen base was prepared as a 10x stock, sterile filtrated, and added to the media after autoclaving.

**Transformation:** *S. cerevisiae* were transformd using the previously reported LiAc/SS carrier DNA/PEG method (Gietz & Schiestl, 2007) with minor changes. Cells were streaked out on YPD plates and incubated at 28°C overnight. The next day a single colony was inoculated in 5 ml YPD media and again grown overnight at 28°C in an incubator at 140 rpm. The following day 1 ml of dense culture was harvested via centrifugation (2 min, 12000 rpm, standard tabletop centrifuge). The pellet was washed once in 1 ml of 0.1 M TE buffer (1 M Tris-HCl pH 8.0, 0.1 M EDTA) and subsequently resuspended in 300  $\mu\text{l}$  40% Poly(ethylene glycol) (PEG) 4000 (Fluka, Cat.No. 95904) in LiAc/TE buffer. 74.8  $\mu\text{g}$  salmon sperm DNA (10 mg/ml in TE buffer) were added as well as 2  $\mu\text{l}$  of plasmid DNA (ca 0.5-1  $\mu\text{g}$ ). Cells were mixed with buffer and DNA and incubated overnight at room temperature. The next day, the emulsion was re-mixed by pipetting and heat-shocked at 42°C for 10 min and subsequently incubated on ice for 2 min. The whole reaction was then streaked out on selective media and incubated at 28°C. Single colonies were distinguishable after two to three days.

**Colony PCR:** From each transformation eight colonies were screened for the presence of the correct transgene. Each of the colonies was sub-cultivated on a fresh minimal selective media plate to ensure growth. Following, some of the cells were scraped off using an inoculation loop and resuspended in 500  $\mu$ l H<sub>2</sub>O. Cells were pelleted and washed once more with H<sub>2</sub>O before being resuspended in 100  $\mu$ l H<sub>2</sub>O. The cell suspension was then boiled for 10 min at 96°C. Cell debris was pelleted by centrifugation and 5  $\mu$ l of the clear supernatant were used as a template in a standard PCR reaction.

## 2.4 Drosophila work

**Cell line:** *D. melanogaster* Kc (Echalier & Ohanessian, 1969) cell lines were used.

**Cultivation conditions:** *D. melanogaster* cells were cultivated in 3 ml Schneider's medium (Gibco) supplemented with 10% (v/v) fetal bovine serum (FBS) at 24°C. To keep cultures vital and healthy cells were passaged every 5 days in a 1:10 dilution.

**Transfection:** Cells were transfected using the Effectene Transfection Reagent (Quia-gen; Cat.No. 1054250) in 12-well plates according to the manufacturer's protocol for semi-adherent cells.

## 2.5 Plant work

**Seed sterilization:** *A. thaliana* seeds for aseptic cultivation were sterilized using chlorine gas. Seeds were placed into a 2 ml reaction tube (Eppendorf) and exposed to chlorine gas for at least 1 h but never more than 4 h to prevent damage to the seeds. Generation T<sub>0</sub> seeds, obtained after floral dip transformation of *Arabidopsis thaliana*, were sterilized for full four hours. The chlorine gas was created by mixing 10 ml of sodium hypochlorite (Carl Roth; NaOCl, 12%) with 5 ml of hydrochloric acid (Carl Roth; HCl, 37%)<sup>10</sup> in a closed box.

**Plant cultivation:** Plants were grown either on steamed (sterilized for 3 h at 90°C) soil mixture (Einheitserde Classic Kokos (45% (w/w) white peat, 20% (w/w) clay, 15% (w/w) block peat, 20% (w/w) coco fibers; 10-00800-40, Einheitserdewerke Patzer, Gebr. Patzer); 25% (w/w) Vermiculite (grain size 2-3 mm; 29.060220, Gärtnereibedarf Kamlott); 300-400 g/m<sup>3</sup> soil substrate of Exemptor (100 g/kg thiacloprid, 802288, Hermann Meyer)), on 1/2 Murashige & Skoog (MS) (2.16 g/l MS salts, Duchefa; 0.5% Glucose, Carl Roth; 8 g/l phytoagar, Duchefa; pH to 5.6-5.8 using KOH) plates, or in liquid culture in 1/2 MS + 2-(N-morpholino)ethanesulfonic acid (MES) (2.16 g/l MS salts + vitamins, Duchefa; 0.1% Glucose; Carl Roth; 0.5 g/l MES) in different conditions according to the general demands of the experiment. Normal or intermediate growth temperatures refer to 21°C. Cold and warm temperatures refer to 14°C and 28°C respectively. Long day growth conditions refer

---

<sup>10</sup>NaClO + 2 HCl > Cl<sub>2</sub> + H<sub>2</sub>O + NaCl

to a light/dark period of 16/8 h as opposed to short day conditions which refers to a light/dark period of 8/16 h. Plants grown at intermediate or warm temperatures were stratified for at least three days at 4°C in the dark. Seeds destined for germination at 14°C were never stratified since this significantly decreased germination efficiency at low temperatures. For controlled environment experiments, plants were cultivated either in growth cabinets (Percival Scientific; AR-66L2/AR-66L3) or in phyto chambers (Johnson Controls) at a humidity of 60%. During temperature shift experiments plants were watered with pre-cooled or pre-heated water to avoid temperature effects in response to irrigation. Plants destined for selection of transgenic plants on soil or for seed propagation were cultivated in greenhouses at long day conditions.

**High-throughput plant genotyping:** *A. thaliana* plants were genotyped in a 96-well format as described previously (Dissmeyer & Schnittger, 2011). The *lfy-12* plants were genotyped using a dCAPS marker and primers BstAPI\_frw and BstAPI\_rev (Neff *et al.*, 1998). Digestion of the PCR product with the enzyme BstAPI results in elimination of an additional small molecular weight signal in the mutant allele visible through a band weight difference on a 4% agarose gel (WT: 345, 25; *lfy-12* 370).

The genetic identity of the AGA T-DNA insertion line (SALK\_014999, Urbanus *et al.* 2009) was confirmed using primer pairs AG\_WT\_frw/AG\_WT\_rev and AG\_WT\_frw/AG\_LB. Degron constructs were identified using primers DHFR\_frw and DHFR\_rev. The PRT1 mutant allele *prt1-1* was genotyped using primers N130 and N131. The allele contains an EMS-introduced CAPS-marker which can be identified through digestion of the PCR product with the enzyme MnlI.

**Generation and selection of stable lines:** Stable lines of *A. thaliana* were generated using the floral-dip method (Clough & Bent, 1998). In brief: A single colony of *A. tumefaciens* that carried the desired *pEXPR* clone was used to inoculate 5 ml of YEB media and grown overnight. The next day the dense culture was used to inoculate the transformation culture. This culture was grown again until it appeared opaque and orange. Depending on the size of the culture this took between eight hours to overnight. Prior to transformation 5 g/l glucose and 500 µl of the surface surfactant L-77 were added to the culture. Flowering *A. thaliana* plants showing many unopened inflorescences were transformed by submerging the shoots in the *A. tumefaciens* suspension for 20 s. Subsequently, plants were covered and incubated overnight in the greenhouse without direct exposure to lights. The next day cover was taken off, plants re-erected, and cultivated until seed setting. To select for transgenic plants seedlings were either grown on soil or aseptically on plates. Selection on plates was achieved using either kanamycin sulfate (Carl Roth; 50 mg/ml stock in H<sub>2</sub>O, dilution 1:1000) or glufosinate (Duchefa; 10 mg/ml stock in H<sub>2</sub>O, dilution 1:1000). Selection on soil was achieved by spraying in two day intervals with BASTA (Bayer CropScience; dilution 1:1000 in tap water) at least three times or until non-resistant plants turned white and died.

**Trypan blue staining:** Trypan blue is a stain commonly used to stain dead tissues (described in Strober 2015). *A. thaliana* leaves or whole seedlings were stained as previously reported<sup>11</sup> with little changes. In brief: Tissue of interest was added into the staining solution and boiled for one minute. Samples were de-stained using chloral hydrate and finally stored in 50% (v/v) glycerol.

**Polarized light microscopy:** To visualize leaf hairs polarized light microscopy was used, exploiting the birefringent properties of trichomes. When analyzed under a microscope with dual polarization filters trichomes light up in a bright appearance (Gudesblat *et al.* , 2012, Pomeranz *et al.* , 2013). However, I used chloral hydrate for destaining of the leaves. For better analysis and visibility of trichomes color of the images was inverted to display trichomes as black on white background. True leaves three to six were used for analyzed.

**Agarose imprints of leaf surfaces:** To analyze leaf surface morphology imprints on agarose were produced as described previously (Mathur & Koncz, 1997) with minor changes. First, only a 2% agarose suspension was used. Second, a few mg of bromphenol blue was added to the agarose which yielded a light blue color significantly enhancing the contrast under the stereo microscope.

**Seed mucilage visualization:** Seed mucilages was visualized by submerging them in diluted ink followed by macroscopic analysis using a stereo microscope (Rerie *et al.* , 1994).

**Documentation of plants and microscopy:** Pictures of plants *in situ* were taken using a Canon DSLR EOS750D camera equipped with a 50 mm Canon macro lens. For more detailed analysis a Nikon AZ100 stereo microscope equipped with a DS-Fi2 color camera was used. A confocal laser scanning microscope (Zeiss, LSM780) was used for microscopic analysis.

**Protoplast isolation and transfection:** Mesophyll protoplasts from plants of the mutant allele *prt1-1* were isolated using the Tape-*Arabidopsis* Sandwich technique described previously (Wu *et al.* , 2009) with minor changes. The digestive enzymes were purchased from Serva (Macerozyme R-10, Cat.No. 28302.03 and Cellulase "Onozuka" R-10, Cat.No. 16419.03). Also, protoplasts were isolated from the leaf by a three hours incubation period without shaking and protected from direct light in an air-conditioned room set to 18°C. To isolate the protoplasts after the incubation period, leaves were shaken delicately in the solution until cells were released. Protoplasts were transfected according to the protocol in the same publication (Wu *et al.* , 2009) again with minor changes. Mainly, after transfection, cells were just washed once with solution W5 and finally incubated overnight in the dark at 14°C. Transfections were done in 12 ml cell culture tubes (Greiner Bio One; Cat.No. 163160). DNA for transformation was purified using the NucleoBond PC 500 Maxi kit (Machery Nagel; Cat.No. 740571). DNA yield and purity was monitored using a photospectrometer (Tecan; M200pro). For storage and simplified transfection, DNA was

---

<sup>11</sup><http://www.unifr.ch/plantbiology/eng/Home/research/mauch-group/protocols/trypan-blue>

diluted to a final concentration of 1 µg/µl in H<sub>2</sub>O.

**Proteasome inhibitor treatments of *Arabidopsis* seedlings:** For proteasome inhibitor (PI) treatments, seedlings were grown aseptically in 20 ml MS+vitamins/MES on a rocking platform. After two weeks, the media was taken away and the seedlings separated into three samples: Untreated, PI-treated, and mock (Dimethyl sulfoxide (DMSO))-treated. Each sample was treated with 10 ml of the growth media supplemented with the proper chemicals (PI-treated: MG132 to a final concentration of 50 µl (from a 50 mM stock in DMSO); mock-treated: 1 µl DMSO/10 ml media (1:1000)). After five hours samples were harvested, proteins extracted, and analyzed via Western Blot (see section 2.8). 20 µg of total protein were loaded in each lane.

**DAPI staining:** 4',6-diamidino-2-phenylindole (DAPI) staining was performed to stain nuclei in intact *A. thaliana* leaves. Plant material was fixed using a solution of 3.7% formaldehyde in PBT (0.1% Tween in PBS) overnight. After fixation material was washed twice with PBT and subsequently submerged in DAPI staining solution (2.5 µg/ml DAPI, 5% DMSO in PBT), vacuum infiltrated and incubated again overnight. Samples were washed with PBT and destained using EtOH using different concentration (30%, 50%, 70%, 50%, 30%) each for one hour and finally transferred to PBT.

## 2.6 Expression, purification, and *in vitro* stability of recombinant proteins

**Expression and purification of PRT1 in BL21(DE3):** PRT1 was expressed as a C-terminal 8xHIS:MBP-tagged fusion protein from the vector *pVP16* (Invitrogen) (construct *pVP16-8xHIS:MBP:PRT1*, kind gift from C. Naumann). Protein was expressed as followed:

One colony was picked and grown overnight in 5 ml Luria Miller broth (LB) + Carb. This pre-culture was used to inoculate the main culture (250 ml). The culture was grown to an OD<sub>600</sub> of 0.6 in baffled flasks and induced using Isopropyl-β-D-thiogalactopyranosid (IPTG) at a final concentration of 1 mM. Protein was expressed for three hours at 37°C. Cells were harvested through centrifugation (4°C, 3000 g, 20 min), resuspended in 10 ml Ni-buffer (100 mM Tris-HCl, pH 8; 300 mM NaCl; 0.25% Tween; 10% glycerol), and pre-lysed by incubation with lysozyme at a final concentration of 1 mg/ml on ice. After pre-lysis cells were further cracked by sonication. Cell lysate was cleared by centrifugation (4°C, 12000 g, 20 min) and the supernatant loaded on a column (Quiagen; Polypropylene Column, 5 ml volume, Cat.No. 34924) packed with 1 ml Ni-NTA agarose beads (Quiagen; Cat.No. 30230) equilibrated with Ni-buffer. After re-loading the flow-through once on the column, it was washed with 20 ml of Ni-buffer. The bound protein was eluted using 5 ml of the Ni-buffer supplemented with 400 mM imidazole. 1 ml fractions were collected and stored at -20°C until further use. All purification steps *on column* were executed at room temperature.

**Expression and purification of K2-variants in BL21(DE3):** Proteins were es-

entially expressed and purified as described above for PRT1 with only changes in buffer composition. A more stringent Ni-buffer (Ni<sub>K2</sub>-buffer, 50 mM Tris pH 8, 400 mM NaCl, 4% glycerol, 2 mM EDTA, 25 mM imidazole) was used. Elution was done as described above with the Ni<sub>K2</sub>-buffer plus 400 mM imidazole.

**TEV cleavage of N-terminal tags:** TEV protease<sup>12</sup> was used to cleave N-terminal tags for exposure of desired N-termini. Homemade TEV protease was used (Kapust *et al.* , 2001) according to a previously published protocol (Naumann *et al.* , 2016).

**Stability of fluorescent K2-variants in crude plant extract:** Recombinant proteins were labeled using the red dye provided in the SPL starter kit according to the manufacturers instructions (NH Dyeagnostics; Smart Protein Layers, excitation 650 nm, emission 665 nm<sup>13</sup>, Spl Red Kit, Cat.No. PR914) and incubated with a crude protein extract generated using a previously described buffer (Kim & Kim 2013 with only 1/10 of the ATP concentration). To analyze stability in regard to proteasomal dependent degradation the proteasome inhibitor MG132 was used. Every 1.5 hours samples were taken, boiled in loading dye, and subjected to SDS-PAGE (see 2.8). Fluorescence was measured using a Typhoon FLA 9000 (GE Healthcare Life Sciences) with the photomultiplier set to 700 V. Intensities were analyzed using the ImageJ software suite<sup>14</sup> following a protocol for Western Blot intensity analysis<sup>15</sup>.

## 2.7 Degron stability assays *in vivo*

**Qualitative GUS assay:** *In situ*  $\beta$ -glucuronidase (GUS) assays were performed as a simplified version of the protocol described in (Kim *et al.* , 2006). Whole plants were submerged in a GUS staining solution containing 1 mM of the glucuronidase substrate X-glucuronide sodium salt (X-Gluc) (Santa Cruz Biotechnology; sc-208490). After vacuum infiltration for 30 minutes, samples were incubated overnight at 37°C and subsequently fixed in GUS fixation solution (ethanol : glacial acetic acid 9:1) at room temperature for at least four hours, or until tissue became completely destained of chlorophyll, and finally analyzed using a standard stereo microscope.

**Quantitative GUS assay:** GUS activity in seedlings/leafs was measured using a previously described approach (Kim *et al.* , 2006) in a streamlined and optimized version. For each sample five or more seedlings were harvested. Protein extraction was performed using GUS extraction buffer. 196 $\mu$ l of assay solution supplemented with 1 mM 4-methylumbelliferyl- $\beta$ -D-glucuronide (4-MUG) (Santa Cruz Biotechnology; sc-280452) were mixed with 4 $\mu$ l of the crude plant extract containing the GUS protein and transferred into a white 96-well plate (Thermo Scientific; FluoroNunc). The fluorescence measurements were

---

<sup>12</sup>In this work TEV protease refers to the 27 kDa C-terminal fragment of the full length protein that is used in biology and biotechnology, reviewed in Waugh 2011.

<sup>13</sup>[http://www.dyeagnostics.com/site/wp-content/uploads/2012/05/SPL\\_Rot\\_40W.pdf](http://www.dyeagnostics.com/site/wp-content/uploads/2012/05/SPL_Rot_40W.pdf)

<sup>14</sup><http://imagej.nih.gov/ij/>

<sup>15</sup><http://lukemiller.org/index.php/2010/11/analyzing-gels-and-western-blots-with-image-j/>



performed in a preheated photospectrometer (Tecan; M1000) at 37°C for 60 min. One data point was recorded every minute for 1.5 h.

The product of the reaction of the GUS enzyme with its substrate 4-methylumbelliferone (4-MU), is fluorogenic and has an excitation maximum at 365 nm and an emission maximum at 455 nm. Individual stopping and measurement of the completed reaction, as described in the original publication, is hence not necessary. The curve was plotted and the slope of the linear part of the curve was used to calculate the total GUS activity as pmol 4-MU per min and mg total protein using a 4-MU calibration curve (produced with different dilutions of 4-MU, Santa Cruz Biotechnology; sc-206910, see supplementary figure 5.3A) and through normalization to the total protein content of the sample. In case of activity measurement in *A. thaliana* protoplast 10µl of the protoplast suspension were directly resuspended in 190µl of GUS extraction buffer including the substrate in the 96-well plate and measured as described before. All biological replicates were measured as three technical replicates and averaged.

**Temperature shift experiment in plants:** Plants were grown at 14 or 28°C respectively. After ten days plates with plants grown at 14°C were shifted to 28°C and vice versa. Samples were taken at indicated time points. For every sample between 5 and 10 seedling were pooled. Proteins were extracted using a suitable extraction buffer and subjected to quantitative (K2:GUS) or western blot analysis (K2:GUS, K2:GFP).

**Temperature shift experiments in fruit fly cell culture:** After transfection, cells were incubated at 24°C. At the indicated time points plates were shifted to either 15 or 28°C respectively. Subsequently cells were harvested and protein content analyzed through western blot.

**Temperature tuning experiment:** Plants were grown at 14 or 28°C respectively for 10 days. Samples were taken (for every sample five seedlings were pooled) every 24 h and following temperature was shifted for 2.8°C up or down. This was repeated until both, samples grown at 14 or 28°C respectively, completed a full cycle (14°C > 28°C > 14°C; 28°C > 14°C > 28°C). Harvested samples were snap-frozen in liquid nitrogen, stored at -80°C and analyzed all together after the completion of the experiment, using a quantitative GUS assay.

**Split-luciferase assay:** After transfection, using 4.5 µg *Pro35S:cLUC:PRT1\_C29A* DNA, 4.5 µg *Pro35S:K2:nLUC* DNA, and 1 µg *ProUBQ:GUS* (Norris *et al.*, 1993) DNA, for normalization, per 100 µl of protoplast suspension, the cells were incubated for 19 h at room temperature in the dark. To measure the luciferase activity the substrate d-luciferin (Carl Roth; Cat.No. 4096.2) was added to a final concentration of 1 mM (from a 10 mM stock in H<sub>2</sub>O). 200 µl of protoplasts were transferred to a white 96-well plate (Thermo Scientific, FluroNunc) and measured in a luminometer (Tecan; M200 pro) with an integration time of 20 s. GUS activity of every sample was determined as described previously. The software GraphPad Prism 5 was used for statistical analysis and data

representation in BoxBlots.

**Luciferase stability assay:** The *p1-1* protoplasts were transfected with 4µg of *pAM-PAT-Pro35S:K2:LUC* DNA, 2µg of *ProUBQ10:GUS*(Norris *et al.* , 1993) DNA, and 2µg of *pAM-PAT-ProUBQ:PRT1<sub>WT/C\_29A</sub>* DNA (kind gift of Maria Klecker) per 100 µl of protoplast suspension. After 16 h of incubation at 18°C in the dark 140µl of protoplast suspension of every sample was measured for their luciferase activity as described previously with the only difference that a 10 s integration time was used. GUS activity of every sample was determined as described previously and used for signal normalization. Stability of the individual K2 variants was determined as: Stability = LUC-activity in PRT1<sub>WT</sub> co-transfected cells/(LUC-activity in PRT1<sub>C29A</sub> co-transfected cells/100). The software GraphPad Prism 5 was used for statistical analysis and data representation using BoxBlots.

**Degron stability in yeast:** Verified colonies were used for degron stability and degradation assays. The different yeast expression clones described above (see section 2.1.1) were transformed into the different yeast strains. To assess stability, cells were pre-grown on selective plates. Cells were scraped off and inoculated in liquid selective minimal media with 2% galactose to induce the protein expression. Cells were grown overnight. The next day cells were harvested and pellets washed twice with H<sub>2</sub>O and OD<sub>600</sub> was measured. Cells were pelleted once more and resuspended again in minimal selective media now with 2% glucose to a final OD<sub>600</sub> of 1. Glucose was used to shut off promoter activity. 300µl of the cell suspension was transferred into a black 96-well plate (Thermo Scientific; Nunclon). EGFP fluorescence was measured in a fluorescence reader (Thermo Scientific; VarioScan, 28°C, 488 nm excitation, 509 nm emission, 500 ms integration time).

## 2.8 Protein Techniques

**Protein extraction and quantification:** For protein extraction from *D. melanogaster*, cells from one well were transferred into a standard 1.5 ml reaction tube and sedimented through centrifugation (4°C, 5 min 300 g). The pelleted cells were washed once with ice cold PBS. To lyse the cells a radioimmunoprecipitation assay (RIPA) buffer (50 mM Tris-Cl pH 8, 120 mM NaCl, 20 mM NaF, 1 mM EDTA, 6 mM EGTA, 1 mM benzamidine hydrochloride (sc-207323, Santa Cruz Biotechnology) 15 mM Na<sub>4</sub>P<sub>2</sub>O<sub>7</sub>, and 1% Nonidet P-40; EDTA-free Complete Protease Inhibitor cocktail (Roche Diagnostics) was added to the freshly made buffer and aliquots were stored at -20°C for later use) was used with lysis happening in a pre-chilled thermo shaker (Eppendorf ThermoMixer, 4°C, 800 rpm, 20 min). The cell lysate was cleared of insoluble cell debris via centrifugation (>20,000 g, 4°C, 20 min). The clear supernatant was transferred to a fresh tube and protein concentration determined using the BCA kit (see below).

For protein extraction from *A. thaliana*, material (seedlings or tissues such as leaves or flowers) was collected in standard 2 ml reaction tubes containing three metal beads

(Mühlmeier; Nirosta stainless steel beads; 3.175 mm; Cat.No. 75306). Samples were flash frozen in liquid nitrogen and either stored at  $-80^{\circ}\text{C}$  for later experiments or used directly. A bead mill (Retsch; 45 s, 30 Hz; with collection microtube blocks (Qiagen; adapter set from TissueLyser II, Cat.No. 69984)) was used for grinding. After grinding, extraction buffer, either RIPA buffer, GUS extraction buffer (Kim *et al.*, 2006) (50 mM Na-phosphate, 10 mM EDTA, 0.1% (w/v) SDS, 0.1% (v/v) Triton X-100, and 10 mM  $\beta$ -mercaptoethanol freshly added), or the extraction buffer from Kim *et al.* (Kim & Kim, 2013) with only  $1/10$  of the ATP use, was added and lysis was carried out for 20 min at  $4^{\circ}\text{C}$  on a thermoshaker at 1000 rpm. Subsequently, the protein extract was cleared through centrifugation (20 min,  $4^{\circ}\text{C}$ ,  $>20000\text{g}$ ) and the supernatant transferred to a fresh 1.5 ml reaction tube. Protein content was quantified using either DirectDetect or BCA for RIPA extracts and either DirectDetect or 2-D Quant for GUS extracts (see below).

Protein content was quantified using either the DirectDetect system (MerckMillipore), a Pierce BCA Protein Assay Kit (Thermo Scientific; Cat.No. 23225) according to the manufacturer's instructions for plate reader and measured in a photospectrometer (Tecan M200pro, Tecan), or the 2-D Quant Kit (GE Healthcare Life Sciences; Cat.No. 80-6483-56) according to the manufacturer's instructions.

**Immunoprecipitation of K2:GUS from plant extract:** *ProUBQ10:K2:GUS* expressing plants were grown on selective  $1/2\text{MS}$  plates at permissive temperatures. Proteins were extracted (Dissmeyer *et al.*, 2007) and two individual reactions were set in individual 1.5 ml reaction tubes each containing 250  $\mu\text{l}$  of cleared plant extract with a concentration of 1.5  $\mu\text{g}/\mu\text{l}$  (determined using DirectDetect). Pre-clearing was performed using 100  $\mu\text{l}$  of an equilibrated 50% bead slurry (GE Healthcare; nProtein A Sepharose 4 Fast Flow Cat.No. 17-5280-01) for two hours on a rotating wheel at  $6^{\circ}\text{C}$ . Beads were pelleted by centrifugation, the supernatant transferred into a fresh tube, and 50  $\mu\text{l}$  of a-DHFR antibody were added (tab. 5.2). Samples were incubated with the antibody overnight again on a rotating wheel at  $6^{\circ}\text{C}$ . The next day 250  $\mu\text{l}$  of an equilibrated 50% bead slurry were added to the reaction and incubated for three hours on a rotating wheel at  $6^{\circ}\text{C}$ . Finally, beads were harvested by centrifugation (400 g, 2 min,  $4^{\circ}\text{C}$ ) and washed twice with bead buffer (Dissmeyer *et al.*, 2007). To analyze bound proteins, beads were boiled with 30  $\mu\text{l}$  of 5x loading dye at  $96^{\circ}\text{C}$  for five minutes. Insoluble bead remnants were cleared by centrifugation and the supernatant was pooled. A small fraction was run on a standard SDS-PAGE and analyzed by Western Blotting using an a-HA antibody (tab. 5.2) to verify the success of the Immunoprecipitation (IP). The rest of the sample was run on a gel and subjected to a mass spectrometry compatible silver staining.

**TUBE-based enrichment of the ubiquitome:** A Tandem Ubiquitin Binding Entities (TUBE) approach was used to enrich the ubiquitome from K2:GUS expressing plants grown under cold and warm temperatures to evaluate the ubiquitination state of the protein at the different conditions. Plants (*ProUBQ10:K2:GUS*-expressing and wild type)

were grown aseptically on petri dishes. 3-week old seedlings were harvested and immediately snap-frozen in liquid nitrogen. Plant material was ground using mortar and pestle and protein was extracted using the extraction buffer from Kim et al. (see above) with added proteasome (100  $\mu$ M MG132) and DUB inhibitors. 1 ml of a protein extract, at a concentration of 1.5 $\mu$ g/ $\mu$ l, was incubated with 40 $\mu$ l of a 50% slurry of TUBE matrix (LifeSensors; Agarose-TUBE 2, Cat.No. UM402) equilibrated in the extraction buffer. The bead matrix was incubated with the plant extract for 1.5 h at 6°C on a 3D-shaker. Following, beads were washed with 500  $\mu$ l of extraction buffer and resuspended in 50  $\mu$ l of 5x SDS loading dye, boiled at 95°C for 10 min, and centrifuged (20000 g, 5 min) to remove insoluble cell and bead debris. 20  $\mu$ l of the supernatant were used for SDS-PAGE and subsequent analyzed using UB and HA-specific antibodies (tab. 5.2).

**SDS PAGE and Western Blot:** Defined amounts of protein were diluted with 5x loading dye (0.2 % [v/v] bromophenol blue, 0.5 M DTT, 50 % [v/v] glycerol, 10% [v/v] SDS, 0.25 M TRIS-Cl pH 6.8). Proteins were denatured at 96°C for ten minutes. Separation was achieved using standard SDS-polyacrylamide gel equipment (BioRad; Protean Mini). For Western Blot analysis, gels were blotted using a semi-dry blotting system (Bio-Rad; Trans-Blot SD Semi-Dry Transfer Cell) at 0.85 V/cm<sup>2</sup> of membrane and a standard PVDF membrane (GE; Amersham Hybond P 0.45 PVDF, Cat.No. 10600023 ). Subsequently, the blot was blocked for one hour (at room temperature) to overnight (at 6°C) in TBST (50 mM Tris, 150 mM NaCl, 0.1%Tween 20) + 4% milk on a rocking platform. Blots were incubated with primary and secondary antibody in 4% milk in TBST for always 1 h each with a 30 min washing step in between (3x10 min TBST).

**Three buffer blotting system:** SPOT-array-bound proteins were blotted using the three buffer blotting system (Kyhse-Andersen, 1984) that has recently been established for SPOT assays (Klecker & Dissmeyer, 2016).

**Detection of HRP-signals:** Depending on signal intensity HRP signals were detected using either a chromogenic substrate (Thermo Scientific; Novex HRP Chromogenic Substrate (TMB), sensitivity range 1 ng, Cat.No. WP20004), or chemo-luminescent substrates of one of two different strengths (Thermo scientific; SuperSignal West Pico, sensitivity range 10-50 ng/mL, Cat.No. 34077 or SuperSignal West Femto, sensitivity range 2-10 ng/ml secondary antibody, Cat.No. 34094) with a standard film developing unit and X-ray films (Hartenstein; Fujifilm Super RX, Cat.No. RF11).

**Gel and blot loading controls:** Coomassie Brilliant Blue (CBB) (Carl Roth; Rotiphorese Blau R, Cat.No. 3074.1) was used to stain membranes and gels. This stain is irreversible and was therefore only used after analysis by e.g. Western Blot was completed. Gels or membranes were incubated in the CBB solution followed by destaining using destaining solution (40% methanol, 10% acetic acid). Ponceau S (Saturated solution in 5% acetic acid, Sigma Aldrich; Cat.No. 141194) was used after blotting and before blocking of membranes to ensure proper transfer and loading. Ponceau S staining is reversible and membranes

were first destained with destaining solution followed washing by TBST. In some cases blots were re-probed with a primary antibody against a housekeeping gene. In this case the membrane was stripped ( Carl Roth; Roti-Free stripping buffer, Cat.No. 0083.1) first.

**Silver staining:** All solutions were used at a 25 ml scale. After gel run the gel was incubated for at least one hour in fixing solution (40% (v/v) methanol (10 mL), 10% (v/v) acetic acid (2.5 mL) in H<sub>2</sub>O). The gel was pretreated for 30 minutes in a solution of 0.8 mM Na<sub>2</sub>S<sub>2</sub>O<sub>3</sub>, 0.8 M CH<sub>3</sub>COONa, 30% (v/v) methanol in H<sub>2</sub>O. After washing three times in water for at least 5 min the staining was performed for 20 minutes using 12 mM AgNO<sub>3</sub> in H<sub>2</sub>O. The staining was developed in 0.2 M NaCO<sub>3</sub>/0.04% formaldehyde in H<sub>2</sub>O. The reaction was stopped by incubation in 0.3 M Na<sub>2</sub>-EDTA for at least 10 minutes. Bands were excised and proteins analyzed by mass spectrometry.

## 2.9 SPOT assays

**Membrane synthesis and Synthetic Peptide On membrane support Technique (SPOT) assay:** Membranes were synthesized as described previously (Kleckler & Dissmeyer, 2016). At least four replicates of the same membrane were synthesized (Membrane 1 - 6x, Membrane 2 - 4x). Dry membranes were sealed in foil and stored at -20°C. After de-protection and activation (Kleckler & Dissmeyer, 2016), membranes were blocked in TBST<sub>SPOT</sub> (20 mM Tris-HCl, pH 7.4, 135 mM NaCl, 0.1% (v/v) Tween 20) + 10% milk overnight. 8xHis:MBP:PRT1 was used at various concentrations to distinguish the optimal signal to background ratio. For initial experiments 8xHis:MBP:PRT1 was used in a concentration of 200 nM, for the final and quantified assays the enzymes was diluted to a final concentration of 18.5 nM in binding buffer (TBST<sub>SPOT</sub> + 5 mM dithiothreitol (DTT) + 10 mM maltose + 0.75% milk). 8xHis:MBP:PRT1 was always pre-incubated for 30 minutes in the binding buffer subsequently followed by a two hour incubation with the membrane. After washing with TBST<sub>SPOT</sub> (3 intervals a 10 minutes, 30 minutes total) the membrane was blotted using a three buffer blot system (Kyhse-Andersen, 1984, Kleckler & Dissmeyer, 2016) or later used for immediate detection of bound proteins.

**Antibody based detection of PRT1 binding:** After blotting the PVDF membrane was blocked for one hour in TBST + 4% at room temperature. 8xHis:MBP:PRT1 or 8xHis:MBP were probed using an a-His tag antibody (tab. 5.2) followed by detection using an HRP-coupled secondary antibody (tab. 5.3).

**Fluorescence based analysis of PRT1 binding:** To quantify and normalize binding efficiency of 8xHis:MBP:PRT1 on and between the SPOT membranes a quantifiable approach using fluorescence was developed, since the dynamic range of X-ray films is too limited to allow adequate quantification (Faden *et al.* , 2016a). Three different approaches, or rather optimization steps, were established. For detection a Typhoon FLA 9000 (GE Healthcare Life Sciences) was used. The signal intensity was analyzed using the ImageJ

software<sup>16</sup> together with an embedded MicroArray analysis profile<sup>17</sup>. To analyze the binding efficiency, the measured values were exported to Excel 2016 (Microsoft). For every membrane the average binding intensity of six K2 wild type controls was determined. This value was set as 100% and subsequently all other values obtained from a given membrane was normalized to the binding efficiency of the K2 sequence in %/K2. A sequence starting with a stabilizing residue served as blank normalization.

**Immuno Blue based detection:** The PVDF membrane, as obtained after the assay, blotting, and blocking procedure was incubated with Immuno Blue, a fluorescent chromogenic HRP substrate (NH Dyeagnostics; Cat.No. PR840) according to the manufacturer's instructions and analyzed using the same ImageJ procedure as described above.

**Detection of labeled 8xHis:MBP:PRT1 on a PVDF membrane:** Before incubating the 8xHis:MBP:PRT1 enzyme in the binding buffer, it was labeled using the same red dye as mentioned above (see section 2.6). This red dye allows a direct detection of the fluorescence signal thus eliminating the need for a specific antibody. To label 8xHis:MBP:PRT1, the appropriate amount of protein was labeled in a 5x reaction according to the manufacturer's instruction, however internal standards for Western Blot analysis, as provided with the kit, were neglected. After the labeling procedure, the whole reaction was diluted in the binding buffer to a final concentration of 18.25 nM and the SPOT assay was carried out as described above. After washing, the membrane was blotted on PVDF and the blot directly analyzed in the Typhoon reader.

**Detection of labeled 8xHis:MBP:PRT1 on the SPOT membrane:** As a final optimization step, and to exclude signal alterations by the blotting procedure, the fluorogenically labeled 8xHis:MBP:PRT1 fusion protein was directly analyzed on the SPOT membrane without any blotting. The SPOT assay itself was carried out as described before.

**Regeneration of SPOT membranes:** After use, membranes were stripped (Klecker & Dissmeyer, 2016). Subsequently membranes were either dried, sealed, and stored at -20°C or washed with TBST<sub>SPOT</sub> and reused directly. Membranes were re-used for up to six times without noticing signal alterations.

---

<sup>16</sup><http://imagej.nih.gov/ij/>

<sup>17</sup>Bob Dougherty, [www.optinav.com/MicroArray\\_Profile.htm](http://www.optinav.com/MicroArray_Profile.htm)

## 3 Results

### 3.1 The degron cassette mediates temperature dependent control over protein abundance over a wide variety of proteins of interest

To demonstrate the capabilities of the degron approach and to further characterize the degron's behavior on a molecular level, different reporters were fused to the optimized N-degron cassette (K2, Gowda *et al.* 2013, Faden *et al.* 2016b). All reporter proteins offered an easy readout and/or were well established proteins that have been used widely in a biological/biochemical context, therefore being of general interest to the science community<sup>1</sup>. To confirm true regulation on protein level, transcripts of many of the reporter lines were analyzed.

#### 3.1.1 Generation of a K2:GUS expressing reporter line

$\beta$ -glucuronidase (GUS) is an enzyme from *E. coli* that has been used extensively in higher plants for promoter and expression studies (Jefferson *et al.* , 1987). It catalyzes the hydrolysis of  $\beta$ -glycosidic bonds, which in enzyme assays with either 5-bromo-4-chloro-3-indolyl glucuronide (X-Gluc) or 4-methylumbelliferyl-beta-D-glucuronide (4-MUG) results in easily measurable read-outs which are a bright blue precipitate for X-Gluc and a fluorescence signal for 4-MUG. K2:GUS expression in stably transformed *A. thaliana* plants was driven by either ProCaMV35S (Pro35S), ProUBQ10, or ProCDKA;1.

**Identification of responsive K2:GUS expressing lines:** T<sub>2</sub> plants were screened for degron functionality through a qualitative GUS assay of plants grown at 14°C or 28°C. In the initial screen, two lines, one for the CDKA;1 and one for the UBQ10 promoter construct, were identified that showed a temperature dependent accumulation of the active GUS protein, as made visible by a blue color precipitate. However, expression of K2:GUS in the ProCDKA;1 controlled line seemed weak (fig. S 5.3B). Most of the other lines either did not show any color, or showed color independent of the growth temperature. Mainly Pro35S driven lines behaved in this way, most likely due to strong expression from the viral promoter (fig. 3.1A). The two identified lines were grown again at 14°C or 28°C and

---

<sup>1</sup>An overview over this first generation of K2-reporter constructs, depicting overall organization as well as used promoters and primary destabilizing residues, can be found in fig. S 5.2.

subjected to a quantitative GUS assay. The ProCDKA;1 line proved to be a false positive since it did not show significant GUS activity (fig. S 5.3C).

**Protein analysis:** To evaluate whether the qualitative differences would correlate with abundance of GUS protein, samples were generated from cold and warm grown plants and subjected to Western Blot analysis. Signals for the K2:GUS fusion protein always appeared specifically as two distinct species over and below 100 kDa (fig. 3.2B). The lower molecular weight signal occurred at the *in silico* predicted mass weight of the K2:GUS fusion protein of 94.3 kDa. Longer exposure of blots always resulted in both signals being visible in both samples (14°C or 28°C) with different intensities (fig. S 5.3D). The higher molecular weight signal was found to be stronger in samples extracted from cold grown plants, whereas the lower molecular weight signal was usually more abundant in samples isolated from warm grown plants. Longer exposure led to both signal appearing in both samples, whereas weaker exposure of the blot led to a characteristic "zig-zag" scheme of bands (figs. 3.1B and 3.2).

#### 3.1.1.1 Characterization of the *ProUBQ10:K2:GUS* reporter line

**A qualitative GUS assay confirms the response of K2:GUS levels to temperature:** To analyze the GUS activity, a *Pro35S:GUS*<sup>2</sup>, as well as a non-responsive *Pro35S:K2:GUS* expressing line were used as controls. GUS activity in the two control lines was significantly higher than in the degron expressing lines. Also the dynamics of the GUS accumulation was inverted. Were non-responsive lines accumulated more active GUS enzyme under warm conditions, the *ProUBQ:K2:GUS* expressing line accumulated significantly more active GUS enzyme when grown at 14°C than when grown at 28°C, indicating functionality of the degron in regard to temperature dependent accumulation of the K2:GUS fusion protein (fig. 3.1A).

**A quantitative GUS assay reveals inverse accumulation kinetics between the responsive *ProUBQ10:K2:GUS* expressing line and non-responsive control lines:** Plant lines used for the qualitative assay were now subjected to quantitative analysis. GUS activity in the two control lines was found to be 3 to 23 times higher than in the K2:GUS expressing lines. Also, the dynamics of the GUS accumulation was inverted. Were non-responsive lines accumulated more active GUS enzyme at 28°C, *ProUBQ10:K2:GUS* reliably accumulated significantly more active GUS enzyme at 14°C (fig. 3.1C). Also it appeared as if the fusion of the degron to the GUS enzyme influenced overall protein levels as the activity in the *Pro35S:K2:GUS* expressing plants was significantly lower compared to the GUS activity found in the *Pro35S:GUS* expressing lines. This data confirms the results obtained in the qualitative GUS assay (fig. 3.1A)

**Temperature shift experiments show a quick and timely responsive of K2:GUS**

---

<sup>2</sup>Expression from the binary plasmid *pBI121* (Jefferson *et al.*, 1987); kind gift of Diana Schmidt (Leibniz Institute of Plant Biochemistry, Halle)



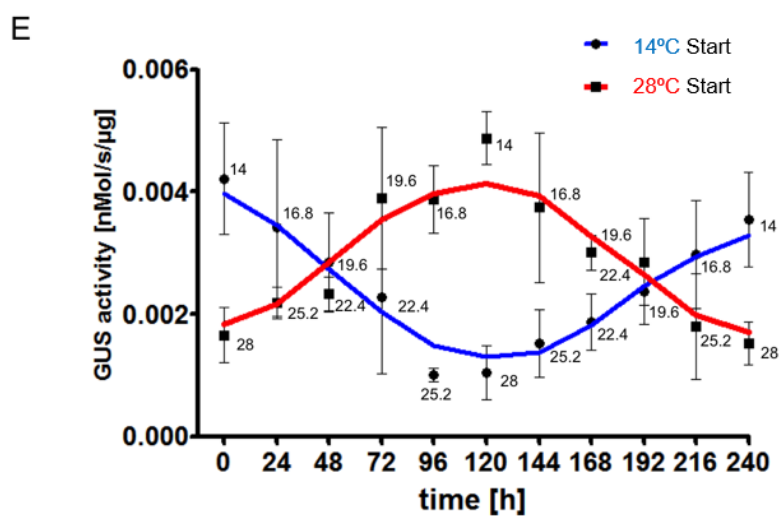
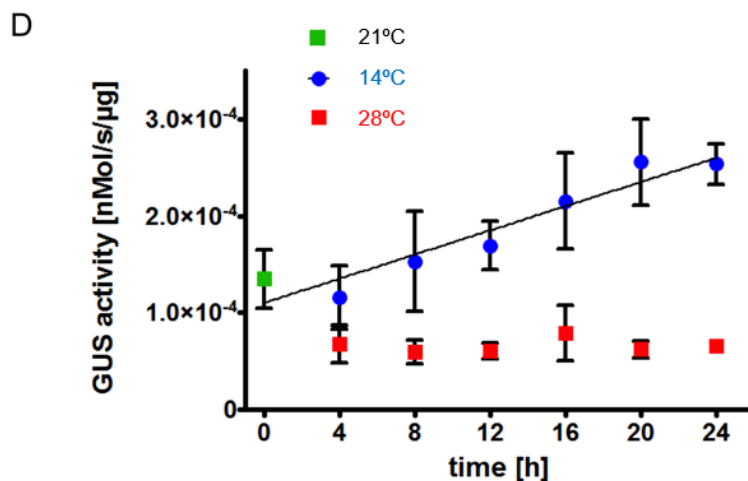
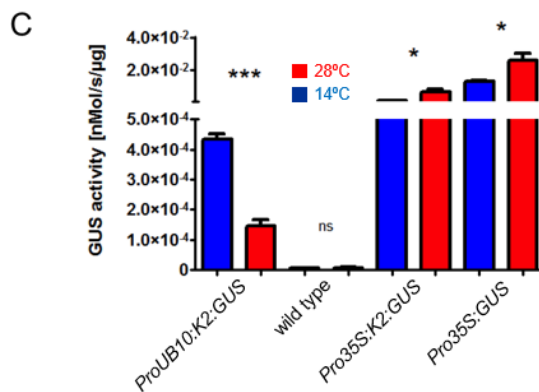
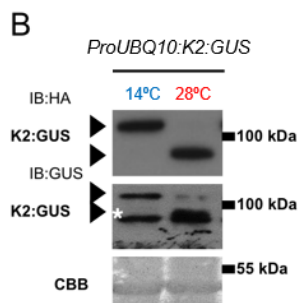
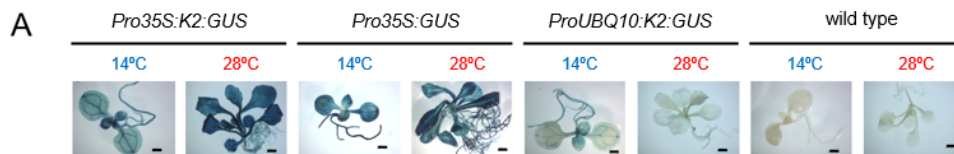


**Figure 3.1 – The degron cassette stirs K2:GUS accumulation in a highly responsive, temperature dependent manner.** (A) Qualitative GUS assays of different lines expressing K2:GUS under the control of different promoters reveal a temperature dependent stability only when expression is driven by the weaker UBQ10 promoter. (B) Western Blot analysis of cold and warm grown, K2:GUS expressing, plants reveal double banding with a typical zig-zag signal appearance. Blots were probed with anti-Ha (targeting the degron cassette) and anti-GUS (directly targeting the GUS moiety) antibodies respectively. (C) Quantitative analysis confirms the observation made in (A).  $N = 6$  for *ProUBQ:K2:GUS* and  $N = 3$  for all others.  $p < 0.5$  \*,  $p < 0.01$  \*\*,  $p < 0.001$  \*\*\*. unpaired ttest. (D) The degron reacts to a temperature shift within hours. Stabilization at 14°C is not completed 24 hours past shift.  $N = 3$  (E) Degron stability and linked GUS activity is flexible and tunable following a temperature stimulus in teh transgenic GUS-expressing plants.  $N = 3$

**levels to altered temperatures:** To dissect the resolution of the degron accumulation in regard to temperature and time, two different shift experiments were employed. In a first approach, plants were grown at 21°C temperature on plates. After two weeks, plates were shifted to either 14°C or 28°C respectively. Upon temperature shift, activity increased or decreased in a temperature dependent manner, indicating accumulation or degradation of the K2:GUS fusion protein (fig. 3.1D). The level of GUS activity dropped quickly and reached a low steady-state already after eight hours as indicated by reached statistically significant differences in activity as compared to time point zero (for values see additional data in table 5.1). The changed activity correlated with the total amount of K2:GUS fusion protein (fig. S 5.3D).

**A temperature tuning experiments shows a linear link between K2:GUS stability and temperature:** Additionally to the first experiment, where the reaction time of the stabilization of the K2:GUS fusion protein was assessed, a second experiment was performed to show tuneability as well as (de)stabilization kinetics of the K2:GUS fusion protein. Plants were grown at 14°C or 28°C. Every 24 h a sample was taken and the temperature shifted for 2.8°C up or down. The degron quickly responded to changed temperatures, which allows to tune protein content to desired levels (fig. 3.1E). The response of the degron to switching temperatures seemed linear, thus confirming the results of the temperature shift experiment (fig. 3.1D/E).

**An inhibitor treatment indicates proteasomal degradation of the K2:GUS fusion protein:** The previous experiments indicated that K2:GUS stability, and therefore the enzymatic GUS activity per  $\mu\text{g}$  of total protein, is linked to temperature. However, it remained unclear whether the K2:GUS fusion protein is readily degraded by the Ubiquitin Proteasome System (UPS) as predicted. Treatment of seedlings with the proteasomal inhibitor MG132 clearly showed accumulation of higher molecular weight signals after treatment of plants grown at 28°C. This indicates that the K2:GUS fusion protein is indeed degraded by the proteasome. Also, it suggests that the higher molecular species of K2:GUS represent the fraction of total K2:GUS protein, that confers the activity, sensitive to temperature dependent accumulation/degradation (fig. 3.2A).

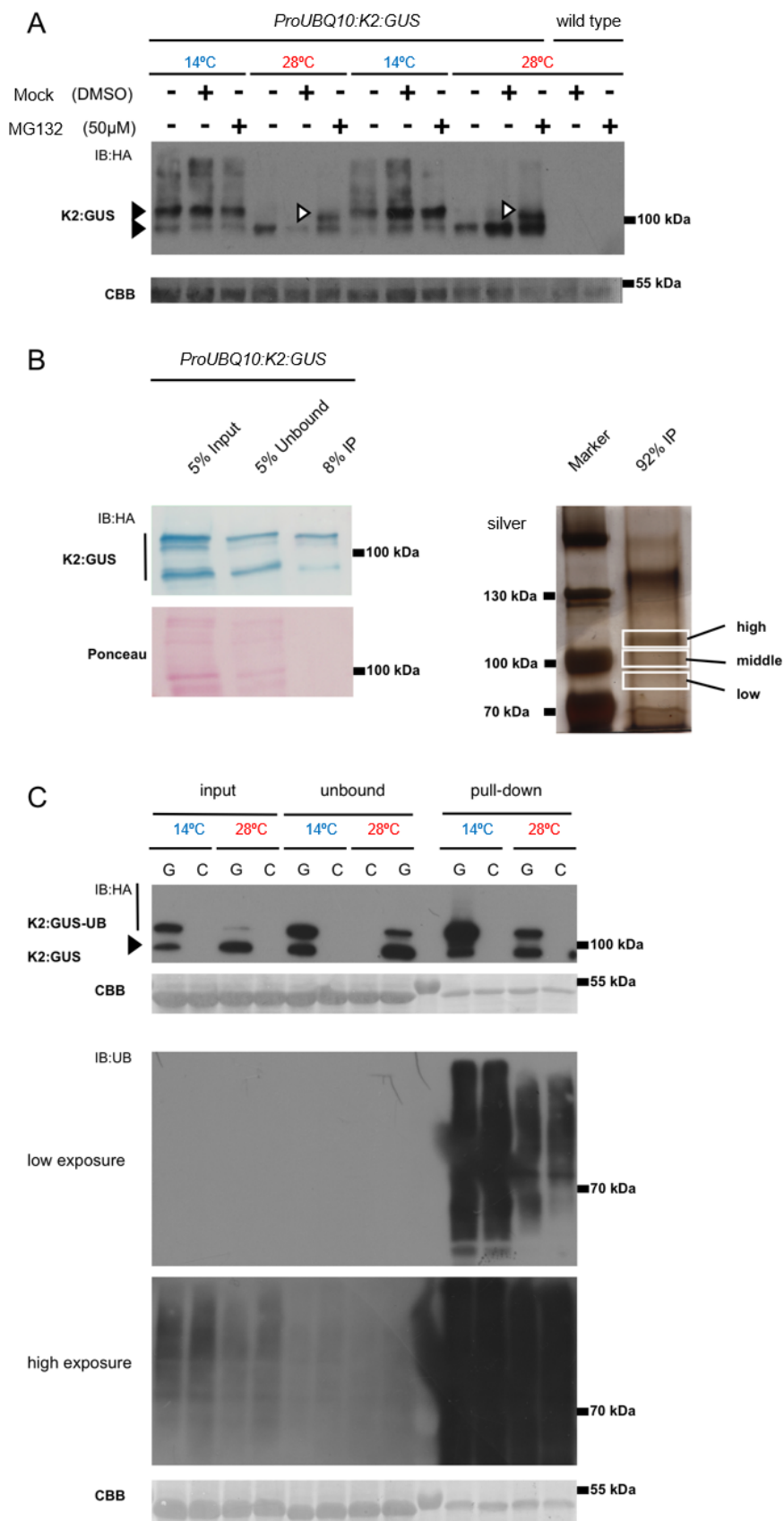


**Figure 3.2 – Inhibitor treatments, enrichment, and mass spectrometric analysis suggest potential distinct ubiquitinated species of K2:GUS and its degradation via the UPS.** (A) Treatment of stable transgenic seedlings expressing *ProUBQ10:K2:GUS* with the proteasomal inhibitor MG132 indicates degradation of the K2:GUS fusion protein via the proteasome as indicated by appearance of higher molecular species after treatment (white triangles). (B) Immunoprecipitation of K2:GUS from stable transgenic *ProUBQ10:K2:GUS* expressing plants using a DHFR specific antibody. The left panel shows success of the pulldown. Not only the two previously identified signals appear but also numerous others of intermediate molecular masses indicating a higher diversity of different sub-species. The right panel indicates the three different samples (high, middle, low) cut from the gel and subjected to mass spectrometric analysis. Peptides specific for the fusion K2:GUS fusion protein were identified in all samples (compare Faden *et al.* 2016b for exact results). (C) Ubiquitome enrichment of stable transgenic plants expressing *ProUBQ10:K2:GUS*, using a TUBE matrix, indicates that the multiple signals observed in K2:GUS expressing plants indeed represent various ubiquitinated subspecies of the fusion protein. Especially the higher molecular weight species are enriched in the elution fraction when the starting material was grown at cold temperatures.

**Immunoprecipitation (IP) and Mass Spectrometry confirm the identity of the different protein sub-species:** To analyze the different species of K2:GUS, the fusion protein was immunoprecipitated and subjected to mass spectrometric analysis. The success of the IP was monitored via SDS-PAGE. For better resolution of the high molecular weight signals, a low acrylamide percentage of 8% was chosen. The number of K2:GUS species, as indicated by the different specific signals appearing, seemed to be even higher than initially observed. Whereas other Western Blots always showed a separation into only two species (figs. 3.1A, 5.3D, and 3.2A/C), the analysis on a low percentage gel suggested at least four species of the K2:GUS fusion protein (fig. 3.2B left panel). However, the two species previously identified were the most abundant ones. To test whether these species contained the K2:GUS fusion protein the larger part of the IP reaction was loaded on another gel and silver-stained. Three different parts of the gel were cut out and subjected to mass spectrometric analysis (fig. 3.2B left panel). Indeed, in all three fractions peptides specific for the GUS enzyme could be identified (compare Faden *et al.* 2016b).

**Enrichment of the Ubiquitome of K2:GUS expressing plants reveal over-representation of discrete sub-populations of the ubiquitinated fusion protein:** To elucidate the ubiquitination state of the K2:GUS fusion protein under different temperatures, a Tandem Ubiquitin Binding Entities (TUBE) based enrichment of the entire ubiquitome of plants grown at 14°C or 28°C was carried out. Wild type plants were used as a control to ensure specificity of the immunosignals in the elution fraction. Especially the higher molecular weight signals always appeared specifically enriched in the TUBE-enriched ubiquitome fraction (fig. 3.2C). Additionally, a typical ubiquitination smear is visible atop the upper K2:GUS elution signal. This might indicate that the higher band of the two bands always visible in the K2:GUS line represents a specific state of ubiquitination. Interestingly, the control blot probed with an anti-Ub antibody revealed that the overall abundance of ubiquitinated proteins seemed to be lower in plants grown at 28°.

Also no difference between transgenic and wild type plants in regard to total ubiquitination levels was apparent.

### 3.1.2 Cloning and expression of Tobacco Etch Virus protease as a degron fusion protein

TEV protease, or rather the 27 kDa C-terminal domain of full length TEV protease conferring cleavage activity, has widely been used *in vitro* and *in vivo* for protein cleavage at its conserved recognition site (E-N-L-Y-F-Q-(G/S)) (reviewed in Waugh 2011). Due to its high specificity it represents a protein of a certain biotechnological importance. Transgenic T<sub>2</sub> lines expressing *Pro35S:K2:TEV* were screened for the presence of the fusion protein by Western Blot analysis. For every line samples from plants grown at either 14°C or 28°C were analyzed to identify lines accumulating K2:TEV in a temperature dependent manner. Three lines were initially identified, however, one line showed silencing effects in generation T<sub>3</sub>, leaving two lines that reproducibly showed a temperature dependent accumulation of the K2:TEV fusion protein (fig. 3.3A).

### 3.1.3 Cloning and expression of the BASTA resistance protein PAT as a degron fusion protein

The aim was to generate a conditionally BASTA-resistant<sup>3</sup> *A. thaliana* line. Transgenic T<sub>1</sub> were directly selected through BASTA spraying at 14°C to recover only K2:PAT expressing lines that showed the desired stability phenotype of the K2:PAT fusion protein.

**K2:PAT expressing lines show neither a clear macroscopic nor protein level phenotype:** Responsive lines should survive at 14°C, but not at 28°C, due to the temperature dependent accumulation of the K2:PAT fusion protein. No *Pro35S:K2:PAT* expressing and responsive line showing the desired phenotype could be isolated. All lines showed resistance to BASTA regardless of growth temperature (fig. 3.3B).

To exclude possible effects of the temperature on the efficiency of the BASTA selection, also wild type plants were grown at 14°C and 28°C with or without BASTA. BASTA selection was not influenced by the growth temperature and killed non-transgenic plants efficiently under any growth condition tested (fig. S 5.4). Since it proved impossible to isolate a responsive line expressing K2:PAT under the control of the strong ProCaMV35S, a set of new *pEXPR* vectors with the weaker ProUBQ10 and ProCDKA;1 driving expression was generated. These vectors were termed *pAM-NOP*<sup>4</sup>. As opposed to previous experiments, where only phenylalanine starting degron cassettes (K2) were used, now also version with

<sup>3</sup>BASTA (glufosinate, phosphinothricin) is a widely used herbicide. Resistance to BASTA or its active components is conferred by the *bar* gene coding for the PAT enzyme. Two homologues have been initially isolated from *Streptomyces hygroscopicus* (Thompson *et al.*, 1987) and *Streptomyces viridochromogenes* (Wohlleben *et al.*, 1988). Since then it has been used in a wide variety of plants for research, bio- and agrotechnological applications.

<sup>4</sup>NOP = no PAT

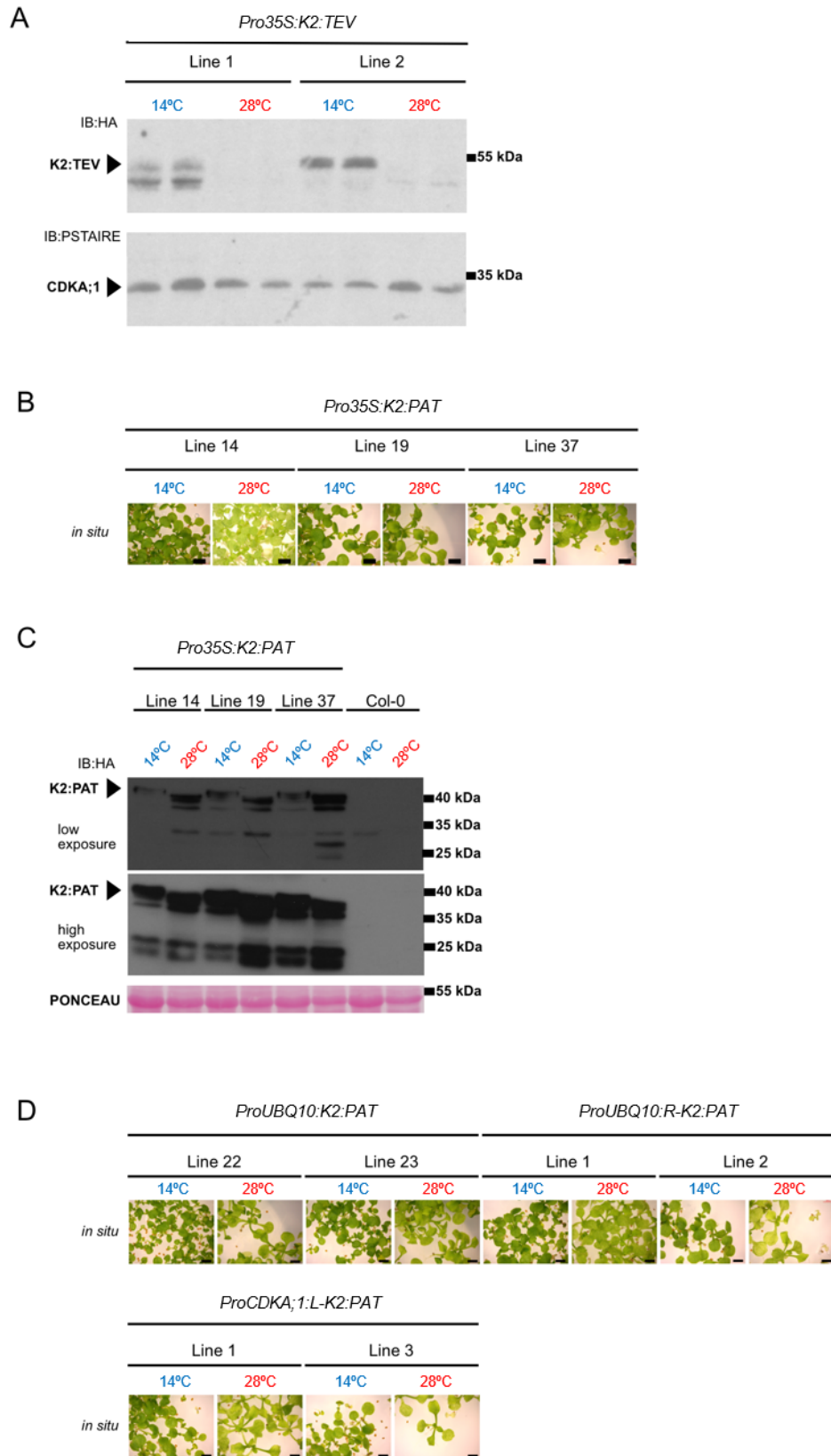


**Figure 3.3 – Analysis of Tobacco Etch Virus (TEV) and phosphinothricin-N-acetyltransferase (PAT) as degron fusions.** (A) K2:TEV expressed under the control of the strong viral ProCaMV35S results in temperature dependent accumulation of the fusion protein. CDKA;1 was used as a housekeeping gene. (B) Representative selection of different lines expressing K2:PAT. All lines showed insensitivity to BASTA independently of the growth temperature (black bar = 1mm). (C) Western blot analysis of three *Pro35S:K2:PAT* expressing lines. Even though some changes in signal intensities and abundance could be observed overall there was no clear phenotype on protein levels which is in line with the observed insensitivity to BASTA. (D) Different promoters or N-termini do not alter the BASTA insensitivity phenotype (black bar = 1 mm).

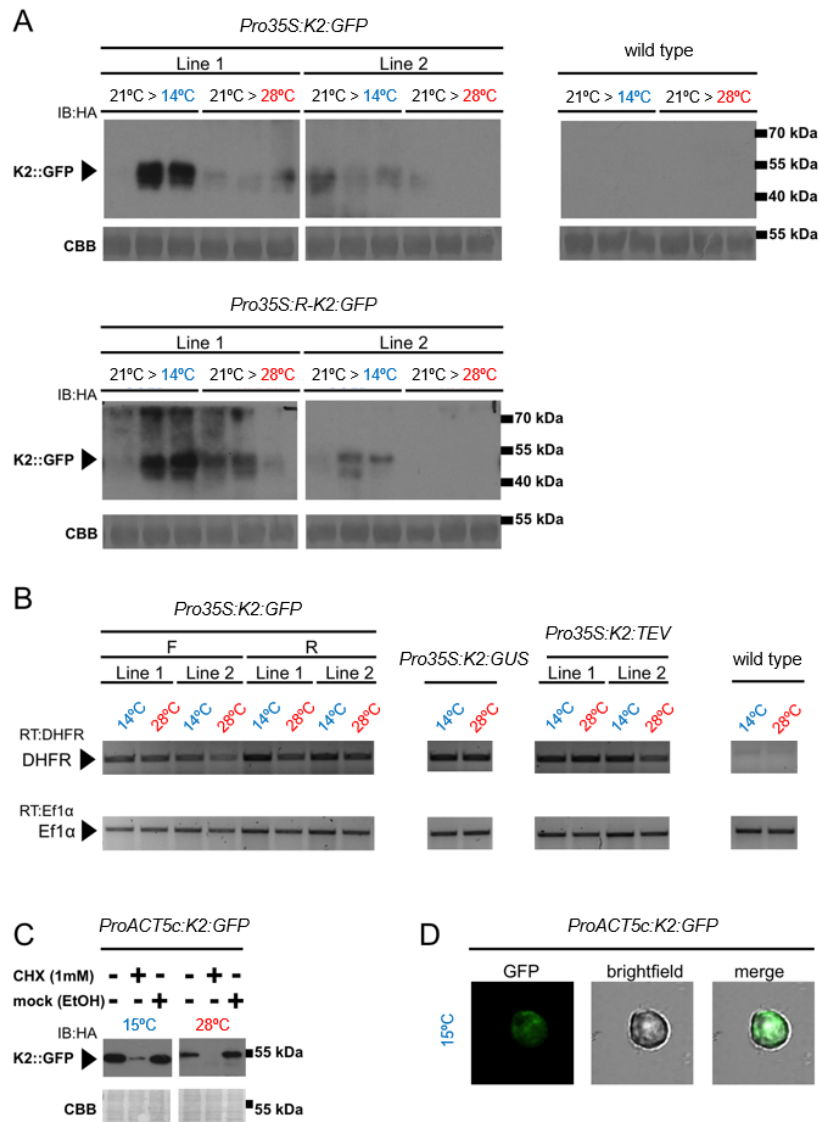
Arginine (R-K2) and Leucine (L-K2) at the N-terminal were used (*pAM-NOP-ProUBQ:K2-PAT/R-K2:PAT/L-K2:PAT* and *pAM-NOP-ProCDKA;1:K2-PAT/R-K2:PAT/L-K2:PAT*). Selection of transgenic lines took place again at 14°C. Transgenic lines for *pAm-NOP-pUBQ:K2-PAT/R-K2:PAT* as well as for *pAM NOP pCDKA;1:L-K2-PAT* could be recovered. These lines were screened again for a temperature responsive BASTA resistance phenotype as described previously. However, no responsive line could be isolated again (for a representative selection fig. 3.3D).

To elucidate whether the temperature insensitive resistance phenotype might still correlate with a responsive phenotype on protein level, meaning less of the K2:PAT fusion protein at 28 than at 14°C, selected lines were analyzed via Western Blot. Samples were harvested from three Pro35S lines (fig. 3.3B) grown at 14°C and 28°C. Multiple specific signals were identified, with the highest molecular weight one under cold growth temperatures correlating with the expected, *in silico* determined, molecular weight of 46.9 kDa for the complete K2:PAT protein and with the other ones representing possible cleavage products. Interestingly, this highest band reliably disappeared under warm growth conditions indicating temperature dependent processing of the fusion protein (fig. 3.3C). No significant difference in overall levels of band intensities could be observed between the two growth conditions correlating with the non-responsive phenotype.

### 3.1.4 Addressing different N-recognins of the plant N-end rule through Phe- and Arg-starting K2:GFP constructs

Green fluorescent protein (GFP), and its various versions, are long established fluorophores, used extensively in cell biology (reviewed in Remington 2011). *Pro35S:K2:GFP* and *Pro35S:R-K2:GFP* expressing lines were screened for presence of the fusion protein at 14°C and 28°C through Western Blot analysis. Two lines expressing K2:GFP as well as two lines expressing R-K2:GFP were isolated that reliably showed the desired phenotype on protein level (data not shown). These lines were subjected to a temperature shift experiment (fig. 3.4A). All lines showed efficient stabilization or degradation of the fusion protein depending on the temperature shift. It is worth noting, that the R-K2:GFP expressing plants performed as well as the K2:GFP expressing ones indicating that the degron is also able to efficiently target R-K2:GFP for degradation through PRT6. Functionality of

the K2:GFP fusion protein was verified using a confocal laser scanning microscope. GFP fluorescence was clearly identified in the root cells of transgenic K2:GFP expressing plants. The identity of the K2:GFP signal was confirmed through a lambda scan (fig. S 5.5).



### 3.1.5 The K2 cassette mediates efficient protein degradation in *D.melanogaster* embryonic Kc cells

To test whether the degron would also be functional in *D. melanogaster*, K2:GFP was expressed in embryonic Kc cells. *D. melanogaster*, as an example for a poikilothermic animal, was chosen to demonstrate the comprehensive applicability of the degron in different organisms. 24 h post transfection cells were treated with either 1 mM of the protein translation inhibitor cycloheximide (CHX) or a mock treatment and shifted for four hours to 15°C or 28°C respectively. The K2:GFP fusion protein was destabilized upon temperature shift. The effect became even more eminent when translation was disrupted through the



**Figure 3.4 – K2:GFP with different N-termini addresses both known N-recognins in plants as well as the N-end rule in *D.melanogaster*. The phenotype is a true protein one and not the result of transcriptional regulation.** (A) K2:GFP addressing the Phe-as well as the Arg-branch of the N-end rule in *A.thaliana*. Plants were grown at 21°C temperature and shifted to 14°C or 28°C respectively. Samples were taken after 0, 6, and 24 h. (B) Semi-quantitative reverse transcriptase analysis shows that the degron phenotype happens on the level of stabilization rather than being a result of transcriptional regulation. (C) The degron is able to mediate degradation/stabilization in embryonic *D.melanogaster* Kc cells. (D) Functionality of the K2:GFP fusion protein in Kc cells is monitored by fluorescence microscopy.

inhibitor (fig. 3.4C). K2:GFP is also functional as indicated by microscopic analysis (fig. 3.4D).

### 3.1.6 Transcript analysis confirms regulation of degron levels on protein level

To ensure that the phenotypes of the different responsive degron lines is dependent on stabilization of the protein, rather than transcriptional regulation, cDNA from the K2:GFP, K2:GUS, and K2:TEV expressing lines was analyzed using a DHFR (= K2) specific primer set. Results clearly showed that the degron transcripts are not responsive to temperature, indicating a real and temperature dependent protein stabilization phenotype (fig. 3.4B).

### 3.1.7 Cytotoxic barnase expressed in *Arabidopsis* trichomes as a degron fusion is able to stir organ formation

In his master thesis, Stefan Mielke isolated a transgenic *A. thaliana* line expressing a K2:BAR fusion under the control of the trichome specific TRYPTICHON promoter (*ProTRY*) (Mielke, 2014). The bacterial ribonucleas (BAR) is an enzyme possessing RNase activity, synthesized and secreted by the soil bacterium *Bacillus amyloliquefaciens* (Buckle & Fersht, 1994). It is potentially cytotoxic in all eukaryotic and prokaryotic cells. The *ProTRY:K2:BAR* expressing line showed a temperature dependent presence of trichomes. When grown at 14°C trichomes were absent, most probably due to the cytotoxic effects of the stabilized K2:BAR fusion protein. When grown at 28°C plants appeared wild type-like (Mielke, 2014).

This line was now further characterized using different microscopic approaches to further define the K2:BAR fusion protein as a conditional cell-death module for higher plants. *A. thaliana* trichomes, due to their unicellular organization and good characterization (reviewed e.g. in Schwab *et al.* 2000, Hülkamp 2004), represent a versatile model system for the expression of (toxic) proteins and their effects also due to the ease of trichome observation using well established microscopic methods.

**Trichome formation in the *ProTRY:K2:BAR* expressing line is a dynamic process controlled by temperature:** Plants were grown at 14°C and 28°C respectively.

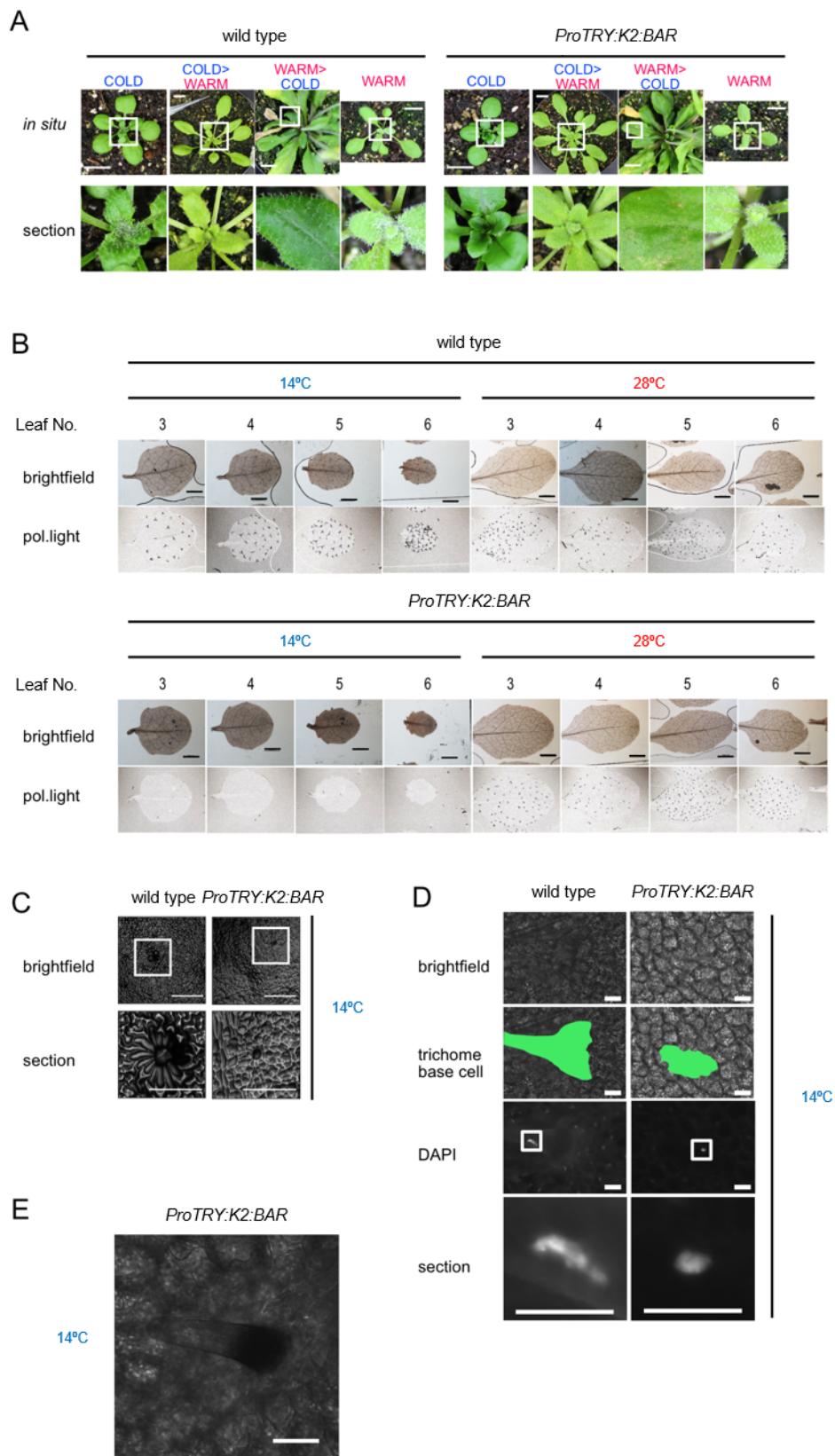


**Figure 3.5 – A K2:BAR fusion protein expressed in *A.thaliana* trichomes controls organ formation in a temperature dependent manner.** (A) Abrogation of trichomes can be stirred through conditional stability of the K2:BAR fusion protein, using a temperature stimulus. Plants were grown at either 14°C or 28°C. Cold grown plants were shifted to warm temperatures for 9 d before being shifted back to cold temperatures. Trichome formation on newly formed leafs was monitored (white bar = 1 cm). (B) Polarized light analysis of cleared true leafs three to six. The plants expressing *ProTRY:K2:BAR* show completely glabrous trichomes (black bar = 500 µm). Trichomes appear as black. (C) Agar imprints of the leaf surface of K2:BAR expressing plants. K2:BAR expressing plants were compared with wild type plants. Plants were grown at 14°C. The trichome base of the transgenic plants has collapsed and is severely altered compared to wildtype plants. (D) DAPI staining of K2:BAR expressing plants grown at cold temperatures show a trichome phenotype similar to the *gl2* phenotype. Trichome cells remain in a state of growth arrest as indicated by the still present nuclei. (E) Older leafs of *ProTRY:K2:BAR* expressing plants show occasional induction of trichomes similar to the previously described *gl2* phenotype.

The previously reported phenotype (Mielke, 2014) was completely reproducible. Plants expressing *ProTRY:K2:BAR* reliably abolished trichomes when grown at 14°C (fig. 3.5A). To test whether the trichome phenotype is dynamically responsive to temperature switches, plants grown at 14°C were switched to 28°C for nine days. New leaves clearly exhibited a normal, wild type like, trichome patterning. After a switch back to cold growth temperatures the K2:BAR fusion protein was stabilized and new leaves appeared glabrous<sup>5</sup> again. This clearly indicates that the K2:BAR fusion protein reacts dynamically to changing temperatures (fig. 3.5A).

To analyze trichome spacing and number in more detail, I used a polarized light microscopy approach to visualize trichomes. Leafs of plants grown at either 14°C or 28°C were harvested and visualized. The pictures clearly confirmed the macroscopic data shown in figure 3.5A. Cold grown plants of *ProTRY:K2:BAR* expressing plants appear indeed glabrous (fig. 3.5B)

**The K2:BAR fusion protein significantly alters the structure of the trichome base:** To gain further insight into the process of trichome abolition in K2:BAR-expressing plants, agar imprints of the surface were obtained. The imprints clearly showed significant alterations in the overall structure of the trichome base. Namely, the cells around the central trichome-forming cells did not form. However, the central, barnase expressing, cell is still present in the tissue indicating a growth arrest rather than a complete ablation of the cell (fig. 3.5C).

**DAPI staining of nuclei reveals a cell growth arrest similar to the *gl2* mutant allele phenotype:** To finally distinguish whether the trichome forming cells of the K2:BAR expressing plants grown at cold temperatures have collapsed or are only in a state of growth arrest I performed microscopy analysis of DAPI stained leafs (fig. 3.5D). If the cells are indeed dead they should no longer contain DNA. The analysis of stained leafs revealed that the glabrous leaf phenotype elicited through K2:BAR strongly resembles the

---

<sup>5</sup>glabrous = smooth, without hairs

phenotype of the GLABRA2 knockout allele (*gl2*) (Rerie *et al.* 1994, reviewed in Hül-skamp 2004). Similar to this phenotype, the cells arrested in a state of enlargement prior to forming the actual trichome indicating that the initiation and differentiation process was interrupted. Comparable to the *gl2* phenotype, also some cells, even though very rarely, were able to start trichome initiation, something that was also reported for the *gl2* phenotype. However, this only happened solemnly and predominantly on older leaves (fig. 3.5D).

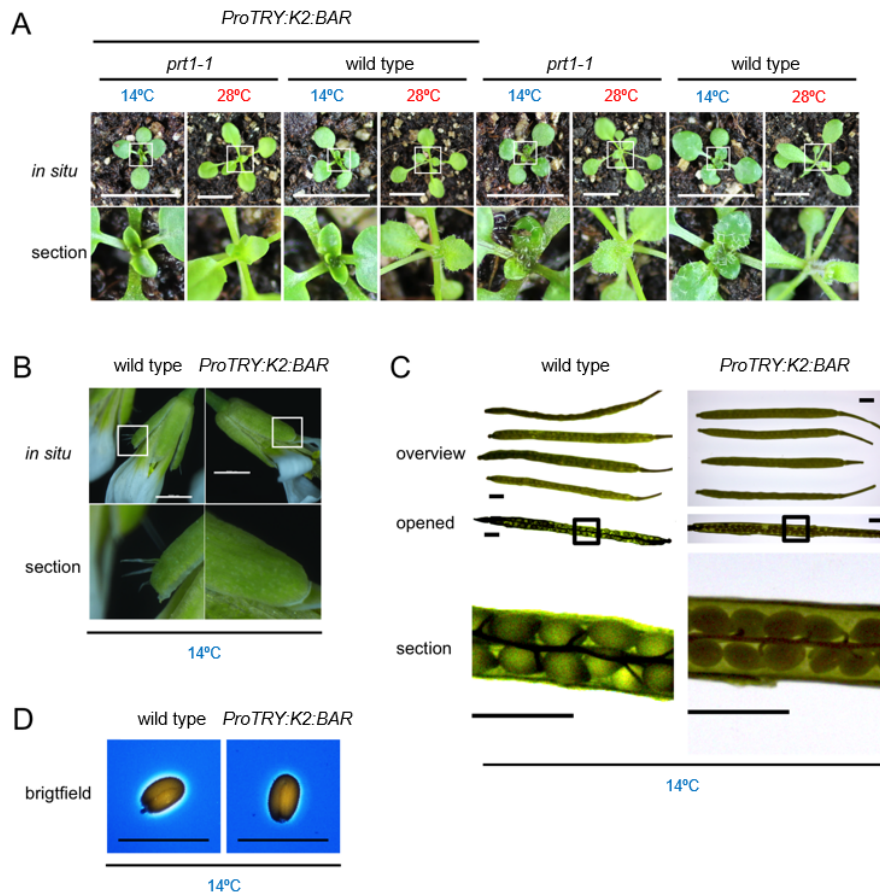


**Figure 3.6 – The K2:BAR fusion protein is degraded by the E3 ubiquitin ligase PRT1 and the phenotype is organ specific.** (A) Crossing of *ProTRY:K2:BAR* into the *prt1-1* mutant background results in a temperature independent stabilization of the fusion protein (white bar = 1 cm). (B) K2:BAR is also active in flowers (white bar = 500 μm). (C) K2:BAR does not lead to increased seed abrogation under cold temperatures. Late stage siliques of wild type and *ProTRY:K2:BAR* expressing plants were opened and analyzed using a stereo microscope. There is no obvious difference between the control and the transgenic plants (black bar = 1 mm). (D) Transgenic and wild type seeds show no difference in mucilage deposition as made visible by a white aureole around seeds after submergence in diluted ink (black bar = 500 μm).

---

**Genetic evidence suggests degradation of K2:BAR by the E3 ligase PRT1:** To test whether the degron is indeed predominantly degraded by the E3 ligase PRT1 and to assess whether barnase activity itself might also be influenced by the changing temperature, I crossed the K2:BAR-expressing line into the PRT1 mutant background (*prt1-1*, Bachmair *et al.* 1993, Potuschak *et al.* 1998). Crossing into *prt1-1* resulted in a temperature independent stabilization of the K2:BAR fusion protein, thus indicating that indeed the degradation by PRT1, and not potential temperature sensitivity of barnase, led to the temperature dependent toxicity phenotype (fig. 3.6A)

**ProTRY is also active in flowers but not in seeds:** Transcript data of the TRYP-TICHON protein obtained from the eFP browser (Winter *et al.* , 2007) (see also figure 5.6) shows that ProTRY is almost ubiquitously active throughout the whole plant with expression maximal in trichomes, early flower stages as well as early seed / silique developmental stages. This led to the question whether the toxic protein K2:BAR would also induce cell death in other tissues than in the leaf/trichomes. The temperature dependent expression of the K2:BAR fusion protein led to abolishment of trichomes on the flowers (fig. 3.6B). Since the expression data also hints towards expression in early seedlings and siliques the question arose whether K2:BAR expressing plants would be sterile under cold growth conditions. This was not the case.

To determine whether expression and activity of the K2:BAR fusion protein at 14°C would result in in abolished seeds, late stage siliques were opened and seeds analyzed using a standard stereo microscope. The K2:BAR expressing line did not show more abolished seeds than the Col-0 wildtype plants grown at the same temperature (fig. 3.6C). Additionally, the seeds showed an indistinguishable mucilage deposition on the seed coat when compared to wild type seeds. Disturbed mucilage deposition in the seed coat is a reported phenotype of *gl2* (Rerie *et al.* , 1994), indicating that the similarity to *gl2* does not extend to the seed but remains exclusive for trichomes (fig. 3.6D).

## 3.2 Using a peptide array to determine N-terminal sequences with improved binding to PRT1

The proposed mode of action of the original heat-inducible degron in yeast suggested an, at least partial, unfolding of the DHFR moiety at the restrictive temperature, allowing the conditional ubiquitination of the fusion protein (Dohmen *et al.* , 1994). This would suggest that PRT1 can always recognize the N-terminal of the degron cassette and that only the ubiquitination and the subsequent degradation, but not the recognition, is conditional. Following this idea, I decided to attempt to improve recognition of the degron cassette by PRT1. This optimized recognition should lead to a more efficient degradation of the degron-fusion protein under restrictive growth temperatures. We choose Synthetic Peptide On membrane support Technique (SPOT) assays using 17mere peptide. The SPOT technique is a well established technique to map protein-protein interaction and has already been applied in the N-end rule field for the determination of binding affinities of different peptides to different N-recognins (Hwang *et al.* , 2010a, Kim *et al.* , 2014, Klecker & Dissmeyer, 2016, Dong *et al.* , 2017).

### 3.2.1 SPOT membrane design

To identify sequences, showing an improved binding affinity to PRT1, an intensive literature search was performed. Different sequences were identified that were discussed, or have been shown previously, to be sequences leading to degradation via the N-end rule pathway of protein degradation. Partially, these sequences have been used to generate probes mapping the N-end rule. Some of these sequences were used in this work as scaffolds to map and optimize binding efficiency. The identity of the sequence, e.g eK or nsP4, refers to amino acids two to 16 as, amino acid 17 was always a Glycine and the amino acid at position one, usually a Phenylalanine or a control amino acid, might not have been the same in the original publication of the sequence.

- **eK** - The eK-sequence is a derivate of the *E. coli* LacZ-gene and has been used to identify and map the N-end rule in yeast with a wide variety of N-termini (Bachmair *et al.* , 1986, Bachmair & Varshavsky, 1989). The 17-mer peptide sequence (in 1-letter code) used is: **F-HGSGAWLLPVSLVKR-G**
- **nsP4** - The nsP4 sequence is a derivate of the Sindbis Virus RNA polymerase and has been used in stability assays with a type 1 (R) and type 2 (Y) primary destabilizing residue (de Groot *et al.* , 1991). The 17-mer peptide sequence (in 1-letter code) used is: **F-IFSTDTGPGHLQKKS-G**
- **W-GUS** - The N-terminal extension sequence of a GUS reporter probe previously described (Worley *et al.* , 1998). The 17-mer peptide sequence (in 1-letter code) used

is: **F-QIPGYGQSLMLRPVE-G**

- **W-LUC** - The N-terminal extension sequence of a Luciferase (LUC) reporter probe previously described (Worley *et al.* , 1998). This reporter has also been used to map the plant N-end rule with various N-termini (Graciet *et al.* , 2010). The 17-mer peptide sequence (in 1-letter code) used is: **F-QICRSTDLHSGTVGK-G**

Unfortunately, no crystal structure is available, neither for PRT1 nor for any other eukaryotic E3, binding type 2 primary destabilizing residues. Only a structure of the *E. coli* protein ClpS, which is the type 2 recognition particle<sup>6</sup> of the bacterial N-end rule, has been published and described in its binding to the N-terminal of peptide sequences (Guo *et al.* , 2002a,b, Erbse *et al.* , 2006, Román-Hernández *et al.* , 2009, Dougan *et al.* , 2012, Stein *et al.* , 2016). I was reasoning that the binding of the same type-2 N-degrons might be reflected in a similar overall domain architecture in ClpS and PRT1, especially since Ubr1, the E3 of the Arg/N-end rule in yeast carries a ClpS-homology domain for recognition of type 2 destabilizing residue. While there is only very limited sequence homology between Ubr1 and PRT1, they share functional homology (reviewed in Tasaki *et al.* 2012). Additionally, a SPOT assay approach has already been applied to map binding efficiencies of different peptides to ClpS (Erbse *et al.* , 2006).

It has been shown that ClpS binds better to peptides with a positive net charge (Erbse *et al.* , 2006), a fact that is further supported through observation of the crystal structures which shows that the binding pocket for the destabilizing residue is surrounded by negatively charged amino acid (fig. S 5.7, Román-Hernández *et al.* 2009).

Also, it has been demonstrated previously that the presence and position of Lysine residues within the N-terminal sequence have an influence on stability, when addressing the Arg/Nend rule in yeast with probes exhibiting type 1 or type 2 destabilizing residues at their N-terminal (Suzuki & Varshavsky, 1999). Therefore, one question to also be addressed in the SPOT assays was, whether the influence of Lysine residues on stability acts on the level of recognition or the subsequent degradation, since Lysine residues are prime targets for ubiquitination crucial for degradation.

**Membrane 1:** Membrane 1 was synthesized with two different sets of positive controls to ensure the suitability of the SPOT assay for K2-binding by PRT1. A set of six wild type K2 sequences was arranged on the first column of the membrane to serve as controls for inter-and intra-experimental normalization. The last column of the membrane consisted of six spots of a sequence derived from the protein ETHYLENE-INSENSITIVE PROTEIN 2 (EIN2), that has been shown to be bound strongly by PRT1 in a SPOT assay (M. Klecker, personal communication). This sequence served as an initial positive control, since it was unknown how the K2 sequence would behave in this type of assay. The membrane was

<sup>6</sup>Particle, because ClpS does not have any modifying activity but only recruits substrates to the protease ClpA.

designed with two things in mind: One the one hand different sequences already used in the N-end rule field were to be tested and compared to the K2 sequence in regard to their binding efficiency. On the other hand different new sequences were modeled following analysis of hydrophobicity and electric surface potential of the type 2 primary destabilizing residue binding pocket of ClpS (fig. S 5.7). Below a full rationale of the chosen sequences is given. An overview over membrane arrangement, as well as a full list of all peptide sequences can be found in the appendix (tab. 5.6 and fig. S 5.8).

- **F-K2 WT control** - The standard amino acids of the K2 degron cassette starting with Phenylalanine. Six spots were synthesized for inter-and intra-experimental normalization.
- **F-H + Glycine stretch** - Previous understanding about the structure of N-Degrone always assumed a high mobility of the N-terminal to be important. This was to be tested using a very mobile Glycine stretch.
- **F + small amino acids** - Using smaller amino acids while trying at the same time to respect charge and hydrophobicity of the original sequence for possible increased mobility.
- **F-R + Glycine stretch** - Same as the previous glycine stretch, only with Arginine at position two.
- **F + G-GUS** - The amino acid sequence used at the N-terminal of a reporter construct leading to the discovery of PRT6 (Garzón *et al.*, 2007).
- **F + nsP4** - The nsP4 sequence as described above with different variations.
- **F + non-aromatic hydrophobic aa + K2** - A test whether a hydrophobic patch close to the N-terminal can alter binding efficiency.
- **F + non-aromatic hydrophobic aa + negative stretch + Glycine** - Same as before with addition of a negative stretch and a mobile Glycine part.
- **F-H + Glycine-Serine walk** - To test whether a combination of mobile (Glycine) and polar (Serine) residues is beneficial.
- **F + W-GUS** - As described above with and without negative charge.
- **F-I + K2** - K2 sequence with Isoleucine at position 2.
- **F + W-LUC** - As described above with and without negative charge and Lysines.
- **K2 with different type 2 destabilizing residues at position one** - To test whether phenylalanine does indeed provide the best binding efficiency.



- 
- **K2 Alanine walk** - Every position replaced once by alanine to determine the influence of every amino acid on binding.
  - **F + eK** - The eK sequence as described above, also with alterations such as e.g. with or without Lysines.
  - **F + EIN2** - The positive control previously identified by M. Klecker (personal communication).

**Membrane 2:** Membrane 2 was designed to reproduce some of the results of membrane 1 as well as to gain more insight into the binding behavior of 8xHis:MBP:PRT1 to some of the sequences. Also, it was attempted to optimize some of the well binding sequences through creation of hybrids.

Below a full rationale of the chosen sequences is given. For arrangement on the membrane see figure S 5.9. A full list of all peptide sequences can be found in the appendix (tab. 5.7).

- **F-K2 WT control** - The standard amino acids of the K2 degron cassette starting with phenylalanine. Six spots were spread over the membrane for inter-and intra-experimental normalization.
- **F + G-GUS** - Same as described above.
- **M/G-2 at position 1 or 2** - ELUCidating the influence of the amino acids Glycine and Methionine at position one and two of the peptide sequence because of their frequent use as negative controls.
- **F + nsP4 variants** - Different versions of the previously described nsP4 sequence.
- **F + W-GUS Alanine walk** - An Alanine walk through the Worley sequence to determine influences of every amino acid position on PRT1 binding.
- **F-K2 Aspartate walk** - An Aspartate walk through the K2 sequence to determine possible positive influence of negative charges at certain positions in the peptide sequence.
- **F + ek** - Different versions of the previously described eK sequence.
- **F + K2/W-GUS hybrids** - Mixtures of the well binding sequences Worley-GUS and K2.
- **F + W-LUC** - Different versions of the well binding Worley-LUC sequence.

### 3.2.2 SPOT assay - detection, optimization, and data analysis

**Assay and data analysis:** Membranes were de-protected once and used for the SPOT assays. Following the assay, membranes were regenerated and stored or reused at a later timepoint. It is important to emphasize that no decrease or change in binding affinity between used or fresh membranes could be observed. Also, since one type of membrane set always originated from one synthesis event they are treated as technical replicates and values were averaged.

**Membrane 1 - blotting and antibody based detection:** A first set of membranes was incubated with the 8xHis:MBP:PRT1 fusion protein as well as with free 8xHis:MBP as a negative control. A starting concentration of 50 nM of recombinant protein used on SPOT membranes has been previously described (Klecker & Dissmeyer, 2016). To account for the fact that a membrane was synthesized, which almost exclusively consisted of sequences binding to PRT1, a higher concentration of 200 nM was chosen to prevent protein depletion. 8xHis:MBP was used in the same concentration as a negative control on an identical membrane. A strong signal was detected when using 8xHis:MBP:PRT1, while 8xHis:MBP did not show any unspecific binding (fig. 3.7A). Additionally, binding efficiency and capacity of the membrane was so high that the recombinant protein was even detectable using CBB staining (fig. 3.7A).

**Membrane 1 - optimization of protein concentration for blotting:** Because of the strong binding of 8xHis:MBP:PRT1 to the SPOT membrane the protein concentration for the assay was lowered to 50 nM as previously described (Klecker & Dissmeyer, 2016). This significantly improved the quality of the assay (fig. 3.7B). Also some of the weaker spots (e.g. C2/3) disappeared compared to the first assay indicating that the lower protein concentration used in this assay led to more stringent binding. The 8xHis:MBP:PRT1 fusion protein reliably showed increased binding to some sequences compared to the K2 wild type control. Especially the spots A7 (nsP4-K), C6 (W-GUS), D2 (W-LUC-K), and E8 (K2 R8A) reliably appeared in five experiments.

**Membrane 1 - quantification using ImmunoBlue:** To quantify the efficiency in binding of 8xHis:MBP:PRT1 to different peptide sequences and to strengthen and validate the results obtained by antibody/ECL-based detection, an optimized approach was introduced, where the detection of the bound protein was still based on an antibody, but the chemoluminescent ECL detection was replaced by the fluorogenic substrate ImmunoBlue enabling quantification. Detection with ImmunoBlue often led to "unclean" results. The spots seemed to diffuse and substrate to be washed away from the spots before forming the fluorogenic precipitate. Nevertheless, these assays led to the first quantifiable results (fig. 3.7C).

A total of three membranes was quantified (fig. S 5.15). The results are consistent with data obtained from the ECL experiments. For example the well binding spots A7 (No.

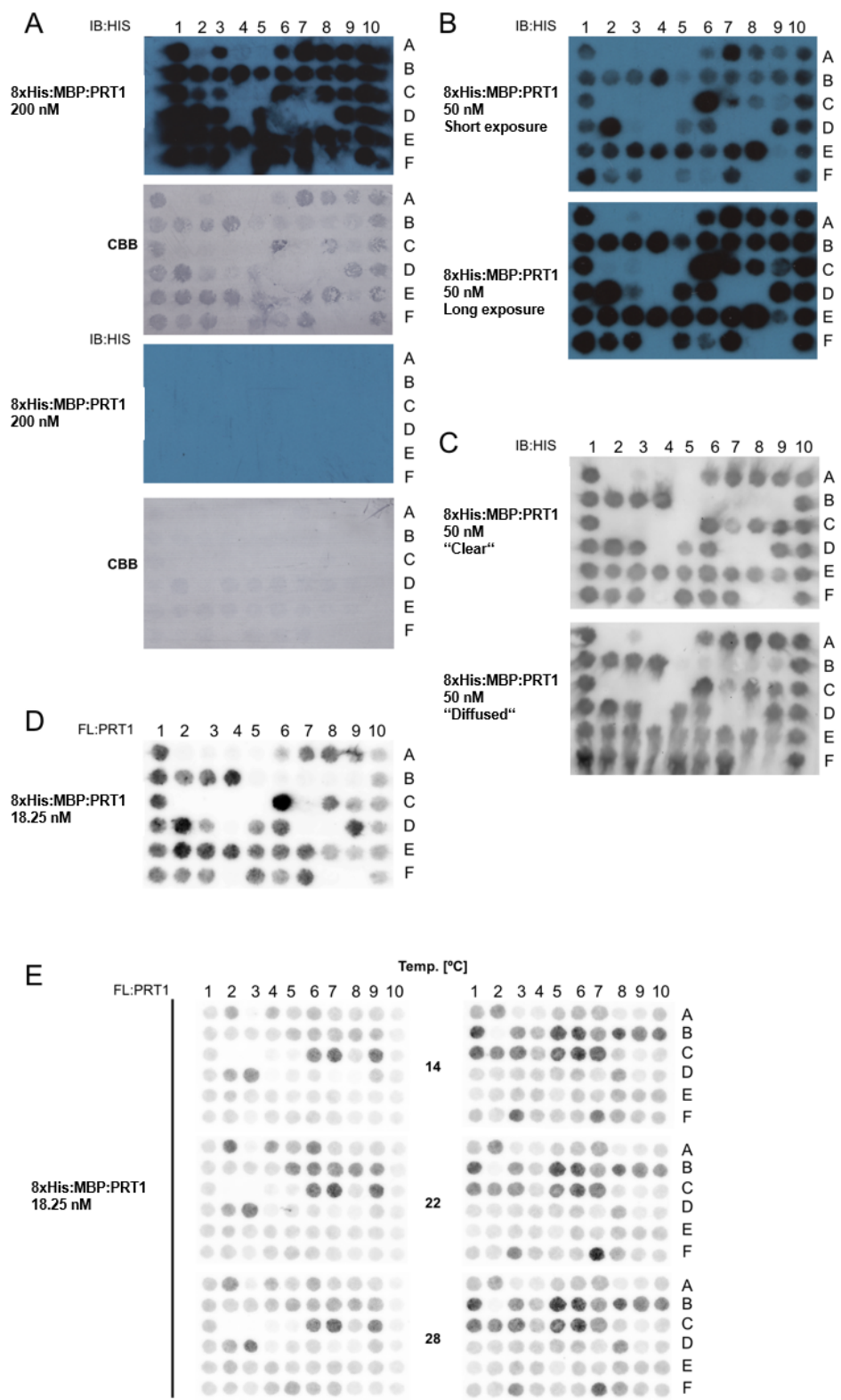


**Figure 3.7 – Optimizing synthetic peptide binding assays from a purely qualitative to a fully streamlined quantitative experiment identifying optimized N-terminal sequences for PRT1 binding.** (A) Incubation of membrane 1 with 200 nM of 8xHis:MBP:PRT1 or 8xHis:MBP results in strong binding in a blotting/antibody-based detection process. 8xHis:MBP does not bind unspecifically to the membrane. (B) Decrease of protein concentration to 50 nM significantly increases experimental quality. (C) Replacing standard ECL substrate with the fluorescent substrate ImmunoBlue allows for quantification but exhibits some problems with substrate dispersal. (D) Direct labeling of PRT1 allows for further reduction of used protein concentration and further increases the experimental quality while resulting in a fully quantifiable signal in a blot based assay (detection strength = 800V). (E) Omission of blotting and direct on-membrane detection further streamlines the experiment. Representative membranes for membrane 1 (left panel) and 2 (right panel) incubated at the indicated temperatures are shown (detection strength = 650V).

6), C6 (No. 21), D2 (No. 25), and E8 (No. 39) still appears. However, the differences in binding did not seem as striking as seen in the ECL experiments (fig. 3.7B and fig. S 5.15).

**Membrane 1 - direct fluorescent labeling PRT1:** To avoid the shortcomings of the ImmunoBlue detection and to streamline the assay procedure further, 8xHis:MBP:PRT1 was labeled using a fluorogenic dye. Additionally, the protein concentration used for the assay was lowered again to a final concentration of 18.25 nM, to avoid unspecific binding and to reduce signal diffusion (fig. 3.7D).

For quantification and comparison of the different experiments all values were normalized to the average of six K2 wild type sequences on each membrane. Also, the value for the peptide starting with Alanine (31/D8) was always subtracted as a blank, since 8xHis:MBP:PRT1 should not interact with this spot and therefore, binding by PRT1 can be considered unspecific, or at least N-terminal independent. Figure S 5.10 shows the normalized binding values for all tested sequences. Analysis of the obtained data can be found below together with data obtained from direct detection of the fluorescent protein on the membrane.

**Membrane 1 - direct *on membrane* detection and binding at different temperatures:** To further simplify and streamline the assay and to improve the quality of the obtained results, a next level of optimization was reached by directly detecting the labeled fusion protein on the membrane. This eliminated the blotting procedure and boosted signal intensities by about 20%, when compared to the blot-based assay. Now, also the binding efficiency of 8xHis:MBP:PRT1 at different temperatures was assessed. 14°C, 22°C, and 28°C were chosen respectively.

The higher and lower temperatures represent the maximum temperature range of the degron when used *in vivo*. The intermediate temperature would help to elucidate the binding behavior at room temperature, as well as making it comparable to the previous assays. This follows the idea that N-terminal mobility, as a function of the temperature, might influence the recognition and therefore destabilization through action of PRT1.

This mobility might be based only on basic underlining principles such as the Brownian motion<sup>7</sup> or could be directly connected to the primary sequence of the peptide chain adopting different conformations or states of increased or decreased mobility dependent on temperature, something that has been previously described however for longer sequences (e.g. see review in Mackay & Chilkoti 2008) .

Figure 3.7E (left column) shows representative images for binding of 8xHis:MBP:PRT1 to membrane 1 at each of the indicated temperatures. Figure 5.10 shows the comparative and quantified binding efficiency of 8xHis:MBP:PRT1 to membrane 1 at different temperatures. Overall it can be seen that the signal intensity of many sequences is boosted. Also a large set of sequences previously found not to bind 8xHis:MBP:PRT1 now shows very high binding efficiency (compare signal intensities of peptide sequences 12-16 in figure 5.10 for blot-based and direct detection) indicating a qualitative and quantitative difference between the two experimental approaches.

### 3.2.3 *In depth* analysis of binding of PRT1 to membrane 1 comparing direct and blot-based detection as well as different temperatures

**Sequences known to follow the N-end rule also bind to PRT1 *in vitro*:** These sequences have all been used to address, or have at least been discussed to be recognized by, potential N-recognins (fig. 3.8A).

The binding efficiency varied significantly between the different peptide sequences (fig. 3.8A). The G-GUS sequence, used in a reporter probe to identify the N-recognin PRT6 (Garzón *et al.* , 2007), was found to not confer binding in the blot-based assay. However, this sequence actually exhibited strong binding in the direct detection approach with even an increased binding at ambient temperature compared to 14°C and 28°C respectively (fig. 3.8 lane 1). Also the nsP4 sequence (de Groot *et al.* , 1991), which, in the blot-based assay, showed about 40% binding efficiency when compared to the original K2 sequence, exhibited even stronger binding than the G-GUS sequence in the direct detection assay again with a peak at ambient temperature (fig. 3.8A lane 2). Elimination of Lysines (K) in this sequence through replacement with Glycines (G) resulted in increased signal intensity in the blot-based assay but showed the opposite effect, namely decreased binding, in the direct detection approach (fig. 3.8A lane 3).

The W-GUS sequence (Worley *et al.* , 1998) shows very high binding efficiencies in both approaches (direct and blot-based). It also exhibits a lower influence of the assay temperature on binding of the E3 ligase (fig. 3.8A lane 4). Still, elimination of the negatively charged Glutamic acid (E) at position 16 of the peptide sequence leads to a complete loss of signal in the blot-based assay. Contrarily, in the direct detection assay the signal is boosted by more than 100%, now also showing even more improved binding at ambient

<sup>7</sup>Brownian motion describes the random motion of a particle in a gas or liquid through random collisions with the molecules of that liquid or gas.

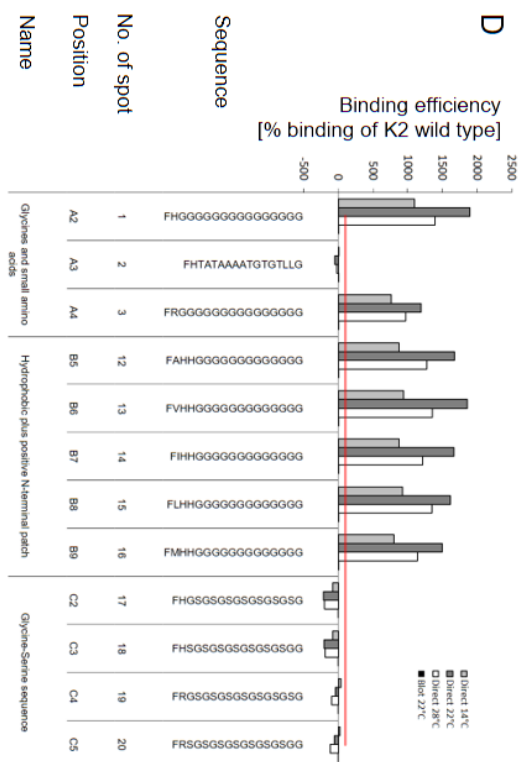
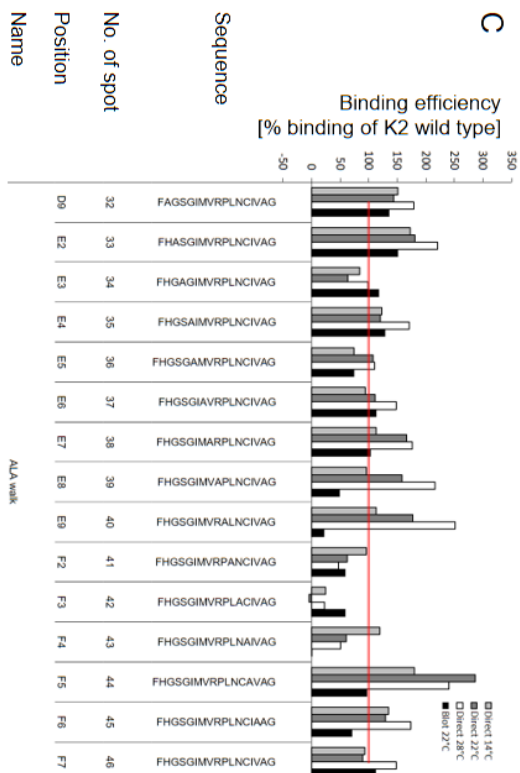
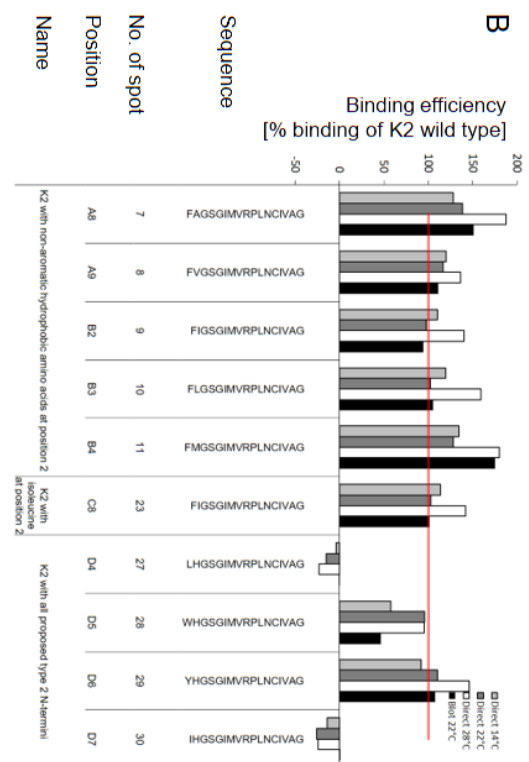
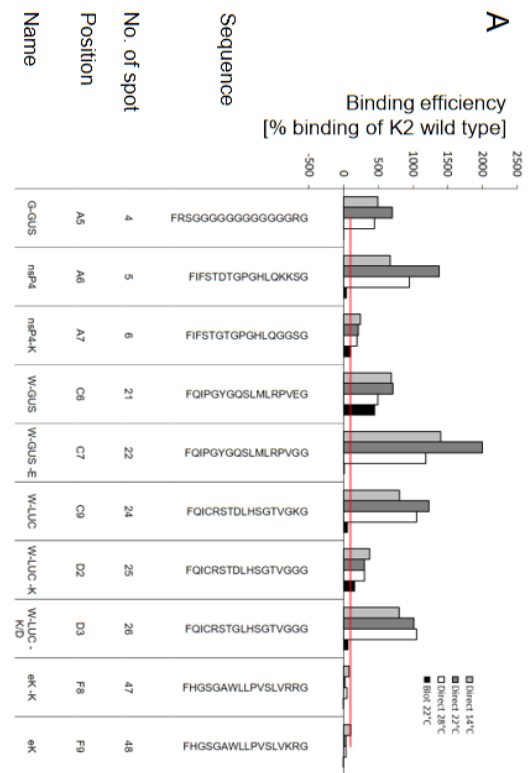


**Figure 3.8 – In-depth analysis of different experimental setups synthesized on membrane one.** (A) Binding efficiency of 8xHis:MBP:PRT1 to known N-degron sequences. Different sequences known to follow the N-end rule were assessed. A huge difference between the direct and the blot-based detection is visible. All sequences get bound by 8xHis:MBP:PRT1 at least in the direct detection assay. However some sequences show significantly higher binding efficiencies. The red line marks 100% binding of the K2 WT sequence. (B) Binding efficiency of 8xHis:MBP:PRT1 to variations of the K2 WT sequence. Different variations of the K2 WT sequence were tested. The first six lanes show binding efficiencies after replacing the histidine at position two with different non-aromatic hydrophobic amino acids which leads to an overall relatively low change in binding efficiency but results in throughout higher binding of 8xHis:MBP:PRT1 to set sequences when incubated at 28°C. Spots number 9 and 23 (lane 3 and 6) are identical but were on different places on the membrane. Lanes seven to ten show that elimination of the aromatic ring at the N-terminal by replacing the original Phenylalanine (F) with either Leucine (L) or Isoleucine (I) leads to abolished binding. Only the aromatic amino acids Tryptophane (W) and Tyrosine (Y) are able to maintain binding. The red line marks 100% binding of the K2 wild type sequence. (C) Alanine walk through the K2 wild type sequence. All amino acids from position 1-16 were replaced with alanine. Position 1 is not depicted since it served as negative control for reduction of background binding therefore setting its binding value to zero. Overall the results for the blot-based detection follow the ones obtained using the direct detection approach except for position seven to ten (lane 6-9) were signal intensities decrease in the blot-based assay but increase when using direct detection. Overall one can clearly see that especially modifications in the last third of the sequence (position 11-13) lead to a decreased binding. (D) Binding of 8xHis:MBP:PRT1 to long mobile Glycine (G) stretches is very efficient and disrupted through introductions of Serines at alternating positions. Binding of 8xHis:MBP:PRT1 to long Glycine stretches is very efficient with a clear maximum at ambient temperatures (lanes one and three to eight). Increasing hydrophobicity through replacing any other Glycine with Serine (S) abolishes binding (lanes nine to twelve). Replacing every amino acid in the K2 sequence with a smaller counterpart whilst retaining charge and hydrophobicity also abolishes binding completely.

temperatures (fig. 3.8A lane 5). So, like the nsP4 sequence described before, this sequence shows the opposite behavior in the direct detection compared to the blot-based assay.

The next sequence to be analyzed was the W-LUC sequence (Worley *et al.* , 1998). This sequence shows binding in all conditions however with a significantly increased binding in the direct detection based assay (fig. 3.8A lane 5). Elimination of Lysines (K) led to an increased binding in the blot-based, but to a decreased binding in the direct detection assay (fig. 3.8A lane 6). Additional elimination of the negatively charged Aspartic acid (D) led to the opposite effects, increasing binding in the direct detection but decreasing binding in the blot-based assay, showing a similar pattern as the previously described sequences, with opposite behavior between blot-based and direct detection approaches. This sequence however, did not show a high dependency on temperature.

The last sequence assessed was the eK sequence which has been extensively used in the N-end rule field (Bachmair *et al.* , 1986, Bachmair & Varshavsky, 1989) in various probes. It did not exhibit very high binding efficiencies when compared to the wild type K2 sequence and even did not bind at all in the blot based assay. Also, it showed a higher dependency on temperature in the direct detection assay, with an increased binding at 14°C. The elimination of a Lysine (K) through replacement by an Arginine (R) did not significantly alter the binding efficiency to 8xHis:MBP:PRT1 (lanes 9/10).

**Sequence variations of K2 slightly alter binding behavior:** Different variations of the K2 sequence were compared (fig. 3.8B). The first six lanes show that the replacement of the amino acid at position two (originally a Histidine (H)) through different non-aromatic, hydrophobic amino acids only slightly altered the binding efficiency. Also, one can see that all sequences showed a binding maximum at 28°C in the direct detection assay with the sequence possessing a Methionine (M) at position two also showing this increase in binding in the blot-based detection method.

Lanes seven to ten show that an elimination of the aromatic ring at the N-terminal of the degrons sequence disrupted binding of the E3 ligase. Only the aromatic amino acids Tryptophane (W) and Tyrosine (Y) were able to maintain binding with Tryptophane performing worse, especially at cold temperatures and in the blot-based assay (fig. 3.8B). Overall, all these sequences show much less alterations in binding efficiency between the blot-based and the direct detection approach than the known N-degron sequences discussed before (fig. 3.8A).

**An Alanine-walk through the K2 sequence reveals the importance of different positions for binding of PRT1:** In this experimental setup amino acids on position one to 16 of the K2 wild type sequence were replaced with Alanine (A) to determine the influence of every position on binding. Alanine-walks are a commonly used tool to map epitopes for the significance of the individual peptides residues (e.g. see Weiss *et al.* 2000, Morrison & Weiss 2001, Gauguin *et al.* 2008, Dey *et al.* 2007, Trott *et al.* 2014).

The reaction of the binding efficiency of 8xHis:MBP:PRT1 to the sequence with Alanine



at different positions can be subdivided into four sections. In the first part (fig. 3.8C lanes one to six), the direct detection and blot-based assay follow the same scheme. Signal intensities oscillated when modifying these positions. Overall, replacing the Glycine at position three seemed to have the biggest effect. From position eight on (lane seven) until position ten (lane eight), results from the blot-based approach and the direct detection approach behaved adversely with the signal intensities for the blot-based method decreasing and the signal intensities for the direct detection approach increasing.

Also, modification in this part, especially when replacing the Proline (P) at position ten (lane nine), rendered the whole sequence more temperature susceptible with a clear increase in binding efficiency at 28°C. Modifications between position ten to twelve altered this effect and significantly diminished binding activity regardless of the experimental approach. Modifications toward the end of the sequence again increased binding with a peak at position thirteen (lane twelve), however, without the clear peak at higher temperatures. Overall, one can see that modification in the K2 sequence altered its binding behavior especially at intermediate or higher temperatures, with binding efficiencies obtained when the assay was performed at 14°C remaining the least influenced.

**Long mobile Glycine but not Serine/Glycine stretches lead to highly increased binding of 8xHis:MBP:PRT1:** Since the G-GUS sequence contains a high number of Glycines the effect of these mobile sequences was to be elucidated further. Glycine based sequences showed the highest binding efficiencies in the direct detection assay, with binding maxima at ambient temperatures and the lowest binding potential at cold temperatures (fig. 3.8D lanes one and three to eight). Replacing every second Glycine with Serine, rendering the chain more hydrophobic, resulted in complete loss of binding sometimes even below zero also indicating the the K2 sequence starting with Alanine, that was used as a blank, still retained residual binding efficiency (see figs. 3.8D lanes 9-12 and also 3.8B). The Glycine based sequences showed the highest discrepancy between the blot-based and the direct detection approach with no binding in the former and very high binding in the latter.

Lane number two (fig. 3.8D lane two) shows a modified K2 sequence where every amino acid was replaced by a smaller one while trying to retain charges and hydrophobicity at every position. This completely abolished binding.

### 3.2.4 Membrane 2 - direct on SPOT detection and binding of PRT1 at different temperatures

The second membrane was only analyzed in regard to its binding efficiency using the direct detection approach, since it offered superior results and significantly easier handling than the blot-based approach. 8xHis:MBP:PRT1 bound efficiently to membrane 2 at different temperatures as expected (fig. 3.7E, right column and fig. S 5.12 ) Binding values obtained from membrane 2 were again normalized to six wild type K2 sequences this time spread

all around the membrane as well as blank subtraction of spot no. 2 (A3) which carries a Methionine at position one making it a non-target for PRT1.

Overall, one thing directly met the eye and that is the fact, that the overall binding strength of membrane 2 seemed to be lower than that of membrane 1 (figs. S 5.12 and S 5.10). However, analysis of the raw data showed this to be no effect due to real lower binding of the protein to membrane 2, but rather a result of the fact that the labeled PRT1 protein bound stronger to the positive controls on membrane 2 than to the ones on membrane 1 thereby attenuating the signal strength. This could be due to the different position of the six K2 wild type sequences on membrane 1 (column on on the very left) and membrane 2 (one in each corner plus two more within the membrane).

**Previously tested sequences and some of their variations confirm results of previous experiments:** The G-GUS sequence already tested on membrane 1 (fig. 3.8A) showed again efficient binding with a binding peak at room temperature (22°C, fig. 3.9A lane one).

Replacing the N-terminal amino acid of the K2 sequence with either Methionine (fig. 3.9A lane 2) or Glycine (fig. 3.9A lane 3) almost completely abolished binding, confirming and justifying approaches where these amino acids have been used as negative controls. Also, sequences carrying non-destabilizing N-terminal amino acids seemed to retain residual binding properties, indicated by the fact that after normalization some sequences showed negative binding efficiencies (fig. 3.9A lane 7).

Replacing the amino acid at position two of K2 with a Methionine (hydrophobic) or a Glutamine (polar) did not significantly alter binding behavior.

The last six lanes again showed that modifications within the Lysine containing parts of most of the tested sequences resulted in significantly reduced binding efficiency to PRT1. In a first part (fig. 3.9A lanes six to eight), behavior of the nsP4 sequence with Lysine replaced by either Glycine (lane seven) or Glutamate (lane eight) is shown. Clearly, mutation of the Lysine to either of the two residues led to an almost complete abrogation of binding. This effect was already visible on the previous membrane (fig. 3.8A) even though the same sequence (Glycine instead of Lysine) did retain binding potential on the first membrane indicating possible (synthesis) differences between the two membranes.

Lanes nine to eleven show a similar effect also on the W-LUC sequence. Replacing the C-terminal Lysine with Glycine again results in strongly diminished binding, as seen previously (fig. 3.8A). Interestingly, the introduction of another negative charge in place of the Lysine even further diminished the binding potential, indicating that not only is a Lysine at this position beneficial but also that the newly introduced Glutamate has additional negative effect (fig. 3.9A lane eleven).

**An Alanine walk through the W-GUS sequence reveals the importance of amino acids at position three, six, and 13:** As previously performed with the K2 sequence (fig. 3.8C), an Alanine walk through the W-GUS sequence was performed. Com-

pared to the original sequence (fig. 3.8C lane one), only a few sequence positions showed a strong effect on binding of the labeled PRT1 protein. Among these, replacing the Arginine at position 13 resulted in the most dramatic loss of binding. Replacing positions three (Isoleucine) and six (Tyrosine) did have similar, albeit not as dramatic, effects. Interestingly, replacing the Glutamate at position 16 with an Alanine as compared to the Glycine used on membrane 1 (fig. 3.8A) did not have a similarly high positive effect on binding of PRT1. This is unexpected, since both Alanine and Glycine are small, hydrophobic residues and eliminate a negative charge (fig. 3.9B).

**An Aspartate walk through the K2 sequence indirectly confirms the detrimental effect of Proline at position nine:** To determine the effects of an additional negative charge on the binding potential of the K2 sequence an Aspartate walk through the sequence was performed. As expected replacing almost every position with Aspartate led to decreased binding as a negative charge is clearly detrimental in this case. However, replacing the Proline at position nine (fig. 3.9C lane nine) boosted binding significantly, especially under warm and intermediate temperatures. This suggests a strong negative effect of Proline.

**Hybrids of K2 and W-GUS do not lead to a superior binding sequences:** To determine the effect of the N- and C-terminal part of the 17mer on binding to PRT1, two mixed sequences that each consisted of one half of the K2 and one half of the W-GUS sequence were tested (fig. 3.9D). If the first seven amino acids originated from the K2 sequence, binding was significantly diminished. However, if the first seven amino acids originate from the W-GUS sequence the complete sequence binds better. This indicates that the part more N-terminal towards the primary destabilizing residue has a potentially higher influence on overall binding of the peptide sequence. However, since also the K2 binding sequence is a well binding sequence, the C-terminal part still must play a role in binding.

A sequentially mixed sequence did not show significantly improved binding but surprisingly retained binding activity even with a stabilizing Glycine at the N-terminal indicating, again that in these artificial *in vitro* situations well binding backbones retain residual binding potential, even with a stabilizing N-terminal.

**Mutations within the last amino acids of the eK sequence increase binding to PRT1 strongly:** Surprisingly, the eK sequence, which is a well established and commonly used sequence in the context of N-end rule research, did not show high binding affinity to PRT1 in the first assay (fig. 3.8A). In a new approach different mutations were introduced into the eK sequence which all resulted in more or less improved affinity to PRT1 (fig. 3.9E). Introducing a Cysteine at position 13 (L13C), the same position the K2 wild type sequence carries a Cysteine, results in improved binding by PRT1. Mutating the Lysine at position 15 to an Aspartate (K15D) also improves binding, albeit not that drastically. This is surprising since it was previously believed that Lysines support N-recognition binding. The

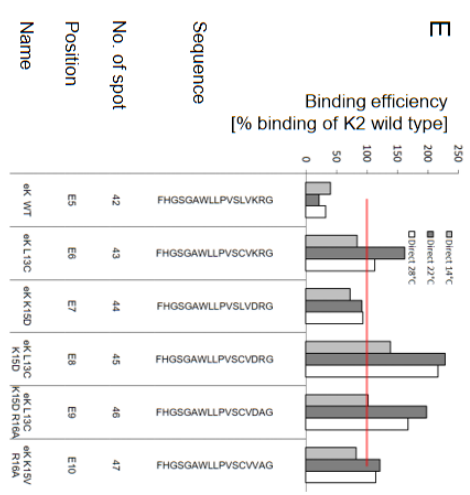
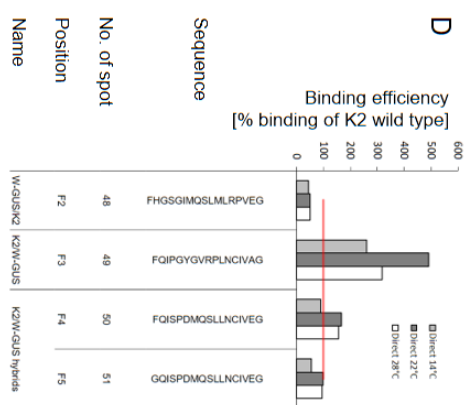
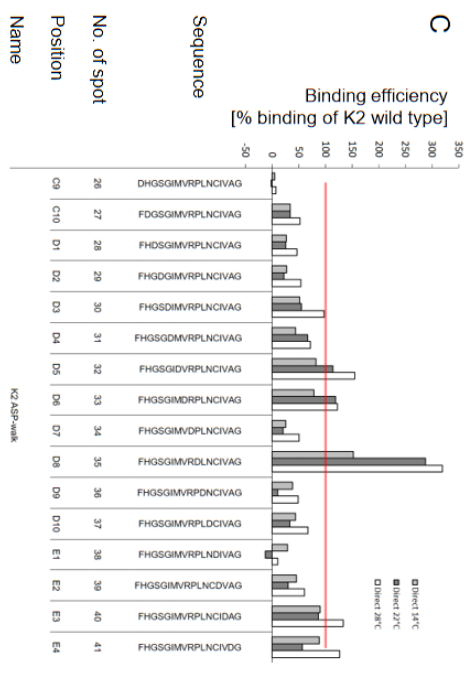
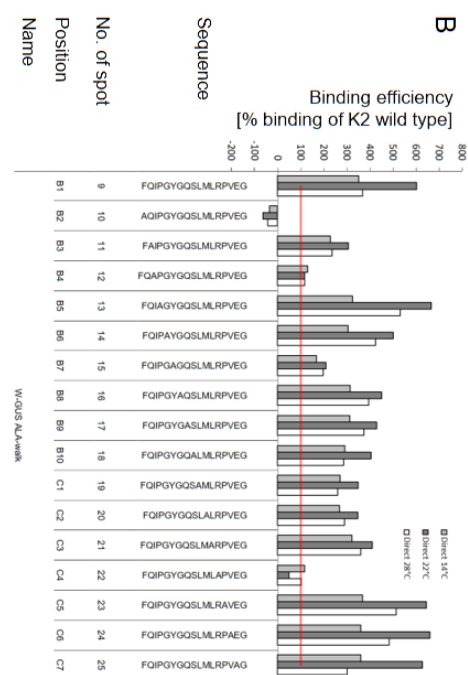
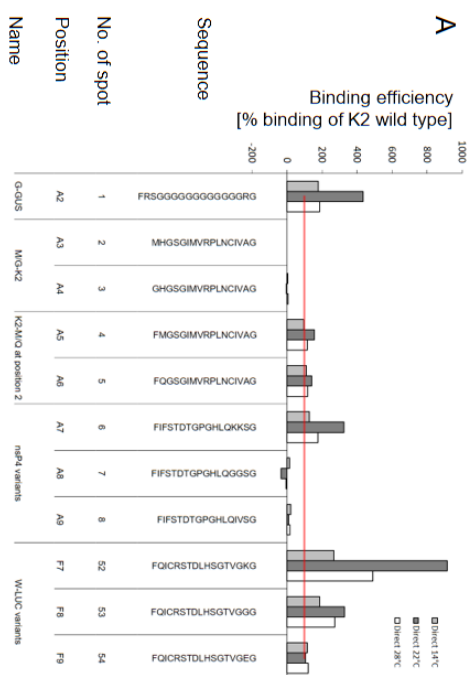


**Figure 3.9 – In-depth analysis of different experimental setups synthesized on membrane two.** (A) Binding of 8xHis:MBP:PRT1 to previously tested sequences and their derivatives. Binding of 8xHis:MBP:PRT1 to Bachmair sequence (lane 1) is reproducible on this membrane. Modification of the amino acid at position one or two of the K2 sequence leads to either abolished binding (lane two and three) or slightly improved binding (lane four and five). Modification of the Lysine at the C-terminal of the nsP4 sequence leads to binding abrogation. (B) Alanine walk through the W-GUS sequence. Compared to the original sequence (lane one) especially amino acid at positions three, six, and 13 seem to influence binding. Replacing the C-terminal Glutamate with Alanine does not have the same dramatic effect on binding as the previous replacement with Glycine. (C) Aspartate walk through the K2 sequence. Introducing the Aspartate at all positions of the K2 sequence mainly results in decreased binding to PRT1 except when replacing the Proline at position nine. (D) Hybrid sequences of K2 and W-GUS. A sequence with the first seven amino acids from the K2 sequence shows significantly diminished binding whereas a sequence with inversed parts (W-GUS at the N-terminal) still shows good binding (lane one and two). A sequentially mixed sequence of K2 and W-GUS did not show much improved binding but retained this binding potential almost completely with a stabilizing N-terminal residue. (E) Different mutations within the eK sequence increase binding efficiency by PRT1.

positive effect of these two mutations (L13C and K15D) was additive. Introducing a third mutation, replacing Arginine 16 with Alanine (R16A), the same amino acid again as in the K2 wild type sequence, did not have drastic effects, only attenuating binding by PRT1 slightly. Mutating the Lysine at position 15 to Valine, as in the K2 wild type sequence. Keeping the R16A mutation negatively influences binding compared to the triple mutated sequence, while still maintaining higher binding efficiency than the original eK wild type sequence.

### 3.3 Influence of altered N-terminal sequences on degron/E3 interaction and stability *in vitro* and *in vivo*

**Stability of two different K2-variants in an *in vitro* degradation assay using crude plant extract:** K2 variants F/M-K2 and F/M-W-GUS-K2 were expressed in *E. coli*. Expression of the 8xHis:MBP:K2 variants was always very strong, already after two hours of induction at 37°C (fig. 3.10A). Following TEV cleavage to expose the N-terminal Phenylalanine or Methionine, the recombinant TEV, as well as uncleaved protein, were depleted from the sample via a second purification step (fig. 3.10B). Purified recombinant protein was used in a cell free degradation assay and monitored via Western Blot analysis or fluorescent labeling.

Western blot analysis of a cell free degradation assay showed that the degradation of the recombinant protein in the crude plant extract is proteasomal dependent, as indicated by increased stability after proteasome inhibitor treatment. However, the stability seemed to be independent of the N-terminal since Methionine as well as Phenylalanine starting proteins exhibited the same degradation pattern (fig. 3.10C). To quantify degradation patterns, an alternative labeling approach was carried out. Quantification showed that

there was no difference in the degradation between a degron with the wild type or the optimized (W-GUS) sequence. Proteasomal degradation was confirmed once more. Both versions efficiently stabilized upon MG132 treatment. Initial degradation is a result of the inhibitor not functioning instantly (fig. 3.10D).

**Cloning a PRT1:K2 co-expression construct for yeast expression:** As an alternative for the optimization of the binding efficiency of PRT1 to the degron cassette, a construct expressing PRT1, as well as the K2 cassette from the same open reading frame was cloned. This way of expression should boost K2 degradation since it raises the enzyme to substrate ratio to equimolar. Functionality of PRT1 in yeast has been demonstrated previously (Stary *et al.* , 2003).

The approach is a mixture of the widely adopted ubiquitin-protein-reference (UPR) technique<sup>8</sup> (Varshavsky, 2005) and the approach to co-express enzyme and substrate to reach beneficial ratios of enzyme to substrate to achieve faster processing. This has been done already, albeit not from the same reading frame, by co-expressing TEV protease (Shih *et al.* , 2005) or a de-ubiquitinating enzyme (Piatkov *et al.* , 2013) together with a substrate from the same plasmid in bacteria.

For this construct, a vector *pENTR:3xHA:PRT1:UBQ<sub>K29/48/63R</sub>:K2*, termed pREF, with N-terminals being the original K2 wild type sequence or the well binding W-GUS sequence was generated which was expressed in yeast as a GFP fusion. A mutated ubiquitin was introduced due to the fact that, contrarily to the UFT ,where free ubiquitin is released, the ubiquitin moiety will remain on the PRT1 protein after processing. Even though has been postulated that at least a chain of four ubiquitin residues is necessary to induce proteasomal degradation (Ciechanover *et al.* , 1980a,b, Thrower *et al.* , 2000), ubiquitin was mutated to prevent chain formation on the newly exposed ubiquitin moiety. The Lysines at positions 29, 48, and 63<sup>9</sup> were mutated<sup>10</sup>. Then a degron stability assay in regard to PRT1 and Ubr1 was performed.

PRT1, when expressed from the pREF construct, led to efficient degradation of the K2:GFP fusion protein (fig. 3.11). However, there were no stability differences between the WT-K2:GFP and the W-GUS-K2:GFP protein. Strangely, the stability of K2:GFP or K2-W-GUS:GFP did not differ significantly when expressed in either wild type or *ubr1-Δ* yeast cells. Since this was only an initial test, mainly aiming on elucidating if sequences, identified in the SPOT assays to show superior binding to PRT1, would confer the same effect *in vivo*. Since this was not the case, and the wild type as well as the modified K2-version were degrade at the same speed and efficiency, no further sequences were tested.

### Assessing the stability of different versions of the K2-degron cassette carrying

---

<sup>8</sup>In UPR a stable reference protein is cloned upstream of the ubiquitin moiety that is cleaved upon translation to expose desired N-termini in fusion proteins using the ubiquitin-fusion-technique (UFT).

<sup>9</sup>Although K63 is commonly not associated with degradation it was nevertheless mutated to exclude other effects, such as re-localisation initiated through K63 linked chains.

<sup>10</sup>It is noteworthy that the original UFT approach does not use a mutated lysine (Varshavsky, 2005).

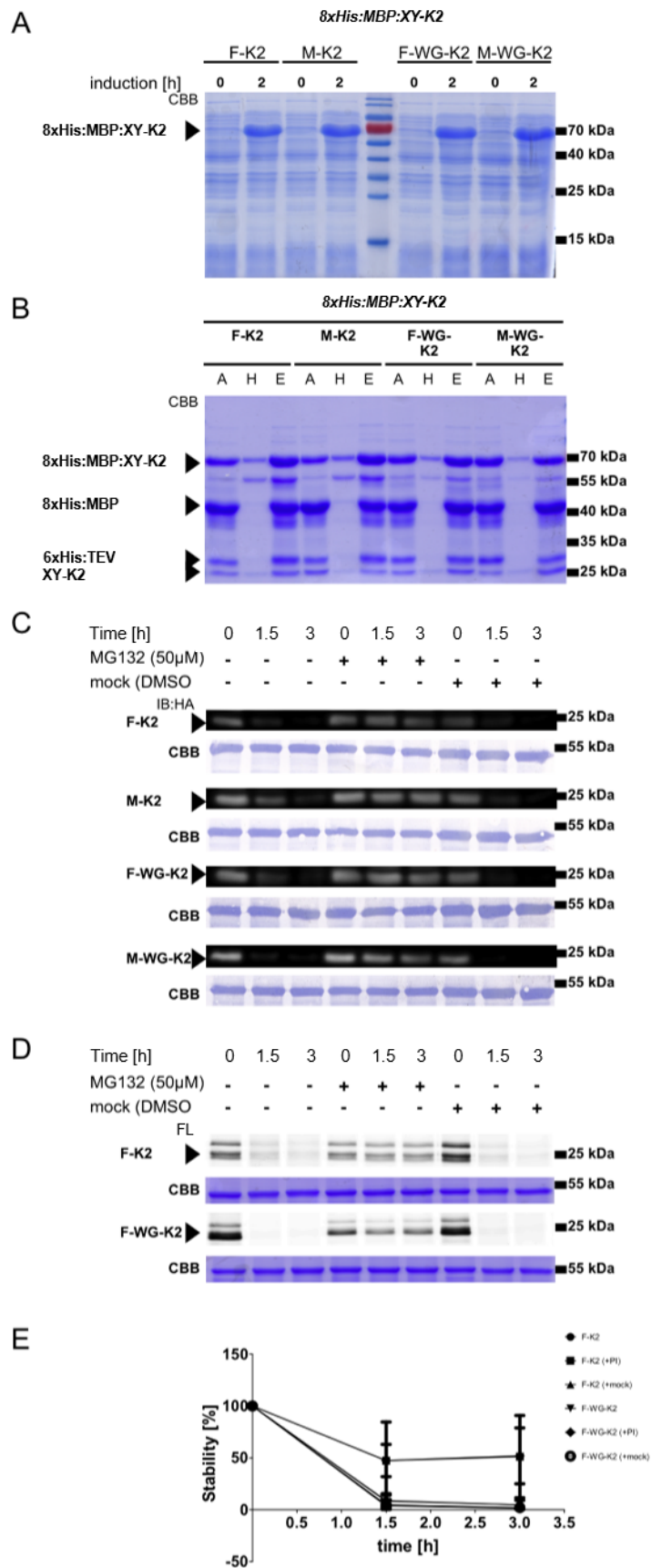


**Figure 3.10 – Recombinant degron protein is readily degraded in a proteasomal dependent albeit N-terminal independent manner in crude plant extract.** (A) All versions of K2 are efficiently induced as 8xHis:MBP fusions after 2 h of induction at 37°C. 20 µl of crude *E. coli* extract was boiled and subjected to SDS PAGE. (B) TEV-processing and purification of degron versions. (C) Recombinantly expressed K2 variants are efficiently degraded in a cell free degradation assay in a proteasomal dependent but N-terminal independent manner. 3 µl of recombinant protein were incubated in 80 µl of crude plant extract ( $c = 1 \mu\text{g} / \mu\text{l}$ ). At timepoint zero MG132 was added were indicated. At the indicated timepoints 20 µl of the reaction were taken and immediately boiled in loading dye. Samples were subjected to western blot analysis and visualized using an a-HA antibody. Detection was carried out using a camera. (D) Fluorescently labeled protein was used in an assay as described in (C), however, after SDS PAGE gels were directly analyzed using Typhoon scanner at a set photomultiplier strength of 650V. (E) Quantification of results obtained in (D) ( $N = 3$ , whiskers = standard deviation).

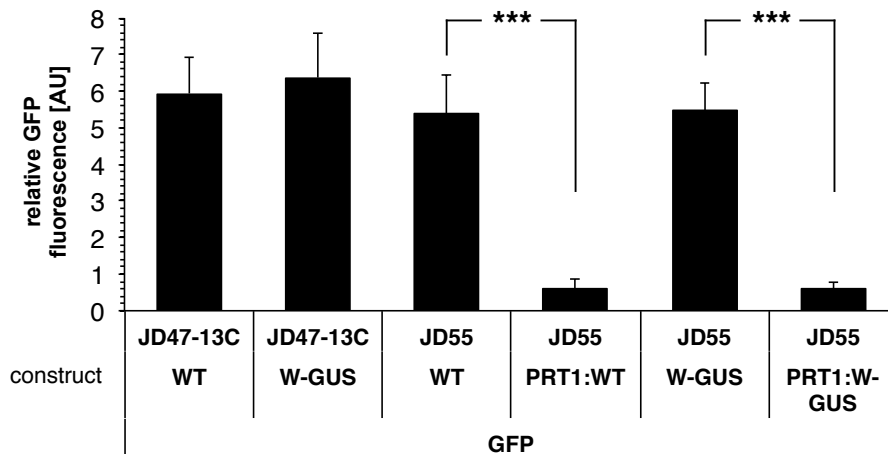


**Figure 3.11 – PRT1 dependent instability of K2:GFP variants in yeast.** Degradation of K2 variants is mediated through PRT1 in yeast by complementing the *ubr1-Δ* dependent degradation phenotype.  $N = 8$ , two-sided unpaired ttest,  $p < 0.001$  \*\*\*



**various N-terminal sequences identified via SPOT assays *in vivo*:** The SPOT assays identified and highlighted a number of sequences showing altered binding behavior and affinity to PRT1. To verify and further assess the *in vivo* relevance of these results, a number of N-terminal sequences was introduced into the K2-degron cassette replacing the original N-terminal. Through a split-luciferase assay, using a stabilized and inactive version of PRT1 (PRT<sub>C29A</sub>, kind gift of Maria Klecker), as well as a luciferase stability assay the behavior of these altered K2 variants in regard to target/E3 interaction as well as PRT1-dependent stability was assessed in *A. thaliana* mesophyll protoplasts. Following sequences were introduced into the K2-degron cassette (details about the sequences can be found in tabs. 5.6 and 5.7):

- **WT** - The original wildtype sequence as found in the K2 cassette
- **W-GUS** - The W-GUS sequence
- **W-GUS-E** - The W-GUS sequence without negative Glutamic acid (E)
- **W-LUC** - The W-LUC sequence
- **W-LUC-D** - The W-LUC sequence without negative Aspartic acid (D)
- **W-LUC-K** - The W-LUC sequence without Lysine (K)
- **nsP4** - The nsP4 sequence
- **nsP4-K** - The nsP4 sequence without Lysines (K)
- **eK** - The eK sequence
- **G-GUS** - The original sequence used by Garzon and colleagues
- **poly-G** - Long Glycine stretch
- **poly-GS** - Long Glycine/Serine stretch
- **M** - Methionine starting wild type sequence - unrecognizable/stable control
- **G** - Glycine starting wild type sequence - unrecognizable/stable control

These sequences were chosen, because most have already been shown to follow the N-end rule *in vivo*, making them strong candidates for an improved degron with minimized risks of choosing a sequence that only shows efficient binding in an *in vitro* environment. However, also the poly Glycine/poly Glycine/Serine sequences were tested since their behavior on the SPOT membrane was unexpected.

**Different N-terminal sequences alter the interaction strength between the degron and PRT1 *in vivo*:** To verify *in vivo* interaction between the different K2 versions and PRT1 a split-luciferase assay was chosen<sup>11</sup>.

The different versions of the degron cassette, carrying the various altered N-termini, were expressed as a C-terminal fusion with the N-terminal part of firefly luciferase. Its interacting partner, the E3 ligase PRT1, was expressed as an N-terminal fusion with the C-terminal part of luciferase. To prevent degradation effects of the different degron proteins an inactive version of PRT1, where Cysteine 29 was mutated to Alanine was chosen. The C29A version of PRT1 (kind gift of Maria Klecker) is potentially unable to interact with E2 proteins (seen through loss of auto-ubiquitination *in vitro*, Maria Klecker,; personal communication) rendering it significantly more stable and also preventing substrate degradation during simultaneous expression of K2 and PRT1 proteins in mesophyll protoplasts.

To further confirm that PRT1<sub>C29A</sub> does not show an altered substrate interaction behavior compared to PRT1<sub>WT</sub> the SPOT assay was repeated using 8xHis:MBP:PRT1<sub>C29A</sub>. This assay revealed that the C29A mutation does not significantly alter binding behavior to the SPOT membrane (figs. S 5.11 and S 5.13). The N-terminal fusion was chosen again, because already in the SPOT assays an N-terminal tagged 8xHS:MBP:PRT1 was used, which showed reliable binding to the membrane. The K2 proteins on the other hand relied on a C-terminal fusions to still be able to expose the desired N-terminal. Signal intensity was normalized to the activity of a stable, co-expressed GUS protein (Norris *et al.* , 1993). Protoplasts were generated from *prt1-1* plants to prevent influence by endogenous PRT1.

The interaction between PRT1<sub>C29A</sub> and the different degron versions is altered by the modification of the N-terminal sequences (fig. 3.12A). Most sequences were recognized more efficiently. However, some sequences, such as nsP4-K as well as the M and G starting controls, did not seem to interact. Also, some sequences did show interaction with PRT1<sub>C29A</sub>, however, without any statistically significant differences to the wild type sequence. Almost all sequences did show a high variability over the range of the experiments indicating some experimental issues.

**Different N-termini alter the stability of the degron *in vivo*:** To further elucidate the stability and to determine whether an increased interaction with PRT1 would translate into decreased stability of the degron cassette, a luciferase based stability assay was used. The K2 versions described above were transiently expressed in *A. thaliana* mesophyll protoplasts, isolated from *A. thaliana prt1-1* plants, as a C-terminal luciferase fusion together with either PRT1<sub>WT</sub> or PRT1<sub>C29A</sub> (two individual reactions, constructs kind gifts of Maria Klecker) as well as the *ProUBQ:GUS* construct for transformation normalization.

---

<sup>11</sup>The split-luc assay offers many advantages over the well established Bi-molecular fluorescence complementation (BIFC) assay, mainly because it enables a quantifiable measurement in a 96-well format as well as a dynamic interaction read-out since the individual fragments of the luciferase, as opposed to the traditional YFP based BIFC assay, can still dissociate. Therefore measured interaction represents a dynamic steady state. Additionally, the technique has been applied extensively in protoplasts (Luker *et al.* , 2004, Fujikawa & Kato, 2007, Gehl *et al.* , 2011, Li *et al.* , 2011a)



Stability was determined by measuring GUS and LUC activity. Luciferase activity of every sample was normalized to the samples' GUS activity and stability was calculated as percentage of luciferase activity of the sample co-transformed with PRT1<sub>WT</sub>, compared to the one co-transformed with PRT1<sub>C29A</sub>. Most sequences exhibited a decreased stability. The stable controls (M and G starting) showed high stability even over 100% indicating a higher stability when co-transformed with PRT1<sub>WT</sub> then with PRT1<sub>C29A</sub>. Variability of the results was significantly lower than in the split-luc assay. Also, almost all sequences exhibited a statistically lower stability than the wild type sequence which, for some sequences such as nsP4-K or WL (W-Luc), is not entirely in agreement with the results of the split-luc assay.

### 3.4 Using a newly cloned vector for easy degron tagging

To strengthen the application of the degron as a biochemical tool and to facilitate degron fusions by circumventing fusion PCRs, a new *pDEST* was assembled, based on the *pAM-PAT* backbone, where the K2 cassette was introduced between the promoter and the gateway site. These vectors, carrying either the UBQ10 or the CDKA;1 promoter, were named *pLTDK2-ProUBQ10/CDKA;1*.

**Application of the *pLTDK2* vectors for expression of two different transcription factors involved in flowering:** To test whether the degron could be used to complement sterile mutant phenotypes, two transcription factors, AGAMOUS (AGA, AT4G18960) and LEAFY (LFY, AT5G61850), were chosen. AGA and LFY belong to the class of homeotic genes regulating flower development (Yanofsky *et al.*, 1990, Huala & Sussex, 1992, Weigel & Meyerowitz, 1994). The AGA mutant plants grow a second flower instead of reproductive organs. In LFY knockout plants petals are converted into leaves (fig. 3.13A). Complementation of the mutant phenotype should result in morphologically normal flowers and finally in fertile seeds and therefore represent an easy experimental read-out.

**pLTDK2 driven expression of K2:AG and K2:LFY does not complement the mutant phenotype:** Since homozygous mutants of either LFY or AG are sterile (fig. 3.13B) heterozygous plants were transformed. For LFY the strong *lfy-12* allele was chosen. This allele is an EMS-allele which contains a premature STOP-codon close to the start of the coding sequence (Huala & Sussex, 1992). For AGA a T-DNA insertion line (SALK\_014999) was used (Urbanus *et al.*, 2009).

After BASTA selection a total of 192 plants per construct plants was selected, transferred into single pots, and genotyped for homozygosity of the mutant allele. Additionally, plants were genotyped for the presence of the transgene using a DHFR specific primer set (tab. 5.4). Homozygosity appeared at the expected rate of about 25%. Most of them were also positive for the transgene. However, when grown under cold conditions, no phenotypic

complementation could be detected<sup>12</sup>.

Expression of K2:AG from the weaker pCDKA;1 promoter neither resulted in any complementational effect. There was no influence on the phenotype by the construct. However, *ProCDKA;1:K2:LFY* expressing plants showed a phenotype. Unfortunately this phenotype was dominant negative, indicated by the fact that plants heterozygous for the *lfy-12* allele, that normally appear wild type like, looked mainly like homozygous mutants when the K2:LFY fusion protein was expressed (fig. 3.13C).

**Cloning a high-flexibility Gateway-based vector for easy degron-POI expression:** To offer a higher level of flexibility for the degron as a tool, also in regard to choice of promoter and potential stable references, the *pLTDK2* vector was further modified (fig. S 5.16). The promoter was replaced through a multiple cloning site (MCS) offering a total of 13 restriction sites for easy promoter insertion. Downstream of the MCS and the following TMV leader sequence, restriction sites were introduced for easy insertion of a stable reference protein allowing an ubiquitin-protein-reference (UPR) approach as described previously (Varshavsky, 2005).

One has to take into account that the UB protein within the whole cassette is still a wild type UB. While it has not been described for the UPR that mutation of ubiquitin is necessary (Varshavsky, 2005), one must be careful to never use a Lysine-mutated ubiquitin without a reference protein, as processing of the fusion protein leading to cleavage and release of the ubiquitin will result in build-up of mutated and inert ubiquitin within the cell leading to disturbances within the Ubiquitin-System resulting in overall increased stability of proteins destined for proteasomal degradation.

---

<sup>12</sup>Unfortunately, it was discovered that the vector *pAMPAT-ProUBQ10* that was used to generate *pLTDK2-ProUBQ10* carried a formerly unknown and non-annotated insertion of 134 bp. This insertion did change the reading frame and inserted a stop codon when translating the K2:AG/LFY fusion protein. However, some plants did show some phenotype that can be explained by translation of only AGA from the vectors since both of them retained a start codon (ATG) (fig. 3.13C). This eliminated 50% of all plants to be analyzed.

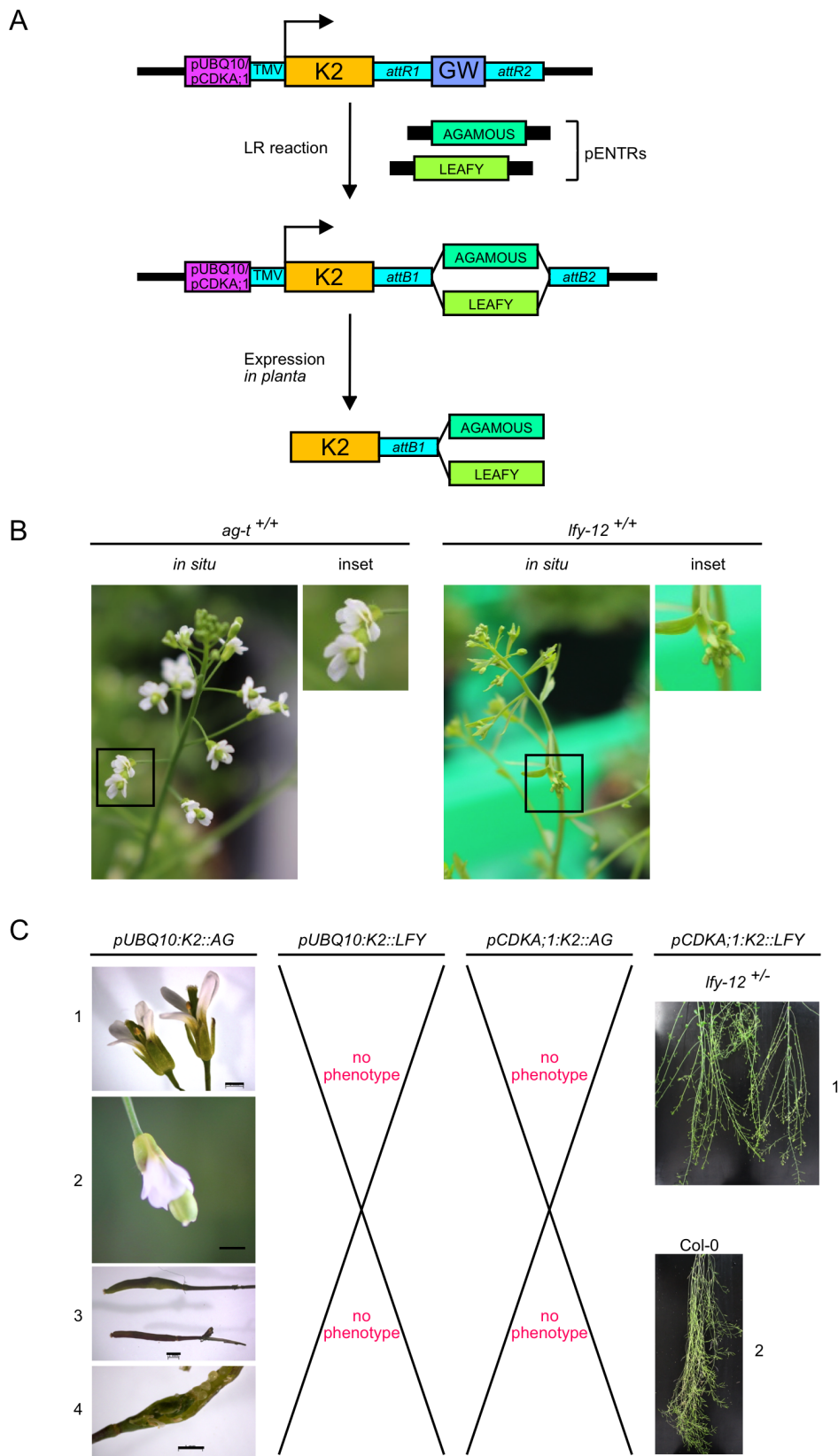


**Figure 3.13 – Cloning and expression of *pLTDK2-ProUBQ10:AG/LFY* and *pLTDK2-ProCDKA;1:AG/LFY* in the respective mutant backgrounds.** (A) Cloning overview of *pLTDK2-ProUBQ10/ProCDKA;1:AG/LFY* constructs. (B) Greenhouse phenotype of the *ag* and *lfy-12* allele. (C) Phenotypes of plants expressing the different constructs in the respective mutant background. *pLTDK2-ProUBQ10:AG* expressing plants exhibited a phenotype as a result of expression of only the AGAMOUS protein through a second start codon<sup>13</sup>. Flowers still appeared different than wild type with enlarged pistills (1/2) and siliques that contained, besides seeds, also a structure that appeared to be an additional flower organ (3/4). *pLTDK2-ProUBQ10:LFY* did not show any phenotype. Plants looked like the mutant allele depicted in (B). *pLTDK2-ProCDKA;1:AG* did not show any phenotype and plants looked like the mutant allele depicted in (B). *pLTDK2-ProCDKA;1:LFY* showed a dominant negative phenotype when expressed in a heterozygous background. Plants showed altered flower morphology with significantly reduced amounts of siliques and seeds when compared to the wild type.





## 4 Discussion

### 4.1 The degron is an efficient tool to mediate phenotypes *on demand in vivo*

#### 4.1.1 Different POIs expressed as degron fusions show plasticity and responsiveness of the degron approach

The first, and most thoroughly, analyzed protein of interest (POI) was the commonly used  $\beta$ -glucuronidase (GUS). Though already introduced in the late 1980s (Jefferson *et al.* , 1987), it is still used, mainly for promoter expression studies. However, the GUS protein possesses some unique features that should be taken into account, when analyzing the data at hand.

It functions as a homotetramer, which represents the only active form of the GUS protein, due to the fact that the two active sites of each tetramer are made up by surfaces of two monomers from opposite dimers. Tetramer formation is restricted by two rate limiting steps after translation (monomer to dimer and dimer to tetramer formation) (Matsuura *et al.* , 2011). Examination of the dimer structure indicates that the N-terminal of each monomer points away from the active center and is not buried within the protein (Wallace *et al.* , 2010, Raju *et al.* , 2015, Wallace *et al.* , 2015), making it likely that the degron fusion at this N-terminal will not hamper with GUS monomer and tetramer structure and therefore its activity (fig. S 5.17A left panel).

A schematic view of the hypothetical structural arrangement of the GUS homotetramer, with each GUS enzyme carrying the N-terminally fused degron cassette, highlights again that active center and degron cassette point into opposite directions, making hampering of the degron with GUS activity all the more unlikely (fig. 5.17A right panel). Because no *ProCaMV35S:K2:GUS*-expressing line could be isolated, K2:GUS expression in the responsive line was controlled by the weaker UBQ10 promoter. In the case of ProCaMV35S driven expression, plants mostly showed an "always on" phenotype (fig. 3.1)<sup>1</sup>. It seems unlikely that the ubiquitin system itself would be overridden<sup>2</sup>, but maybe the capacity

---

<sup>1</sup>Due to the qualitative nature of the assay it can however not be excluded that different responsive lines showing at least differential, temperature dependent accumulation of the enzyme, were lost in the assay due to a possibly weak phenotype.

<sup>2</sup>Due to its involvement in almost all aspects of plant homeostasis and development, mutation or disabling of the proteasome leads, depending on the position of the mutation, to severe defects and developmental phenotypes (Brukhin *et al.* , 2005, Kurepa *et al.* , 2009, 2010), nothing of which can be observed in the

of PRT1, the E3 ligase responsible for degron degradation, was maxed out, leading, in combination with the high stability of GUS, to the temperature independent accumulation.

However, when the K2:GUS expressing line was analyzed (fig. 3.1), what was most surprising was that the expression by the UBQ10 promoter instead of the CaMV35S promoter downregulates the activity of GUS enzyme by about 100 fold (fig. 3.1C). At a first glance, this effect seems very high, but it can be explained through different effects coming into play. First of all, it has been shown in transient expression experiments, that the expression strength of the CaMV35S exceeds that of the UBQ10 promoter by about 50% (Grefen *et al.* , 2010). The vector backbone (*pAM-PAT-Pro35S*) used for Pro35S driven expression of K2:GUS contains even a double CaMV35S promoter. Also copy and position effects might play a role. However, all these effects become multiplied by properties of GUS tetramer formation. It has been shown that tetramer assembly is a fourth order reaction, therefore a decrease in DNA/expression/monomer availability by 2-fold will result in a decrease in the rate of tetramer formation of 16 ( $=2^4$ )-fold (Matsuura *et al.* , 2011), thus, in combination with the other effects, explaining the differences in accumulation of active GUS in these lines. Additionally, it can not be excluded that the degron itself has a certain influence on the kinetics of tetramer formation.

Also, there is also a significant difference in regard to GUS activity between plants expressing *Pro35S:GUS* or *Pro35S:K2:GUS*. This can be explained by the presence of the degron cassette. Even though it does not lead to the desired temperature dependent protein accumulation phenotype, it might hamper with tetramer formation or might put some other kind of restraint on protein transcription/translation.

The difference in GUS activity between the *Pro35S:K2:GUS* and the *ProUBQ10:K2:GUS* expressing lines can be explained by position effects (discussed in Finn *et al.* 2011) and copy numbers multiplied by the effect of tetramere formation explained above. Higher levels of GUS activity at warm temperatures might reflect either increased tetramere abundance potentially caused by increased assembly, or increased velocity of protein translation. It is most likely not a transcription-related phenotype, as transcript analysis of different degron-expressing lines showed absolutely no changes in transcript abundance at different temperatures (fig. 3.4B). The potentiating effects of tetramere assembly functions in both ways, therefore minor changes in GUS expression will lead to more drastic effects of active GUS accumulation, which is one of the reasons why GUS is very sensitive especially in lower expression ranges (Matsuura *et al.* , 2011).

When plants expressing *ProUBQ10:K2:GUS* were grown at a standard growth temperature of 21°C and then shifted to either restrictive or permissive temperature, the GUS activity showed an immediate reaction already after 4h (fig. 3.1D). The initial activity at 21°C seemed to be of an intermediate state, indicating that degron instability, in regard to temperature, does not represent a simple on/off state but rather a continuous process.

---

*ProCaMV35S:K2:GUS* expressing lines.

---

Plants shifted to the permissive temperature started to accumulate active GUS enzyme in nearly linear manner with a plateau not yet reached after 24 h (fig.s 3.1D and supplementary figure 5.3D). This is interesting because GUS assembly into a tetramer has been shown to be a fourth order reaction in an *in vitro* transcription/translation system with monomer to dimer and dimer to tetramer formation being the rate limiting steps, thereby resulting in a convex curve shape influenced strongly by the concentration of available DNA (Matsuura *et al.* , 2011).

The linear accumulation behavior in transgenic plants is another hint for a relatively low expression/availability of GUS monomers in the functional reporter line, where the rate of the tetramer formation is solely limited by the amount of available GUS, and therefore expression strength and stability, and not significantly influenced by the speed of dimer formation. Additionally, it has been demonstrated *in vitro* that tetramer dissociation is neglectable highlighting once more the high stability of GUS (Matsuura *et al.* , 2011). Overall this assay also demonstrated the degron's fast reaction to temperature shifts, but also that accumulation of the active protein is most likely not finished after 24 h.

This behavior was also evident on protein level as assessed by western blot (fig. 5.3D). The responsiveness was not restricted to the K2:GUS fusion protein but could also be observed when repeating the experimental with a K2:GFP fusion protein which behaved similarly indicating once more that the observed (de)stabilization effect is mediated by the degron rather than the POI (fig. 3.4A). Also, it has been demonstrated *in vitro* that GFP accumulation is a linear function of DNA concentration not showing any higher order relation behavior (Matsuura *et al.* , 2011). This highlights that in this situation of rather low expression the degron represents the governing entity with limited influence of the POI on stabilization kinetics, as opposed to the high-expression situation in the 35S drive GUS control lines..

Another shift-based assay, where transgenic plants were continuously shifted by 2.8°C higher or lower every 4 h (fig. 3.1E) showed that the amount of active GUS protein can be efficiently tuned in response to temperature and especially highlights the fact that the degron is able to target the very stable tetramer for destruction. This also indicates, that, at least for GUS as a POI, the degron-fusion reacts quickly to the temperature stimulus. This was surprising, since GUS is an intrinsically stable protein, with a reported half-life of 50 h mesophyll protoplasts (Jefferson *et al.* , 1987).

This assay conclusively highlights the power of the degron by enabling full control over the pool of active protein that can be tuned as desired. Higher or lower temperatures than 14 or 28°C respectively were not assayed due to possible side effects on plant development and stress response. The data also suggests that the temperature range from 14 to 28°C could be only slightly adapted to a range from 16.8 to 25.2°C thus potentially decreasing effects of temperature on plant growth and development. Ubiquitome enrichment from warm grown plants indicated that overall ubiquitination is reduced in plants grown at

28°C suggesting that this is not a state of heat stress, which has been previously linked in yeast to a strong increase of overall ubiquitination levels due to protein misfolding (Fang *et al.* , 2011).

Still, levels of GUS activity never reached zero. This might be due to an equilibrium of synthesis and degradation or rather between tetramer formation and degradation and is somewhat surprising taking into account that only the tetramer represents the active conformation highlighting once more the high sensitivity of GUS (Matsuura *et al.* , 2011). This also means that newly synthesized K2:GUS is still able to reach the tetrameric state to some extent without being caught efficiently by the degradation machinery. This probably being once more a reflection of the intrinsically high stability of the GUS enzyme, counteracting the instability imposed by the degron cassette at restrictive conditions.

Analysis of the K2:GUS protein revealed a surprising behavior. If one would deduce from the activity and the histological phenotype (fig. 3.1A/C) to protein levels one would expect a significantly higher concentration of protein under permissive than under restrictive temperature (even though one would not expect a total absence of protein, due to the retained low activity at restrictive temperature). However, this did not seem to be the case but rather two distinct sub-species with highly distinctive molecular weights were identified in Western Blot analysis. Proteasome inhibitor treatments of permissively and restrictively grown plants indicated that the higher molecular subspecies is indeed the one responsible for the phenotype and the one targeted by the degradation machinery, since it accumulates after treatment (fig. 3.2A). Strikingly, the treatment of permissively grown plants does not lead to further stabilization of the degron indicating that K2:GUS is completely stable at the permissive temperature of 14°C, contrarily to what might have been expected when comparing reporter activity of *Pro35S:K2:GUS* and *Pro35S:GUS* expressing plants.

The TUBE-based ubiquitome enrichment from K2:GUS-expressing plants grown at 14°C or 28°C suggest following process: At the permissive temperature, the synthesized K2:GUS protein is, two a large extend, ubiquitinated but remains stable thus resulting in a higher abundance of the heavier molecular weight signal. Under restrictive conditions, ubiquitinated K2:GUS is removed from the cell, therefore leaving only the lower molecular weight signal representing the equilibrium between degradation and synthesis. The fact that these ubiquitinated species can accumulate at the permissive temperature highlights the influence of the protein of interest's intrinsic stability on the degron fusion, since it was shown previously that a K2:TTG1 fusion in the *prt1-1* mutant background, where the E3 ligase responsible for degron degradation is absent, also additionally stabilizes the protein under permissive temperature (compare Faden *et al.* 2016b figure 1f).

Even though proteasome inhibitor treatments and an E3 knockout are not exactly addressing the same process (degradation vs. ubiquitination), they target the same pathway and should therefore lead to comparable results. Further implications of these findings in context with other data will be discussed in section 4.8.

Albeit K2:GUS was the best characterized protein, the degron also proofed applicability with other proteins of different classes, as well as trans-species functionality in *D. melanogaster*, as expected from conservation of the N-end rule pathway (reviewed in Varshavsky 2011). Additionally, transcript analysis clearly confirmed a real degradation/stabilization phenotype and excluded transcriptional regulation of the degron in response to temperature.

#### 4.1.2 A degron-barnase fusion protein is able to control trichome formation in *A.thaliana*

The bacterial ribonuclease (barnase, BAR), which is secreted by the soil bacterium *Bacillus amyloliquefaciens*, is a potent non-specific RNase (Buckle & Fersht, 1994). It has been used in a variety of applications such as creation of male sterile mutants in *A. thaliana*, tobacco, and wheat (Mariani *et al.* , 1992, Burgess *et al.* , 2002, Gils *et al.* , 2008), as a sort of "kill-switch" to prevent uncontrolled spread of transgenes in birch, *A. thaliana*, and wheat (Lannanpaa *et al.* , 2005), or as part of a defense strategy against the pathogen *Phytophthora infestans* in potato (Strittmatter *et al.* , 1995). Furthermore, barnase has been used as a cell ablation tool in mammalian cell culture (Leuchtenberger *et al.* , 2001), to map cell populations in the murine nervous system (Bar-On & Jung, 2010), or for cell regeneration studies in the zebra fish (Curado *et al.* , 2007). Additionally, barnase is discussed as a therapeutical anti-cancer tool (Edelweiss *et al.* , 2008).

The fusion of the degron cassette K2 with barnase (K2:BAR) was able to efficiently control formation of trichomes. At permissive conditions, potentially<sup>3</sup> due to the activity of the barnase protein, the leafs of plants appeared glabrous<sup>4</sup> while loosing this phenotype completely under restrictive temperatures (fig. 3.5A/B).

The first interesting observation is that K2:BAR seems to drive the cells rather into a state of growth arrest than into induction of cell death. This is unexpected since barnase has been known to be a potent RNase, usually inducing apoptosis in cell culture or ablation in plant organs (see references above). The barnase-elicited phenotype strikingly resembles a previously described transcription factor mutant, namely the GLABRA 2 (GL2) loss-of-function allele *gl2*. GL2 is a transcription factor crucial for cell fate determination and trichome formation and acts downstream of TRANSPARENT TESTA GLABRA 1, GLABRA 1/3, and ENHANCER OF GLABRA 3 (Rerie *et al.* 1994, Szymanski *et al.* 1998, reviewed in Hülskamp 2004). The *gl2* allele has been shown to arrest trichome cell differentiation in an early state of cell fate determination without proceeding to the next step of trichome formation. *Gl2* plants show an almost glabrous leaf surface where the trichome forming cells are easily spotted due to their size and elongated shape. Some of these cells are able to produce a small "stichel" like structure which does not develop into

<sup>3</sup>Unfortunately the K2:BAR fusion protein could never be directly identified in Western Blot analysis.

<sup>4</sup>glabrous = smooth, without hairs

a full trichome (Rerie *et al.* , 1994, Szymanski *et al.* , 1998).

However, *gl2* plants completely maintain cell spacing, indicating that proteins such as TRYPTICHON (TRY), a key regulator of trichome spacing suppressing trichome formation in neighboring cells, are still translated and transported to their target location, where they efficiently suppress downstream GL2 synthesis and activity (Schnittger *et al.* , 1998, Pesch & Hülskamp, 2011). The observed phenotype roughly defines the point of cell growth arrest. However, it does not allow to accurately determine the point of TRY promoter activity. It has been shown that the TRY promoter is active in trichomes (Pesch & Hülskamp, 2011) using expression of ProTRY:GUS. Due to the high stability of GUS this only signifies that the TRY promoter has been active in the trichome but does not indicate when this has been the case. Additionally data from the eFP browser highlights a more or less constitutive activity of the TRY promoter, only being shut off in later stage siliques (Schmid *et al.* 2005, Winter *et al.* 2007, fig. 5.6)

Trichome formation already takes place in the leaf primordia (Larkin *et al.* , 1996). Since the appropriate spacing requires action of TRY, K2:BAR would start to accumulate relatively early during leaf development, thus indicating that toxicity of the K2:BAR fusion protein cannot be very high, since the cells are still able to complete the spacing process and also do not die later. This fact supports two different models. Either the TRY promoter indeed shuts off after spacing is complete. This seems to be a state where the cells have accumulated enough active K2:BAR to stop further development but not enough to have fatal consequences. Or, if one assumes that the degron partially destabilizes the barnase protein already at permissive temperatures, then this state could also be an equilibrium between synthesis and degradation, where the TRY promoter remains active.

The first model would suggest that activator gene expression in the mature leaf is turned off, since no new cells start differentiation into trichomes and trichome spacing itself is not disturbed in the K2:BAR expressing plants. However, due to the fact that we failed to show presence of the protein by western blot analysis, it remains elusive whether the cell is able to cope and degrade the fusion protein and then rests in the state of arrest due to the overall developmental stage of the leaf, or whether the amount of active barnase in the cell results in a sort of steady-state situation. Still, due to the well known toxicity of barnase which is so high that even cloning without an artificial intron is impossible, makes it more likely that the TRY promoter does shut off at an early time point of leaf development and that the degron itself is slightly leaky in regard to its degradation, as observed previously for a degron-TTG1 fusion (see discussion above and Faden *et al.* 2016b fig. 1f). This would result in degradation of small amounts of the fusion protein even at the permissive temperature, allowing the cell to gradually overcome the toxicity phenotype and survive.

Naturally, one can not exclude sterical hindrance/influence of the degron cassette on the barnase protein. The degron cassette could disturb either structural conformation or activity of the barnase protein itself. However, analysis of the crystal structure of barnase

indicates that the N-terminal, where the degron cassette is fused, faces away from the active site (fig. S 5.18). Hence, if indeed the degron influences barnase activity itself, other mechanisms such as splicing of the artificial intron or disturbance of target recognition might play a role.

What can be stated, however, is that the activity of the barnase moiety itself is not influenced by temperature as introduction into the *prt1-1* mutant allele background leads to efficient and temperature independent stabilization providing strong genetic evidence that the observed phenotype is indeed a protein stabilization/degradation phenotype, rather than being a result of altered barnase activity or synthesis.

Therefore, the K2:BAR module represents a highly efficient, conditional tool to control organ fate in *A. thaliana*. The possibility to control the generation of a plant organ offers high potential. By combining the K2:BAR module with a tissue specific promoter full control over a specific subset of cells could be achieved. This offers great possibilities in basic research, where deletion of a certain subset of cells during plant development could be studied. Additionally, the conditional control over barnase paves the way towards a more efficient molecular pharming. Molecular pharming, as a way to produce cytotoxic peptides, has been increasingly investigated since a while now. For example peptides, such as the family of lectins from the mistletoe or others, have long been discussed as a potent class of cancer therapeutics. However, their production, due to their toxicity, is challenging (Desai *et al.* , 2002, Pryme *et al.* , 2007, Boohaker *et al.* , 2012, Cho *et al.* , 2013, Gameraith *et al.* , 2014), something that should be overcome by using the degron to specifically accumulate protein e.g. in storage organs and at later developmental stages. The possibility to destabilize the (toxic) target protein provides efficient means for easy maintenance of the transgene.

Similar attempts for targeted organ formation/destruction have been undergone using the A-chain from Diphtheria toxin (DT-A). Diphtheria toxin (DT) is an exotoxin from *Corynebacterium diphtheriae* which consists of two fragments, namely the A- and B-chain, where the A-chain confers toxicity through blockage of protein synthesis, and the B-chain is responsible for cellular uptake (Pappenheimer Jr., 1977). It is so toxic that one molecule was found to be sufficient to kill a cell (Yamaizumi *et al.* , 1978). DT, as well as DT-A, have been used extensively for cell ablation studies. In mice mainly full-length DT has been used. Due to the natural resistance of mice to DT, due to mutation in the receptor responsible for cellular uptake, in this system toxicity of injected DT is guided through tissue specific promoters (Saito *et al.* , 2001b, Brockschneider *et al.* , 2004, Buch *et al.* , 2005). In plants expression of DT-A is toxic (Czako & An, 1991), but has also been applied in deciphering processes in seed and pollen development as well as in the root (Thorsness *et al.* , 1993, Twell, 1995, Tsugeki & Fedoroff, 1999, Weijers *et al.* , 2003). Also temperature-sensitive versions of DT are known and have been applied in yeast and *D. melanogaster* (Bellen *et al.* , 1992), as well as in plants (Guerineau *et al.* , 2003).

It was shown previously that DT-A fails to deliver a temperature-sensitive phenotype when expressed in *A. thaliana* trichomes as a degron fusion (Mielke, 2014). The K2:BAR module therefore represents a potent alternative with the advantage of a lower toxicity of the protein itself, making handling potentially simpler.

## 4.2 Reporter that do not support the degron fusion

As with every other protein fusion, issues linked to the fusion of the degron cassette can arise. In this paragraph three examples of degron-protein fusions are discussed which did not show a phenotype as it would be expected from an instability effect mediated by the degron fusion. Even though these experiments failed to deliver the desired results, they still provided knowledge over the functionality of the degron and help to select proteins suitable to function with the degron approach.

### 4.2.1 The degron is unable to confer conditional BASTA-resistance when fused to the resistance protein PAT

BASTA is a common herbicide used in a large scale on fields. The chemical compound behind the trademark is phosphinothricin, that is contained in the solution as a DL-racemate with L-phosphinothricin being the active compound. L-phosphinothricin irreversibly inhibits the enzyme glutamine synthetase ultimately leading to a collapse of photosynthesis and death of the plant (Wendler *et al.* , 1990). Resistance to BASTA/L-phosphinothricin is conferred by the *bar* (bialaphos resistance) and *pat* (phosphinothricin acetyltransferase) genes from *Streptomyces*<sup>5</sup>, two genes that code for highly similar gene products with identical functionality (Thompson *et al.* , 1987, Wehrmann *et al.* , 1996). L-phosphinothricin is metabolized quickly and the final metabolites also exhibit mobility within the plant (Droege *et al.* , 1992, Droege-Laser *et al.* , 1994). The enzyme phosphinothricin-N-acetyltransferase specifically acetylates L-phosphinothricin thereby inactivating it. Acetylated ac-L-phosphinothricin remains stable within the plant.

K2:PAT fails to deliver a temperature dependent resistance phenotype. This effect might be due to expression strength, because the strong constitutive CaMV35S promoter initially used, might shift the synthesis/degradation equilibrium more in the direction of stability, as it was observed in the case of plants expressing *ProCaMV35S:K2:GUS* (fig.s 3.1C and 3.3B/D). Also, down-regulating the expression strength or choosing different N-terminal amino acids to address different N-recognins, did not alter the non-responsive phenotype.

Analysis carried out on protein level showed that the K2:PAT fusion protein does not seem to be efficiently removed from the cell (fig. 3.3C), again with potentially more protein accumulating when plants are grown at 28°C then at 14°C. Comparing plants grown at 14 or

---

<sup>5</sup>Also a mutated version of the glutamine synthetase has been identified that also confers resistance to phosphinothricin (Tian *et al.* , 2015).



28°C shows that different potential degradation products are always visible in a temperature independent manner. Therefore, one explanation might be that the degron cassette gets, for some unknown reason, cleaved off the PAT protein resulting in a free PAT that could confer resistance regardless of temperature or the presence or absence of the degron. Since degron detection is mediated by the HA-tag within the degron cassette, a free PAT would be invisible” in Western Blot analysis.

Looking at the signals with higher molecular weight one can observe that the initial higher molecular weight signal seen at permissive conditions seemed to disappear and additional signals appear. One explanation would be that degradation of the protein starts but, for some reason, cannot be continued. This is however an unlikely explanation since the degron alone should be sufficient to mediate degradation of the entire fusion protein. Still, PAT is a rather small (20.6 kDa) and compact protein which might have a negative influence on its degradation efficiency (fig. S 5.20). Still, previously it has been demonstrated that a degron-PAT follows a temperature stimulus when transiently expressed in *N. benthamiana*, however, in this transient environment only the protein and not the resistance phenotype was evaluated (Faden *et al.* , 2016b). Also, in these experiments, K2:PAT did not appear as a single molecular weight signal in the Western Blot analysis, but rather as three distinct sub-species.

Possibly the PAT-protein might also have a sub-cellular localization that is at least partially not cytosolic making it unavailable for the degradation machinery, however this theory remains highly speculative.

#### 4.2.2 The degron disrupts the function of the homeotic proteins LEAFY and AGAMOUS

Flowers consist of four different types of organs namely sepals, petals, stamens, and carpels that are arranged in four rings, so-called whorls. Organ identity is determined through three different classes of homeotic genes termed "A", "B"; and "C", where every class of homeotic genes is active in two adjacent whorls e.g. class A in whorl one and two, class B in whorl two and three and class C in whorl three and four. The classical "ABC" model of homeotic genes describes how these different proteins with overlapping expression patterns shape the floral organ identity in *A. thaliana* (Bowman *et al.* 1991, reviewed in Coen & Meyerowitz 1991, Weigel & Meyerowitz 1994).

**Expression of K2:LEAFY leads to a dominant-negative effect most likely due to disturbance of LFY oligomerization:** LEAFY (LFY) is a transcription factor acting upstream of the homeotic genes and it is responsible for flower organ initiation (Schultz & Haughn, 1991, Weigel *et al.* , 1992). Previous work has highlighted its importance as the master regulator of flower meristem induction across plant species (Weigel & Nilsson, 1995, Kelly *et al.* , 1995, Rottmann *et al.* , 2000, Wada *et al.* , 2002). Even though LEAFY was found to be conserved among many plant species, its DNA binding specificity differs among

species, showing selectivity for different DNA motifs, therefore attenuating its function (Sayou *et al.* , 2014). LEAFY acts directly through transcriptional up-regulation of the homeotic gene APETALA (Wagner *et al.* , 1999). It has been shown that LEAFY itself is activated through the plant hormone auxin (Yamaguchi *et al.* , 2015) and is specifically upregulated under long-day conditions (Blázquez *et al.* , 1997). However, the response of the shoot to LEAFY induction requires also competence of the shoot for said action as indicated by experiments where LFY was ectopically overexpressed under control of the strong CaMV35S promoter. These plants do initiate flowers significantly earlier than the wild type but are still able to grow some leaves indicating that competence for LEAFY action is not acquired immediately after germination (Weigel & Nilsson, 1995). The disruption of the gene coding for LEAFY results in a complete sterile phenotype with flowers transformed into leaf- and shoot-like structures (Huala & Sussex, 1992).

The degron was fused to the LFY coding sequence using the *pLTDK2* vector. Expression of the K2:LFY fusion protein resulted in a dominant negative *lfy* phenotype. In this case plants homozygous for the *lfy-12* allele did not show any sign of complementation whereas plants heterozygous for the same allele adopted the phenotype of the homozygous plants even though heterozygous plants alone have a wild type like appearance. This phenotype was temperature-insensitive. This supports the notion that not only did the LFY-protein not support the degron fusion, meaning it was not able to fulfill its endogenous tasks, but also that it probably elicits the dominant negative phenotype through interaction with some of its endogenous binding partners titrating them away from the cell.

The structure of the C-terminal DNA-binding domain has been elucidated (Hamès *et al.* , 2008). However, this domain would be relatively far away from the degron cassette and also in regard to the dominant negative phenotype, disturbance directly in the DNA-binding domain seems rather unlikely. Only recently the precise mode of action of the N-terminal domain of LEAFY was determined. Interestingly, an N-terminal domain was identified that was crucial for LFY oligomerization. Additionally, oligomerization was identified as a crucial prerequisite for LFY function *in vivo* and elicitation of downstream effects (Sayou *et al.* , 2016).

The domain responsible for interaction of individual LFY molecules was identified as a SAM domain (and not as previously thought as a leucine-zipper domain, Siriwardana & Lamb 2012), a type of domain not yet fully characterized in plants. To date, the SAM domain has been described in other eukaryotes to interact with proteins, DNA, RNA, and lipids (reviewed in Qiao & Bowie 2005). The N-terminal LFY domain belongs to a type of SAM domain that enables protein self-association through two interaction surfaces, called the mid-loop (ML) and end-helix (EH) domain (Sayou *et al.* , 2016). Interaction happens in an ML-EH fashion. Mutations in one or both of these two domains abolished interaction *in vitro* as well as functionality *in vivo*, since a mutated version of LFY was unable to fully complement the mutant phenotype. Interestingly, the two single mutants of each domain

were still able to interact forming a dimer indicating that only one functional complementary interaction domain on each monomer is sufficient for dimer formation (Sayou *et al.* , 2016). The oligomerization has strong implications *in vivo*, with its function being important for higher specificity to the target sequences as indicated to less binding to truncated promoter elements (Sayou *et al.* , 2016).

Most likely the degron-LFY fusion protein interacts with the endogenous LFY in the heterozygous mutant background disabling its function. Different models are possible. Since the N-terminal SAM domain is close to the degron it could be structurally disturbed, or sterically hindered to interact with other LFY molecules. Since the dominant-negative phenotype indicates that only one interaction surface is impaired in its function, the spatial proximity of the SAM-domain to the degron cassette makes it the most likely candidate.

In this case the degron-LFY protein could still interact with a WT-LFY protein forming a dimer. This dimer, on the WT side, could still interact with further free WT-LFY proteins forming multimers. This might be where expression strength and copy number come into play. If one assumes that the amount of the degron-LFY protein is higher than that of the WT-LFY protein, due to stronger expression of the promoter (CDKA;1 promoter vs. LEAFY promoter, see eFP browser Schmid *et al.* 2005, Winter *et al.* 2007) and a higher copy number (since there is only one copy of the LFY-gene in the heterozygous mutant background and possibly a multitude of transgenes) then most WT-LFY proteins will bind a degron-LFY protein leading to a predominant formation of non-functional dimers, or shorter-than-necessary multimers.

Another possibility would be that the degron fused to the N-terminal of LFY results in structural disturbance of the oligomere possibly disrupting or altering its DNA binding affinity or leading to restructuring of the individual LFY moieties within the oligomere. Also this possibility would bind functional WT-LFY protein within a non-functional complex with degron-LFY proteins, hence the dominant negative phenotype.

**Expression of K2:AGAMOUS disrupts its transcription factor functionality:** AGAMOUS (AGA) is a class C homeotic gene crucial for the specification of carpel and stamen identity (Bowman *et al.* , 1991, Mizukami & Ma, 1997). AGA is activated late in flower development through a cooperation of LFY and WUSCHEL, which plays a role in stem cell maintenance. Additionally AGA acts on WUSCHEL in a negative feedback loop (Lohmann *et al.* , 2001). AGA itself is a MADS domain (for MCM1, AGA, DEFA and SRF) transcription factor. It is able to homodimerize or to heterodimerize with other homeotic genes (Riechmann *et al.* , 1996, Fan *et al.* , 1997) or with one of the four SEPALLATA genes using its L- and K-motive (reviewed in Irish 2010). Interaction with different proteins is thought to alter its DNA-binding affinity and specifies its differential action between whorl three and four (reviewed in Irish 2010).

Interestingly, AGA is one of the few genes translation of which is not initiated by a standard AUG but rather by an ACG codon even though artificial addition of an AUG

and disruption of the ACG codon does not hamper activity (Riechmann *et al.* , 1999). Unfortunately, AGA fused to the degron cassette was not able to elicit a phenotype, namely was unable to complement, or at least partially complement, the sterile mutant phenotype resulting in fertile plants. Only plants where the degron fusion was expressed under the control of the UBQ10 promoter showed an almost complete complementation (fig. 3.13C). However, as it was realized in the course of the experiments, the ProUBQ10 containing vector backbone included a previously unknown and undescribed insertion that induced a frame-shift within the degron-AGA fusion protein. The complementation effect can therefore only be a result of translation initiation at the ATG of AGAMOUS. This point was further strengthened by the fact that the observed phenotype was temperature insensitive.

Plants expressing the fusion protein under the control of the CDKA;1 promoter failed to show any complementation phenotype hinting towards a complete disruption of AGA functionality by the degron. Since AGAMOUS functionality relies on two principles, dimerization with other homeotic proteins through its K-box, and DNA interaction through its MADS-box, it is probable that one or both of these features is influenced and disrupted by the degron. Since the MADS domain is close to the N-terminal it is more likely to be negatively influenced by the degron fusion. However, this suggests that the degron-AGA fusion protein would retain its dimerization ability resulting in ectopic expression of an AGA version that can still interact with other proteins but not anymore with DNA. It has been previously reported that strong ectopic overexpression of AGA from the CaMV35S promoter induces an APETALA2 (AP2) mutant phenotype (*ap2*) (Mizukami & Ma, 1992). This phenotype has also been reported in other plant species (Benedito *et al.* , 2004).

AP2 has been shown to repress AGA (Drews *et al.* , 1991, Bomblies *et al.* , 1999) and proper initiation and identity of the two inner whorl has been proposed to be a result of the balanced action of AP2 and AGA (Wollmann *et al.* , 2010). If a degron-AGA fusion protein would retain its dimerization activity, one might expect a phenotype similar to the one reported for the AGA overexpression because the degron-AGA protein would interact with numerous other proteins (among them AP2) without being able to elicit a downstream response. Therefore one can conclude that non-functionality of the degron-AGA fusion protein might be a result of an either overall disturbed structure or sterical hindrance preventing dimerization with its interaction partners. MADS-domain disturbance and therefore impairment of DNA binding can not be excluded but is secondary since the AGA monomer is not able to bind DNA on its own. Also, it has been shown that the N-terminal domain of AGA, the part that is most likely influenced by the addition of the degron, is not important for DNA binding *in vitro* and that ectopic expression of an N-terminally truncated version of AG still elicits the same *ap2*-like phenotype as observed when expressing the full length protein (Mizukami, 1996).

### 4.3 An improved and completely quantifiable SPOT assay design offers tremendous advantages over existing methods

Traditional Synthetic Peptide On membrane support Technique (SPOT) assay analysis is a multi-step procedure: After incubation of the SPOT membrane with the target protein the membrane is blotted (once or several times) and the blot membrane, now carrying the protein formerly bound to the SPOT assay membrane, is subjected to antibody- or radioactive labeling-based methods for visualization of the bound protein (e.g. Erbse *et al.* 2006, Choi *et al.* 2010, Hwang *et al.* 2010a, Kim *et al.* 2014, Klecker & Dissmeyer 2016).

This "classic" approach is time consuming and does not offer accurate quantification possibilities, mainly due to a limited dynamic range of the chemiluminescence signal on films and radioactive labeling is more expensive and needs a special infrastructure. Additionally, every handling step of the SPOT membrane, such as blotting and intermediate washing steps, increases the risk of errors. In this work I developed and optimized a fully quantifiable and high resolution method, based on commercially available labels that allow to execute a full SPOT assay, from incubation of the membrane to target protein detection, in just under three hours, reducing handling time by more than 50%.

The reported method is based on labeling of the target protein, in this case 8xHis:MBP:PRT1, using a fluorogenic dye. The red fluorescent dye was chosen over an also available blue dye, to avoid interference with natural occurring fluorescence, especially of the aromatic amino acid containing peptides, in the UV spectrum. The red dye exhibits a detection sensitivity of less than 1 ng with a dynamic range of  $10^{4-5}$ . Labeling takes only 30 minutes. SPOT membranes were incubated with the labeled protein for two hours, washed for 30 minutes and subjected to fluorescence detection of the bound proteins. The method offers some advantages when comparing it to the "classical" approach (fig. 3.7), mainly an increased velocity and less material consumption due to the omission of blotting and antibody-based detection.

Thanks to its fluorescent nature the signal could be quantified accurately. Due to the fact that protein could be detected directly on the membrane, signal strength was boosted, because less protein was lost thanks to the significantly decreased amount of handling steps (no blotting, less washing). Much less protein was needed for the assay saving time and resources, also on protein purification. Maybe the biggest advantage was that also extremely strong binders could be identified that bound so tightly to the membrane that the standard blotting procedure could not transfer them to the PVDF membrane. This problem might be circumventable by repeating several subsequent blotting steps however this would split the signal onto several membranes, making the assay overall longer, more material consuming, and the results significantly more tedious to analyze.

Overall the reported method represents a significant improvement over the existing workflow. Another advantage is the possibility, to now also being able to analyze tag-free protein. This could be advantageous in cases where a fusion tag used for protein quantification disturbs proper protein functionality. Naturally the labeling process represents a modification of the protein. Therefore it is crucial that a blot-based trial assay is performed to ensure that the label does not disturb binding behavior.

## 4.4 SPOT assay based degron optimization suggests limited importance of the N-terminal degron sequence on recognition by PRT1 *in vitro*

### 4.4.1 Membrane 1

**Comparison of sequences known to follow the N-end rule:** Comparing the binding efficiency of the wild type degron cassette to N-termini of known N-end rule reporter constructs shows that all established N-end rule reporters, except for the commonly used eK sequence, indeed show a strong, often even stronger than K2, binding to the SPOT membrane (fig. 3.8A). Interestingly a few general tendencies are perceivable: First of all, the elimination of negative charges seems to increase the binding efficiency. If the Glutamic acid at position 16 in the N-terminal of the GUS reporter extension from Worley et al. (Worley *et al.*, 1998) is replaced by Glycine, binding efficiency is doubled. This indicates that negative charges within the N-terminal sequence must influence binding/recognition to PRT1 in a disadvantageous way, potentially reflecting a negatively charged surface of the binding domain. Another effect observed is that the elimination of Lysine residues decreases binding efficiency, possibly because Lysine is positively charged so the overall charge of the protein becomes more negative which might be disadvantageous. This feature has already been described in yeast where it was shown that spiking an N-terminal sequence with Lysines can indeed influence the stability of the reporter protein (Suzuki & Varshavsky, 1999). The results that an overall more positive net charge of the peptide sequence is in agreement with findings regarding the substrate specificity of *E. coli* ClpS (Erbse *et al.*, 2006), highlighting once more that the structure of N-degrons is, at least to a certain extent, transferable between species.

On the other hand, the fact that the very commonly used eK sequence is such a poor binder is surprising. Even though it binds to PRT1, its binding efficiency seems much reduced in comparison to the wild type degron sequence. The fact that the eK sequence is still functioning so well *in vivo* hints towards effects that do not play a role *in vitro*. One possibility would be that the overall higher hydrophobicity compared to the degron sequence plays a role. However, this remains highly speculative.

**PRT1 recognizes the aromatic amino acids F, W, and Y but not I and L at**

**the N-terminal:** Replacing the residue in the penultimate position with different non-aromatic, hydrophobic amino acids does not significantly alter the recognition efficiency by PRT1 (fig. 3.8 B). Isoleucine at position two was tested twice, both times resulting in almost the same results, again highlighting the robustness of the method. Replacing the N-terminal with different postulated type 2 destabilizing amino acids resulted in the expected outcome: While the aromatic amino acids Tryptophane (W) and Tyrosine (Y) still enabled PRT1 binding, replacement of the N-terminal Phenylalanine with Leucine (L) or Isoleucine (I) completely abolished binding. This is consistent with previous results obtained for L when expressing PRT1 and different reporters in yeast mapping their stability (Stary *et al.*, 2003). Still, initial work on the N-end rule pathway in yeast showed that I and L starting reporters are unstable, albeit with I being about ten times more stable (30 min compared to 3 min) than L (Bachmair & Varshavsky, 1989) in yeast.

In contrast to these findings, in plants only a slightly decreased stability for L and I starting reporters, when transiently expressed in tobacco (Graciet *et al.*, 2010). Still, these two amino acids are proposed primary type 2 destabilizing residues according to the N-end rule. SPOT results now finally suggest that I and L are not recognized by PRT1 and therefore probably cannot be considered primary destabilizing residues in *A. thaliana*, provided that there is no further type 2 N-recognin present in the genome of *A. thaliana*.

In contrast to structural data from the adapter protein ClpS, the type 2 degron recognizing particle of the bacterial N-end rule, which has been crystallized from two different bacterial species (*E. coli* and *Caulobacter crescentus*) both in complex with L starting peptides (Schuenemann *et al.*, 2009, Román-Hernández *et al.*, 2009), PRT1 seems to behave like ClpS2 from *A. tumefaciens*.

In this species two different version of the ClpS adapter protein (ClpS1/2) were identified. These two ClpS versions exhibit differential binding with ClpS1 binding F, Y, W, and I starting peptides and ClpS2 binding only F peptides well and already Y and W peptides to a lesser extent, exhibiting no binding to L at all. Additionally, the two different ClpS versions are expressed at different phases of bacterial culture growth (Stein *et al.*, 2016). The findings highlight the evolutionary development and flexibility of the N-end rule pathway and make it tempting to speculate about a similar mechanism in plants, where PRT1 behaves more like ClpS2, only binding a more limited number of N-terminals, and the ClpS1 functional homologue might have been lost, or at least is conferred by a different N-recognin with either a very low activity or a very high selectivity for the structural context, as reported for Gid4 in yeast (Chen *et al.*, 2017), thus explaining the only slightly decreased stability of I- and L-starting probes in tobacco (Graciet *et al.*, 2010).

**An ALA-walk through the K2 sequence reveals a stretch of importance for binding by PRT1:** An Alanine walk was used to identify potential residues important for PRT1 binding. This well established technique is used to map the influence of every amino acid by replacing it with an Alanine (Weiss *et al.* 2000, Morrison & Weiss

2001, Gauguin *et al.* 2008, Dey *et al.* 2007, Trott *et al.* 2014, fig. 3.8C)<sup>6</sup>. The Alanine walk reveals importance of the residues 11-13 especially at temperatures higher than 14°C, with replacing the Asparagine at position twelve eliciting the most severe effect almost completely interrupting binding. The other two mutations mainly seem to have effects at higher temperatures. Overall it seems that the binding is more uniform over all residues at lower temperatures. This is insofar surprising as it does not seem to abolish binding but making it only less prone to react to amino acid exchanges. One possibility might be that these changes mainly influence mobility of the peptide chain thereby modulating PRT1 binding, an effect being likely less strong under colder temperatures as general mobility of the peptide chain might be lower. In this regard one also has to take into account that all values are normalized so the effects seen are always relative to a control.

**Long Glycine but nor Glycine-Serine stretches result in extremely tight binding of PRT1:** The influence of long Glycine stretches, ergo very mobile sequences, was elucidated. Long poly-Glycine stretches, like the sequence previously used to identify PRT6 (fig. 3.8D, Garzón *et al.* 2007) increased binding significantly. However, sequences with alternating Serine-Glycine sequences completely abolished binding despite the Phenylalanine residue at position one. This is surprising as the strong binding to long Glycine stretches suggests that the identity of amino acids is of limited importance. However, later *in vivo* assays, using a non-binding Glycine-Serine containing sequence, revealed that this effect is a SPOT-assay specific effect and that mobile sequences show overall improved binding indicated also by decreased stability (see 4.6, fig. 3.12).

---

<sup>6</sup>The Results for Alanine at position one of the sequence are not shown, as this value serves for as an internal normalization spot(fig. 5.10, spot D8).



#### 4.4.2 Membrane 2

**The effects of different amino acid exchanges in sequences known to follow the N-end rule are confirmed and extended:** Modifications in different sequences known to follow the N-end rule have an effect on on PRT1 binding (fig. 3.9A). First, the good binding efficiency to the formerly used sequence from Garzon et al. could be confirmed. This sequence was used again on this membrane because it did not appear in the initial blot-based analysis of membrane 1 (fig.s 5.10 and 3.8A), which was highly unexpected and required confirmation. After analysis of directly bound PRT1 to membrane 1 however, this sequence was already confirmed to be recognized extremely well by PRT1 in these experiments. Secondly, binding of PRT1 to a wild-type degron sequence with Methionine or Glycine at position one was elucidated. The Methionine starting sequence was used as negative control since it had been shown previously that it is not recognized by PRT1 (Stary *et al.* , 2003)<sup>7</sup>. Also, it has been shown for the bacterial ClpS N-end rule adapter protein that its binding pocket poorly fits Methionine (Román-Hernández *et al.* , 2009), making N-terminal Methionine an adequate negative control.

As expected Glycine exhibited no binding to PRT1, which is in line with results that have been previously reported, namely that a Glycine- as well as Methionine-starting reporters are stable, when expressed transiently in tobacco (Graciet *et al.* , 2010).

Modifications at position two of the degron sequence also did not alter binding. This was tested to see if the positively charged Histidine residue plays an important role in coordination of the peptide chain into the binding pocket. Neither replacement with the more hydrophobic Methionine nor the polar Glutamine showed any influence highlighting the low selectivity of PRT1 for the amino acid at the penultimate position.

The widely used nsP4 sequence originating from the Sindbis virus RNA polymerase (de Groot *et al.* , 1991, Tasaki *et al.* , 2005, Xia *et al.* , 2008c) has already been shown to exhibit increased binding to PRT1 compared to the degron (K2) sequence (fig. 3.8A). These results were confirmed. Not only did PRT1 bind better to nsP4 than the degron (K2) but also elimination of the two internal Lysines disrupted binding regardless if they were altered to Glycines or to the more hydrophobic and aliphatic Isoleucine and Valine (as present in the K2 wild type sequence). This is similar to previous results obtained for yeast Ubr1 in regard to type 1 N-degrons, where it had been shown that Lysines at defined positions of the degron sequence increase degradation rates of a reporter (Suzuki & Varshavsky, 1999).

Similar results are seen when looking at different versions of the luciferase degron sequence from Worley and colleagues (Worley *et al.* , 1998). Elimination of a C-terminal lysine decreased binding significantly. Replacing this Lysine with a negatively charged

---

<sup>7</sup>It can be recognized in *in vivo* in yeast, when acetylated, by a specialized E3 ligase called Doa10 (Hwang *et al.* , 2010a). However, this does not play a role *in vitro*. Additionally, this process has not yet been described in plants.

Glutamic acid further decreased binding, indicating that negative charges might be detrimental for proper degron recognition and binding by PRT1 possibly due to increased surface clashes with the potentially negatively charged surroundings of the type 2 N-degron binding pocket of PRT1, as inferred from the analysis of the ClpS domain from bacteria (fig. 5.7, Erbse *et al.* 2006).

In the end it is difficult to separate recognition and degradation processes when comparing the SPOT results (recognition/binding) with published results regarding reporter stability, since these processes might only be partially dependent on each other. On the one hand degradation is dependent on foregone recognition by the E3, resulting in ubiquitination. On the other hand, recognition of the target by the E3 might not be dependent on the ability to subsequently ubiquitinate the bound target. Initial experiments that highlighted the importance of Lysine residues for the stability of reporter probes cannot differentiate if the observed stability phenotype is either a result of disrupted recognition or degradation (Bachmair & Varshavsky, 1989, Suzuki & Varshavsky, 1999).

Results obtained in the SPOT assay hint more towards a decreased recognition upon elimination of Lysine residues, likely partially due to a decreased positive net charge of the peptide sequence. Also, data published monitoring *in vitro* ubiquitination of a fluorescent and eK-based probe by PRT1 show that elimination of Lysines in the eK sequence, that leads to stabilization of an L-starting reporter *in vivo*<sup>8</sup> (Bachmair & Varshavsky, 1989), leads to altered, albeit not abolished ubiquitination of a reporter, possibly being a result of altered interaction between the target sequence and PRT1 and the fact that, after elimination of Lysines within the eK sequence, now other Lysines are ubiquitinated, that might not be in the ideal distance (Mot *et al.* , 2017).

**An Alanine walk through the W-GUS sequence reveals residues with importance for recognition by PRT1:** An Alanine walk through the Worley-GUS sequence, found to be a well-bound sequence, was analyzed (fig. 3.9B). It reveals that many positions in this sequence indeed have an influence on binding behavior. Especially, the Arginine at position 14 significantly decreased binding albeit not abolishing it. Replacing Arginine with Alanine eliminates a positively charged amino acid, again possibly having a negative influence on binding to the (potentially) negatively charged surface of the binding pocket (Erbse *et al.* , 2006).

**An Aspartate walk through the K2 sequence reveals positions sensitive to introduction of negative charges:** An Aspartate walk through the K2 wild type sequence was done to identify residues where the negative charge of the Aspartate interrupted the binding to PRT1 highlighting positions with potentially close proximity to the surface of the degron binding motif (fig. 3.9C). Not surprisingly, replacing the N-terminal phenylalanine resulted in loss of binding. All other positions, especially in the first half, as well as

---

<sup>8</sup>While L cannot be bound by PRT1 (this work, Mot *et al.* 2017) it is a type 2 destabilizing residue in yeast (Bachmair & Varshavsky, 1989).

the last third, showed that introduction of a negative charge does indeed have detrimental effects on binding. The only exception was the replacement of the Proline at position ten. Probably the negative effects of the Proline is higher than the influence of the negative charge at this position. The same effect had been observed previously when replacing the Proline with Alanine (fig. 3.8C), interestingly however, to a weaker extend. Proline itself is somewhat a special amino acid due to its ring-forming side chain and the inability to adopt many conformations and its preference to introduce a turn structure (Levitt, 1981, Betts & Russell, 2003).

The replacement of residues one to four, especially with a negative charge, probably hinders proper binding within the binding pocket as reported previously for ClpS (Erbse *et al.*, 2006), indicating at least a low sequence selectivity for these peptides. As with the previously executed Alanine walk, replacing residues 12 to 13, results in decreased binding. This effect is however significantly more pronounced when introducing an Aspartate instead of Alanine. This again suggests a certain importance of the last third of the peptide sequence for binding to PRT1, at least when found in the structural context of a more heterogenous peptide chain as opposed to the well binding Glycine stretches (fig. 3.8D).

**W-GUS/K2 hybrid sequences show a mixed behavior in regard to PRT1 binding:** Hybrid sequences (fig. 3.9D) show mixed results. Combining the N-terminal part of the wild type degron sequence with the C-terminal part of the W-GUS sequence results in a sequence that is bound efficiently by PRT1, albeit less than the two original sequences. Inversing results in a well binding sequence behaving more like a W-GUS wild-type sequence. This might indicate that the reason for better binding to PRT1 is to be searched more towards the N-terminal meaning that the difference between the binding of the W-GUS and the K2 wild type sequence to PRT1 is a result of differences in this part. This seems logical as this is the part being closer to the binding pocket therefore also being in closer proximity to the proteins surface.

Surprisingly, a W-GUS/K2 hybrid sequence did not show significantly improved binding by PRT1 but retained binding when the N-terminal Phenylalanine was replaced by a Glycine. This is opposed to results from the K2 wild-type sequence with a Glycine at position one that abolished binding (fig. 3.9A). This means that either there is a synthesis mistake and there is no Glycine at the N-terminal of this specific peptide sequence, or that this sequence somehow interacts with PRT1 in an N-terminal independent manner, which is something that should be elucidated further.

**Modifications of the eK sequence increase affinity to PRT1:** Surprisingly in all experiments the wild type e sequence starting with Phenylalanine only showed about 50% of the affinity to PRT1 than the K2 degron sequence (fig.s 3.8A and 3.9E). This is astonishing, since this is one of the widest applied sequences in the N-end rule field and has been used in many different reporter constructs (e.g. Bachmair *et al.* 1986, Bachmair & Varshavsky 1989, Mot *et al.* 2017), and was therefore to be expected to be recognized

well by PRT1.

Introducing a Cysteine at the same position as in the K2 degron sequence increased binding significantly, an effect that was additive, when also introducing a negative charge, in form of an Aspartate, for the Lysine at position 15. As opposed to the K2 sequence (fig. 3.9C), the eK sequence seems to benefit from elimination of positive charges, a feature which is highly unexpected. Additional mutation of an Arginine to Alanine does not change the binding behavior. The positive effect of Lysine elimination does not seem to be specific to Cysteine as also introduction of a Valine at said position increases binding by about the same amount. In total one can say, that the eK sequence behaves very unexpectedly, since introduction of a negative charge increased binding by PRT1, a feature rarely seen in other sequences.

### 4.4.3 Conclusions

Summing up, the temperature dependent binding of PRT1 to various sequences has not been discussed in depth. This is because the question arises whether this experiment is actually able to reflect an *in vivo* situation or whether a change of temperature *in vitro* mainly results in *in vitro* specific effects. This setup has been chosen to account for the possible mode of action of conditional recognition of the degron by PRT1.

However, it seems unlikely that the effect would be perceivable in a SPOT assay, even if conditional (temperature dependent) recognition would be the mode of action. This is because the tested peptides, since there is only 17mers tested, are not tested in their structural *in vivo* environment but rather only fixed on a membrane. Two effects are imaginable, namely that the peptides, depending on their sequence, do also, to a certain extent, interact with or influence themselves thereby modulating availability for PRT1, or additionally changing temperature will most likely influence the mobility of all peptides, however probably to a different extent, depending on their primary structure.

While peptide mobility and conformational changes in regard to temperature have been described for significantly longer sequences (Mackay & Chilkoti, 2008), on the membranes the used PEG-linker, that is used to anchor the peptides to the membrane, might play a role. It has been shown before that the length of a PEG-linker is able to influence binding of live cells in a binding study (Heon Lee *et al.*, 2012). While cells and an E3 ligase are by no means comparable, these assays highlight the possible influence of the PEG linker on availability of the ligand.

Another possibility to explain temperature-dependent binding difference of PRT1 to the different peptides would be a certain, albeit low, amount of temperature-dependent conformational plasticity of the PRT1 N-degron binding pocket. Conformational plasticity means that a protein can exist in different conformational stages, induced possibly through factors such as pH, temperature, or ligand binding. Conformation plasticity has been reported in a wide variety of proteins (e.g. Miletto *et al.* 2015, Plattner & Noé 2015,

Kovermann *et al.* 2015), and might play a role in PRT1 binding to the membrane-bound peptides. However, this is purely speculative and would need additional experimental confirmation through means such as e.g. Circular Dichroism (CD) measurements.

Comparison between membranes one and two, at least when looking at the absolute values of PRT1/peptide interaction, is difficult, mainly due to different spacing of the controls and therefore also differential behavior of the sequences. The fact that sequences on the membrane also behave in a certain way connected to their position is somewhat worrying and should be considered.

On membrane 1 all six positive controls were situated on the left side of the membrane. Respectively, this was not beneficial since the overall interaction of PRT1 with the peptides was lower, which in exchange artificially amplified the interaction strength of all other peptides since all values were normalized to that control. This might or might not be an artifact of incubation or synthesis however it should be taken into account when interpreting the results. All in total, it is perceivable that on the one hand the SPOT assay procedure is a very valuable tool to find and identify sequences showing improved binding to PRT1, but that the absolute quantification of interaction data should be interpreted carefully. To my best knowledge this protocol using fluorescently labeled protein is one of the fastest protocols available for SPOT assays regardless if a full quantification is carried out in the end. Additionally, avoidance of an antibody/HRP-based readout (Cushman, 2008, Klecker & Dissmeyer, 2016) significantly simplifies handling and also very strongly binding sequences are efficiently detectable.

Finally, I believe the protocol I developed and implemented offers high potential for large-scale interaction screening, however, I believe that SPOT assays, the way they are currently used, offer merely an idea about interaction and need extensive *in vitro* and *in vivo* verification. Even though the readout can (and was by me) quantified I think the actual output of the assay is more of a qualitative to semi-quantitative nature.

## 4.5 *In vitro* stability assays and heterologous expression do not confirm SPOT assay results

Two variants of the degron N-terminal (namely the wild type (standard K2) N-terminal and the GUS N-terminal from Worley *et al.* 1998) were successfully cloned, purified, and TEV-processed to generate exposed degron versions that were used in cell free degradation assays in plant extract. The W-GUS sequence was chosen because after the first, blot-based, SPOT assays it presented as the strongest candidate.

Unfortunately, the versions starting with the stabilizing residue failed to stabilize indicating an N-end rule independent mode of degradation. However, addition of the potent proteasome inhibitor MG132 indeed stabilized the protein suggesting a proteasome dependent degradation. In a more in-depth approach, the two F-starting versions were labeled

with a fluorescent dye and their degradation patterns measured through in-gel fluorescence. This approach has the advantage that a really quantifiable signal is generated and additionally the blotting steps are omitted subtracting one layer of complexity.

Again, there was no difference in the degradation patterns between the wild type and the optimized W-version. Also, addition of MG132 stabilized both proteins, thus confirming the proteasomal dependent degradation. Summing up, one can say that a cell free plant extract does not seem to be the appropriate system to test degradation rates of the degron cassette due to apparent N-end rule independent degradation effects (fig. 3.10).

Similar results were obtained when the degron versions were co-expressed with PRT1 from the same open reading frame (ORF). The constructs were expressed in the *S. cerevisiae* PRT1 knockout homologue *ubr1-Δ* (Reiss *et al.* , 1988, Gonda *et al.* , 1989, Bartel *et al.* , 1990) to exclude influence by the endogenous Ubr1. The fact that there was no obvious stability differences, when expressing a sole degron construct, without the PRT1 fusion, as a GFP fusion in the wild type or *ubr1-Δ* cells (fig. 3.11), confirms the strong promoter expression, leading to similar effects as observed in *A. thaliana* with a strong equilibrium of the degradation towards stability.

When the degron is co-expressed with PRT1, a strong reduction in GFP fluorescence is detectable. Unfortunately, there is no difference between the two version of the degron's N-terminal used (wild type and W-GUS) (fig. 3.11), still this result shows that the degron is degraded in a PRT1 dependent manner confirming results published previously (Stary *et al.* , 2003, Faden *et al.* , 2016b). However, due to the high ratio of E3 to target of 1:1, differences in the recognition efficiency of the respective N-terminal most likely do not play a role resulting in an efficient degradation in both cases regardless of the N-terminal. The leftover fluorescence can be explained with small amounts of free GFP and with the fact that probably a steady state situation between synthesis and degradation is reached. A control by Western Blot analysis was not successful due to the almost identical size of the two parts of the reference construct (HAT:PRT1:UBQ<sup>mut</sup> = 58,5 kDa, F-K2:GFP = 53,2). Strong signal intensities made a clear distinction impossible.

## 4.6 *In vivo* testing of different N-terminal sequences reveals altered interaction and stability patterns

To confirm the results of the SPOT assays and to elucidate their *in vivo* relevance, protoplast based assays were carried out. A split luciferase assay was used to confirm the altered binding efficiency of different N-terminal sequences to PRT1. A total of 14 different sequences was elucidated. The wild type F-K2 degron sequence showed only weak interaction with PRT1<sub>C29A</sub>. When the wild type version of PRT1 was used there was no signal (data not shown), most likely a result of the ubiquitin ligase activity of PRT1 resulting in degradation of the target or itself through autoubiquitination, therefore not allowing

the luciferase to reconstitute. This was the initial reason to use the PRT1<sub>C29A</sub> mutant that is inactive, due to its proposed inability to interact with E2 enzymes thus blocking all ubiquitination processes such as autoubiquitination (might influence E3 stability) as well as target degradation (Maria Klecker, personal communication).

It is difficult to judge whether this interaction is strong or not because to my knowledge no exact  $K_d$  value of the interaction of an E3 ubiquitin ligase with its target has been determined *in vivo*<sup>9</sup>. Since this particular version of PRT1 is probably not able to recruit an E2 ubiquitin conjugating enzyme it might, or might not, release the target again. Additionally, the interaction with an E2 enzyme can have different effects on the E3 itself. For example it has been described that the interaction of the Anaphase Promoting Complex (APC), a large multi-subunit E3 ligase, with the E2 UbcH10 limits APC activity and enables more stringent target selection (Summers *et al.* , 2008). In the end however, it remains highly speculative whether the disruption of E2-PRT1 interaction does indeed play a role in its target recognition since this mutation will additionally also influence PRT1s auto-ubiquitination ability, an general feature of many E3 ligases that has been linked to several effects such as self-destruction via the proteasome or, contrarily, even enhancement of activity (Scaglione *et al.* , 2007, Amemiya *et al.* , 2008, Ranaweera & Yang, 2013). However, since SPOT assays function in the absence of E2 enzyme one expect that, if any at all, the effect of the E2 on E3-target interaction has only modulatory character.

The different biological replicates gave very various results when compared to the wild type degron, strikingly with high standard deviations making an overall statistical interpretation beyond pure qualitative or semi-quantitative questions somewhat questionable. Additionally, many of the different sequences tested *in vivo* gave results very different to what was deducible from the SPOT assays. On the one hand sequences like W-GUS, W-LUC, and nsP4 behaved as expected, namely by showing increased interaction (albeit not statistically significant for Worley-LUC). Other sequences, on the other hand, such as G-GUS, poly-Glycine, and poly-Glycine-Serine sequences showed a behavior diametral to what was expected after interpretation of the SPOT assays.

While the G-GUS and poly-Glycine sequences, that showed high affinity *in vitro* for PRT1 binding, did not interact strongly with PRT1<sub>C29A</sub>, the thought to be non-binding poly-Glycine-Serine sequence mediated a significantly increased interaction with PRT1<sub>C29A</sub>, a result completely opposite to the SPOT assays. Also, the eK sequence, not binding well to PRT1 *in vitro* showed such increased interaction. Other effects, such as the improvement of interaction upon elimination of negatively charged amino acids or the elimination of Lysines leading to decreased binding could mainly not be confirmed in this assay. Neither did the elimination of the negatively charged Glutamic acid (E) in the Worley-GUS sequence or Aspartic acid (D) in the Worley-LUC sequence result in increased interaction nor did the elimination of Lysine in this sequence lead to dramatically decreased binding

---

<sup>9</sup>Yeast Ubr1 has a  $K_d$  of ca. 2  $\mu$ M *in vitro* (Xia *et al.* , 2008c).

affinity. The only other sequences that behaved as expected were the nsP4 sequence without Lysines (nsP4-K) as well as the non-interacting controls starting with Methionine and Glycine.

Another issue might be of a structural nature. Since the first 16/17 amino acids of the degron cassette starting from the N-terminal Phenylalanine were exchanged also the first eleven amino acids of the DHFR are modified. The last seven of these amino acids are part of a  $\beta$ -sheet and modification of these amino acids might influence the structural integrity of the DHFR. For example it would be possible that the long Glycine stretch containing sequences tested fit better into the structure and are more hidden being actually less available than on the SPOT assay where they are surface-exposed and potentially very mobile. Other sequences might also fit into the existing DHFR structure or might have influences on the overall structure of the protein.

Still, this experimental setup had some properties that might not have made it a perfect choice for verification of SPOT results. First of all normalization happened via a second construct (*ProUBQ10:GUS*), also because the almost identical size of the expressed proteins impeded a satisfactory separation and analysis using SDS-PAGE and antibody based detection. Moreover, the normalization of transformation efficiency using reporters such as GUS or full length luciferase (see e.g. Guo *et al.* 2012, Jeon *et al.* 2007, Sheikh *et al.* 2016), can be problematic when elucidating protein binding affinity and interaction.

The absolute interaction strength, measured by the luminescence output, depends on the ratio of the two interactors as well as their absolute concentration. This is so because the  $K_d$  of the protein is defined by a saturation curve rather than a linear curve. This means that a sample with low concentrations of both interactors, due to insufficient transformation efficiency would significantly underestimate interaction strength when using the secondary GUS signal to normalize it to a second sample with good transformation efficiency. Naturally, such an effect also would hold true the other way around. Additionally, recently it has been discussed that the intensity of luminescence in a split-luciferase assay actually is not linearly correlated itself with interaction strength and it tends to underestimate especially samples with high luminescence signals. It was suggested that the correlation between the interaction strength of a protein pair and the emitted luminescence is indeed non-linear (Dale & Kato, 2016).

All this, the obvious discrepancy in regard to the *in vitro* data as well as the recently defined shortcomings of the split luciferase system in regard to kinetic analysis suggests at least a certain cautiousness when interpreting the results. Also, if the reporter constructs featuring the nsP4-k or G-GUS variant at their respective N-terminals do not interact, even they were shown to be (strong) interactors in the SPOT assays, that indicates that the sensitivity of this approach, especially in the range of potential weaker interaction, is very limited.

To see whether *in vitro* and *in vivo* interaction data would actually translate into de-



creased stability, a luciferase based stability assay was carried out determining the PRT1-dependent stability again in protoplasts (fig. 3.12 B). All sequences except the W-GUS sequence without Glutamic acid as well as the W-LUC sequence without Lysines led to a significantly decreased stability. While this effect is in line with SPOT results (elimination of Lysines led to weaker interaction) for the W-LUC sequence without Lysines, it is contradictory for the W-GUS sequence without Glutamic acid since elimination of negative charges should lead to better interaction with PRT1 and therefore to decreased stability.

Notably, the standard deviation for all sequences tested, except the stable M and G starting controls, exhibited far lower scattering and variability in case of the stability assays than the split luciferase assays did. The sequences containing long Glycine stretches indeed conferred high instability. This includes the Glycine-Serine containing sequence, indicating that the absence of interaction in the SPOT assay is actually not a propensity of this sequence but apparently only an artifact/false negative result of the SPOT method. The problem of the luciferase stability assay, besides the possible appearance of structural "stress" due to the exchanged N-terminal, as mentioned above, is that it can only be carried out at room temperature, because of the transient nature of the system and the observation that especially elevated temperatures lead to a generally increased protein accumulation, probably as a combination of a high copy number of transgenes and faster translation. It therefore only catches a glimpse of the whole kinetic range of the degron. One possibility would be for example that the alternative N-terminal sequences do not influence stability *per se* but rather alter the (de)-stabilization kinetics. This would be beneficial to know since already the protein of interest does have a severe influence on said kinetic (see section 4.8).

Maybe, sequence optimization of the degron's N-terminus using SPOT assays and protoplasts is overall misguided. If indeed conditional degradation/ubiquitination is the degron's mode of action then introduction of sequences potentially disturbing the degron's structure and introducing higher conformational flexibility might alter the whole protein stability making the already existing point mutations functionally obsolete and rendering the degron cassette intrinsically more stable. Additionally, if the exchange of the N-terminal peptide chain leads indeed to structural rearrangements or disturbances within the DHFR moiety, this process itself might act as a degron e.g. by exposure of hydrophobic patches degradation at any temperature could happen in a PRT1 independent way. In animal cells it has been shown that exposure of hydrophobic patches recruits chaperones such as HSP (Heat-Shock Protein) 40/70 which facilitate recognition by the E3 ligase CHIP resulting in proteasomal-dependent degradation (reviewed in Goldberg 2003). Also in *A. thaliana* the existence of an HSP70/CHIP mediated degradation pathway has been shown (Lee *et al.* , 2009, Zhou *et al.* , 2014), making the possibility, that N-terminal exchanges and the resulting possible exposure of hydrophobic patches through misfolding of the DHFR moiety within the degron result in increased degradation rates, all the more likely.

Still, also such a more destabilized degron version might have its benefits e.g. for destabilization of very stable proteins of interest. Problematic is also the fact that the kinetics of degron (in)stability can not properly be addressed in a transient transformation environment since in protoplasts, but also in tobacco, temperature is directly connected to transformation efficiency as well as protein expression from the introduced transgene. This, together with the strong promoters usually used in these experiments, lead to an effect where cells usually accumulate more protein under warm conditions when e.g. performing shift experiments (data not shown). Therefore, the degron should best be optimized and tested in stably transformed *A. thaliana* lines, or another kind of stable transgenic system, using weaker promoters and ideally also different proteins of interest exhibiting different stability such as e.g. GUS and LUC (stable (50 Jefferson *et al.* 1987) vs. instable (1 h Koksharov & Ugarova 2011)).

### 4.7 Conclusions from the degron optimization approach

The newly developed and improved SPOT assay represents a valuable tool for the science community. However, the results obtained by the method in regard to the goal of improving the degron is rather limited, at least by the means of verifications obtained here. There is two main issues, one being the still unclear mode of degradation of the degron, the other one being that a temperature stimulus is difficult to screen in transiently transformed organisms.

It is not surprising that many sequences could be identified that bind better to PRT1 than the wild type sequences. Judging from the fact that, in the *in vitro* environment, the long Glycine-containing sequences bound best to PRT1 suggests that an old dogma of N-degron definition is actually accurate namely that the N-terminal must be mobile and accessible. Following that logic, only the N-terminal Phenylalanine plays an important role and the nature of the subsequent amino acids is rather insignificant as long as they do not create structural clashes with the surface of PRT1. The fact that the original degron also addressed the Arg-branch of the N-end rule, taken together with the fact that also degron-GFP stably expressed in *A. thaliana* were efficiently degraded regardless if an Arginine or Phenylalanine was presented at the N-terminal, hints more towards a mode of degradation mostly independent of the primary structure subsequent to the N-terminal. The fact that an alternating Glycine-Serine sequence did not bind in the SPOT environment could be most easily explained with a synthesis problem, since the sequence behaved as expected in the other assays. However, since the peptides are covalently bound to the cellulose membrane and are not elutable verification via e.g. mass spectrometry is not possible right now. Also a scenario could be imaginable where the massive amounts of Serines within this sequence produces hydrogen bonds, e.g with the neighboring peptide chains or even with the cellulose matrix, thereby altering secondary structure and making the sequence

unavailable for PRT1.

The degron cassette is, due to its structural context, also not the appropriate environment for the verification and mapping of more general properties of an N-degron. If such an attempt is undergone, N-terminal exchanges should be carried out in a destabilizing sequence such as e.g. the eK sequence, something that has been started in yeast (Bachmair & Varshavsky, 1989).

In the end, three different parameters are available for optimization and changing that define the degrons capabilities. For once the range of stabilization (high stability at permissive temperatures and low stability at restrictive temperatures), a more narrow range between temperature extremes to prevent phenotypic differences in the used organism, and altered kinetics e.g. versions with a small transition zone for efficient and fast changing between states of stable or unstable protein versus versions with longer transition zones better suited for tuning of intermediate protein stability situations. Unfortunately, the POI has a rather strong influence on this behavior so additional work should be done reach at least a basic scheme of classification of POI in regard to their behavior as a degron fusion protein.

Additionally, the SPOT assays indicated a reliable and strong recognition of the degron sequence by PRT1, overall indicating that optimization in regard to PRT1 binding might not be necessary, or at least might not play a role *in vivo*, since in an endogenous environment with significantly lower amounts of available PRT1 it might not play a role whether the target sequence is well-binding or extremely well-binding.

## 4.8 The degron's mode of action is most likely a predominant mix of conditional ubiquitination and conditional degradation

Overall the detailed mode of action of the degron on a molecular level is unclear. However, DHFR proteins have a long history of serving as stability reporters (e.g. Tasaki *et al.* 2005, Xia *et al.* 2008c), therefore, together with the results found in the making of this work, allowing to postulate a model of degron degradation that mainly relies on conditional ubiquitination and conditional degradation and not excessively on conditional recognition by PRT1

The original mode of action postulated for the original yeast degron system was that of conditional ubiquitination. It was argued then that through increased structural flexibility at the restrictive temperature, the mutated DHFR moiety would reach a state of higher conformational flexibility making some Lysines, previously inaccessible in the tertiary structure of the DHFR, now available for ubiquitination, finally leading to the degradation of the degron (and its fused POI) (Dohmen *et al.* , 1994). This mode of action has been

proposed as well for the degron version used in this work, supported by *in silico* modeling data, suggesting mainly Lysines in the vicinity of the E173D mutation of K2 becoming accessible after a shift to restrictive temperature (Faden *et al.* , 2016b)<sup>10</sup>.

The proposed mode of conditional ubiquitination indeed fits to previous results obtained when mapping the stability of the eK sequence *in vivo*. In these experiments, different versions of the eK-sequence, fused to a non-mutated DHFR, were tested for their stability in yeast (Bachmair & Varshavsky, 1989). The eK-DHFR reporter stabilizes efficiently, when the two Lysine residues within the eK-sequence are eliminated. This shows that a non-mutated DHFR cannot be ubiquitinated or degraded *in vivo*, which most likely reflects the degron's behavior at the permissive temperature. No Lysines are available for ubiquitination therefore the protein remains stable<sup>11</sup>. The ek-DHFR reporter probe has also been shown to be recognized by PRT1 in plants as it has been used to identify the *prt1-1* mutant allele via a mutagenesis screen, where the ek-DHFR probe stabilized efficiently after disruption of PRT1 functionality (Bachmair *et al.* , 1993).

The second prerequisite of proteasomal degradation, namely the presence of flexible regions needed for degradation initiation, has to be taken into account. It has been demonstrated conclusively that proteins, such as e.g. Rad23 in yeast (Fishbain *et al.* , 2011), can be heavily ubiquitinated but still escape proteasomal degradation due to their structural rigidity (Takeuchi *et al.* , 2007, Fishbain *et al.* , 2011, Yu *et al.* , 2016). Intriguingly, this work also uses a DHFR protein for *in vitro* stability assays with purified yeast proteasome, showing once more that a DHFR, without addition of flexible regions, remains stable. Flexible regions at the N- or C-terminal of a protein can be as short as 25 amino acids to confer instability (Verhoef *et al.* , 2009) and proteins become more unstable with increasing length of the flexible regions (Takeuchi *et al.* , 2007, Fishbain *et al.* , 2011, Yu *et al.* , 2016). This fits well to the stability behavior of the ek-DHFR protein described previously (Bachmair & Varshavsky, 1989) that stabilizes also, when decreasing the length of the eK sequence which is originally 42 amino acids long and has therefore a length found to be sufficient to mediate instability (Verhoef *et al.* , 2009).

This is another strong hit towards the hypothesis that a non-mutated DHFR itself does not even offer Lysine residues accessible for ubiquitination since the ek-DHFR probe with the long eK linker but without Lysines in this linker remains stable (Bachmair & Varshavsky, 1989). While it would be possible that the DHFR is not ubiquitinated due to the Lysines not being in the right spatial distance to the E3, this seems unlikely since the DHFR contains a total of 16 Lysines, with many of them in the vicinity of the C-terminal, where they, since the N- and C-terminal are in close vicinity (fig. 5.21) should be ubiquitinated, if they were available. The fact that an eK-starting probe is still ubiquitinated by

---

<sup>10</sup>The original yeast degron carries one P66L mutation (Dohmen *et al.* , 1994), whereas K2 carries two mutations, namely T39A and E173D (Gowda *et al.* , 2013, Faden *et al.* , 2016b).

<sup>11</sup>While the nsP4 sequence could not be recognized anymore by PRT1 in the SPOT assay upon Lysine mutation (fig. 3.9A), this is not the case for the eK sequence (fig. 3.9A, Mot *et al.* 2017).

PRT1 *in vitro*, even if no Lysines in the direct vicinity of the probe's N-terminal are available, shows that PRT1 shows a certain flexibility in its ubiquitination activity (Mot *et al.*, 2017).

The N-terminal extension of the K2-construct, that can also be found in the original yeast degron, consists of five amino acids starting at the penultimate positions (the ultimate position being the primary destabilizing residue). Exactly this extension (X-HGSGI-M; X = primary destabilizing residue, M = Methionine of the DHFR), combined with an unmutated DHFR, has been shown to be completely stable in yeast (Bachmair & Varshavsky, 1989).

Two questions now remain. For once, if the degron also relies on flexible regions in order to initiate degradation, where are these to be found, and secondly what is the influence of the POI on the behavior of the degron-POI fusion?

The N-terminal linker of the degron is significantly too short to serve as a region of initiation of degradation at the proteasome. This raises the question how exactly the degron initiates its degradation after being ubiquitinated and recruited to the proteasome. It was shown that flexible regions for efficient degradation initiation at the proteasome, that are situated within the protein, have to have a minimal length of 95-100 amino acids to initiate degradation (Fishbain *et al.*, 2011, Yu *et al.*, 2016). Since the whole DHFR is only 189 amino acids long this would mean a more or less complete unfolding, or at least drastically increased structural flexibility which seems a bit far fetched, since the T39A mutations does not seem to induce any conformation distress on the overall structure and only the E173D mutation induces structural clashes (fig. 5.21). If one postulates unfolding this would be the result of only one mutation. Therefore degradation initiation via either the N- or C-terminal seems more likely. While the N-terminal in the wildtype DHFR which, according to the structure (fig. S 5.21, Pettersen *et al.* 2004), would have a flexible sequence of only ten amino acids, which would not be sufficient for degradation initiation, it might be possible that overall higher structural flexibility leads to elongation of this stretch enabling degradation via the N-terminal.

However, it seems more likely that the C-terminal might be the access point crucial for degradation initiation. When recombinantly expressed and purified K2-versions were incubated in a plant extract they were degraded in a proteasome dependent manner (fig. 3.10). This indicates that a degron cassette, even without the a fused POI, can be degraded by the proteasome. In this case the free C-terminal, consisting of linker regions and a triple-HA tag might be the starting point of degradation. Since the E173D mutation that was shown to induce structural flexibility (fig. 5.21, Faden *et al.* 2016b), is close to the N-terminal it is tempting to speculate that it would also be responsible for an increased flexibility in this region allowing the initiation of proteasomal degradation.

The degron itself, without a POI, would therefore rely on a mixed mechanism of conditional ubiquitination and conditional degradation most likely happening simultaneously at

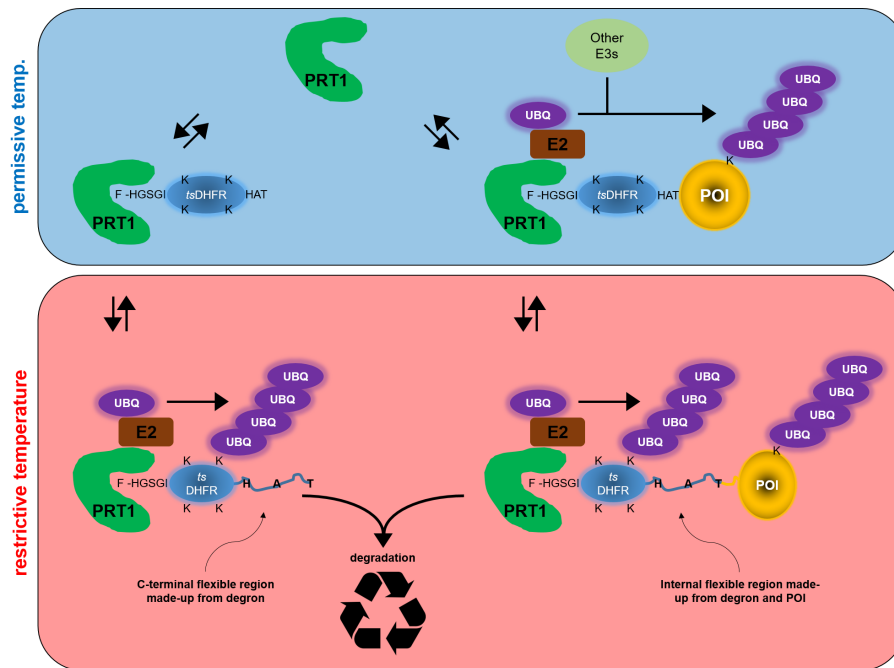


**Figure 4.1 – Model of degron degradation.** At the permissive temperature the degron cassette cannot be ubiquitinated or degraded. However, a fused POI might potentially be ubiquitinated, also by other E3s than PRT1. Upon shift to the restrictive temperature the degron itself is ubiquitinated and flexible regions allow initiation of degradation.

the restrictive temperature.

How might the POI now influence the kinetics of the entire fusion protein? Ubiquitome enrichment of K2:GUS from the *ProUBQ10:K2:GUS*-expressing line showed that also at the permissive temperature the protein is ubiquitinated (fig. 3.2C). If one follows the hypothesis of the conditional ubiquitination of the degron this would mean that ubiquitination, in this case, would be exclusive to the GUS moiety. Analysis of the crystal structure of the murine DHFR (fig. S 5.21) indicates that N- and C-terminal of the protein are in close proximity to each other. This might indicate that also in the case of a ubiquitination event, PRT1 would be in close vicinity of the protein of interest located at the C-terminal of the DHFR possibly facilitating ubiquitination of the POI in a temperature independent manner.

Naturally, it cannot be excluded that other E3 ligases might play a role in this ubiquitination process. Interestingly, ubiquitinated species of K2:GUS remain completely stable as indicated by proteasome inhibitor treatments of K2:GUS expressing seedlings where no accumulation of K2:GUS at the permissive temperature could be observed (fig. 3.2A). This is most likely based on the intrinsically high stability and rigidity of the GUS protein that does not offer flexible regions for proteasomal degradation.

Contrarily, it has been demonstrated previously that a degron fusion with the transcription factor TRANSPARENT TEST GLABRA1 (TTG1) also further stabilizes at the permissive temperature when crossed into the *prt1-1* mutant background indicating that

---

here ubiquitinated subpecies are removed from the cell (Faden *et al.* , 2016b), possibly because TTG1 offers a higher degree of conformational flexibility than GUS. The fact that POIs can potentially be ubiquitinated at the permissive temperature probably decreases the influence of the conditional degradation of the mutated DHFR in the degon cassette in response to the different temperatures making conditional degradation the prevalent mechanism of degon-POI degradation through the proteasome.

Still, one question remains. If one assumes that the C-terminal of the free degon cassette serves as the point of degradation initiation then fusion with a POI poses a problem since now the C-terminal region becomes an internal region. While terminal regions have been shown to confer degradation also when they are relatively short (Verhoef *et al.* , 2009), internal regions need at least a length of 95 to 100 amino acids to efficiently confer degradation (Fishbain *et al.* , 2011, Yu *et al.* , 2016). The only explanation would be that this region now consists of a large portion of the DHFR, plus the HA-linker, as well as the N-terminal of the POI to reach a length sufficient for degradation initiation.

In the end also conditional recognition could play a minor role. This would mean that the N-terminal can only be recognized by PRT1 at the permissive temperature. The SPOT assays, where binding at different temperatures was elucidated, rather hinted towards conditional recognition not playing an immense role. While some sequences show different binding affinity by PRT1 no sequence abolishes binding upon temperature. Of course one has to take into account that the 17mere peptides on the membrane are not in their natural structural context, therefore they might not completely reflect the *in vivo* situation. The stability and interaction studies using the luciferase-based approaches only offer limited insights into this question as they were all carried out at ambient temperature. While interaction behavior of PRT1 with the different N-terminals is clearly altered this might be a result of the N-terminal exchange disturbing the overall DHFR-structure (see section 4.6 and 4.7).

Summing up, I suggest a mechanism where, at permissive conditions only the POI can potentially be ubiquitinated, which might be due to the action of PRT1 or other endogenous E3 ligases. If the POI can provide a degradation initiation point these species are removed from the cell. If the POI does not possess such a region the ubiquitinated species remain stable. The ubiquitination itself hints towards conditional recognition not playing an important role in degon ubiquitination and degradation. Once switched to restrictive conditions the point mutation close to the C-terminal of the DHFR induces conformation flexibility which should increase the length of the flexible region to a point sufficient for degradation initiation. Now, also additional ubiquitination through availability of Lysine residues on the DHFR will most likely play a role.

## 4.9 The degron system compared to other conditional degron techniques

A degron is defined as a peptide sequence within a protein conferring its instability and therefore its degradation (Varshavsky, 1991). A conditional degron therefore would be such a degradation initiation sequence that is not constitutively exposed but that would only be accessible to the degradation machinery upon a certain stimulus. Following, the N-degron system is compared to other well established systems of conditional protein degradation.

However, only systems functioning directly on the level of active protein are assessed as they represent the direct competitors to the degron system. Also potential other degron sequences that have not yet been used in the context of biotechnological or synthetic biology, such as the widely adopted eK (extensions containing Lysines) sequence (Bachmair & Varshavsky, 1989), the discussed jasmonate-based degron (Sheard *et al.* , 2010), or various destabilizing viral sequences (Sen *et al.* , 2007) will not be discussed, because this part of the discussion focuses on comparison with already established and applied techniques to evaluate strength and weaknesses of the system and to offer potential adopters the possibility to make an informed choice about which system to use.

The auxin-induced degron (AID) is a system based on the transfer of the plant auxin-dependent degradation pathway into a heterologous organism (Nishimura *et al.* , 2009). In plants auxins, a family of plant hormones, bind to the F-box protein TRANSPORT INHIBITOR RESPONSE 1 (TIR1) and regulates its binding to the IAA transcription repressor. TIR1 is part of the SCF-TIR1 complex *in planta*, a multi-subunit E3 ligase, capable of recruiting an E2 ubiquitin conjugating enzyme. Auxin serves as a sort of molecular glue promoting the interaction of the IAA transcription repressor with the SCF complex therefore promoting its ubiquitination and subsequent degradation. SCF complexes can be found in all eukaryots with only the adapter protein, in this case TIR1, differing. Therefore, fusing a protein of interest to the IAA transcription repressor, and parallel ectopic expression of the TIR1 adapter protein, will mediate the destruction of the IAA-carrying protein in response to auxin.

The auxin inducible degron has been used successfully in a variety of different organisms, however mostly, on the level of cell culture or single-celled organisms (Nishimura *et al.* , 2009, Holland *et al.* , 2012, Kreidenweiss *et al.* , 2013, Heider *et al.* , 2015). The only example where this system has been used in an intact multi-cellular organism has been described recently in the nematode *C. elegans* (Zhang *et al.* , 2015). Also, a combination with transcriptional repression to generate more tightly controlled conditional mutants in yeast has been reported (Tanaka *et al.* , 2015). A further improvement of the technique now allows for a CRISPR/CAS-based tagging of endogenous proteins, therefore generating conditional mutants, however, again only in cell culture (Natsume *et al.* , 2016). Compared to the N-degron approach described in this work there is some shortcomings of the auxin-



based system. First of all its general applicability in higher organisms has yet to be demonstrated, even though initial experiment in *C.elegans* indeed look promising. Control of Auxin uptake can be difficult, e.g. an age-dependent efficiency of the system in *C.elegans*, depending on the developmental stage of the nematodes presumably based on "differences in the rates of auxin uptake or diffusion through tissues", has been described (Zhang *et al.* , 2015).

Even though the degradation rates of the auxin-based system appear superior to that of the N-degron approach, with the auxin-based system removing proteins from cells within 30 minutes to one hour post induction, depending on the auxin concentration, washing out of the elicitor can be significantly more tedious because efficiency of the removal is highly dependent on the applied concentration of the elicitor (Zhang *et al.* , 2015). This issue is efficiently circumvented by the temperature stimulus controlled N-degron.

Another disadvantage of the auxin-based system is the limited ability for tuning of protein amounts. While the N-degron allows for efficient tuning of amounts of active protein based on the exposure to intermediate temperatures (fig. 3.1E) intermediate amounts of auxin only result in changes in the degradation kinetics but do not seem to result in intermediate protein levels. Also, even if such a stage could be reached, this would require to constantly grow the organism on a certain level of auxin, something that might be very difficult to monitor and additionally costly. Last, the auxin-based system is only available in heterologous, ergo non plant, systems as opposed to the N-degron.

Another system, also engaging an SCF-complex, is based on the degradation of a GFP moiety called deGradFP. In this technique an engineered F-box protein combined with an anti-GFP antibody fragment recruits GFP, and proteins fused to it, to the SCF complex initiating their degradation. In *D. melanogaster* embryos this approach has been used successfully to generate conditional null mutants (Caussin *et al.* , 2011). The fact that a GFP moiety is used as a degron allows for easy monitoring of degradation efficiency. Even though proteins are removed relatively quickly from the cell, within approximately four hours in cell culture, the applicability of this technique in multicellular organisms has still to be demonstrated. Here, usually a second layer of control over protein abundance is needed, e. g. the adjustment of the expression level of the F-box protein mediating recruitment to the SCF. Nevertheless the deGradFP approach constitutes one of the few techniques available which are also able to act on transmembrane proteins if the GFP is on the cytosolic side of the protein making it available for the ubiquitin system, something that has not been attempted with the N-degron yet. In the end the deGradFP approach possesses the advantage of velocity and monitoring but again does not allow for easy tuning and reversion of degradation effects.

Another well established system relies on an engineered FK506- and rapamycin-binding protein (FKBP12) that confers conditional instability by adding a so called destabilizing domain (DD) to a fused protein of interest, but can be saved from degradation through

addition of a small compound termed Shield1 (Shld1), efficiently stabilizing the fusion protein (Banaszynski *et al.* , 2006). This system allows a rapid depletion as well as tunability of protein amounts using intermediate concentrations of the stabilizing compound Shld1. The DD-based approach has been successfully applied to cell cultures (Banaszynski *et al.* , 2006, An *et al.* , 2015), single celled organisms such as *Toxoplasma gondii* (Herm-Götz *et al.* , 2007) or *Plasmodium* (Armstrong & Goldberg, 2007), and even whole mice (Berdeaux *et al.* , 2007, Banaszynski *et al.* , 2008, Rodriguez & Wolfgang, 2012). Like the N-degron approach, this system allows a real tunability of protein content however long term tuning to intermediate protein amounts might be difficult due to the needed monitoring and maintenance of Shld1 levels.

An additional, also Shld1 based, system has been established in the same group. In this case a different version of the FKBP protein, termed LID-FKBP, confers instability when Shld1 is added. Even though it has not yet been applied widely, it shows interesting prospects since the concomitant use of DD-FKBP12 and LID-FKBP12 potentially allows for simultaneous stabilization and degradation of two different POIs in the same cell (Bonger *et al.* , 2011).

A new, conditional degron system that has emerged recently is based on blue light illumination as the environmental stimulus for degradation. It consists of a LIGHT OXYGEN VOLTAGE SENSING DOMAIN 2 (LOV2) from *A. thaliana* PHOTOTROPIN 1 (PHOT1) combined with the murine ornithine decarboxylase-like degradation sequence (cODC1) (Renicke *et al.* , 2013a), termed the photosensitive degron (psd). The system mediates efficient degradation via the UPS within four hours of blue light illumination. Treatments with cycloheximide, a strong inhibitor of protein synthesis, showed even that the half-life of proteins fused to the psd is less than 30 minutes in yeast indicating a strong destabilization effect (Renicke *et al.* , 2013b). Additionally, tunability using intermediate light intensities, high spatial and temporal resolution, and the ability to use the psd module for the generation of conditional mutants were demonstrated (Renicke *et al.* , 2013b). The degradation mechanism of cODC1 is conserved in yeast, vertebrates, and plants potentially making the degron extendable to these systems, naturally with limitations in organisms, such plants, mammals, and birds, that are able and/or rely on blue light perception. The psd module has been further optimized with various cassettes with different stabilization/destabilization behavior being available (Usherenko *et al.* , 2014). Also it has been applied successfully in the nematode *C.elegans* to create a conditional knock down situation in the central nervous system (Hermann *et al.* , 2015).

An engineered version of the LOV2 domain from *Avena sativa* combined with an alternative peptide degron, replacing the cODC1 degron to control protein stability in mammalian cells as well as zebrafish embryos, thus expanding the use of light induced protein destabilization to these important model systems was used (Bonger *et al.* , 2014). Compared to the N-degron system the light induced system shares the benefit of a potentially non-toxic,

however possibly developmental influential, inducer as well as the possibility for efficient tuning of protein amounts.

The use of light restricts these systems to small or single celled organisms or to outer cell layers due to probably decreased light penetration into deeper tissues as well as it excludes organisms that sense and/or need blue light for survival.

Recently, the auxin inducible degron (see above) was combined with a chemically modified photoactivatable auxin, hence increasing the spatiotemporal resolution of the AID-system in yeast and mammalian cells. Although the idea is appealing, this system has not been adopted widely yet (Delacour *et al.* , 2015).

Yet another system that was applied in yeast is the TEV Induced Protein Inactivation (TIPI) system (Taxis *et al.* , 2009, Jungbluth *et al.* , 2010). It relies on a dormant degron containing a conserved TEV protease cleavage site. The original approach only contained an N-degron resulting, after TEV cleavage, in an N-terminal fragment showing a primary destabilizing residue according to the N-end rule which leads to rapid removal of the protein from the cell. The N-terminal fragment would serve as a stable control. An adapter protein fused to the TEV protease with its recognition site close to the site of targeted cleavage resulted in rapid and efficient cleavage upon TEV induction (Taxis *et al.* , 2009) by recruiting the protease directly to its destination. In a later approach the system was extended through introduction of the cODC1 degron upstream of the TEV cleavage site. Therefore, both fragments would carry a degradation signal upon TEV cleavage. Through this approach the system acquired higher flexibility, because now target proteins can be tagged for degradation via their respective N- and C-terminal (Jungbluth *et al.* , 2010). However, the system has only been applied in yeast so far and because the regulatory unit is the TEV protease, which is controlled through promoter induction, it inherits all the disadvantages of regulation on transcriptional/translational level, namely induction speed and poor reversibility. Therefore the TIPI system remains more a system for rapid and targeted protein depletion rather than offering tuning and adjustment properties such as the N-degron approach.

In general *ts* allele approaches are naturally the most comparable to the optimized N-degron approach. Such temperature sensitive alleles have long been used in basic research as they allow direct control over a protein of interest in its natural biological context. However, identification of these alleles is tedious as it usually requires large mutational screens and is therefore, with few examples, restricted to unicellular organisms or cell cultures with short generation times. A work-around was published, however the reported approach for plant *ts*-alleles employs targeted mutagenesis based on structural information as well as heterologous testing of the mutations in the moss *Physcomitrella patens* (Vidali *et al.* , 2009), an approach that still (A) relies on structural information being available on the protein of interest (POI) as well as (B) requiring that said tested POI can elicit a phenotype in the heterologous organism. Western Blot analysis, in the absence of a

phenotype, would be theoretically possible but impracticable due to the large amount of samples.

The original *ts*-degron cassette was the first system to circumvent the problems of *ts*-allele identification by introducing the N-degron cassette generating artificial *ts*-alleles of a given POI (Dohmen *et al.* , 1994). This approach has been used extensively in yeast and also in some other organisms, however mainly in cell culture (reviewed in Faden *et al.* 2014). Another work-around is the use of temperature sensitive inteins resulting in temperature dependent splicing of the POI (Zeidler *et al.* , 2004). A library of different intein switches is readily available (Tan *et al.* , 2009). This technique has two downsides, namely the fact that the intein sequences have to be introduced into the POI, making cloning more difficult and secondly the splicing process adds another layer of processing. To date this technique has been applied in *D. melanogaster* and yeast.

Later applications of similar systems combine the self-processing abilities of inteins with the formerly mentioned LOV2 domain to obtain light-splicable modules in mammalian cells, bacteria, and yeast (Wong *et al.* , 2015, Jones *et al.* , 2016). Even a salt inducible version has been successfully demonstrated to function *in vitro* (Reitter *et al.* , 2016). This shows broad potential for the application of inteins. Still, to-date no large scale experiment, using the technique, has been performed and detailed kinetics of the system's behavior have yet to be elucidated. So far the original work suggests tuneability via intermediate temperatures but this has not yet been looked at intensively (Zeidler *et al.* , 2004).

Summing up the degron approach presented in this work is one of the most versatile solutions available in the field. It suffers from only very few species restrictions and is not burdened by secondary effects of chemical elicitors or prone to uneven induction through insufficient tissue diffusion of said elicitor. The sole limitations of the degron is its restriction to poikilothermic and eukaryotic organisms. This should still make it available in mammalian cell cultures but definitely makes it unavailable in higher animals such as mice. What makes the optimized N-degron approach superior to many of the aformentioned techniques is the possibility for protein tuning as well as the fact that its applicability has been demonstrated in the most important model organisms.

Similar possibilities have been demonstrated for the Shld1 based system (Banaszynski *et al.* , 2006) in mammalian cells, albeit the same potential in multicellular organisms has yet to be demonstrated and might be impossible due to penetration difficulties of the Shld1 compound into the organism. While the different degrons discussed above all have their respective strength and advantages, the optimized N-degron approach presents the optimal compromise between ease of use and efficiency.

Generation of N-degron fusion constructs is now more straightforward than ever since the assembly of a new vector for easy degron-tagging, which offers high variability through use of the gateway system.

## 4.10 Outlook - How to map degron kinetics, mode of action, and the influence of the POI

This work highlights the general applicability of the degron technique and the wide array of possible applications in different organisms. However, a real and in depth characterization of the degron cassette with or without different proteins of interest is still not completed and would be crucial for a better understanding and therefore improved application of the technique. For now, the system has never been analyzed *in vivo* without any protein of interest fused to its C-terminal, an approach crucial for determining the influence of the protein of interest on the overall behavior of the degron. Two important questions would have to be answered: First, what are the exact stabilization/degradation kinetics of the degron cassette and second, what is the precise mode of action (see section 4.8).

The accurate characterization of the degron actually poses some intrinsic difficulties, such as detection of the cassette in a large scale and screenable format. It seems logical that stably transformed *A. thaliana* lines do not necessarily represent the quickest screening system, mainly since the generation of reporter lines is lengthy and large scale generation of material needs at least some phytocabinets with a tightly controlled environment. A pre-screen could be done using *D. melanogaster* cell culture. They are stably transformable, especially since there is vector sets available that co-express GFP or other fluorescent markers in a multicistronic way similar to the Ubiquitin-Reference-Technique (González *et al.* , 2011) and they grow at an ideal temperature of 25°C. While this is not exactly the intermediate temperature for the degron it was shown that they support the temperature shift associated with degron usage (fig. 3.4C/D, Faden *et al.* 2016b).

Stably transformed *D. melanogaster* cells carrying a degron cassette, additionally tagged with a FLAG or STREPII tag, could offer a system that is easily maintainable, offers high protein yields, reacts to the temperature stimulus, and should be relatively easy to generate. Yeast or also mammalian cells would conceivably be suitable systems as well, however protein extraction from yeast can be more tedious and mammalian cells' ideal growth temperature of 37°C is far away from the degrons usual temperature range. These cells would be more suitable for work with the original yeast degron such as it has already been done in chicken cells where a restrictive temperature of even 42°C was used (Su *et al.* , 2008, Bernal & Venkitaraman, 2011). FLAG or STREPII tags could be incorporated in the linker region up- or downstream of the already present triple HA-tag. They present a good compromise of cost, purity, and yield of the purified protein when used for production of recombinant proteins in different organisms (Lichty *et al.* , 2005). Additionally, modification of this linker region could already provide some experimental data on whether this region might be involved in the degradation initiation of the degron cassette, as hypothesized (see section 4.8)

Quantification of degron stability could be achieved using a quantifiable Western Blot

analysis, best using fluorescent antibodies (Faden *et al.* , 2016a) where the signal could be normalized to the co-expressed GFP. The tagging would enable to purify the degron cassette to quantify its amount in different assays to properly elucidate its degradation/stabilization kinetics. Quantification of degron stability could be achieved through a DHFR activity assay, which is commercially available. The advantage of the DHFR activity assay would be a direct, plate reader based readout enabling higher throughput and automation by avoiding Western Blot.

As a shortcut for pre-screening purposes also an reticulocyte extract for *in vitro* transcription/translation could be used. Reticulocyte extracts are a long established test system in the ubiquitination and N-end rule field (compare introduction). The degron could be expressed containing the *ts*DHFR or a wild type version as a control and stability after cycloheximide-mediated shut down of translations could be monitored. Since the reticulocyte extract functions at an optimal temperature of 30°C temperature shifts would not be applicable in this system rendering it a system solely suitable for initial testing and pre-screening purposes. However, its commercial availability and ease of use make it a well suitable system. Analysis would be performed again by fluorescent Western Blotting or e.g by expressing the degron as a GFP fusion protein for direct live monitoring. Initial tests showed that GFP fluorescence can be measured in a reticulocyte extract even when diluted with plant extract (fig. 5.22).

To further elucidate the degrons precise way of action and to shed light on the question which precise mode of recruitment and degradation via the proteasome, conditional recognition/ubiquitination/degradation, several experiments should be performed. First, a simple *in vitro* assay to measure the unstructuredness of the degron could be done. Fishbain and colleagues used a simple protease degradation assay to measure the unstructuredness of their test proteins (Fishbain *et al.* , 2011). They used a DHFR, which itself escaped degradation, while flexible regions at its respective C-and N-terminal, which were shown to be crucial for initiation of proteasomal degradation, were destroyed.

*In vitro* ubiquitination assays with PRT1 and the degron might yield another piece of the puzzle. Since temperature shifts *in vitro*, to mimic degron behavior *in vivo*, are difficult to analyze, because the changed temperature would most likely influence ligase activity, a wild type DHFR should be used as a control. Comparison of ubiquitination levels of the *ts* and the wild type DHFR would provide further insight into the contribution of conditional ubiquitination to degron degradation. For proper quantification, fluorescent ubiquitin should be used which is commercially available. Alternatively, and since the labeled ubiquitin might be differentiating between auto- and target ubiquitination difficult, a recently described fluorescence label could be used which enables the fluorescent tagging of Cysteine residues (Mot *et al.* , 2017). The DHFR has exactly one Cysteine at position seven.

Naturally, the experiments of Fishbain and colleagues using purified yeast proteasome

should be repeated (Fishbain *et al.* , 2011). Using the ubiquitinated proteins from the ubiquitination assay, one would compare degradation efficiency of the wild type DHFR to the *ts*-DHFR. This would further indicate whether flexibility of the DHFR is needed for degradation initiation at the proteasome. In this context the question remains if pre-ubiquitinated degron protein could re-acquire its structural rigidity upon a shift to the permissive temperature, because the attached ubiquitin moieties might influence the structural flexibility.

Other experiments should address the question of conditional recognition by PRT1. Here *in vitro* and *in vivo* pull downs could indicate whether this scenario plays a role. Using wild type and mutated DHFRs as baits one could compare the pull down efficiencies in regard to PRT1. This experiment could be performed also in a transient environment, such as *A. thaliana* mesophyll protoplasts, since no temperature shift is required and transient environments allow for high yield production of protein. However the assay itself should be carried out at 28°C to maintain degron flexibility. Naturally, *in vivo* the previously described PRT1 mutant C29A should be used to prevent degradation and N-terminal extension should be used that do not potentially disturb the structural integrity of the DHFR.

Depending on the precise mode of action, improvement and optimization of the degron could be achieved. Since data obtained by the SPOT assays suggests only a very limited influence of the N-terminal's primary sequence, other means of optimization should be attempted. If indeed the degrons primary mode of action is conditional degradation and conditional ubiquitination, than indeed co-expression of PRT1, as it was done in this work in yeast, could offer a valuable possibility to increase the degrons capacity, albeit maybe only in connection with very stable POIs since increasing amounts of E3 might result in increased amounts of POI ubiquitination and subsequent degradation. However, this would be something that would have to be carefully characterized since it has been shown that also at the permissive temperature, depending on the protein of interest, small amounts of degron are degraded (Faden *et al.* , 2016b), depending on the protein of interest. Co-expression of PRT1 might shift this equilibrium more into a state of instability thus diminishing the degrons potential, albeit this scenario might be desirable when working with very stable POIs.

Similar experiments would then have to be repeated in a structured fashion with different POIs, best representing different classes of enzymes and proteins. Stable proteins as well as established reporters of different sizes should be tested. In the end, only proteins of known stability and/or structural information should be used to be able to accurately identify, measure, and quantify the effects these different proteins would have on the degrons stability and kinetics.

At the end of the day, the following questions would be important: Which traits make a protein an ideal target for the degron? How much do protein traits influence degron behavior and therefore modulate degron kinetics? Data suggests a more continuous

(de)stabilization behavior and not a real switch-like reaction of the degron (mode 1 vs mode 2, fig. S 5.19). Still, different POIs might modulate and shift the fusion proteins behavior from one mode to another. On the other hand, would the degron be able to significantly modulate the behavior of a POI, e.g. be able to still confer temperature dependent effects when fused to other intrinsically stable proteins? Finally, if the linker region between the degron cassette and the POI plays a role in degradation initiation at the proteasome, how can this be exploited/optimized? Experiments, where the degron is directly fused to the POI or where the POI is contained in the vector backbone thus elongating the linker could already provide first hints.

All these questions, when answered, will make the degron technique an easy to use and probably further widely applicable approach.



## 5 Supplementary information

### 5.1 Supplementary Tables

**Table 5.1** – Statistical analysis of GUS activity from temperature shifted seedlings. TTest (2-sided, unpaired) n./s.  $p > 0.05$ ; \*  $p < 0.05$ ; \*\*  $p < 0.01$ ; \*\*\*  $p < 0.001$

time past shift [h]	temperature	value	level of significance.
4	cold	0.436175407	n./s.
8	cold	0.617174884	n./s.
12	cold	0.126783787	n./s.
16	cold	0.091448048	n./s.
20	cold	0.02564107	*
24	cold	0.00056953	***
4	warm	0.005650286	n./s.
8	warm	0.000762829	***
12	warm	0.000735725	***
16	warm	0.049483404	*
20	warm	0.00083785	***
24	warm	0.001248274	**

**Table 5.2** – List of primary antibodies (ABs) in TBST (0.1% TWEEN / 4% milk)

Type of AB	Antigen	Risen in	Cat.No.	Supplier	Dillution
monoclonal	HA tag	mouse	MMS-101	Eurogentec	1:1000
polyclonal	<i>AtCDKA;1</i>	goat	sc-12826	Santa Cruz	1:1000
polyclonal	GFP	rabbit	sc-8334	Santa Cruz	1:1000
monoclonal	<i>HsDHFR</i>	mouse	sc-74593	Santa Cruz	1:500
polyclonal	GUS	rabbit	A-5790	Molecular Probes	1:500
polyclonal	HIS tag	mouse	27-4710-01	GE healthcare	1:3000
monoclonal	ubiquitin	mouse	sc-8017	Santa Cruz	1:5000

**Table 5.3** – List of secondary antibodies (ABs) in TBST (0.1% TWEEN / 4% milk)

Detection	Antigen	Risen in	Cat.No.	Supplier	Dillution
HRP	mouse	goat	31430	Thermo scientific	1:5000
HRP	rabbit	goat	sc-2004	Santa Cruz	1:2500
HRP	goat	rabbit	sc-2768	Santa Cruz	1:2500

**Table 5.4** – Primers used in this work

Name	Application	Sequence
K2(P2)_frw	cloning	GGGGACAAGTTTGTACAA AAAAGCAGGCTTACTCGA GCTGCAGAATTAC
K2(P2)_rev	cloning	GGGGACCACTTTGTACAA GAAAGCTGGGTAAGCACC AGCACCAGCGTA
att_GUS_rev	cloning	GGGGACCACTTTGTACAA GAAAGCTGGGTAttattgtttgc ctccctgctgc
K2_Phe-Leu_frw	site directed mutagenesis	taagacttagaggtgggctccacggatctg gaatc
K2_Phe-Leu_rev	site directed mutagenesis	gattccagatccgtggagcccacctctaag tctta
K2_Phe-Arg_frw	site directed mutagenesis	cttaagacttagaggtgggcccacggatc tggaatcatg
K2_Phe-Arg_rev	site directed mutagenesis	catgattccagatccgtggcggcccacctcta agtcttaag
EF1_ss	transcript analysis	ATGCCCCAGGACATCGTG ATTTCAT
EF1_as	transcript analysis	TTGGCGGCACCCTTAGCT GGATCA
DHFR_frw	transcript analysis and genotyping	CCATTGAACTGCATCGTC GC
DHFR_rev	transcript analysis and genotyping	GCCTTTGTCCTCCTGGACC TC
eK_frw	cloning GeK:CO	ctcgagctgcagaattactatttaca
eK_rev_OH_CO	cloning GeK:CO	ttgtttcaacatagcaccagcaccagcgta a
CO_frw_OH_eK	cloning GeK:CO	ggtgctggtgctatgttgaacaagagagt aacgacatag
CO_rev	cloning GeK:CO	tcagaatgaaggaacaatccca
eK_frw_BP	cloning GeK:CO	GGGGACAAGTTTGTACAA AAAAGCAGGCTTACTCGA GCTGCAGAATTACTAttaca
CO_rev_BP	cloning GeK:CO	GGGGACCACTTTGTACAA GAAAGCTGGGTATCAGAA TGAAGGAACAATccca
K29R_frw	generating UBQ <sub>K29/48/63R</sub>	cttctctgtctctggattctagccttgacgtg tcgatggtgctc
K29R_rev	generating UBQ <sub>K29/48/63R</sub>	gacaccatcgacaacgtcaaggctagaatc caggacaaggaag
K48R_frw	generating UBQ <sub>K29/48/63R</sub>	agttctaccgtctcaagctgcctaccggca aagatcaat
K48R_rev	generating UBQ <sub>K29/48/63R</sub>	attgatctttgccggtaggcagcttgagga cggtagaact

Continued on next page

Table 5.4 – continued from previous page

Name	Appliation	Sequence
K63R_frw	generating UBQ <sub>K29/48/63R</sub>	agatgtaaggtcgattccctctgaatattgt agtcagcaagagttc
K63R_rev	generating UBQ <sub>K29/48/63R</sub>	gaactcttgctgactacaatattcagaggg aatcgaccttacatct
K2(WT)_tev_frw	cloning variants for <i>E.coli</i> ex- pression	gcttagaaaacctgtattttcagttccacgg atctggaatcatg
K2(WORL)_tev_frw	cloning variants for <i>E.coli</i> ex- pression	gcttagaaaacctgtattttcagtttcaa tcttgatatggaca
K2(WT)_M_tev_frw	cloning variants for <i>E.coli</i> ex- pression	gcttagaaaacctgtattttcagatgcacg gatctggaatcatggttc
K2(WORL)_M_tev_frw	cloning variants for <i>E.coli</i> ex- pression	gcttagaaaacctgtattttcagatgcaaa ttctggatatggacaatcttt
adapter_tev	adapter for TEV rec. site (Nau- mann <i>et al.</i> , 2016)	ggggacaagttgtacaaaaagcaggct tagaaaacctgtattttcaggaatg
K2-TEV_BP_frw	cloning variants for <i>E.coli</i> ex- pression	GGGGACAAGTTTGTACAA AAAAGCAGGCTTACTCGA GCTGCAGAATTA
K2-TEV_BP_rev	cloning variants for <i>E.coli</i> ex- pression	GGGGACCACTTTGTACAA GAAAGCTGGGTATTACCC TTGCGAGTACAC
KillXhoI_frw	eliminating XhoI site in ubiqui- tin (K2)	gttctaccgtcctcaagctgcttaccggc
KillXhoI_rev	eliminating XhoI site in ubiqui- tin (K2)	gccgtaagcagcttgaggacggtagaac
HA_XhoI_frw	amplifying 3xHAT:PRT1 for cloning into K2	agctctcgagatgggatcctaccatacga tg
PRT1_Bgl_rev	amplifying 3xHAT:PRT1 for cloning into K2	tagaagatctgcatttctgtgcttgatgact cattagaag
SalI_re_frw	reconstitute SalI in K2	gatgtaagtcgactccctctgaatattgta gtcagcaa
SalI_re_rev	reconstitute SalI in K2	ttgctgactacaatattcagagggagtcga ccttacatc
prt_kill_ec1_frw	eliminating Eco31I site 1 in PRT1	gaaagtgaacatcagggcctcatatcg gacaatgag
prt_kill_ec1_rev	eliminating Eco31I site 1 in PRT1	ctcattgtccgatatgtaggaccctatgt tcactttc
prt_kill_ec2_frw	eliminating Eco31I site 2 in PRT1	cagaacctgaggagaacgtgcaagctcaa gc
prt_kill_ec2_rev	eliminating Eco31I site 2 in PRT1	gcttgagcttgacgcttctcctcaggttctg
K2_XhoI_frw	amplification of K2 for pLTDK2	gcaggcttactcgagctgcag
K2_XhoI_rev	amplification of K2 for pLTDK2	tcagggtacctcgagccagcaccagcacca gcgtaatc
pLTDK2_seq1	sequencing pLTDK2 insertion	ggccacaacctcttcagttg
pLTDK2_seq2	sequencing pLTDK2 insertion	ctgctccgactatccaaacc

Continued on next page

Table 5.4 – continued from previous page

Name	Appliaction	Sequence
AG.1_att_frw	cloning pENTR:AGA	GGGGACAAGTTTGTACAA AAAAGCAGGCTTAatggcgtag caateggagc
AG_att_rev	cloning pENTR:AGA	GGGGACCACTTTGTACAA GAAAGCTGGGTATTACAC TAACTGGAGAGCGGtttG
LFY_att_frw	cloning pENTR:LFY	GGGGACAAGTTTGTACAA AAAAGCAGGCTTAatggatcct gaaggtttcacg
LFY_att_rev	cloning pENTR:LFY	GGGGACCACTTTGTACAA GAAAGCTGGGTActagaaacgc aagtcgtcgc
BstAPI_frw	<i>lfy-12</i> dCAPS primer	AAGCAGCCGTCTGCGGTG TCAGCAGCTGTT
BstAPI_rev	<i>lfy-12</i> dCAPS primer	CTGTCAATTTCCCAGCAAG ACAC
AG_WT_frw	AGAMOUS gDNA primer	agttaaaggagatctgagtgagagt
AG_WT_rev	AGAMOUS gDNA primer	ttttacattatacaacaccagatc
AG_LB	left border primer for <i>ag</i> geno- typing	TGGTTCACGTAGTGGGCC ATCG
Kill_XhoI_ref_frw	Elimination of XhoI	gtggatcctctttctagagccagcaccagc a
Kill_XhoI_ref_rev	Elimination of XhoI	tgctggctggctctagaagaggatcca c
SelA	pENTR sequencing	tcgcttaacgctagcatggatctc
SelB	pENTR sequencing	gtaacatcagagattttgagacac
N130	<i>prt1-1</i> genotyping	CAGAGGAAGAGCAAGAAC GAGAAT
N131	<i>prt1-1</i> genotyping	CCACCTTCTGTTTATCTAC AC

Table 5.5 – Newly synthesized N-terminal sequences (highlighted in capitals)

Name	Sequence
W-	tcgaccttacatctgtcttaagacttagaggtgggTTTCAAATTCCTGGATATGGACA
GUS_frw	ATCTTTGATGTTGAGACCTGTTGAAGGAtcccaaatatggggattggcaa
W-	gttcttgccaatccccatatttgggaTCCTTCAACAGGTCTCAACATCAAAGATT
GUS_rev	GTCCATATCCAGGAATTTGAAAcccactctaatgcttaagacaagatgtaagg
W-GUS-	tcgaccttacatctgtcttaagacttagaggtgggTTTCAAATTCCTGGATATGGACA
E_frw	ATCTTTGATGTTGAGACCTGTTGGAGGAtcccaaatatggggattggcaa
W-GUS-	gttcttgccaatccccatatttgggaTCCTCCAACAGGTCTCAACATCAAAGATT
E_rev	GTCCATATCCAGGAATTTGAAAcccactctaatgcttaagacaagatgtaagg
W-	tcgaccttacatctgtcttaagacttagaggtgggTTTCAAATTTGTAGATCTACTGA
LUC_frw	TTTGCATTCTGGAAGTGTGGAAAGGGAtcccaaatatggggattggcaa

Continued on next page

Table 5.5 – continued from previous page

Name	Sequence
W-	gttcttgccaatcccatatTTTgggaTCCCTTTCCAACAGTTCCAGAATGCAAAT
LUC_rev	CAGTAGATCTACAAATTTGAAAaccacctaagtcttaagacaagatgtaagg
W-LUC-	tcgacctacatctgtcttaagacttagaggtgggTTTCAAATTTGTAGATCTACTGG
D_frw	ATTGCATTCTGGAAGTGTGGAAAGGGAatcccaaatatggggattggcaa
W-LUC-	gttcttgccaatcccatatTTTgggaTCCCTTTCCAACAGTTCCAGAATGCAATC
D_rev	CAGTAGATCTACAAATTTGAAAaccacctaagtcttaagacaagatgtaagg
W-LUC-	tcgacctacatctgtcttaagacttagaggtgggTTTCAAATTTGTAGATCTACTGA
K_frw	TTTGCATTCTGGAAGTGTGGAGGAGGAatcccaaatatggggattggcaa
W-LUC-	gttcttgccaatcccatatTTTgggaTCCTCCTCCAACAGTTCCAGAATGCAAAT
K_rev	CAGTAGATCTACAAATTTGAAAaccacctaagtcttaagacaagatgtaagg
nsP4_frw	tcgacctacatctgtcttaagacttagaggtgggTTTATTTTTTCTACTGATACTGG
	ACCTGGACATTTGCAAAAAGAAGTCTGGAatcccaaatatggggattggcaa
nsP4_rev	gttcttgccaatcccatatTTTgggaTCCAGACTTCTTTTGCAAATGTCCAGGTC
	CAGTATCAGTAGAAAAAATAAAaccacctaagtcttaagacaagatgtaagg
nsP4-	tcgacctacatctgtcttaagacttagaggtgggTTTATTTTTTCTACTGATACTGG
K_frw	ACCTGGACATTTGCAAGGAGGATCTGGAatcccaaatatggggattggcaa
nsP4-K_rev	gttcttgccaatcccatatTTTgggaTCCAGATCCTCCTTGCAAATGTCCAGGTC
	CAGTATCAGTAGAAAAAATAAAaccacctaagtcttaagacaagatgtaagg
G-GUS_frw	tcgacctacatctgtcttaagacttagaggtgggTTTAGATCTGGAGGAGGAGGAG
	GAGGAGGAGGAGGAGGAGGAGGAAGAGGAatcccaaatatggggattggcaa
G-GUS_rev	gttcttgccaatcccatatTTTgggaTCCTCCTCCTCCTCCTCCTCCTCCTCCTC
	CTCCTCCTCCTCCAGATCTAAAccacctaagtcttaagacaagatgtaagg
poly-G_frw	tcgacctacatctgtcttaagacttagaggtgggTTTCATGGAGGAGGAGGAGGAG
	GAGGAGGAGGAGGAGGAGGAGGAGGAGGAatcccaaatatggggattggcaa
poly-G_rev	gttcttgccaatcccatatTTTgggaTCCTCCTCCTCCTCCTCCTCCTCCTCCTC
	CTCCTCCTCCTCCATGAAAccacctaagtcttaagacaagatgtaagg
poly-	tcgacctacatctgtcttaagacttagaggtgggTTTCATGGATCTGGATCTGGATC
GS_frw	TGGATCTGGATCTGGATCTGGATCTGGATatcccaaatatggggattggcaa
poly-	gttcttgccaatcccatatTTTgggaTCCAGATCCAGATCCAGATCCAGATCCAG
GS_rev	ATCCAGATCCAGATCCATGAAAccacctaagtcttaagacaagatgtaagg
eK_frw	tcgacctacatctgtcttaagacttagaggtgggTTTCATGGATCTGGAGCTTGGTT
	GTTGCCTGTTTTCTTTGGTTAAGAGAGGAatcccaaatatggggattggcaa
eK_rev	gttcttgccaatcccatatTTTgggaTCCTCCTTAACCAAAGAAACAGGCAACA
	ACCAAGCTCCAGATCCATGAAAccacctaagtcttaagacaagatgtaagg
M-K2_frw	tcgacctacatctgtcttaagacttagaggtgggATGCATGGATCTGGAATTATGGT
	TAGACCTTTGAATTGTATTGTTGCTGGAatcccaaatatggggattggcaa
M-K2_rev	gttcttgccaatcccatatTTTgggaTCCAGCAACAATACAATTCAAAGGTCTAA
	CCATAATTCAGATCCATGCATcccacctaagtcttaagacaagatgtaagg
G-K2_frw	tcgacctacatctgtcttaagacttagaggtgggTTTCATGGAGGAGGAGGAGGAG
	GAGGAGGAGGAGGAGGAGGAGGAGGAGGAatcccaaatatggggattggcaa
G-K2_rev	gttcttgccaatcccatatTTTgggaTCCTCCTCCTCCTCCTCCTCCTCCTCCTC
	CTCCTCCTCCTCCATGAAAccacctaagtcttaagacaagatgtaagg

**Table 5.6** – All sequences of membrane 1 - Color code: green = hydrophobic, red = polar/uncharged, green = special, violet = charged/positive, tan = charged/negative

No.	Sequence	Info
A1	F H G S G I M V R P L N C I V A G	K2 WT
A2	F H G G G G G G G G G G G G G G	H P2+polyG
A3	F H T A T A A A A T G T G T L L G	small AA
A4	F R G G G G G G G G G G G G G G	R P2+polyG
A5	F R S G G G G G G G G G G G R G	G-GUS
A6	F I F S T D T G P G H L Q K K S G	nsP4
A7	F I F S T G T G P G H L Q G G S G	nsP4 -K/D
A8	F A G S G I M V R P L N C I V A G	hydroph. AA at P2
A9	F V G S G I M V R P L N C I V A G	hydroph. AA at P2
A10	F R S L S G E G G S G T G S L S G	EIN2
B1	F H G S G I M V R P L N C I V A G	K2 WT
B2	F I G S G I M V R P L N C I V A G	hydroph. AA at P2
B3	F L G S G I M V R P L N C I V A G	hydroph. AA at P2
B4	F M G S G I M V R P L N C I V A G	hydroph. AA at P2
B5	F A H H G G G G G G G G G G G G	A+HH+pG
B6	F V H H G G G G G G G G G G G G	V+HH+pG
B7	F I H H G G G G G G G G G G G G	I+HH+pG
B8	F L H H G G G G G G G G G G G G	L+HH+pG
B9	F M H H G G G G G G G G G G G G	M+HH+pG
B10	F R S L S G E G G S G T G S L S G	EIN2
C1	F H G S G I M V R P L N C I V A G	K2 WT
C2	F H G S G S G S G S G S G S G S G	H+pGS
C3	F H S G S G S G S G S G S G S G	H+pSG
C4	F R G S G S G S G S G S G S G S G	R+pGS
C5	F R S G S G S G S G S G S G S G	R+pSG
C6	F Q I P G Y G Q S L M L R P V E G	W-GUS
C7	F Q I P G Y G Q S L M L R P V G G	W-GUS -E
C8	F I G S G I M V R P L N C I V A G	K2+I at P2
C9	F Q I C R S T D L H S G T V G K G	W-LUC
C10	F R S L S G E G G S G T G S L S G	EIN2
D1	F H G S G I M V R P L N C I V A G	K2 WT
D2	F Q I C R S T D L H S G T V G G G	W-LUC -K
D3	F Q I C R S T G L H S G T V G G G	W-LUC -D/K
D4	L H G S G I M V R P L N C I V A G	K2+type 2 PDS
D5	W H G S G I M V R P L N C I V A G	K2+type 2 PDS
D6	Y H G S G I M V R P L N C I V A G	K2+type 2 PDS
D7	I H G S G I M V R P L N C I V A G	K2+type 2 PDS
D8	A H G S G I M V R P L N C I V A G	K2 Ala-walk (1)
D9	F A G S G I M V R P L N C I V A G	K2 Ala-walk (2)
D10	F R S L S G E G G S G T G S L S G	EIN2
E1	F H G S G I M V R P L N C I V A G	K2 WT
E2	F H A S G I M V R P L N C I V A G	K2 Ala-walk (3)
E3	F H G A G I M V R P L N C I V A G	K2 Ala-walk (4)
E4	F H G S A I M V R P L N C I V A G	K2 Ala-walk (5)

Continued on next page

Table 5.6 - continued from previous page

No.	Sequence	Info
E5	F H G S G A M V R P L N C I V A G	K2 Ala-walk (6)
E6	F H G S G I A V R P L N C I V A G	K2 Ala-walk (7)
E7	F H G S G I M A R P L N C I V A G	K2 Ala-walk (8)
E8	F H G S G I M V A P L N C I V A G	K2 Ala-walk (9)
E9	F H G S G I M V R A L N C I V A G	K2 Ala-walk (10)
E10	F R S L S G E G G S G T G S L S G	EIN2
F1	F H G S G I M V R P L N C I V A G	K2 WT
F2	F H G S G I M V R P A N C I V A G	K2 Ala-walk (11)
F3	F H G S G I M V R P L A C I V A G	K2 Ala-walk (12)
F4	F H G S G I M V R P L N A I V A G	K2 Ala-walk (13)
F5	F H G S G I M V R P L N C A V A G	K2 Ala-walk (14)
F6	F H G S G I M V R P L N C I A A G	K2 Ala-walk (15)
F7	F H G S G I M V R P L N C I V A G	K2 Ala-walk (16)
F8	F H G S G A W L L P V S L V R R G	eK + K to R
F9	F H G S G A W L L P V S L V K R G	eK WT
F10	F R S L S G E G G S G T G S L S G	EIN2

Table 5.7 – All sequences of membrane 2 - Color code: green = hydrophobic, red = polar/uncharged, green = special, violet = charged/positive, tan = charged/negative

No.	Sequence	Info
A1	F H G S G I M V R P L N C I V A G	K2 WT
A2	F R S G G G G G G G G G R G	G-GUS
A3	M H G S G I M V R P L N C I V A G	M-K2
A4	G H G S G I M V R P L N C I V A G	G-K2
A5	F M G S G I M V R P L N C I V A G	M P2
A6	F Q G S G I M V R P L N C I V A G	Q P2
A7	F I F S T D T G P G H L Q K K S G	nsP4 WT
A8	F I F S T D T G P G H L Q G G S G	nsP4 KK>GG
A9	F I F S T D T G P G H L Q I V S G	nsP4 KK>IV
A10	F H G S G I M V R P L N C I V A G	K2 WT
B1	F Q I P G Y G Q S L M L R P V E G	W-GUS Ala-walk co.
B2	A Q I P G Y G Q S L M L R P V E G	W-GUS Ala-walk (1)
B3	F A I P G Y G Q S L M L R P V E G	W-GUS Ala-walk (2)
B4	F Q A P G Y G Q S L M L R P V E G	W-GUS Ala-walk (3)
B5	F Q I A G Y G Q S L M L R P V E G	W-GUS Ala-walk (4)
B6	F Q I P A Y G Q S L M L R P V E G	W-GUS Ala-walk (5)
B7	F Q I P G A G Q S L M L R P V E G	W-GUS Ala-walk (6)
B8	F Q I P G Y A Q S L M L R P V E G	W-GUS Ala-walk (7)
B9	F Q I P G Y G A S L M L R P V E G	W-GUS Ala-walk (8)
B10	F Q I P G Y G Q A L M L R P V E G	W-GUS Ala-walk (9)
C1	F Q I P G Y G Q S A M L R P V E G	W-GUS Ala-walk (10)
C2	F Q I P G Y G Q S L A L R P V E G	W-GUS Ala-walk (11)

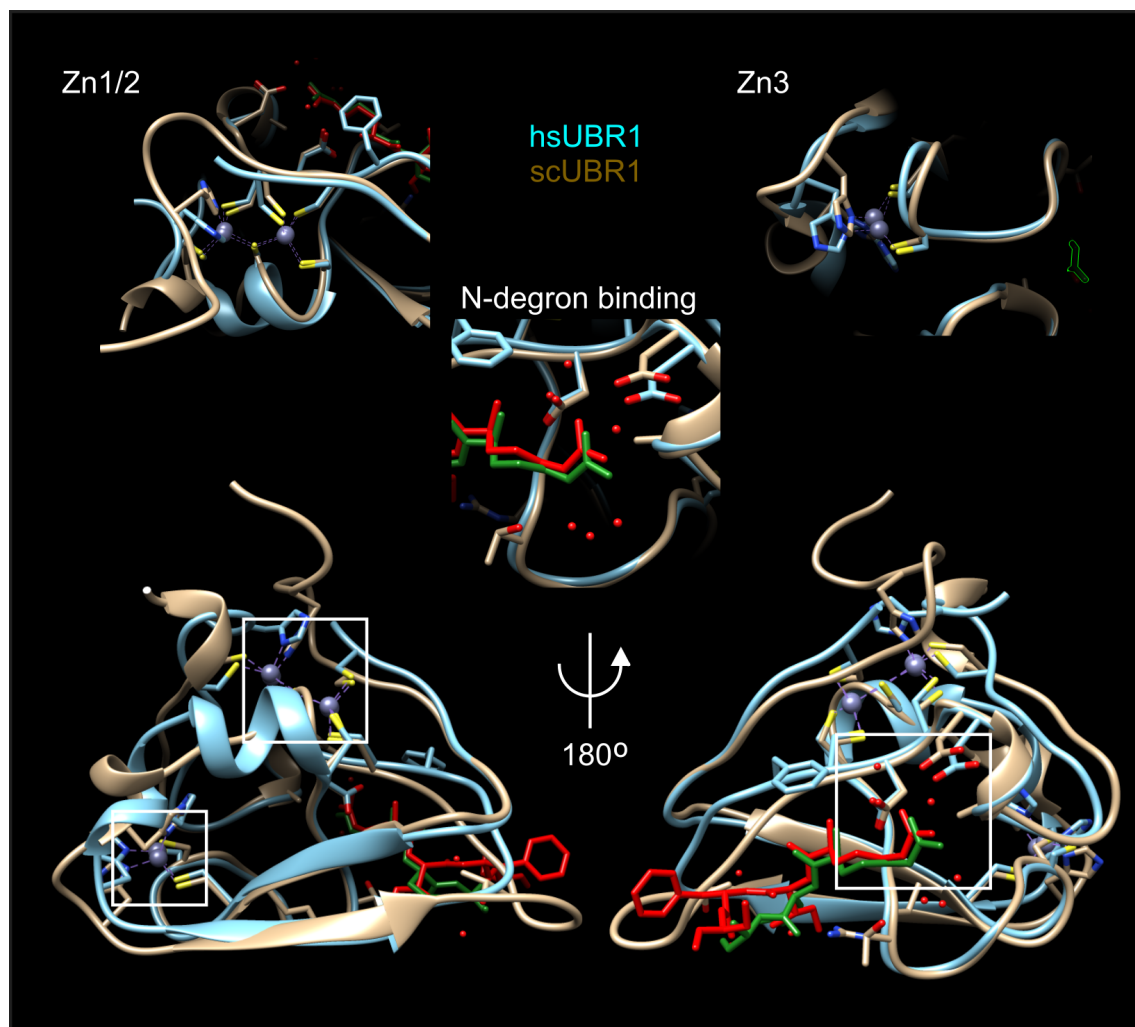
Continued on next page

Table 5.7 - continued from previous page

No.	Sequence	Info
C3	F Q I P G Y G Q S L M A R P V E G	W-GUS Ala-walk (12)
C4	F Q I P G Y G Q S L M L A P V E G	W-GUS Ala-walk (13)
C5	F Q I P G Y G Q S L M L R A V E G	W-GUS Ala-walk (14)
C6	F Q I P G Y G Q S L M L R P A E G	W-GUS Ala-walk (15)
C7	F Q I P G Y G Q S L M L R P V A G	W-GUS Ala-walk (16)
C8	F H G S G I M V R P L N C I V A G	K2 WT
C9	D H G S G I M V R P L N C I V A G	K2 Asp-walk (1)
C10	F D G S G I M V R P L N C I V A G	K2 Asp-walk (2)
D1	F H D S G I M V R P L N C I V A G	K2 Asp-walk (3)
D2	F H G D G I M V R P L N C I V A G	K2 Asp-walk (4)
D3	F H G S D I M V R P L N C I V A G	K2 Asp-walk (5)
D4	F H G S G D M V R P L N C I V A G	K2 Asp-walk (6)
D5	F H G S G I D V R P L N C I V A G	K2 Asp-walk (7)
D6	F H G S G I M D R P L N C I V A G	K2 Asp-walk (8)
D7	F H G S G I M V D P L N C I V A G	K2 Asp-walk (9)
D8	F H G S G I M V R D L N C I V A G	K2 Asp-walk (10)
D9	F H G S G I M V R P D N C I V A G	K2 Asp-walk (11)
D10	F H G S G I M V R P L D C I V A G	K2 Asp-walk (12)
E1	F H G S G I M V R P L N D I V A G	K2 Asp-walk (13)
E2	F H G S G I M V R P L N C D V A G	K2 Asp-walk (14)
E3	F H G S G I M V R P L N C I D A G	K2 Asp-walk (15)
E4	F H G S G I M V R P L N C I V D G	K2 Asp-walk (16)
E5	F H G S G A W L L P V S L V K R G	eK WT
E6	F H G S G A W L L P V S C V K R G	eK L13C
E7	F H G S G A W L L P V S L V D R G	eK K15D
E8	F H G S G A W L L P V S C V D R G	eK L13C K15D
E9	F H G S G A W L L P V S C V D A G	eK L13C K15D R16A
E10	F H G S G A W L L P V S C V V A G	eK K15V R16A
F1	F H G S G I M V R P L N C I V A G	K2 WT
F2	F H G S G I M Q S L M L R P V E G	K2/W-GUS
F3	F Q I P G Y G V R P L N C I V A G	W-GUS/K2
F4	F Q I S P D M Q S L L N C I V E G	F hybrid
F5	G Q I S P D M Q S L L N C I V E G	G hybrid
F6	F H G S G I M V R P L N C I V A G	K2 WT
F7	F Q I C R S T D L H S G T V G K G	W-LUC WT
F8	F Q I C R S T D L H S G T V G G G	W-LUC K16G
F9	F Q I C R S T D L H S G T V G E G	W-LUC K16E
F10	F H G S G I M V R P L N C I V A G	K2 WT



## 5.2 Supplementary Figures



**Figure 5.1 – Superimposition of human and yeast UBR1 structures.** Structures from the human UBR1 N-degron binding domain (pdb structure 3NY3, Matta-Camacho *et al.* 2010) and the yeast Ubr1 N-degron binding domain (pdb structure 3NIL, Choi *et al.* 2010) were superimposed using chimera. The overall structure is highly conserved. Detailed views of zinc ion coordination as well as substrate binding modes are almost indistinguishable.

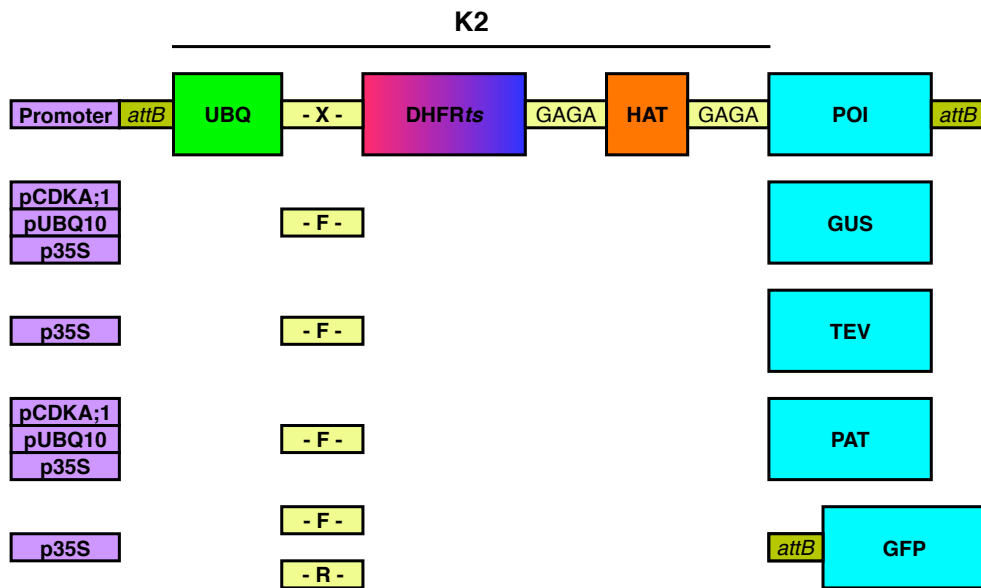


**Figure 5.2 – Schematics of the first generation of K2-reporter constructs used to generate stable *A. thaliana* lines.** K2 = Full degron cassette consisting of UB (UBQ), a primary destabilizing residue (-X-), a temperature sensitive DHFR (DHFR $ts$ ), Glycin-Alanin linkers (GAGA), and a triple Human influenza hemagglutinin-tag (HAT); *attB* sites for Gateway cloning (upstream and downstream of K2), as well as different promoters ProUBQ10 = ubiquitin-10 promoter, Pro35S = CaMV35S promoter, ProCDKA;1 = CYCLIN DEPENDENT KINASE A;1 promoter. In the GFP-construct the GFP is located after the *attB* site because in this case a pAM PAT derivative was used where the GFP is located in the vector backbone C-terminally of the gateway site.

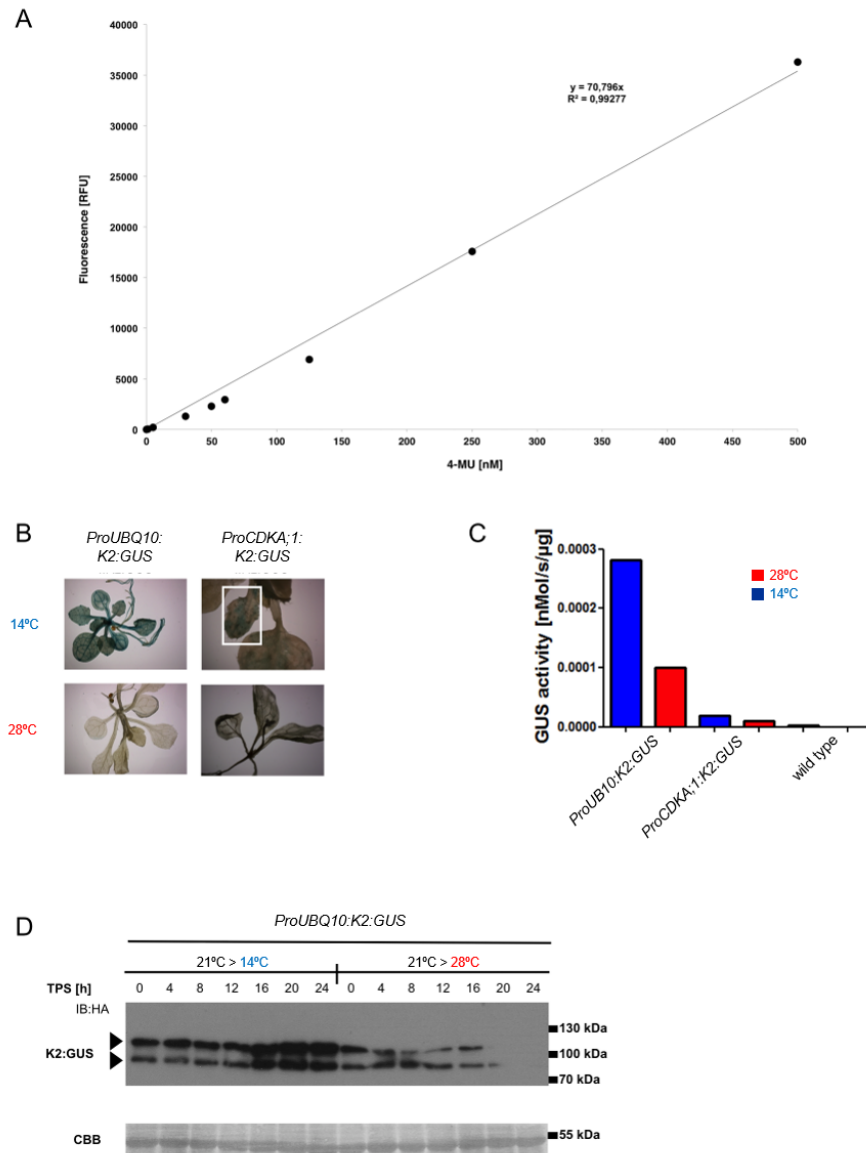


**Figure 5.3 – Supplementary information for the *ProUBQ10::K2::GUS* expressing lines.** (A) 4-MU calibration curve used for quantitative GUS assays. (B) Initial identification of two responsive lines showing temperature dependent GUS activity as shown by a qualitative GUS assay. (C) Quantitative GUS assay for plants seen in (B). n=2 (D) Western Blot analysis of plants shifted from intermediate to cold or warm conditions. Clearly a temperature dependent accumulation of the K2:GUS fusion protein is visible. (TPS = Time Past Shift)

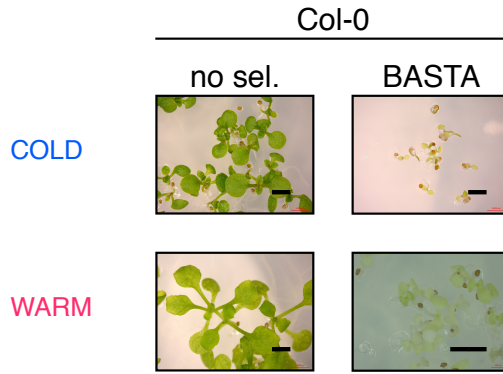


**Figure 5.4** – Col-0 control for BASTA selection under cold and warm temperatures. (scale bar = 1mm)

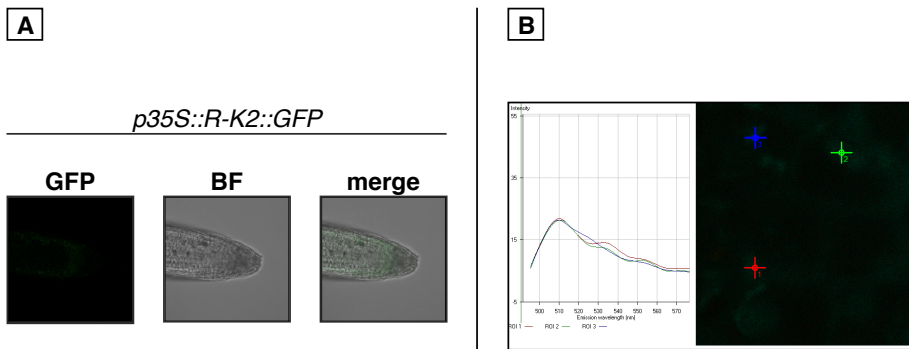


**Figure 5.5** – (A) shows the GFP signal under a confocal laser scanning microscope. (B) shows the confirmation of the signal using a lambda scan. A clear peak of the signal can be seen at 509 nm, the wavelength of GFP fluorescence.

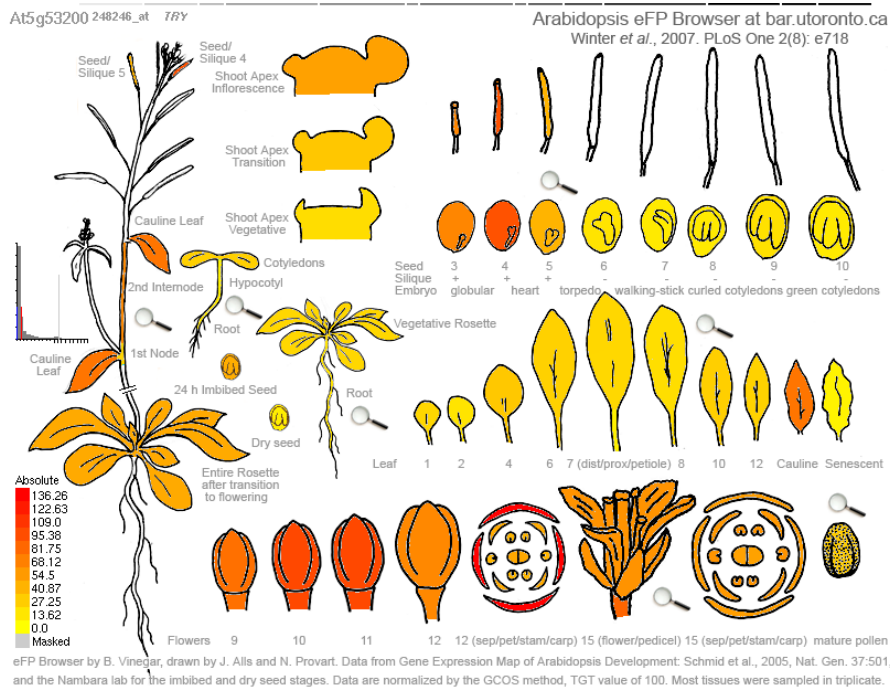


**Figure 5.6** – TRYPTICHON expression data as obtained from the eFP browser. (Winter *et al.*, 2007).

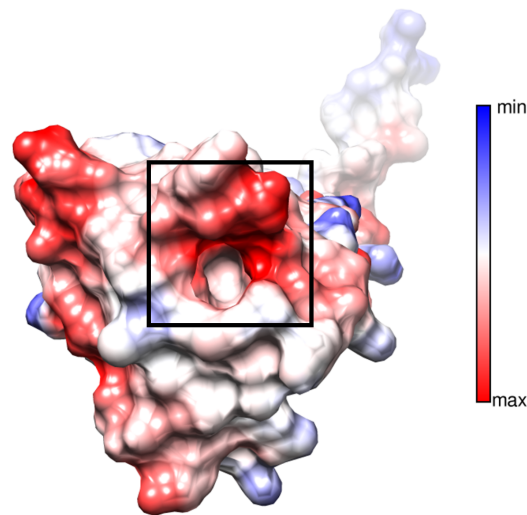


**Figure 5.7 – Electrostatic surface potential of *E. coli* ClpS.** The electrostatic surface potential is displayed in a color range from red (negative) to blue (positive) (modified after Román-Hernández *et al.* 2009, PDB 3O2B modeled with UCSF Chimera Pettersen *et al.* 2004).

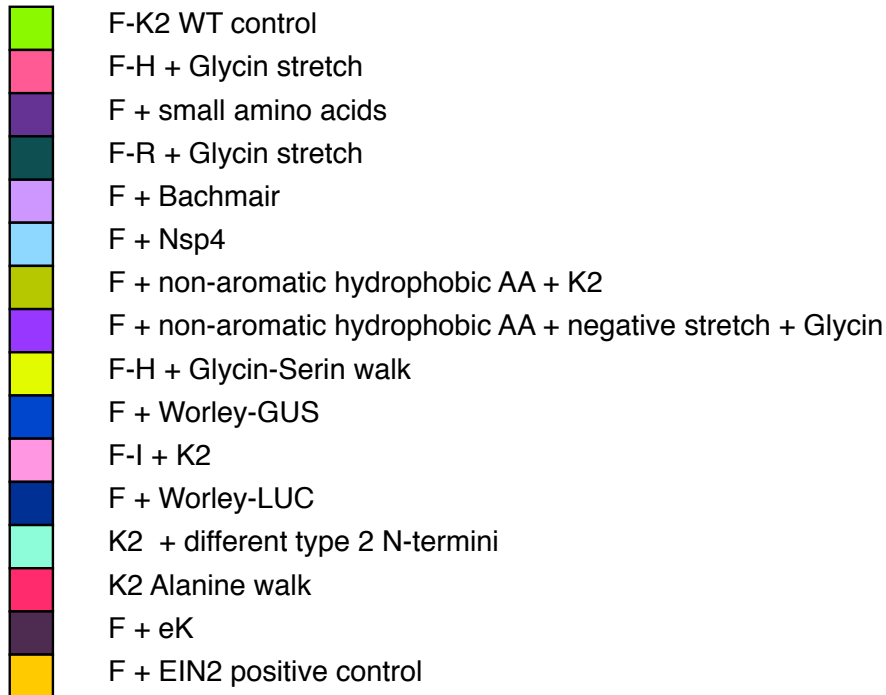


**Figure 5.8 – Design of the first SPOT membrane.** The design of the first membrane is depicted. Different experimental approaches were analyzed on one membrane. Details are given below the membrane pictogramm.

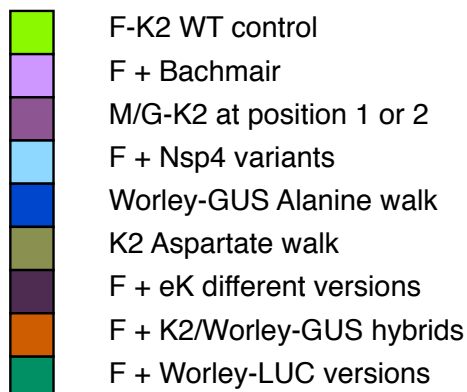
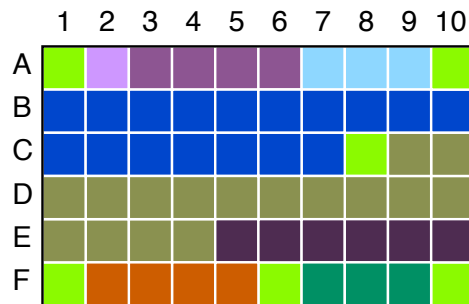


**Figure 5.9 – Design of the second SPOT membrane.** The design of the second membrane is depicted. Different experimental approaches were analyzed on one membrane. Details are given below the membrane pictogramm.

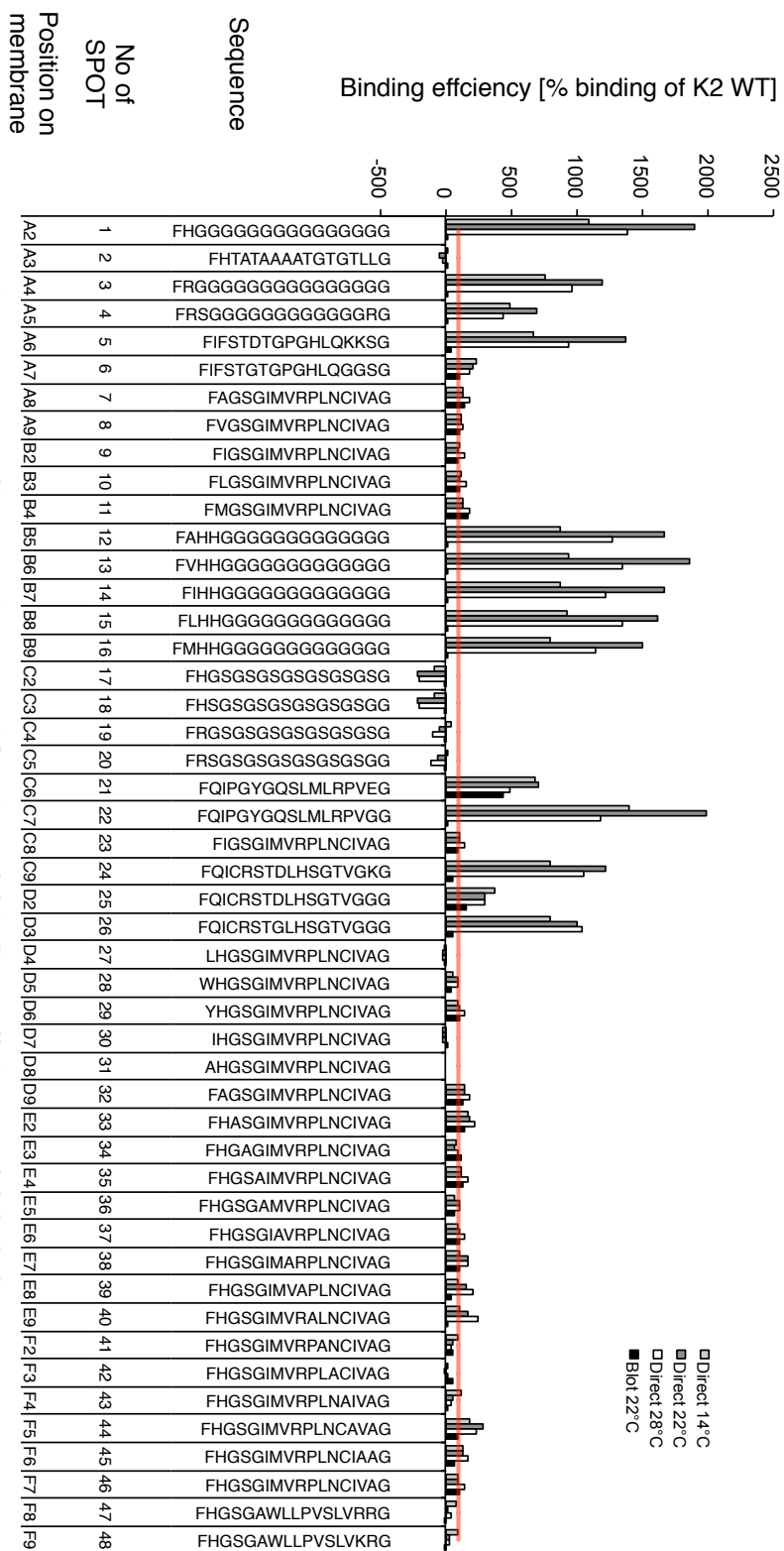


**Figure 5.10 – Comparative quantification of binding efficiency of labeled 8xHis:MBP:PRT1 to the SPOT membrane 1 at different temperatures comparing blot-based and direct detection approaches.** A total of five membranes were analyzed and averaged. The fluorescent protein was visualized using a typhoon scanner at a set photomultiplier strength of 650V (for direct detected protein) or 800V (for blot-based analysis). Values for each membrane were normalized to the K2 wild type control (positive). The values for the Alanine starting sequence No. 31 were subtracted as background blank. The red line marks 100% binding of the K2 WT sequence.



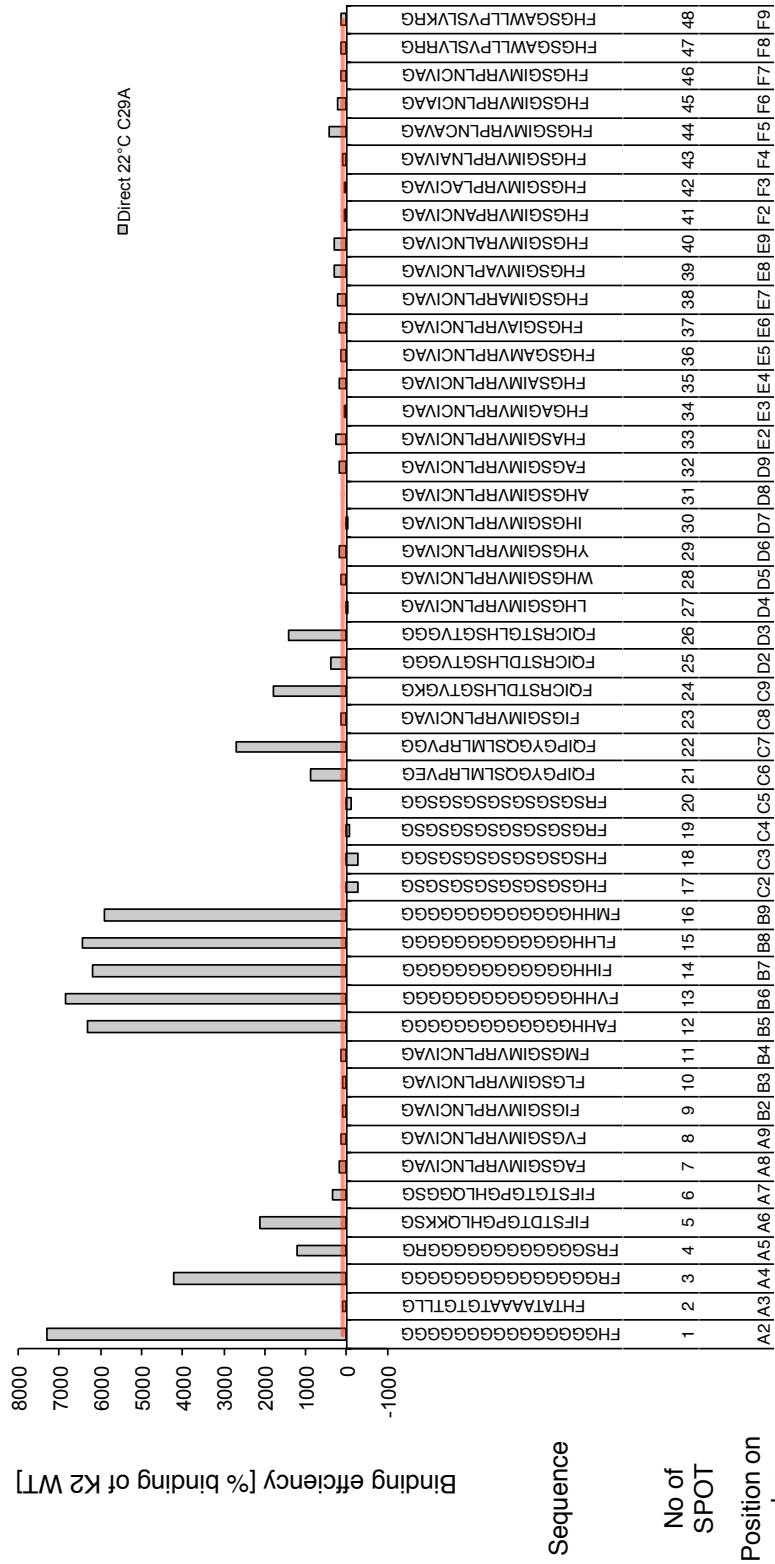


**Figure 5.11 – SPOT assay using recombinant PRT1c29A on membrane 1.**

A total of five membranes were analyzed and averaged. The fluorescent protein was visualized using a typhoon scanner at a set photomultiplier strength of 650V (for direct detected protein) or 800V (for blot-based analysis). Values for each membrane were normalized to the K2 wildtype control (positive). The values for the alanine starting sequence No.31 were subtracted as background blank. The red line marks 100% binding of the K2 WT sequence.

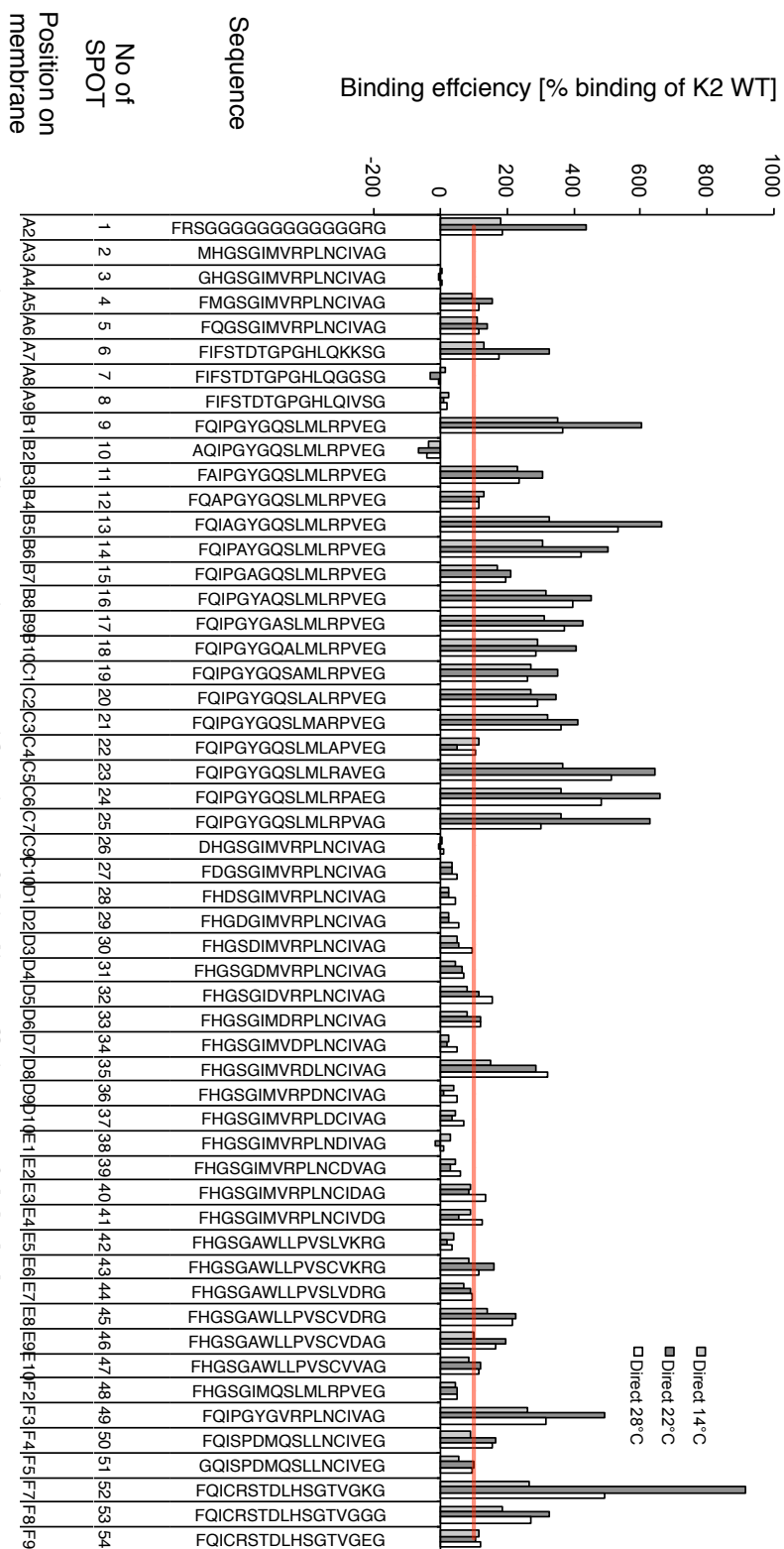


**Figure 5.12 – Comparative quantification of binding efficiency of labeled 8xHis:MBP:PRT1 to the SPOT membrane 2 at different temperatures using the direct detection approach.** A total of four membranes were analyzed and averaged. The fluorescent protein was visualized using a typhoon scanner at a set photo-multiplier strength of 650V. Values for each membrane were normalized to the K2 wild type control (positive) as well as blank subtraction of spot no. 2 (A3) which carries a Methionine at position one making it a non-target. The red line marks 100% binding of the K2 wild type sequence.

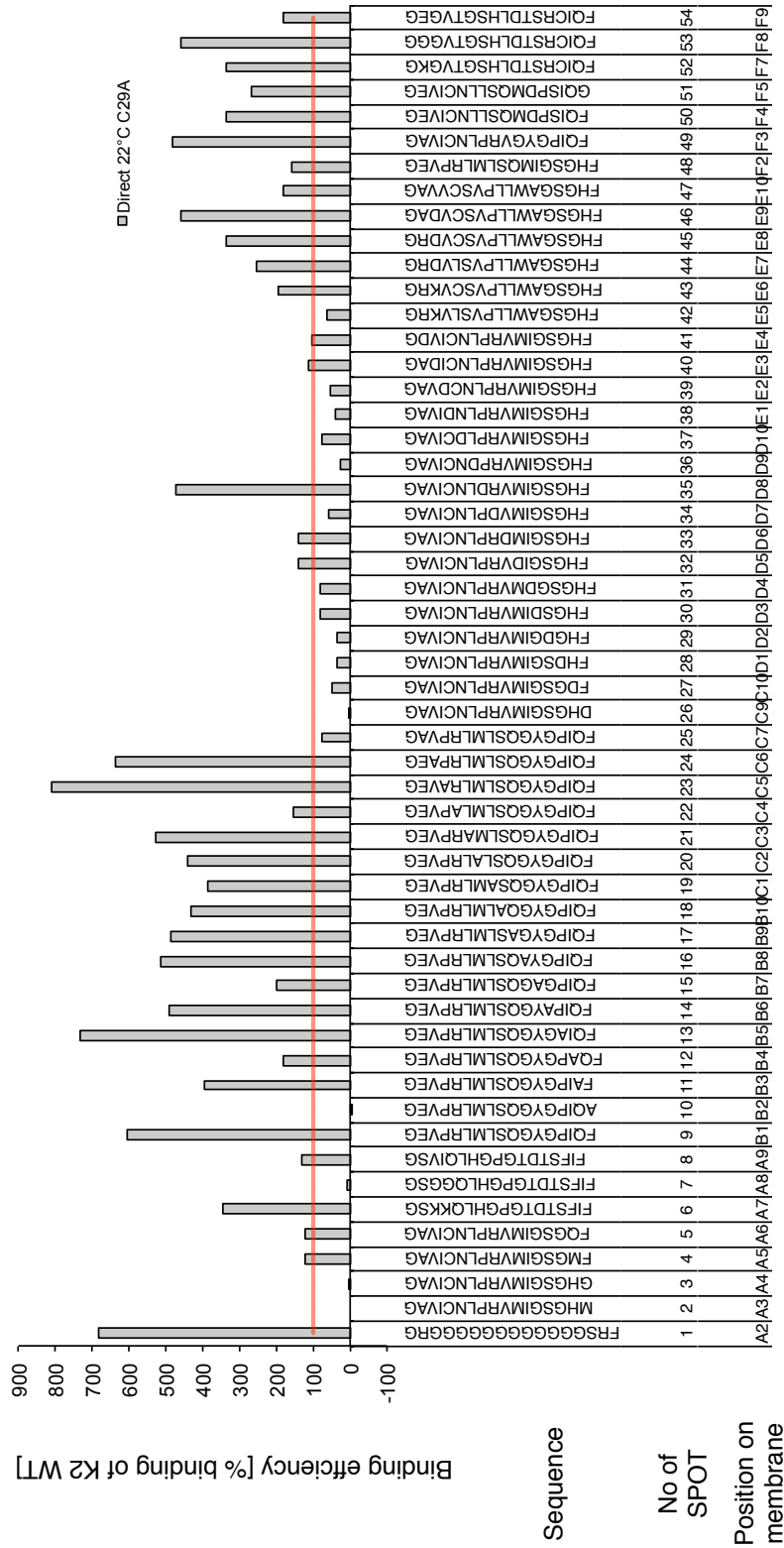


**Figure 5.13 – SPOT assay using recombinant PRT1c29A on membrane 2.**

A total of five membranes were analyzed and averaged. The fluorescent protein was visualized using a typhoon scanner at a set photomultiplier strength of 650V (for direct detected protein) or 800V (for blot-based analysis). Values for each membrane were normalized to the K2 wildtype control (positive). The values for the methionine starting sequence No.2 were subtracted as background blank. The red line marks 100% binding of the K2 WT sequence.

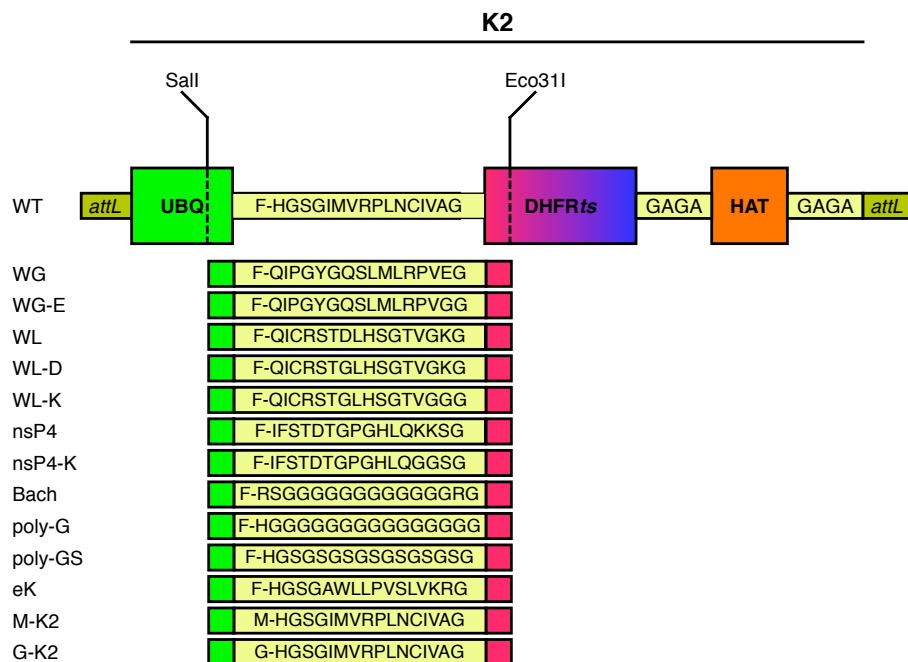


**Figure 5.14 – Schematic overview over the cloning strategy yielding new *pENTR:K2* versions.** After opening the vector pENTR:K2 using SalI and EcoRI the newly synthesized N-terminal sequences were ligated into the vector using standard ligation procedures.

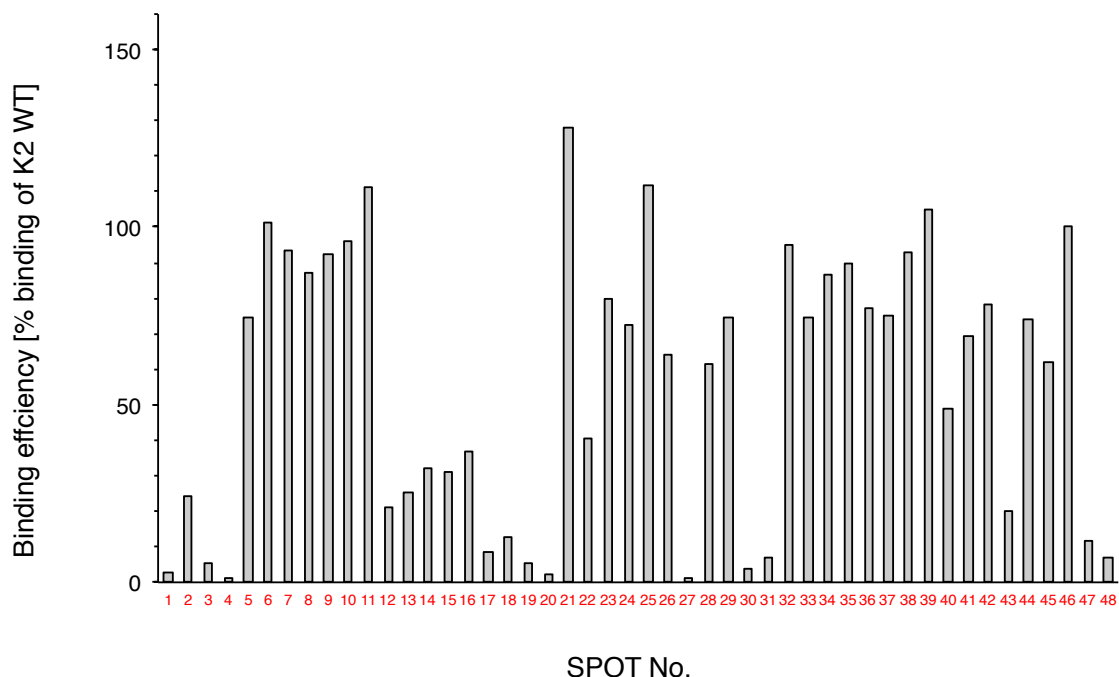


**Figure 5.15 – Quantification of ImmunoBlue based fluorescent detection of 8xHis:MP:PRT1 protein.** The chart shows the average binding of HIS:MBP:PRT1 to the SPOT membrane normalized to the WT control. Three membranes were analyzed.

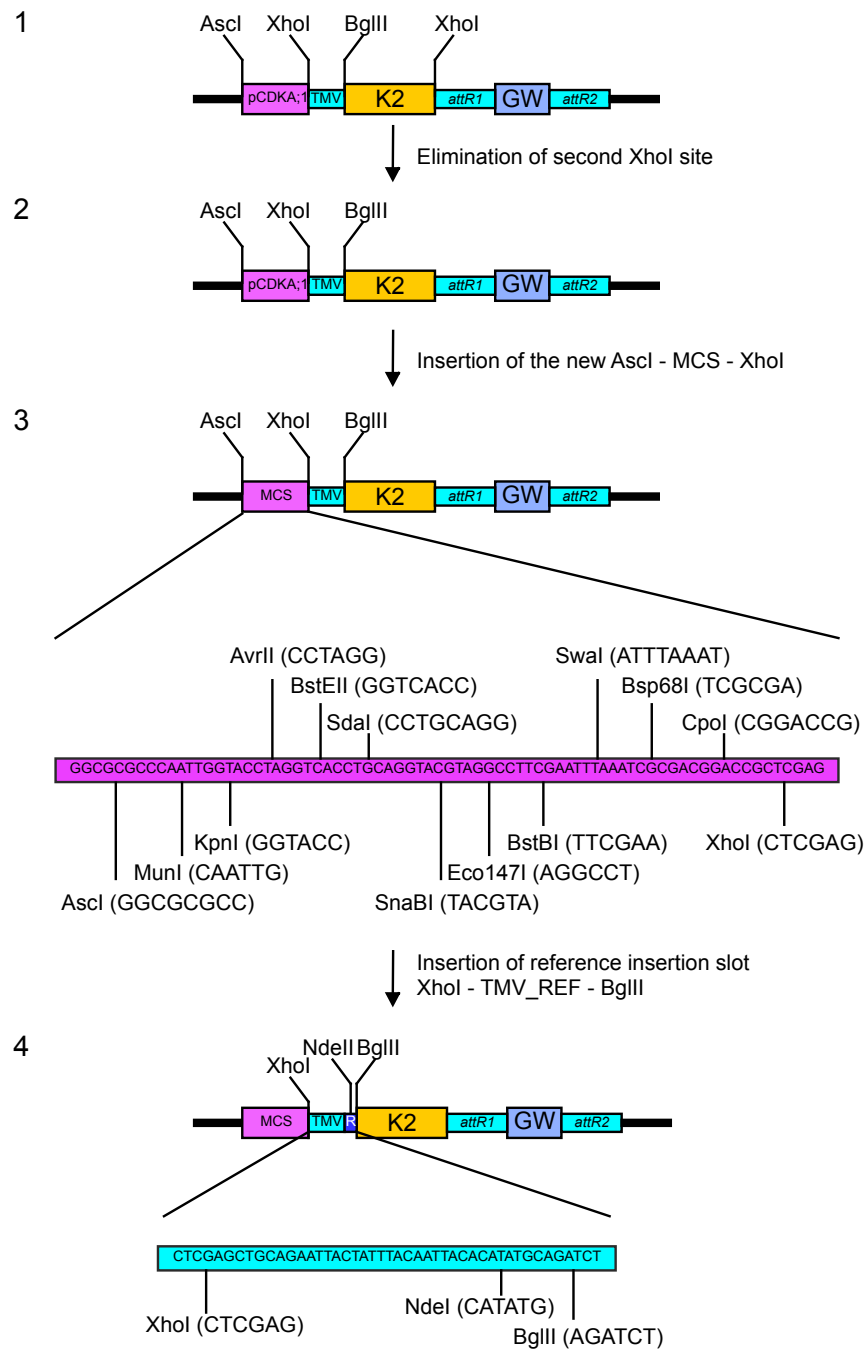


**Figure 5.16 – Cloning strategy of an improved destination vector for easy degdon tagging.** (1) Based on pLTDK2-pCDKA;1 the second XhoI site is eliminated. (2) The promoter is cut out. (3) Insertion of a multiple cloning site (MCS) with 13 restriction sites being unique for the whole vector. (4) Insertion of the reference insertion site.

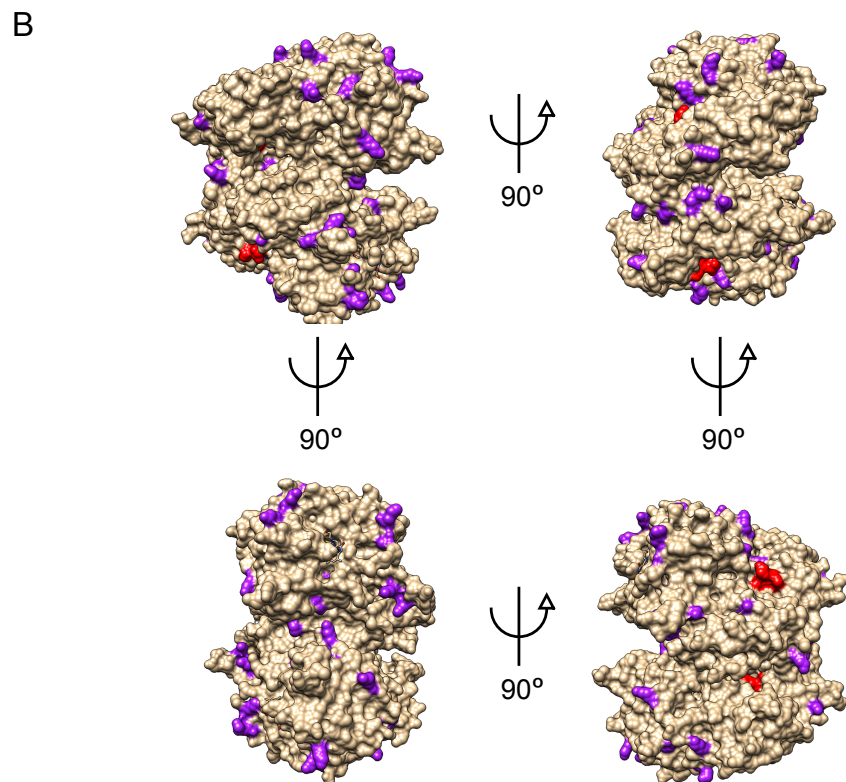
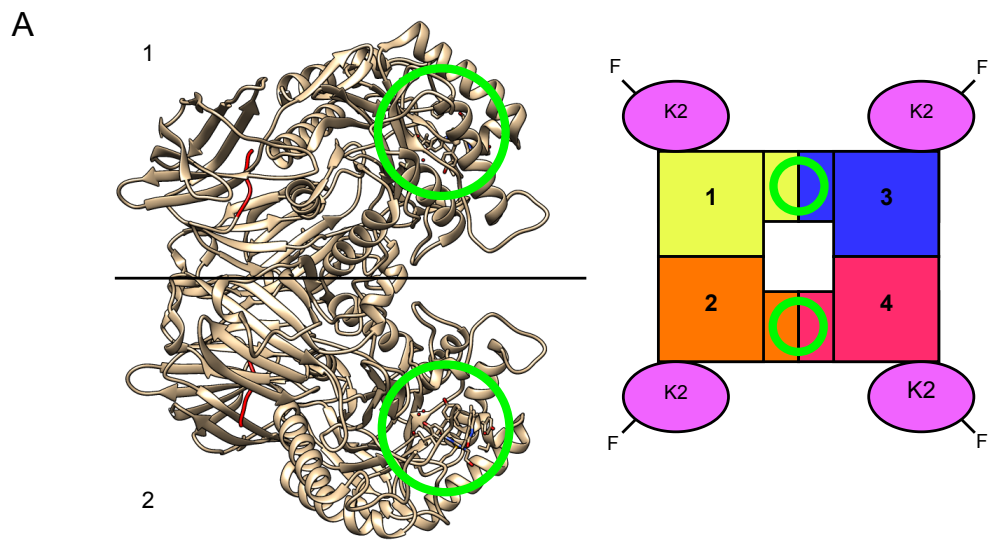


**Figure 5.17 – Crystal structure of the GUS enzyme.**(A) The crystal structure of the GUS dimer is depicted based on pdb structure 5czk (Wallace *et al.* , 2015). Each GUS protein has an inhibitor bound to its active center (green circle). The N-terminal of each monomer are highlighted in red. Structure was analyzed using UCSF Chimera (Pettersen *et al.* , 2004). The right panel depict the hypothetical structure of a tetramer of K2:GUS fusion proteins (based on Wallace *et al.* 2010, Raju *et al.* 2015, Wallace *et al.* 2015). (B) Surface of the same crystal structure from A. Surface exposed Lysines are highlighted in magenta. The forth structure (in clockwise direction) shows Lysines most likely buried within the tetramer due to their position on the interaction surface.

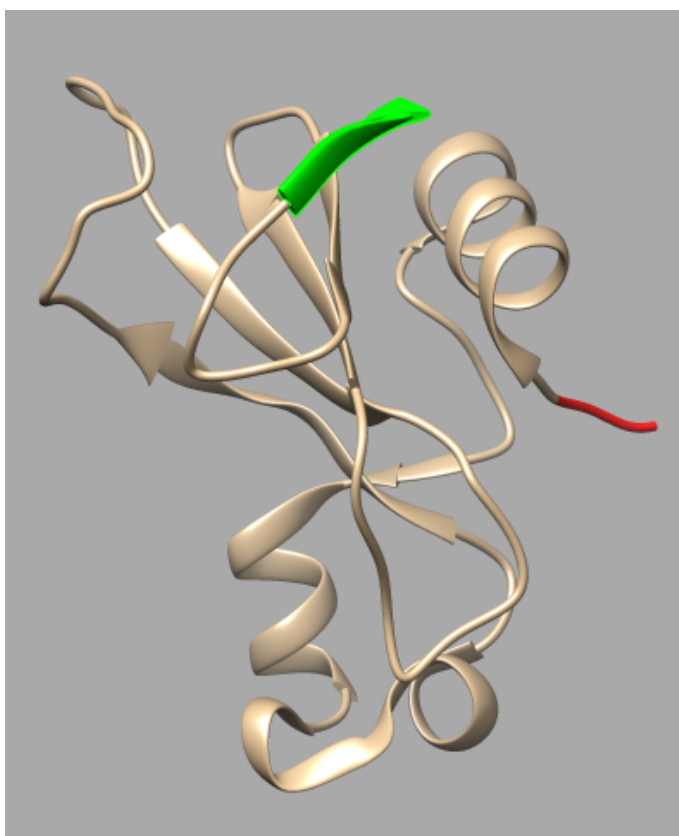


**Figure 5.18 – Crystal structure of barnase.** Side view of the crystal structure of the barnase enzyme adapted from Urakubo *et al.* 2008, pdb file 2ZA4. N-and C-terminal are colored in red and green respectively. The active side can be found on the left side of the structure facing away fro the N-terminal.

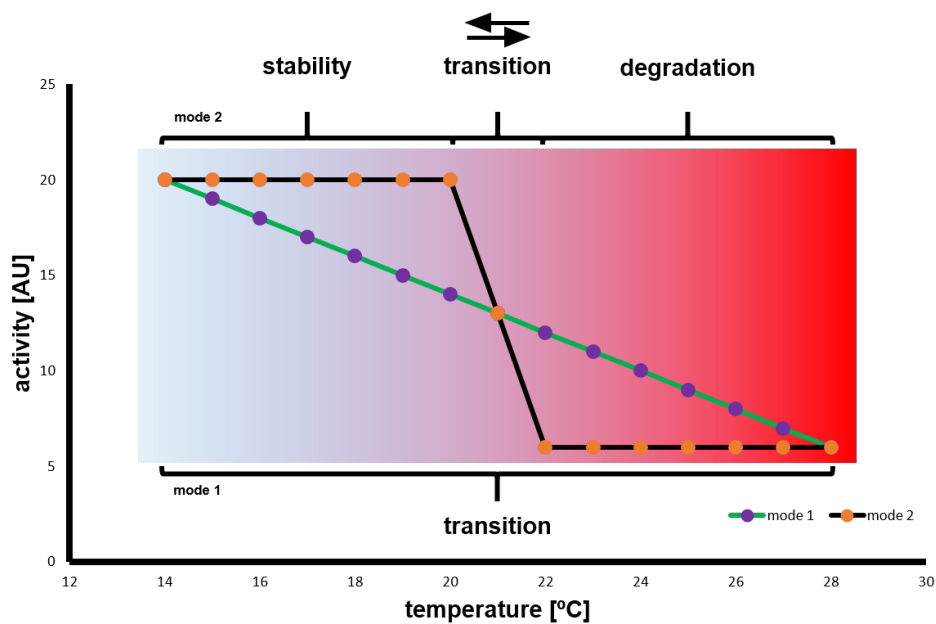


**Figure 5.19 – Possible modes of degron stabilization/destabilization kinetics.** Mode 1 describes a situation where the degron reacts quickly to the temperature change and every switch in temperature is responded by a shift in activity. Mode 2 describes the complete opposite situation, where the degron acts like a switch with long stability and degradation zones and a short transition zone describing the temperature range where the degron starts to be degraded. Naturally every mixture of modes is imaginable as well as e.g. a shifted place of the transition zone.

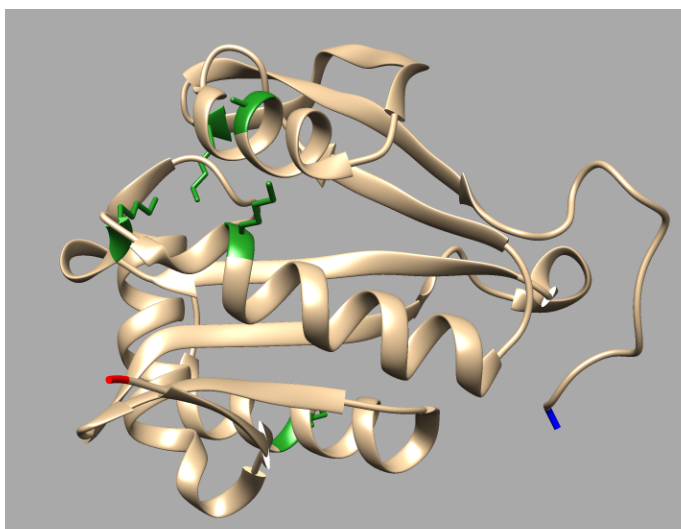


**Figure 5.20 – Crystal structure of Phosphinothricin N-acetyltransferase from *Brucella ovis*.** Adopted from pdb file 5DWM (Clifton *et al*, 2015 (unpublished)). N-terminal in red, C-terminal in blue, Lysines in green.



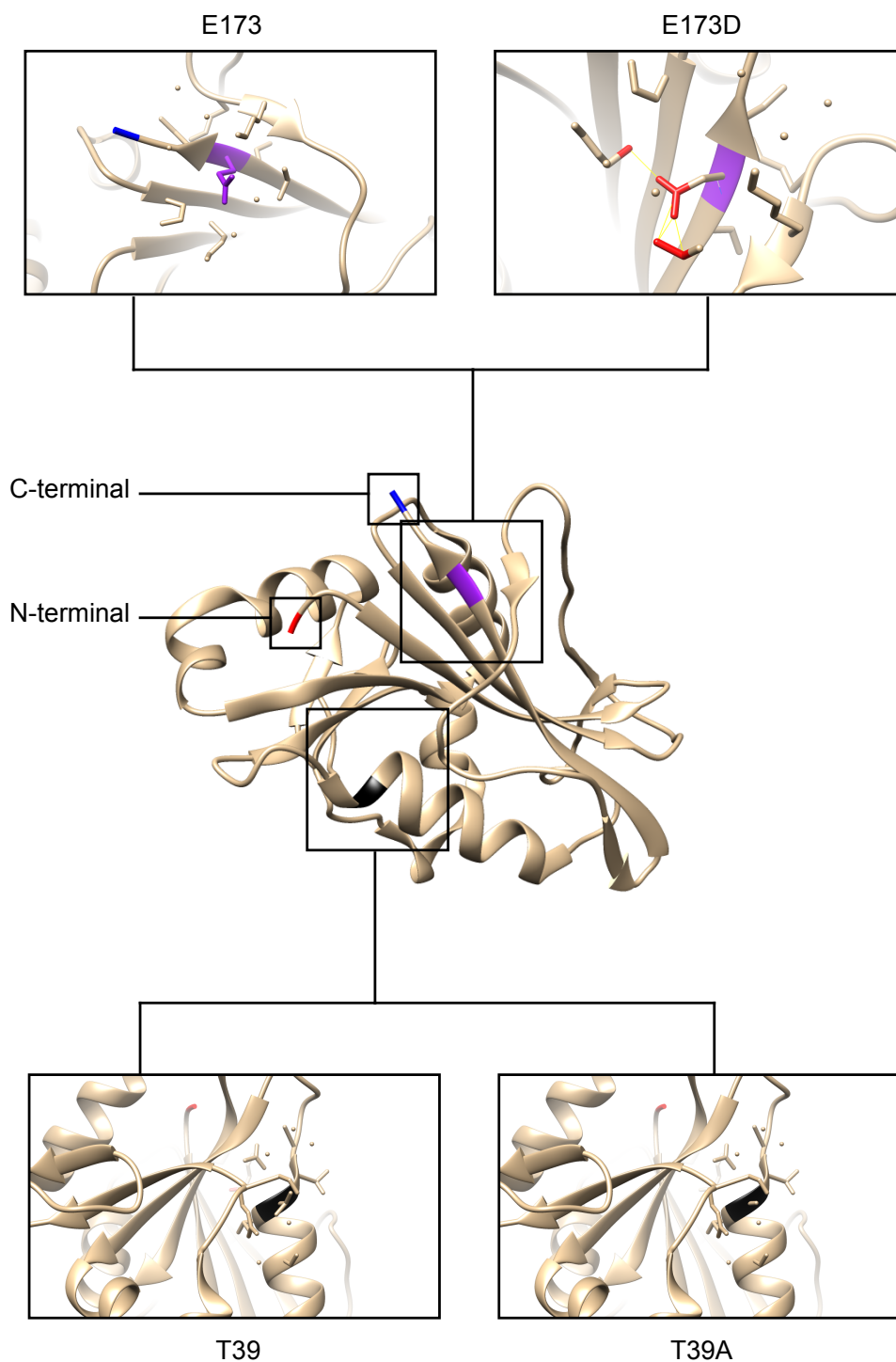


**Figure 5.21 – Structure of murine DHFR and position of K2 mutations.** The *ts*DHFR was modeled using chimera (Pettersen *et al.*, 2004) based on the pdb structure 2FZJ (Cody *et al.*, 2006). N- and C-terminal are highlighted in red and black respectively. The initiation Met as well as the last two amino acids were not part of the crystal structure. Mutations T39A and E173D are shown with a 5 Å sphere around them. As indicated the T39A mutations does not create any structural clashes whereas the E173D mutations induces clashes with amino acids R132 and I159 probably leading to higher conformational flexibility in this region.

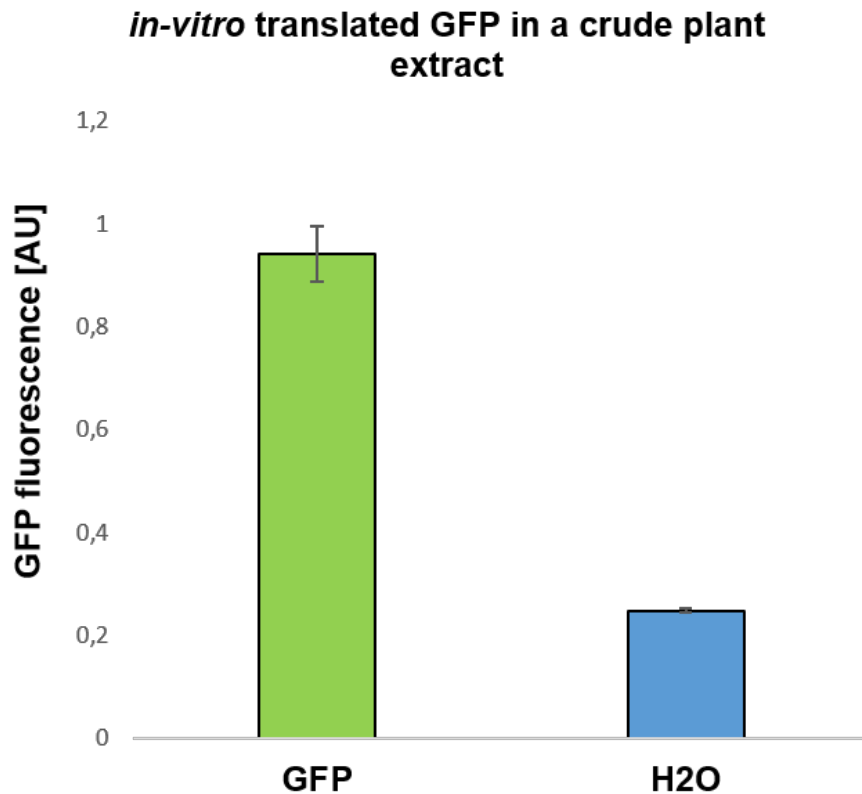


**Figure 5.22 – Fluorescence of *in vitro* generated GFP in a diluted plant extract.** Free GFP was expressed from the pOLENTE backbone.  $\frac{1}{4}$  reaction according to the manufacturer's instructions was used with 250 ng of DNA. Plant extract was obtained using the modified extraction buffer from Kim et al. (see material and methods) without detergents to reduce chlorophyll content in the sample. The full reaction (12.5  $\mu$ l) was diluted with 187.5  $\mu$ l of plant extract at a concentration of 1  $\mu$ g /  $\mu$ l and measured in a fluorescence microplate reader (VarioFluor, 485 nm excitation, 510 nm emission, integration time 1s). N = 3; Whiskers = standard deviation.

## 6 Bibliography

- Alberti, Simon, Gitler, Aaron D., & Lindquist, Susan. 2007. A suite of Gateway cloning vectors for high-throughput genetic analysis in *Saccharomyces cerevisiae*. *Yeast*, **24**(10), 913–919.
- Amann, Egon, Ochs, Birgit, & Abel, Karl Josef. 1988. Tightly regulated tac promoter vectors useful for the expression of unfused and fused proteins in *Escherichia coli*. *Gene*, **69**(2), 301–315.
- Amemiya, Yutaka, Azmi, Peter, & Seth, Arun. 2008. Autoubiquitination of BCA2 RING E3 ligase regulates its own stability and affects cell migration. *Molecular cancer research : MCR*, **6**(9), 1385–1396.
- An, Wenlin, Jackson, Rachel E., Hunter, Paul, Gögel, Stefanie, Van Diepen, Michiel, Liu, Karen, Meyer, Martin P., & Eickholt, Britta J. 2015. Engineering FKBP-based destabilizing domains to build sophisticated protein regulation systems. *PLoS ONE*, **10**(12), 1–12.
- Andersen, Pernille, Kragelund, Birthe B., Olsen, Addie N., Larsen, Flemming H., Chua, Nam Hai, Poulsen, Flemming M., & Skriver, Karen. 2004. Structure and biochemical function of a prototypical Arabidopsis U-box domain. *Journal of Biological Chemistry*, **279**(38), 40053–40061.
- Armstrong, Christopher M, & Goldberg, Daniel E. 2007. An FKBP destabilization domain modulates protein levels in *Plasmodium falciparum*. *Nature methods*, **4**(12), 1007–1009.
- Ashida, Hiroshi, Kim, Minsoo, & Sasakawa, Chihiro. 2014. Exploitation of the host ubiquitin system by human bacterial pathogens. *Nature reviews. Microbiology*, **12**(6), 399–413.
- Bachmair, A, & Varshavsky, A. 1989. The degradation signal in a short-lived protein. *Cell*, **56**(6), 1019–32.
- Bachmair, A, Becker, F, & Schell, J. 1993. Use of a reporter transgene to generate arabidopsis mutants in ubiquitin-dependent protein degradation. *Proceedings of the National Academy of Sciences of the United States of America*, **90**(2), 418–21.
- Bachmair, Andreas, Finley, Daniel, & Varshavsky, Alexander. 1986. In Vivo Half-Life of a Protein Is a Function of its Amino-Terminal Residue. *Science*, **523**(1985).
- Baker, Rohan T, & Varshavsky, Alexander. 1995. Yeast N-terminal Amidase - A New Enzyme And Component Of The N-End Rule Pathway. *The Journal of Biological Chemistry*, **270**(20), 12065–12074.
- Balzi, E, Choder, M, Chen, W N, Varshavsky, A, Goffeau, A, & Goffeaus, Andre. 1990. Cloning and functional analysis of the Cloning and Functional Analysis of the Arginyl-tRNA-protein Transferase Gene ATE1 of *Saccharomyces cerevisiae*. *The Journal of biological chemistry*, **265**(13), 7464–7471.
- Banaszynski, Laura A., Chen, Ling-chun, Maynard-Smith, Lystranne A., Ooi, A. G. Lisa, & Wandless, Thomas J. 2006. A Rapid, Reversible, and Tunable Method to Regulate Protein Function in Living Cells Using Synthetic Small Molecules. *Cell*, **126**(5), 995–1004.
- Banaszynski, Laura A., Sellmyer, Mark A., Contag, Christopher H., Wandless, Thomas J., & Thorne, Steve H. 2008. Chemical control of protein stability and function in living mice. *Nature medicine*, **14**(10), 1123–1127.
- Bar-On, Liat, & Jung, Steffen. 2010. Defining dendritic cells by conditional and constitutive cell ablation. *Immunological Reviews*, **234**(1), 76–89.
- Barbash, O, Lee, E K, & Diehl, J A. 2011. Phosphorylation-dependent regulation of SCF(Fbx4) dimerization and activity involves a novel component, 14-3-3e. *Oncogene*, **30**(17), 1995–2002.
- Bartel, Bonnie, Wunning, Ingrid, & Varshavsky, Alexander. 1990. The recognition component of the N-end rule pathway. *The EMBO journal*, **9**(10), 3179–3189.
- Bass, Steven H, & Yansura, Daniel G. 2000. Application of the *E. coli* trp promoter. *Molecular Biotechnology*, **16**(3), 253–260.
- Baumeister, Wolfgang, Bachmair, Andreas, Chau, Vincent, Cohen, Robert E., Coffino, Philip, DeMartino, George N, Deshaies, Raymond J., Dohmen, R Juergen, Emr, Scott D., Finley, Daniel, Hampton, Randy, Hil, Christopher, Hochstrasser, Mark, Huber, Robert, Jackson, Peter, Jentsch, Stefan, Johnson, Erica, Kwon, Yong Tae, Pagano, Michele, Pickart, Cecile, Rechsteiner, Martin, Scheffner, Martin, Sommer, Thomas, Tansey, William, Tyers, Mike,

- Vierstra, Richard D., Weissmann, Allan, Wilkinson, Keith D., & Wolf, Dieter. 2004. Varshavsky's Contributions. *Science*, **306**.
- Beckwith, Jonathan R., & Zipser, David (eds). 1970. *The lactose operon*. Cold Spring Harbor Laboratory.
- Bellen, H J, D'Evelyn, D, Harvey, M, & Elledge, S J. 1992. Isolation of temperature-sensitive diphtheria toxins in yeast and their effects on Drosophila cells. *Development (Cambridge, England)*, **114**(3), 787–796.
- Ben-Aroya, Shay, Coombes, Candice, Kwok, Teresa, O'Donnell, Kathryn A, Boeke, Jef D, & Hieter, Philip. 2008. Toward a comprehensive temperature-sensitive mutant repository of the essential genes of *Saccharomyces cerevisiae*. *Molecular cell*, **30**(2), 248–58.
- Ben-Aroya, Shay, Pan, Xuewen, Boeke, Jef D, & Hieter, Philip. 2010. Making temperature-sensitive mutants. *Methods Enzymol.*, **470**, 181–204.
- Benedito, Vagner A., Visser, Peter B., Van Tuyl, Jaap M., Angenent, Gerco C., De Vries, Sacco C., & Krens, Frans A. 2004. Ectopic expression of LLAG1, an AGAMOUS homologue from lily (*Lilium longiflorum* Thunb.) causes floral homeotic modifications in Arabidopsis. *Journal of Experimental Botany*, **55**(401), 1391–1399.
- Berdeaux, Rebecca, Goebel, Naomi, Banaszynski, Laura, Takemori, Hiroshi, Wandless, Thomas, Shelton, G Diane, & Montminy, Marc. 2007. SIK1 is a class II HDAC kinase that promotes survival of skeletal myocytes. *Nature Medicine*, **13**(5), 597–603.
- Bernal, Juan A, & Venkitaraman, Ashok R. 2011. A vertebrate N-end rule degron reveals that Orc6 is required in mitosis for daughter cell abscission. *The Journal of cell biology*, **192**(6), 969–78.
- Betts, M J, & Russell, R B. 2003. Amino acid properties and consequences of substitutions. In *Bioinformatics for Geneticists. Pages 311–342 of: Wiley*, vol. 4.
- Blázquez, M A, Soowal, L N, Lee, I, & Weigel, D. 1997. LEAFY expression and flower initiation in Arabidopsis. *Development (Cambridge, England)*, **124**(19), 3835–3844.
- Bombliès, Kirsten, Dagenais, Nicole, & Weigel, Detlef. 1999. Repression of AGAMOUS by APETALA2. *Developmental Biology*, **216**, 260–264.
- Bonger, Kimberly M, Chen, Ling-chun, Liu, Corey W, & Wandless, Thomas J. 2011. Small-molecule displacement of a cryptic degron causes conditional protein degradation. *Nature chemical biology*, **7**(8), 531–537.
- Bonger, Kimberly M, Rakhit, Rishi, Payumo, Alexander Y, Chen, James K, & Wandless, Thomas J. 2014. A General Method for Regulating Protein Stability with Light. *ACS Chemical Biology*, **9**, 111–115.
- Boohaker, R J, Lee, M W, Vishnubhotla, P, Perez, J M, & Khaled, A R. 2012. The Use of Therapeutic Peptides to Target and to Kill Cancer Cells. *Curr Med Chem*, **19**(12), 3794–3804.
- Bourgeois-Daigneault, Marie-Claude, & Thibodeau, Jacques. 2012. Autoregulation of MARCH1 expression by dimerization and autoubiquitination. *Journal of immunology (Baltimore, Md. : 1950)*, **188**(10), 4959–70.
- Bowman, J L, Drews, G N, & Meyerowitz, E M. 1991. Expression of the Arabidopsis floral homeotic gene AGAMOUS is restricted to specific cell types late in flower development. *The Plant cell*, **3**(8), 749–758.
- Breitschopf, Kristin, Bengal, Eyal, Ziv, Tamar, Admon, Arie, & Ciechanover, Aaron. 1998. A novel site for ubiquitination: The N-terminal residue, and not internal lysines of MyoD, is essential for conjugation and degradation of the protein. *EMBO Journal*, **17**(20), 5964–5973.
- Brockschneider, Damian, Lappe-Siefke, Corinna, Boesl, Michael R, Nave, Klaus-Armin, Goebbels, Sandra, & Riethmacher, Dieter. 2004. Cell Depletion Due to Diphtheria Toxin Fragment A after Cre-Mediated Recombination. *Molecular and cellular biology*, **24**(17), 7636–7642.
- Brukhin, Vladimir, Gheyselinck, Jacqueline, Gagliardini, Valeria, Genschik, Pascal, & Grossniklaus, Ueli. 2005. The RPN1 subunit of the 26S proteasome in Arabidopsis is essential for embryogenesis. *The Plant cell*, **17**(10), 2723–37.
- Buch, Thorsten, Heppner, Frank L, Tertilt, Christine, Heinen, Tobias J a J, Kremer, Marcel, Wunderlich, F Thomas, Jung, Steffen, & Waisman, Ari. 2005. A Cre-inducible diphtheria toxin receptor mediates cell lineage ablation after toxin administration. *Nature methods*, **2**(6), 419–426.
- Buckle, a M, & Fersht, a R. 1994. Subsite binding in an RNase: structure of a barnase-tetranucleotide complex at 1.76-Å resolution. *Biochemistry*, **33**, 1644–1653.
- Burgess, Diane G., Ralston, Edward J., Hanson, William G., Heckert, Matthew, Ho, Minh, Jenq, Tina, Palys,

- Joseph M., Tang, Keliang, & Gutterson, Neal. 2002. A novel, two-component system for cell lethality and its use in engineering nuclear male-sterility in plants. *Plant Journal*, **31**(1), 113–125.
- Callis, Judy. 2014. The ubiquitination machinery of the ubiquitin system. In: *The Arabidopsis book 11*.
- Campion, Yannick, Neel, Henry, Gostan, Thierry, Soret, Johann, & Bordonné, Rémy. 2010. Specific splicing defects in *S. pombe* carrying a degron allele of the Survival of Motor Neuron gene. *The EMBO journal*, **29**(11), 1817–29.
- Caussin, Emmanuel, Kanca, Oguz, & Affolter, Markus. 2011. Fluorescent fusion protein knockout mediated by anti-GFP nanobody. *Nature Structural & Molecular Biology*, **19**(1), 117–121.
- Cerutti, Heriberto, & Casas-Mollano, J. Armando. 2006. On the origin and functions of RNA-mediated silencing: From protists to man. *Current Genetics*, **50**(2), 81–99.
- Chau, Vincent, Tobias, John W, Bachmair, Andreas, Marriott, D., Ecker, David J, Gonda, David K, & Varshavsky, Alexander. 1989. A multiubiquitin chain is confined to specific lysine in a targeted short-lived protein. *Science*, **243**(4898), 1576–1583.
- Chen, Li, & Madura, Kiran. 2002. Rad23 promotes the targeting of proteolytic substrates to the proteasome. *Molecular and cellular biology*, **22**(13), 4902–13.
- Chen, Shun-Jia, Wu, Xia, Wadas, Brandon, Oh, Jang-Hyun, & Varshavsky, Alexander. 2017. An N-end rule pathway that recognizes proline and destroys gluconeogenic enzymes. *Science*, **355**(366).
- Cheng, Qian, Cross, Brittany, Li, Baozong, Chen, Lihong, Li, Zhenyu, & Chen, Jiandong. 2011. Regulation of MDM2 E3 Ligase Activity by Phosphorylation after DNA Damage. *Molecular and Cellular Biology*, **31**(24), 4951–63.
- Chini, A, Fonseca, S, Fernández, G, Adie, B, Chico, J M, Lorenzo, O, García-Casado, G, López-Vidriero, I, Lozano, F M, Ponce, M R, Micol, J L, & Solano, R. 2007. The JAZ family of repressors is the missing link in jasmonate signalling. *Nature*, **448**(7154), 666–671.
- Cho, Joonseok, Kim, Inbo, Jeong, Ju-Seong, Jung, Seung-Pil, Kang, Tae-Bong, & Kim, Jong-Bae. 2013. Cytotoxicity of recombinant immunotoxin containing lectin A chain from Korean mistletoe. *Molecular & Cellular Toxicology*, **9**(1), 29–36.
- Choi, Woo Suk, Jeong, Byung-Cheon, Joo, Yoo Jin, Lee, Myeong-Ryeol, Kim, Joon, Eck, Michael J, & Song, Hyun Kyu. 2010. Structural basis for the recognition of N-end rule substrates by the UBR box of ubiquitin ligases. *Nature structural & Molecular biology*, **17**(10), 1175–81.
- Ciechanover, A, Heller, H, Elias, S, Haas, a L, & Hershko, A. 1980a. ATP-dependent conjugation of reticulocyte proteins with the polypeptide required for protein degradation. *Proceedings of the National Academy of Sciences of the United States of America*, **77**(3), 1365–1368.
- Ciechanover, A., Elias, S., & Heller, H. 1980b. Characterization of the heatstable polypeptide of the ATP-dependent proteolytic system from reticulocytes. *Journal of Biological Chemistry*, **255**(16), 7525–7528.
- Ciechanover, A, Heller, H, Katz-Etzion, R, & Hershko, A. 1981. Activation of the heat-stable polypeptide of the ATP-dependent proteolytic system. *Proceedings of the National Academy of Sciences of the United States of America*, **78**(2), 761–765.
- Ciechanover, A., Elias, S., Heller, H., & Hershko, A. 1982. Covalent affinity purification of ubiquitin-activating enzyme. *Journal of Biological Chemistry*, **257**(5), 2537–2542.
- Ciechanover, Aharon, Hod, Yaacov, & Hershko, Avram. 1978. A heat-stable polypeptide component of an ATP-dependent proteolytic system from reticulocytes. *Biochemical and Biophysical Research Communications*, **81**(4), 1100–1105.
- Clough, S J, & Bent, a F. 1998. Floral dip: a simplified method for *Agrobacterium*-mediated transformation of *Arabidopsis thaliana*. *The Plant Journal*, **16**(6), 735–43.
- Cody, Vivian, Pace, Jim, Chisum, Kim, & Rosowsky, Andre. 2006. New insights into DHFR interactions: Analysis of *Pneumocystis carinii* and mouse DHFR complexes with NADPH and two highly potent 5-( $\omega$ -carboxy(alkoxy)) trimethoprim derivatives reveals conformational correlations with activity and novel parallel ring stack. *Proteins: Structure, Function, and Bioinformatics*, **65**(4), 959–969.
- Coen, E S, & Meyerowitz, E M. 1991. The war of the whorls: genetic interactions controlling flower development. *Nature*, **353**(6339), 31–37.
- Coscoy, Laurent, & Ganem, Don. 2003. PHD domains and E3 ubiquitin ligases: Viruses make the connection. *Trends in Cell Biology*, **13**(1), 7–12.

- Curado, Silvia, Anderson, Ryan M., Jungblut, Benno, Mumm, Jeff, Schroeter, Eric, & Stainier, Didier Y R. 2007. Conditional targeted cell ablation in zebrafish: A new tool for regeneration studies. *Developmental Dynamics*, **236**(4), 1025–1035.
- Cushman, Ian. 2008. Utilizing peptide SPOT arrays to identify protein interactions. *Current Protocols in Protein Science*, 1–9.
- Czako, M, & An, G. 1991. Expression of DNA coding for diphtheria toxin chain a is toxic to plant cells. *Plant physiology*, **95**(3), 687–92.
- Dale, Renee, & Kato, Naohiro. 2016. Truly quantitative analysis of the firefly luciferase complementation assay. *Current Plant Biology*, **5**, 57–64.
- Das, Ranabir, Mariano, Jennifer, Tsai, Yien Che, Kalathur, Ravi C., Kostova, Zlatka, Li, Jess, Tarasov, Sergey G., McFeeters, Robert L., Altieri, Amanda S., Ji, Xinhua, Byrd, R. Andrew, & Weissman, Allan M. 2009. Allosteric Activation of E2-RING Finger-Mediated Ubiquitylation by a Structurally Defined Specific E2-Binding Region of gp78. *Molecular Cell*, **34**(6), 674–685.
- Das, Ranabir, Liang, Yu-He, Mariano, Jennifer, Li, Jess, Huang, Tao, King, Aaren, Tarasov, Sergey G, Weissman, Allan M, Ji, Xinhua, & Byrd, R Andrew. 2013. Allosteric regulation of E2:E3 interactions promote a processive ubiquitination machine. *The EMBO journal*, **32**(18), 2504–16.
- de Boer, H A, Comstock, L J, & Vasser, M. 1983. The tac promoter: a functional hybrid derived from the trp and lac promoters. *Proceedings of the National Academy of Sciences of the United States of America*, **80**(1), 21–5.
- de Groot, R J, Rümenapf, T, Kuhn, R J, Strauss, E G, & Strauss, J H. 1991. Sindbis virus RNA polymerase is degraded by the N-end rule pathway. *Proceedings of the National Academy of Sciences of the United States of America*, **88**(20), 8967–71.
- de Marchi, Rémi, Sorel, Maud, Mooney, Brian, Fudal, Isabelle, Goslin, Kevin, Kwaśniewska, Kamila, Ryan, Patrick T., Pfalz, Marina, Kroymann, Juergen, Pollmann, Stephan, Feechan, Angela, Wellmer, Frank, Rivas, Susana, & Graciet, Emmanuelle. 2016. The N-end rule pathway regulates pathogen responses in plants. *Scientific Reports*, **6**(April), 26020.
- Delacour, Quentin, Li, Cheng, Plamont, Marie Aude, Billon-Denis, Emmanuelle, Aujard, Isabelle, Le Saux, Thomas, Jullien, Ludovic, & Gautier, Arnaud. 2015. Light-Activated Proteolysis for the Spatiotemporal Control of Proteins. *ACS Chemical Biology*, **10**(7), 1643–1647.
- Delley, Cyrille L., Striebel, Frank, Heydenreich, Franziska M., Oezcelik, Dennis, & Weber-Ban, Eilika. 2012. Activity of the mycobacterial proteasomal ATPase Mpa is reversibly regulated by pupylation. *Journal of Biological Chemistry*, **287**(11), 7907–7914.
- Desai, U J, & Pfaffle, P K. 1995. Single-step purification of a thermostable DNA polymerase expressed in *Escherichia coli*. *BioTechniques*, **19**(5), 780–2, 784.
- Desai, Urvee a, Sur, Gargi, Daunert, Sylvia, Babbitt, Ruth, & Li, Qingshun. 2002. Expression and affinity purification of recombinant proteins from plants. *Protein expression and purification*, **25**(1), 195–202.
- Dey, Antu K., David, Kathryn B., Klasse, Per J., & Moore, John P. 2007. Specific amino acids in the N-terminus of the gp41 ectodomain contribute to the stabilization of a soluble, cleaved gp140 envelope glycoprotein from human immunodeficiency virus type 1. *Virology*, **360**(1), 199–208.
- Dissmeyer, N., Nowack, M. K., Pusch, S., Stals, H., Inze, D., Grini, P. E., & Schnittger, A. 2007. T-Loop Phosphorylation of Arabidopsis CDKA;1 Is Required for Its Function and Can Be Partially Substituted by an Aspartate Residue. *The Plant Cell*, **19**(3), 972–985.
- Dissmeyer, Nico, & Schnittger, Arp. 2011. Use of Phospho-Site Substitutions to Analyze the Biological Relevance of Phosphorylation Events in Regulatory Networks. *Pages 93–138 of: Dissmeyer, N., & Schnittger, A. (eds), Plant Kinases: Methods and Protocols, Methods in Molecular Biology*, vol. 779. Springer Science+Business Media.
- Ditzel, Mark, Wilson, Rebecca, Tenev, Tencho, Zachariou, Anna, Paul, Angela, Deas, Emma, & Meier, Pascal. 2003. Degradation of DIAP1 by the N-end rule pathway is essential for regulating apoptosis. *Nature cell biology*, **5**(5), 467–473.
- Dohmen, R J, Wu, P, & Varshavsky, A. 1994. Heat-inducible degron: a method for constructing temperature-sensitive mutants. *Science*, **263**(5151), 1273–6.
- Dong, Hui, Dumenil, Jack, Lu, Fu-Hao, Na, Li, Vanhaeren, Hannes, Naumann, Cristin, Klecker, Maria, Prior, Rachel, Smith, Caroline, McKenzie, Neil, Saalbach, Gerhard, Chen, Liangliang, Xia, Tian, Gonzalez, Nathalie,

- Seguela, Mathilde, Inzé, Dirk, Dissmeyer, Nico, Li, Yunhai, & Bevan, Michael W. 2017. Ubiquitylation activates a peptidase that promotes cleavage and destabilization of its activating E3 ligases and diverse growth regulatory proteins to limit cell proliferation in Arabidopsis. *Genes & development (in press)*.
- Dougan, D a, Truscott, K N, & Zeth, K. 2010. The bacterial N-end rule pathway: expect the unexpected. *Molecular microbiology*, **76**(3), 545–58.
- Dougan, D a, Micevski, D, & Truscott, K N. 2012. The N-end rule pathway: from recognition by N-recognins, to destruction by AAA+proteases. *Biochimica et biophysica acta*, **1823**(1), 83–91.
- Downes, B, & Vierstra, R D. 2005. Post-translational regulation in plants employing a diverse set of polypeptide tags. *Biochemical Society transactions*, **33**, 393–399.
- Drews, Gary N., Bowman, John L., & Meyerowitz, Elliot M. 1991. Negative regulation of the Arabidopsis homeotic gene AGAMOUS by the APETALA2 product. *Cell*, **65**(6), 991–1002.
- Drinnenberg, Ines A., Weinberg, David E., Xie, Kathleen T., Mower, Jeffrey P., Wolfe, Kenneth H., Fink, Gerald R., & Bartel, David P. 2009. RNAi in budding yeast. *Science*, **326**(5952), 544–550.
- Droege, W., Broer, I., & Puehler, A. 1992. Transgenic plants containing the phosphinothricin-N-acetyltransferase gene metabolize the herbicide l-phosphinothricin (glufosinate) differently from untransformed plants. *Planta*, **187**(1), 142–151.
- Droege-Laser, Wolfgang, Siemeling, Ulrich, Pühler, Alfred, & Broer, Inge. 1994. The Metabolites of the Herbicide L-Phosphinothricin (Glufosinate). *Plant physiol.*, **105**(1 994), 159–166.
- Du, Fangyong, Navarro-Garcia, Federico, Xia, Zanzian, Tasaki, Takafumi, & Varshavsky, Alexander. 2002. Pairs of dipeptides synergistically activate the binding of substrate by ubiquitin ligase through dissociation of its autoinhibitory domain. *Proceedings of the National Academy of Sciences of the United States of America*, **99**(22), 14110–5.
- Echalier, G, & Ohanessian, A. 1969. Isolement, en cultures in vitro, de lignees cellulaires diploides de Drosophila melanogaster. *Comptes rendus hebdomadaires des seances de l'Academie des Sciences*, **268**, 1771–1773.
- Edelheit, Oded, Hanukoglu, Aaron, & Hanukoglu, Israel. 2009. Simple and efficient site-directed mutagenesis using two single-primer reactions in parallel to generate mutants for protein structure-function studies. *BMC Biotechnology*, **9**(1), 61.
- Edelweiss, Evelina, Balandin, Taras G, Ivanova, Julia L, Lutsenko, Gennady V, Leonova, Olga G, Popenko, Vladimir I, Sapozhnikov, Alexander M, & Deyev, Sergey M. 2008. Barnase as a new therapeutic agent triggering apoptosis in human cancer cells. *PloS one*, **3**(6), e2434.
- Elsasser, Suzanne, Chandler-Mitilello, Devin, Müller, Britta, Hanna, John, & Finley, Daniel. 2004. Rad23 and Rpn10 serve as alternate ubiquitin receptors for the proteasome. *Journal of Biological Chemistry*, **279**(26), 26817–26822.
- Erales, Jenny, & Coffino, Philip. 2014. Ubiquitin-independent proteasomal degradation. *Biochimica et Biophysica Acta - Molecular Cell Research*, **1843**(1), 216–221.
- Erbse, a, Schmidt, R, Bornemann, T, Schneider-Mergener, J, Mogk, a, Zahn, R, Dougan, D a, & Bukau, B. 2006. ClpS is an essential component of the N-end rule pathway in Escherichia coli. *Nature*, **439**(7077), 753–756.
- Faden, Frederik, Mielke, Stefan, Lange, Dieter, & Dissmeyer, Nico. 2014. Generic tools for conditionally altering protein abundance and phenotypes on demand. *Biological chemistry*, **395**(7-8), 737–62.
- Faden, Frederik, Eschen-Lippold, Lennart, & Dissmeyer, Nico. 2016a. Normalized Quantitative Western Blotting Based on Standardized Fluorescent Labeling Frederik. *Chap. 20, pages 247–258 of: Lois, L. Maria, & Matthiesen, Rune (eds), Plant Proteostasis: Methods and Protocols*, vol. 1450. New York, NY: Springer Science+Business Media.
- Faden, Frederik, Ramezani, Thomas, Mielke, Stefan, Almudi, Isabel, Nairz, Knud, Froehlich, Marceli S, Brandt, Wolfgang, Hoehenwarter, Wolfgang, Dohmen, R Jürgen, Schnittger, Arp, & Dissmeyer, Nico. 2016b. Phenotypes on demand via switchable target protein degradation in multicellular organism. *Nature communications*.
- Fan, H Y, Hu, Y, Tudor, M, & Ma, H. 1997. Specific interactions between the K domains of AG and AGLs, members of the MADS domain family of DNA binding proteins. *The Plant Journal*, **12**(5), 999–1010.
- Fang, Nancy N., Ng, Alex H. M., Measday, Vivien, & Mayor, Thibault. 2011. Hul5 HECT ubiquitin ligase plays a major role in the ubiquitylation and turnover of cytosolic misfolded proteins. *Nature Cell Biology*, **13**(11), 1344–1352.

- Farmer, Lisa M, Book, Adam J, Lee, Kwang-Hee, Lin, Ya-Ling, Fu, Hongyong, & Vierstra, Richard D. 2010. The RAD23 family provides an essential connection between the 26S proteasome and ubiquitylated proteins in Arabidopsis. *The Plant Cell*, **22**(1), 124–42.
- Finley, Daniel. 2009. Recognition and Processing of Ubiquitin-Protein Conjugates by the Proteasome. *Annual Review of Biochemistry*, **78**, 477–513.
- Finley, Daniel, Ulrich, Helle D., Sommer, Thomas, & Kaiser, Peter. 2012. The ubiquitin-proteasome system of *Saccharomyces cerevisiae*. *Genetics*, **192**(2), 319–360.
- Finn, Thomas E., Wang, Lei, Smolilo, David, Smith, Neil A., White, Rosemary, Chaudhury, Abed, Dennis, Elizabeth S., & Wang, Ming Bo. 2011. Transgene expression and transgene-induced silencing in diploid and autotetraploid arabidopsis. *Genetics*, **187**(2), 409–423.
- Fire, A, Xu, S, Montgomery, M K, Kostas, S A, Driver, S E, & Mello, C C. 1998. Potent and specific genetic interference by double-stranded RNA in *Caenorhabditis elegans*. *Nature*, **391**(6669), 806–811.
- Fishbain, Susan, Prakash, Sumit, Herrig, Annie, Elsasser, Suzanne, & Matouschek, Andreas. 2011. Rad23 escapes degradation because it lacks a proteasome initiation region. *Nature communications*, **2**, 192.
- Fletcher, Adam J., Mallery, Donna L., Watkinson, Ruth E., Dickson, Claire F., & James, Leo C. 2015. Sequential ubiquitination and deubiquitination enzymes synchronize the dual sensor and effector functions of TRIM21. *Proceedings of the National Academy of Sciences of the United States of America*, 10014–10019.
- Fujikawa, Yukichi, & Kato, Naohiro. 2007. Split luciferase complementation assay to study protein-protein interactions in Arabidopsis protoplasts. *The Plant Journal*, **52**(1), 185–195.
- Gamerith, G, Amann, A, Schenk, B, Auer, T, Huber, JM, Cima, K, Lentzen, H, Löffler-Ragg, J, Zwierzina, H, & Hilbe, W. 2014. P24. Aviscumine enhances NK- cytotoxicity against tumor cells. *Journal for ImmunoTherapy of Cancer*, **2**(Suppl 2), P15.
- Garzón, Marcus, Eifler, Karolin, Faust, Andrea, Scheel, Hartmut, Hofmann, Kay, Koncz, Csaba, Yephremov, Alexander, & Bachmair, Andreas. 2007. PRT6/At5g02310 encodes an Arabidopsis ubiquitin ligase of the N-end rule pathway with arginine specificity and is not the CER3 locus. *FEBS Letters*, **581**(17), 3189–3196.
- Gauguin, Lisbeth, Delaine, Carlie, Alvino, Clair L., McNeil, Kerrie A., Wallace, John C., Forbes, Briony E., & De Meyts, Pierre. 2008. Alanine scanning of a putative receptor binding surface of insulin-like growth factor-I. *Journal of Biological Chemistry*, **283**(30), 20821–20829.
- Gausung, K, & Barkardottir, R. 1986. Structure and expression of ubiquitin genes in higher plants. *European journal of biochemistry / FEBS*, **158**(1), 57–62.
- Gehl, Christian, Kaufholdt, David, Hamisch, Domenica, Bikker, Rolf, Kudla, Jörg, Mendel, Ralf R., & Hänsch, Robert. 2011. Quantitative analysis of dynamic protein-protein interactions in planta by a floated-leaf luciferase complementation imaging (FLuCI) assay using binary Gateway vectors. *The Plant Journal*, **67**(3), 542–553.
- Gibbs, Daniel J, Lee, Seung Cho, Isa, Nurulhikma Md, Gramuglia, Silvia, Fukao, Takeshi, Bassel, George W, Correia, Cristina Sousa, Corbineau, Françoise, Theodoulou, Frederica L, Bailey-Serres, Julia, & Holdsworth, Michael J. 2011. Homeostatic response to hypoxia is regulated by the N-end rule pathway in plants. *Nature*, **479**(7373), 415–8.
- Gietz, R Daniel, & Schiestl, Robert H. 2007. High-efficiency yeast transformation using the LiAc/SS carrier DNA/PEG method. *Nature protocols*, **2**(1), 31–4.
- Gilkerson, Jonathan, Kelley, Dior R., Tam, Raymond, Estelle, Mark, & Callis, Judy. 2015. Lysine Residues Are Not Required for Proteasome-Mediated Proteolysis of the Auxin/Indole Acidic Acid Protein IAA1. *Plant Physiology*, **168**(2), 708–720.
- Gils, Mario, Marillonnet, Sylvestre, Werner, Stefan, Grützner, Ramona, Giritch, Anatoli, Engler, Carola, Schachsneider, Ralf, Klimyuk, Victor, & Gleba, Yuri. 2008. A novel hybrid seed system for plants. *Plant Biotechnology Journal*, **6**(3), 226–235.
- Goldberg, Alfred L. 2003. Protein degradation and protection against misfolded or damaged proteins. *Nature*, **426**(6968), 895–899.
- Goldstein, G, Scheid, M, Hammerling, U, Schlesinger, D H, Niall, H D, & Boyse, E A. 1975. Isolation of a polypeptide that has lymphocyte-differentiating properties and is probably represented universally in living cells. *Proceedings of the National Academy of Sciences of the United States of America*, **72**(1), 11–5.



- Gomez, Tara A, Kolawa, Natalie, Gee, Marvin, Sweredoski, Michael J, & Deshaies, Raymond J. 2011. Identification of a functional docking site in the Rpn1 LRR domain for the UBA-UBL domain protein Ddi1. *BMC biology*, **9**(1), 33.
- Gonda, David K, Bachmair, Andreas, Wunning, Ingrid, Tobias, John W, Lane, William S, & Varshavsky, Alexander. 1989. Universality and Structure of the N-end Rule. *The Journal of Biological Chemistry*, **264**(28), 16700–16712.
- González, Monika, Martín-Ruíz, Itziar, Jiménez, Silvia, Pirone, Lucia, Barrio, Rosa, & Sutherland, James D. 2011. Generation of stable *Drosophila* cell lines using multicistronic vectors. *Scientific reports*, **1**, 75.
- Gossen, M, & Bujard, H. 1992. Tight control of gene expression in mammalian cells by tetracycline-responsive promoters. *Proceedings of the National Academy of Sciences of the United States of America*, **89**(12), 5547–51.
- Gowda, Naveen Kumar Chandappa, Kandasamy, Ganapathi, Froehlich, Marcell S, Dohmen, R Jürgen, & Andréasson, Claes. 2013. Hsp70 nucleotide exchange factor Fes1 is essential for ubiquitin-dependent degradation of misfolded cytosolic proteins. *Proceedings of the National Academy of Sciences of the United States of America*, **110**(15), 5975–80.
- Graciet, Emmanuelle, Hu, Rong-gui, Piatkov, Konstantin, Rhee, Joon Haeng, Schwarz, Erich M, & Varshavsky, Alexander. 2006. Aminoacyl-transferases and the N-end rule pathway of prokaryotic and eukaryotic specificity in a human pathogen. *Proceedings of the National Academy of Sciences of the United States of America*.
- Graciet, Emmanuelle, Walter, Franziska, Maoiléidigh, Diarmuid O, Pollmann, Stephan, Meyerowitz, Elliot M, Varshavsky, Alexander, & Wellmer, Frank. 2009. The N-end rule pathway controls multiple functions during *Arabidopsis* shoot and leaf development. *Proceedings of the National Academy of Sciences of the United States of America*, **106**(32), 13618–23.
- Graciet, Emmanuelle, Mesiti, Francesca, & Wellmer, Frank. 2010. Structure and evolutionary conservation of the plant N-end rule pathway. *The Plant Journal*, **61**(5), 741–51.
- Grefen, Christopher, Donald, Naomi, Hashimoto, Kenji, Kudla, Jörg, Schumacher, Karin, & Blatt, Michael R. 2010. A ubiquitin-10 promoter-based vector set for fluorescent protein tagging facilitates temporal stability and native protein distribution in transient and stable expression studies. *The Plant Journal*, **64**(2), 355–365.
- Gregan, Juraj, Van Laer, Lut, Lieto, Louis D., Van Camp, Guy, & Kearsey, Stephen E. 2003. A yeast model for the study of human DFNA5, a gene mutated in nonsyndromic hearing impairment. *Biochimica et Biophysica Acta (BBA) - Molecular Basis of Disease*, **1638**(2), 179–186.
- Grigoryev, Sergei, Stewart, Albert E., Kwon, Yong Tae, Arfin, Stuart M., Bradshaw, Ralph A., Jenkins, Nancy A., Copeland, Neal G., & Varshavsky, Alexander. 1996. A mouse amidase specific for N-terminal asparagine: The gene, the enzyme, and their function in the N-end rule pathway. *Journal of Biological Chemistry*, **271**(45), 28521–28532.
- Groll, M, Ditzel, L, Löwe, J, Stock, D, Bochtler, M, Bartunik, H D, & Huber, R. 1997. Structure of 20S proteasome from yeast at 2.4 Å resolution. *Nature*, **386**(6624), 463–471.
- Grote, Andreas, Hiller, Karsten, Scheer, Maurice, Münch, Richard, Nörtemann, Bernd, Hempel, Dietmar C., & Jahn, Dieter. 2005. JCat: A novel tool to adapt codon usage of a target gene to its potential expression host. *Nucleic Acids Research*, **33**.
- Gudesblat, Gustavo E., Schneider-Pizoń, Joanna, Betti, Camilla, Mayerhofer, Juliane, Vanhoutte, Isabelle, van Dongen, Walter, Boeren, Sjef, Zhiponova, Miroslava, de Vries, Sacco, Jonak, Claudia, & Russinova, Eugenia. 2012. SPEECHLESS integrates brassinosteroid and stomata signalling pathways. *Nature Cell Biology*, **14**(5), 548–554.
- Guerineau, François, Sorensen, Anna-Marie, Fenby, Nick, & Scott, Rod J. 2003. Temperature sensitive diphtheria toxin confers conditional male-sterility in *Arabidopsis thaliana*. *Plant biotechnology journal*, **1**(1), 33–42.
- Guharoy, Mainak, Bhowmick, Pallab, & Tompa, Peter. 2016. Design principles involving protein disorder facilitate specific substrate selection and degradation by the ubiquitin-proteasome system. *Journal of Biological Chemistry*.
- Guo, Fusheng, Maurizi, Michael R, Esser, Lothar, & Xia, Di. 2002a. Crystal structure of ClpA, an Hsp100 chaperone and regulator of ClpAP protease. *The Journal of biological chemistry*, **277**(48), 46743–52.
- Guo, Fusheng, Esser, Lothar, Singh, Satyendra K., Maurizi, Michael R., & Xia, Di. 2002b. Crystal structure of the heterodimeric complex of the adaptor, ClpS, with the N-domain of the AAA+ chaperone, ClpA. *Journal of Biological Chemistry*, **277**(48), 46753–46762.

- Guo, Jianjun, Morrell-Falvey, Jennifer L., Labbé, Jessy L., Muchero, Wellington, Kalluri, Udaya C., Tuskan, Gerald A., & Chen, Jin Gui. 2012. Highly Efficient Isolation of Populus Mesophyll Protoplasts and Its Application in Transient Expression Assays. *PLoS ONE*, **7**(9).
- Hamès, Cécile, Ptchelkine, Denis, Grimm, Clemens, Thevenon, Emmanuel, Moyroud, Edwige, Gérard, Francine, Martiel, Jean-Louis, Benloch, Reyes, Parcy, François, & Müller, Christoph W. 2008. Structural basis for LEAFY floral switch function and similarity with helix-turn-helix proteins. *The EMBO journal*, **27**(19), 2628–2637.
- Hämmerle, Marcus, Bauer, Jürgen, Rose, Matthias, Szallies, Alexander, Thumm, Michael, Düsterhus, Stefanie, Mecke, Dieter, Entian, Karl Dieter, & Wolf, Dieter H. 1998. Proteins of newly isolated mutants and the amino-terminal proline are essential for ubiquitin-proteasome-catalyzed catabolite degradation of fructose-1,6-bisphosphatase of *Saccharomyces cerevisiae*. *Journal of Biological Chemistry*, **273**(39), 25000–25005.
- Hänzelmann, Petra, Stingele, Julian, Hofmann, Kay, Schindelin, Hermann, & Raasi, Shahri. 2010. The yeast E4 ubiquitin ligase Ufd2 interacts with the ubiquitin-like domains of Rad23 and Dsk2 via a novel and distinct ubiquitin-like binding domain. *Journal of Biological Chemistry*, **285**(26), 20390–20398.
- Hardy, C F. 1996. Characterization of an essential Orc2p-associated factor that plays a role in DNA replication. *Molecular and cellular biology*, **16**(4), 1832–41.
- Hartley, James L., Temple, Gary F., & Brasch, Michael A. 2000. DNA Cloning Using In Vitro Site-Specific Recombination. *Genome Research*, **10**(11), 1788–1795.
- Hartwell, L H, Culotti, J, & Reid, B. 1970. Genetic control of the cell-division cycle in yeast. I. Detection of mutants. *Proceedings of the National Academy of Sciences of the United States of America*, **66**(2), 352–9.
- Hatfield, Peggy M., Gosink, Mark M., Carpenter, Tami B., & Vierstra, Richard D. 1997. The ubiquitin-activating enzyme (E1) gene family in *Arabidopsis thaliana*. *The Plant Journal*, **11**(2), 213–226.
- Heider, Margaret R, Gu, Mingyu, Duffy, Caroline M, Mirza, Anne M, Marcotte, Laura L, Walls, Alexandra C, Farrall, Nicholas, Hakhverdyan, Zhanna, Field, Mark C, Rout, Michael P, Frost, Adam, & Munson, Mary. 2015. Subunit connectivity, assembly determinants and architecture of the yeast exocyst complex. *Nature Structural & Molecular Biology*, **23**(December), 1–10.
- Heon Lee, Jeong, Hyun, Hoon, Cross, Conor J., Henary, Maged, Nasr, Khaled A., Oketokoun, Rafiou, Soo Choi, Hak, & Frangioni, John V. 2012. Rapid and Facile Microwave-Assisted Surface Chemistry for Functionalized Microarray Slides. *Adv Funct Mater.*, **22**(4), 872–878.
- Herm-Götz, Angelika, Agop-Nersesian, Carolina, Münter, Sylvia, Grimley, Joshua S, Wandless, Thomas J, Frischknecht, Friedrich, & Meissner, Markus. 2007. Rapid control of protein level in the apicomplexan *Toxoplasma gondii*. *Nature methods*, **4**(12), 1003–1005.
- Hermann, Anke, Liewald, Jana Fiona, & Gottschalk, Alexander. 2015. A photosensitive degron enables acute light-induced protein degradation in the nervous system. *Current Biology*, **25**(17), R749–R750.
- Hoerberichts, Frank A., Vaeck, Elke, Kiddle, Guy, Coppens, Emmy, Van De Cotte, Brigitte, Adamantidis, Antoine, Ormenese, Sandra, Foyer, Christine H., Zabeau, Marc, Inzé, Dirk, Périlleux, Claire, Van Breusegem, Frank, & Vuylsteke, Marnik. 2008. A temperature-sensitive mutation in the *Arabidopsis thaliana* phosphomannomutase gene disrupts protein glycosylation and triggers cell death. *Journal of Biological Chemistry*, **283**(9), 5708–5718.
- Hoeller, Daniela, Hecker, Christina Maria, Wagner, Sebastian, Rogov, Vladimir, Dötsch, Volker, & Dikic, Ivan. 2007. E3-Independent Monoubiquitination of Ubiquitin-Binding Proteins. *Molecular Cell*, **26**(6), 891–898.
- Holland, Andrew J, Fachinetti, Daniele, Han, Joo Seok, & Cleveland, Don W. 2012. Inducible, reversible system for the rapid and complete degradation of proteins in mammalian cells. *Proceedings of the National Academy of Sciences of the United States of America*, **109**(49), E3350–7.
- Holman, Tara J, Jones, Peter D, Russell, Laurel, Medhurst, Anne, Ubeda Tomás, Susana, Talloji, Prabhavathi, Marquez, Julietta, Schmuths, Heike, Tung, Swee-Ang, Taylor, Ian, Footitt, Steven, Bachmair, Andreas, Theodoulou, Frederica L, & Holdsworth, Michael J. 2009. The N-end rule pathway promotes seed germination and establishment through removal of ABA sensitivity in *Arabidopsis*. *Proceedings of the National Academy of Sciences of the United States of America*, **106**(11), 4549–54.
- Hoppe, Thorsten. 2005. Multiubiquitylation by E4 enzymes: 'One size' doesn't fit all. *Trends in Biochemical Sciences*, **30**(4), 183–187.
- Howles, Paul A., Gebbie, Leigh K., Collings, David A., Varsani, Arvind, Broad, Ronan C., Ohms, Stephen, Birch, Rosemary J., Cork, Ann H., Arioli, Tony, & Williamson, Richard E. 2016. A temperature-sensitive allele of a

- putative mRNA splicing helicase down-regulates many cell wall genes and causes radial swelling in *Arabidopsis thaliana*. *Plant Molecular Biology*, **91**(1-2).
- Hu, Rong-Gui, Sheng, Jun, Qi, Xin, Xu, Zhenming, Takahashi, Terry T, & Varshavsky, Alexander. 2005. The N-end rule pathway as a nitric oxide sensor controlling the levels of multiple regulators. *Nature*, **437**(October), 981–986.
- Hua, Zhihua, & Vierstra, Richard D. 2011. The cullin-RING ubiquitin-protein ligases. *Annual review of plant biology*, **62**(1), 299–334.
- Huala, Eva, & Sussex, Im. 1992. LEAFY Interacts with Floral Homeotic Genes to Regulate Arabidopsis Floral Development. *The Plant Cell*, **4**(8), 901–913.
- Huibregtse, J M, Scheffner, M, Beaudenon, S, & Howley, P M. 1995. A family of proteins structurally and functionally related to the E6-AP ubiquitin-protein ligase. *Proceedings of the National Academy of Sciences of the United States of America*, **92**(7), 2563–2567.
- Hülkamp, Martin. 2004. Plant trichomes: a model for cell differentiation. *Nature reviews. Molecular cell biology*, **5**(6), 471–80.
- Hwang, Cheol-Sang, & Varshavsky, Alexander. 2008. Regulation of peptide import through phosphorylation of Ubr1, the ubiquitin ligase of the N-end rule pathway. *Proceedings of the National Academy of Sciences of the United States of America*, **105**(49), 19188–93.
- Hwang, Cheol-Sang, Shemorry, Anna, & Varshavsky, Alexander. 2010a. N-terminal acetylation of cellular proteins creates specific degradation signals. *Science*, **327**(5968), 973–7.
- Hwang, Cheol-Sang, Shemorry, Anna, Auerbach, Daniel, & Varshavsky, Alexander. 2010b. The N-end rule pathway is mediated by a complex of the RING-type Ubr1 and HECT-type Ufd4 ubiquitin ligases. *Nature Cell Biology*, **12**(12), 1177–1185.
- Hwang, Cheol Sang, Sukalo, Maja, Batygin, Olga, Addor, Marie Claude, Brunner, Han, Aytes, Antonio Perez, Mayerle, Julia, Song, Hyun Kyu, Varshavsky, Alexander, & Zenker, Martin. 2011. Ubiquitin ligases of the N-END rule pathway: Assessment of mutations in UBR1 that cause the Johanson-Blizzard syndrome. *PLoS ONE*, **6**(9).
- Inobe, Tomonao, Fishbain, Susan, Prakash, Sumit, & Matouschek, Andreas. 2011. Defining the geometry of the two-component proteasome degron. *Nature chemical biology*, **7**(3), 161–7.
- Irish, Vivian F. 2010. The flowering of Arabidopsis flower development. *The Plant Journal*, **61**(6), 1014–1028.
- Ivantsiv, Yelena, Kaplun, Ludmila, Tzirkin-Goldin, Regina, Shabek, Nitzan, & Raveh, Dina. 2006. Unique role for the Ubl-Uba protein Ddi1 in turnover of SCFUfo1 complexes. *Mol. Cell. Biol.*, **26**(5), 1579–88.
- Jääntti, Jussi, Aalto, Markku K, Oyen, Mattias, Sundqvist, Lena, Keränen, Sirkka, & Ronne, Hans. 2002. Characterization of temperature-sensitive mutations in the yeast syntaxin 1 homologues Sso1p and Sso2p, and evidence of a distinct function for Sso1p in sporulation. *Journal of cell science*, **115**(Pt 2), 409–20.
- Jefferson, Richard A, Kavanagh, Tony A, & Bevan, Michael W. 1987. GUS fusions: B-glucuronidase as a sensitive and versatile gene fusion marker in higher plants. *EMBO Journal*, **6**(13), 3901–3907.
- Jeon, Joo Mi, Ahn, Nam Young, Son, Bo Hwa, Kim, Cha Young, Han, Chang Deok, Kim, Gun Do, Gal, Sang Wan, & Lee, Sung Ho. 2007. Efficient transient expression and transformation of PEG-mediated gene uptake into mesophyll protoplasts of pepper (*Capsicum annuum* L.). *Plant Cell, Tissue and Organ Culture*, **88**(2), 225–232.
- Johnson, E. S., Ma, P. C M, Ota, I. M., & Varshavsky, A. 1995. A proteolytic pathway that recognizes ubiquitin as a degradation signal. *Journal of Biological Chemistry*, **270**(29), 17442–17456.
- Jones, D. C., Mistry, I. N., & Tavassoli, A. 2016. Post-translational control of protein function with light using a LOV-intein fusion protein. *Mol. BioSyst.*, **12**, 1388–1393.
- Jungbluth, Marc, Renicke, Christian, & Taxis, Christof. 2010. Targeted protein depletion in *Saccharomyces cerevisiae* by activation of a bidirectional degron. *BMC systems biology*, **4**(1), 176.
- Kao, Ai Ling, Lin, Ying Han, Chen, Rita P Y, Huang, Yun Yen, Chen, Ching Chung, & Yang, Chien Chih. 2012. E3-independent ubiquitination of AtMAPR/MSBP1. *Phytochemistry*, **78**, 7–19.
- Kapust, R B, Tözsér, J, Fox, J D, Anderson, D E, Cherry, S, Copeland, T D, & Waugh, D S. 2001. Tobacco etch virus protease: mechanism of autolysis and rational design of stable mutants with wild-type catalytic proficiency. *Protein engineering*, **14**(12), 993–1000.

- Kelly, A J, Bonnlander, M B, & Meeks-Wagner, D R. 1995. NFL, the tobacco homolog of FLORICAULA and LEAFY, is transcriptionally expressed in both vegetative and floral meristems. *The Plant Cell*, **7**(2), 225–34.
- Kim, Do-Young, Scalf, Mark, Smith, Lloyd M, & Vierstra, Richard D. 2013. Advanced proteomic analyses yield a deep catalog of ubiquitylation targets in Arabidopsis. *The Plant Cell*, **25**(5), 1523–40.
- Kim, Heon-Ki, Kim, Ryu-Ryun, Oh, Jang-Hyun, Cho, Hanna, Varshavsky, Alexander, & Hwang, Cheol-Sang. 2014. The N-Terminal Methionine of Cellular Proteins as a Degradation Signal. *Cell*, **156**(1-2), 158–169.
- Kim, Jong Hum, & Kim, Woo Taek. 2013. The Arabidopsis RING E3 ubiquitin ligase AtAIRP3/LOG2 participates in positive regulation of high-salt and drought stress responses. *Plant Physiology*, **162**(3), 1733–49.
- Kim, Kye-Won, Franceschi, Vincent R., Davin, Laurence B., & Lewis, Norman G. 2006.  $\beta$ -Glucuronidase as Reporter Gene. *Chap. 22, pages 263–274 of: Salinas, Julio, & Sanchez-Serrano, Jose J. (eds), Methods in Molecular Biology - Arabidopsis Protocols*, second edn., vol. 323. Totowa, New Jersey: Humana Press.
- Kim, Min Kyung, Oh, Sun Joo, Lee, Byung-Gil, & Song, Hyun Kyu. 2016. Structural basis for dual specificity of yeast N-terminal amidase in the N-end rule pathway. *Proceedings of the National Academy of Sciences of the United States of America*.
- Kirisako, Takayoshi, Kamei, Kiyoko, Murata, Shigeo, Kato, Michiko, Fukumoto, Hiromi, Kanie, Masato, Sano, Soichi, Tokunaga, Fuminori, Tanaka, Keiji, & Iwai, Kazuhiro. 2006. A ubiquitin ligase complex assembles linear polyubiquitin chains. *The EMBO journal*, **25**(20), 4877–87.
- Kish-Trier, Erik, & Hill, Christopher P. 2013. Structural biology of the proteasome. *Annual review of biophysics*, **42**, 29–49.
- Klecker, Maria, & Dissmeyer, Nico. 2016. Peptide Arrays for Binding Studies of E3 Ubiquitin Ligases. *Chap. 7, pages 85–94 of: Lois, Maria L, & Matthiesen, Rune (eds), Plant Proteostasis: Methods and Protocols*. New York, NY: Springer Science+Business Media.
- Kofoed, Megan, Milbury, Karissa L, Chiang, Jennifer H, Sinha, Sunita, Ben-Aroya, Shay, Giaever, Guri, Nislow, Corey, Hieter, Philip, & Stirling, Peter C. 2015. An Updated Collection of Sequence Barcoded Temperature-Sensitive Alleles of Yeast Essential Genes. *G3 (Bethesda, Md.)*, **5**(9), 1879–87.
- Koksharov, Mikhail I., & Ugarova, Natalia N. 2011. Thermostabilization of firefly luciferase by in vivo directed evolution. *Protein Engineering, Design and Selection*, **24**(11), 835–844.
- Koliopoulos, Marios G, Esposito, Diego, Christodoulou, Evangelos, Taylor, Ian A, & Rittinger, Katrin. 2016. Functional role of TRIM E 3 ligase oligomerization and regulation of catalytic activity. *The EMBO journal*, **35**(11), 1–15.
- Koncz, Csaba, & Schell, Jeff. 1986. The promoter of TL-DNA gene 5 controls the tissue-specific expression of chimaeric genes carried by a novel type of Agrobacterium binary vector. *Molecular and General Genetics MGG*, **204**(3), 383–396.
- Kovermann, Michael, Ådén, Jörgen, Grundström, Christin, Elisabeth Sauer-Eriksson, a., Sauer, Uwe H., & Wolf-Watz, Magnus. 2015. Structural basis for catalytically restrictive dynamics of a high-energy enzyme state. *Nature Communications*, **6**(May), 7644.
- Kravtsova-Ivantsiv, Y., & Ciechanover, a. 2012. Non-canonical ubiquitin-based signals for proteasomal degradation. *Journal of Cell Science*, **125**(3), 539–548.
- Kreidenweiss, Andrea, Hopkins, Annika V., & Mordmüller, Benjamin. 2013. 2A and the auxin-based degron system facilitate control of protein levels in Plasmodium falciparum. *PLoS ONE*, **8**(11), 2–7.
- Kurepa, Jasmina, Wang, Songhu, Li, Yan, Zaitlin, David, Pierce, Andrew J, & Smalle, Jan a. 2009. Loss of 26S proteasome function leads to increased cell size and decreased cell number in Arabidopsis shoot organs. *Plant Physiology*, **150**(1), 178–189.
- Kurepa, Jasmina, Karangwa, Consolée, Duke, Liliana Sfichi, & Smalle, Jan A. 2010. Arabidopsis sensitivity to protein synthesis inhibitors depends on 26S proteasome activity. *Plant Cell Reports*, **29**(3), 249–259.
- Kwon, Y T, Kashina, a S, & Varshavsky, A. 1999. Alternative splicing results in differential expression, activity, and localization of the two forms of arginyl-tRNA-protein transferase, a component of the N-end rule pathway. *Molecular and cellular biology*, **19**(1), 182–193.
- Kwon, Y T, Balogh, S a, Davydov, I V, Kashina, a S, Yoon, J K, Xie, Y, Gaur, a, Hyde, L, Denenberg, V H, & Varshavsky, a. 2000. Altered activity, social behavior, and spatial memory in mice lacking the NTAN1p amidase and the asparagine branch of the N-end rule pathway. *Molecular and cellular biology*, **20**(11), 4135–4148.

- Kyhse-Andersen, J. 1984. Electroblotting of multiple gels: a simple apparatus without buffer tank for rapid transfer of proteins from polyacrylamide to nitrocellulose. *Journal of biochemical and biophysical methods*, **10**(3-4), 203–209.
- Lane, Diana R, Wiedemeier, Allison, Peng, Liangcai, Ho, Herman, Vernhettes, Samantha, Hocart, Charles H, Birch, Rosemary J, Baskin, Tobias I, Burn, Joanne E, Arioli, Tony, Betzner, Andreas S, & Williamson, Richard E. 2001. Temperature-Sensitive Alleles of RSW2 Link the KORRIGAN Endo-1, 4- $\beta$ -Glucanase to Cellulose Synthesis and Cytokinesis in Arabidopsis. *Plant Physiology*, **126**(May), 278–288.
- Lannanpaa, M, Hassinen, M, Ranki, A, Holtta Vuori, M, Lemmetyinen, J, Keinonen, K, & Sopanen, T. 2005. Prevention of flower development in birch and other plants using a BpFULL1 :: BARNASE construct. *Plant Cell Reports*, **24**(2), 69–78.
- Larkin, J C, Young, N, Prigge, M, & Marks, M D. 1996. The control of trichome spacing and number in Arabidopsis. *Development*, **122**, 997–1005.
- Lee, Imsang, & Schindelin, Hermann. 2008. Structural Insights into E1-Catalyzed Ubiquitin Activation and Transfer to Conjugating Enzymes. *Cell*, **134**(2), 268–278.
- Lee, Sookjin, Lee, Dong Wook, Lee, Yongjik, Mayer, Ulrike, Stierhof, York-dieter, Lee, Sumin, Jürgens, Gerd, & Hwang, Inhwan. 2009. Heat shock protein cognate 70-4 and an E3 ubiquitin ligase, CHIP, mediate plastid-destined precursor degradation through the ubiquitin-26S proteasome system in Arabidopsis. *The Plant Cell*, **21**(12), 3984–4001.
- Leuchtenberger, S, Perz, A, Gatz, C, & Bartsch, J W. 2001. Conditional cell ablation by stringent tetracycline-dependent regulation of barnase in mammalian cells. *Nucleic acids research*, **29**(16), E76.
- Levitt, Michael. 1981. Effect of proline residues on protein folding. *Journal of Molecular Biology*, **145**(1), 251–263.
- Li, Jian Feng, Bush, Jenifer, Xiong, Yan, Li, Lei, & McCormack, Matthew. 2011a. Large-scale protein-protein interaction analysis in Arabidopsis mesophyll protoplasts by split firefly luciferase complementation. *PLoS ONE*, **6**(11).
- Li, Zhijian, Vizeacoumar, Franco J, Bahr, Sondra, Li, Jingjing, Warringer, Jonas, Vizeacoumar, Frederick S, Min, Renqiang, Vandersluis, Benjamin, Bellay, Jeremy, Devit, Michael, Fleming, James A, Stephens, Andrew, Haase, Julian, Lin, Zhen-Yuan, Baryshnikova, Anastasia, Lu, Hong, Yan, Zhun, Jin, Ke, Barker, Sarah, Datti, Alessandro, Giaever, Guri, Nislow, Corey, Bulawa, Chris, Myers, Chad L, Costanzo, Michael, Gingras, Anne-Claude, Zhang, Zhaolei, Blomberg, Anders, Bloom, Kerry, Andrews, Brenda, & Boone, Charles. 2011b. Systematic exploration of essential yeast gene function with temperature-sensitive mutants. *Nature biotechnology*, **29**(4), 361–7.
- Licausi, Francesco, Kosmacz, Monika, Weits, Daan a, Giuntoli, Beatrice, Giorgi, Federico M, Voesenek, Laurentius a C J, Perata, Pierdomenico, & van Dongen, Joost T. 2011. Oxygen sensing in plants is mediated by an N-end rule pathway for protein destabilization. *Nature*, **479**(7373), 419–22.
- Lichty, Jordan J., Malecki, Joshua L., Agnew, Heather D., Michelson-Horowitz, Daniel J., & Tan, Song. 2005. Comparison of affinity tags for protein purification. *Protein Expression and Purification*, **41**(1), 98–105.
- Liu, Xiang-qin. 2000. Protein -Splicing Intein : Genetic Mobility , Origin , and Evolution. *Annu. Rev. Genet.*, **34**, 61–76.
- Lohmann, Jan U., Hong, Ray L., Hobe, Martin, Busch, Maximilian A., Parcy, François, Simon, Rüdiger, & Weigel, Detlef. 2001. A molecular link between stem cell regulation and floral patterning in Arabidopsis. *Cell*, **105**(6), 793–803.
- Lucas, Xavier, & Ciulli, Alessio. 2017. Recognition of substrate degrons by E3 ubiquitin ligases and modulation by small-molecule mimicry strategies. *Current Opinion in Structural Biology*, **44**, 101–110.
- Luker, Kathryn E, Smith, Matthew C P, Luker, Gary D, Gammon, Seth T, Piwnica-Worms, Helen, & Piwnica-Worms, David. 2004. Kinetics of regulated protein-protein interactions revealed with firefly luciferase complementation imaging in cells and living animals. *Proceedings of the National Academy of Sciences of the United States of America*, **101**(33), 12288–12293.
- Mackay, J. Andrew, & Chilkoti, Ashutosh. 2008. Temperature sensitive peptides: Engineering hyperthermia- directed therapeutics. *Journal of Hyperthermia*, **24**(6).
- Maculins, Timurs, Fiskin, Evgenij, Bhogaraju, Sagar, & Dikic, Ivan. 2016. Bacteria-host relationship: ubiquitin ligases as weapons of invasion. *Cell Research*, **26**(4), 499–510.

- Majovsky, Petra, Naumann, Christin, Lee, Chil-Woo, Lassowskat, Ines, Trujillo, Marco, Dissmeyer, Nico, & Hohenwarter, Wolfgang. 2014. Targeted Proteomics Analysis of Protein Degradation in Plant Signaling on an LTQ-Orbitrap Mass Spectrometer. *Journal of Proteome Research*, **13**(10), 4246–4258.
- Maor, Rudy, Jones, Alex, Nühse, Thomas S, Studholme, David J, Peck, Scott C, & Shirasu, Ken. 2007. Multidimensional protein identification technology (MudPIT) analysis of ubiquitinated proteins in plants. *Molecular & cellular proteomics*, **6**(4), 601–610.
- Mariani, Celestina, Gossele, Veronique, Beuckeleer, Marc De, Block, Marc De, Goldberg, Robert B., Greef, Willy De, & Leemans, Jan. 1992. A chimaeric ribonuclease-inhibitor gene restores fertility to male sterile plants. *Nature*, **357**(6377), 384–387.
- Mason, J O, Kitajewski, J, & Varmus, H E. 1992. Mutational analysis of mouse Wnt-1 identifies two temperature-sensitive alleles and attributes of Wnt-1 protein essential for transformation of a mammary cell line. *Molecular biology of the cell*, **3**(5), 521–33.
- Mathur, Jaideep, & Koncz, Csaba. 1997. Method for preparation of epidermal imprints using agarose. *BioTechniques*, **22**(2), 280–282.
- Matsuura, Tomoaki, Hosoda, Kazufumi, Ichihashi, Norikazu, Kazuta, Yasuaki, & Yomo, Tetsuya. 2011. Kinetic analysis of  $\beta$ -galactosidase and  $\beta$ -glucuronidase tetramerization coupled with protein translation. *Journal of Biological Chemistry*, **286**(25), 22028–34.
- Matta-Camacho, Edna, Kozlov, Guennadi, Li, Flora F, & Gehring, Kalle. 2010. Structural basis of substrate recognition and specificity in the N-end rule pathway. *Nature structural & Molecular biology*, **17**(10), 1182–7.
- McIsaac, R Scott, Silverman, Sanford J, McClean, Megan N, Gibney, Patrick a, Macinskas, Joanna, Hickman, Mark J, Petti, Allegra a, & Botstein, David. 2011. Fast-acting and nearly gratuitous induction of gene expression and protein depletion in *Saccharomyces cerevisiae*. *Molecular biology of the cell*, **22**(22), 4447–59.
- Meierhofer, David, Wang, Xiaorong, Huang, Lan, & Kaiser, Peter. 2008. Quantitative analysis of global ubiquitination in HeLa cells by mass spectrometry. *Journal of Proteome Research*, **7**(10), 4566–4576.
- Mendondo, Guillermina M., Gibbs, Daniel J., Szurman-Zubrzycka, Miriam, Korn, Arnd, Marquez, Julietta, Szarejko, Iwona, Maluszynski, Mirosław, King, John, Axcell, Barry, Smart, Katherine, Corbineau, Francoise, & Holdsworth, Michael J. 2016. Enhanced waterlogging tolerance in barley by manipulation of expression of the N-end rule pathway E3 ligase PROTEOLYSIS6. *Plant Biotechnology Journal*, **14**(1), 40–50.
- Meusser, Birgit, Hirsch, Christian, Jarosch, Ernst, & Sommer, Thomas. 2005. ERAD: the long road to destruction. *Nature cell biology*, **7**(8), 766–72.
- Mielke, Stefan. 2014. *Conditional expression of toxic proteins in plants utilizing the N-end rule pathway*. Tech. rept. Martin-Luther-University Halle-Wittenberg (MLU) / Leibniz Institute of Plant Biochemistry.
- Miletti, Teresa, Di Trani, Justin, Levros, Louis Charles, & Mittermaier, Anthony. 2015. Conformational plasticity surrounding the active site of NADH oxidase from *Thermus thermophilus*. *Protein Science*, **24**(7), 1114–1128.
- Mizukami, Y. 1996. Functional Domains of the Floral Regulator AGAMOUS: Characterization of the DNA Binding Domain and Analysis of Dominant Negative Mutations. *The Plant Cell*, **8**(5), 831–845.
- Mizukami, Y, & Ma, H. 1997. Determination of Arabidopsis floral meristem identity by AGAMOUS. *The Plant Cell*, **9**(3), 393–408.
- Mizukami, Yukiko, & Ma, Hong. 1992. Ectopic expression of the floral homeotic gene AGAMOUS in transgenic Arabidopsis plants alters floral organ identity. *Cell*, **71**(1), 119–131.
- Morrison, Kim L., & Weiss, Gregory A. 2001. Combinatorial alanine-scanning. *Current Opinion in Chemical Biology*, **5**(3), 302–307.
- Mot, Augustin C, Prell, Erik, Klecker, Maria, Naumann, Christin, Faden, Frederik, Westermann, Bernhard, & Dissmeyer, Nico. 2017. Real-time detection of PRT1-mediated ubiquitination via fluorescently labeled substrate probes. *New Phytologist (in press)*.
- Murphy, T. 2003. *The Drosophila Gateway Vector Collection*.
- Nakasone, Mark A., Livnat-Levanon, Nurit, Glickman, Michael H., Cohen, Robert E., & Fushman, David. 2013. Mixed-linkage ubiquitin chains send mixed messages. *Structure*, **21**(5), 727–740.
- Natsume, Toyooki, Kiyomitsu, Tomomi, Saga, Yumiko, & Kanemaki, Masato T. 2016. Rapid Protein Depletion in Human Cells by Auxin-Inducible Degron Tagging with Short Homology Donors. *Cell Reports*, **15**(1), 210–218.

- Naumann, Christin, Mot, Augustin C, & Dissmeyer, Nico. 2016. Generation of Artificial N-end Rule Substrate Proteins In Vivo and In Vitro. *Chap. 6, pages 107–123 of: Lois, L. Maria, & Matthiesen, Rune (eds), Plant Proteostasis: Methods and Protocols*. New York, NY: Springer Science+Business Media.
- Neff, Michael M., Neff, Joseph D., Chory, Joanne, & Pepper, Alan E. 1998. dCAPS, a simple technique for the genetic analysis of single nucleotide polymorphisms: Experimental applications in *Arabidopsis thaliana* genetics. *Plant Journal*, **14**(3), 387–392.
- Ninnin, Robert L, Spall, Sukhdeep K, Talbo, Hert H, Truscott, Kaye N, & Dougan, David A. 2009. *Modification of PATase by L/F-transferase generates a ClpS-dependent N-end rule substrate in Escherichia coli*.
- Nishimura, K., Fukagawa, T., Takisawa, H., Hakimoto, T., & Kanemaki, M. 2009. An auxin-based degron system for the rapid depletion of proteins in nonplant cells. *Nature Methods*, **53**(9), 1689–1699.
- No, D, Yao, T P, & Evans, R M. 1996. Ecdysone-inducible gene expression in mammalian cells and transgenic mice. *Proceedings of the National Academy of Sciences of the United States of America*, **93**(8), 3346–51.
- Nørholm, Morten H H. 2010. A mutant Pfu DNA polymerase designed for advanced uracil-excision DNA engineering. *BMC biotechnology*, **10**, 21.
- Norris, Susan R., Meyer, Sandra E., & Callis, Judy. 1993. The intron of *Arabidopsis thaliana* polyubiquitin genes is conserved in location and is a quantitative determinant of chimeric gene expression. *Plant Molecular Biology*, **21**(5), 895–906.
- Ogunjimi, Abiodun A., Briant, Douglas J., Pece-Barbara, Nadia, Le Roy, Christine, Di Guglielmo, Gianni M., Kavsak, Peter, Rasmussen, Richele K., Seet, Bruce T., Sicheri, Frank, & Wrana, Jeffrey L. 2005. Regulation of Smurf2 ubiquitin ligase activity by anchoring the E2 to the HECT domain. *Molecular Cell*, **19**(3), 297–308.
- O'Rourke, Sean M., Carter, Clayton, Carter, Luke, Christensen, Sara N., Jones, Minh P., Nash, Bruce, Price, Meredith H., Turnbull, Douglas W., Garner, Aleena R., Hamill, Danielle R., Osterberg, Valerie R., Lyczak, Rebecca, Madison, Erin E., Nguyen, Michael H., Sandberg, Nathan A., Sedghi, Noushin, Willis, John H., Yochem, John, Johnson, Eric A., & Bowerman, Bruce. 2011. A survey of new temperature-sensitive, embryonic-lethal mutations in *C. elegans*: 24 alleles of thirteen genes. *PLoS ONE*, **6**(3).
- Pappenheimer Jr., A. M. 1977. Diphtheria Toxin. *Annu Rev Biochem*, **46**, 69–94.
- Park, Sang-Eun, Kim, Jeong-Mok, Seok, Ok-Hee, Cho, Hanna, Wadas, Brandon, Kim, Seon-Young, Varshavsky, Alexander, Hwang, Cheol-Sang, & Rgs2. 2015. Teb4 RGS2 supplemental. *Science*, **347**(6227), 1249–1252.
- Pearce, Michael J, Mintseris, Julian, Ferreyra, Jessica, Gygi, Steven P, & Heran, K. 2008. Ubiquitin-Like Protein Involved in the Proteasome Pathway of *Mycobacterium tuberculosis*. *Science*, **322**(5904), 1104–1107.
- Peng, Junmin, Schwartz, Daniel, Elias, Joshua E, Thoreen, Carson C, Cheng, Dongmei, Marsischky, Gerald, Roelofs, Jeroen, Finley, Daniel, & Gygi, Steven P. 2003. A proteomics approach to understanding protein ubiquitination. *Nature biotechnology*, **21**(8), 921–926.
- Pesch, Martina, & Hülskamp, Martin. 2011. Role of TRIPTYCHON in trichome patterning in *Arabidopsis*. *BMC plant biology*, **11**, 130.
- Petroski, Matthew D, & Deshaies, Raymond J. 2005. Function and regulation of cullin-RING ubiquitin ligases. *Nature reviews. Molecular cell biology*, **6**(1), 9–20.
- Pettersen, E F, Goddard, T D, Huang, C C, Couch, G S, Greenblatt, D M, Meng, E C, & Ferrin, T E. 2004. UCSF Chimera—a visualization system for exploratory research and analysis. *J Comput Chem*, **25**(13), 1605–1612.
- Piatkov, Konstantin, Graciet, Emmanuelle, & Varshavsky, Alexander. 2013. Ubiquitin Reference Technique and Its Use in Ubiquitin-Lacking Prokaryotes. *PLoS ONE*, **8**(6), 1–7.
- Piatkov, Konstantin I, Brower, Christopher S, & Varshavsky, Alexander. 2012. The N-end rule pathway counteracts cell death by destroying proapoptotic protein fragments. *Proceedings of the National Academy of Sciences of the United States of America*, **109**(27), E1839–47.
- Piazzon, Nathalie, Schlotter, Florence, Lefebvre, Suzie, Dodré, Maxime, Méreau, Agnès, Soret, Johann, Besse, Aurore, Barkats, Martine, Bordonné, Rémy, Branlant, Christiane, & Massenet, Séverine. 2012. Implication of the SMN complex in the biogenesis and steady state level of the signal recognition particle. *Nucleic acids research*, **41**(2), 1255–72.
- Pickart, Cecile M., & Eddins, Michael J. 2004. Ubiquitin: Structures, functions, mechanisms. *Biochimica et Biophysica Acta - Molecular Cell Research*, **1695**(1-3), 55–72.

- Pickett, F B, Champagne, M M, & Meeks-Wagner, D R. 1996. Temperature-sensitive mutations that arrest Arabidopsis shoot development. *Development (Cambridge, England)*, **122**(12), 3799–807.
- Plattner, Nuria, & Noé, Frank. 2015. Protein conformational plasticity and complex ligand-binding kinetics explored by atomistic simulations and Markov models. *Nature Communications*, **6**(May), 7653.
- Pomeranz, Marcelo, Campbell, Jeffrey, Siegal-Gaskins, Dan, Engelmeier, Jacob, Wilson, Tyler, Fernandez, Virginia, Brkljacic, Jelena, & Grotewold, Erich. 2013. High-resolution computational imaging of leaf hair patterning using polarized light microscopy. *Plant Journal*, **73**(4), 701–708.
- Potuschak, T, Stary, S, Schlögelhofer, P, Becker, F, Nejinskaia, V, & Bachmair, a. 1998. PRT1 of Arabidopsis thaliana encodes a component of the plant N-end rule pathway. *Proceedings of the National Academy of Sciences of the United States of America*, **95**(14), 7904–8.
- Prakash, Sumit, Tian, Lin, Ratliff, Kevin S, Lehotzky, Rebecca E, & Matouschek, Andreas. 2004. An unstructured initiation site is required for efficient proteasome-mediated degradation. *Nature structural & molecular biology*, **11**(9), 830–837.
- Prakash, Sumit, Inobe, Tomonao, Hatch, Ace Joseph, & Matouschek, Andreas. 2009. Substrate selection by the proteasome during degradation of protein complexes. *Nature chemical biology*, **5**(1), 29–36.
- Pryme, Ian F, Dale, Truls M, & Tilrem, Pontus. 2007. Oral mistletoe lectins : A case for their use in cancer therapy. *Cancer Therapy*, **5**, 287–300.
- Qiao, Feng, & Bowie, James U. 2005. The many faces of SAM. *Science's STKE : signal transduction knowledge environment*, **286**.
- Quint, Marcel, Ito, Hironori, Zhang, Wenjing, & Gray, William M. 2005. Characterization of a novel temperature-sensitive allele of the CUL1/AXR6 subunit of SCF ubiquitin-ligases. *Plant Journal*, **43**(3), 371–383.
- Raasi, Shahri, & Pickart, Cecile M. 2003. Rad23 ubiquitin-associated domains (UBA) inhibit 26 S proteasome-catalyzed proteolysis by sequestering lysine 48-linked polyubiquitin chains. *Journal of Biological Chemistry*, **278**(11), 8951–8959.
- Rademacher, Thomas, Häusler, Rainer E., Hirsch, Heinz Josef, Zhang, Li, Lipka, Volker, Weier, Dagmar, Kreuzaler, Fritz, & Peterhänsel, Christoph. 2002. An engineered phosphoenolpyruvate carboxylase redirects carbon and nitrogen flow in transgenic potato plants. *Plant Journal*, **32**(1), 25–39.
- Rai, Reena, & Kashina, Anna. 2005. Identification of mammalian arginyltransferases that modify a specific subset of protein substrates. *Proceedings of the National Academy of Sciences of the United States of America*, **102**(29), 10123–10128.
- Rajagopalan, Srividya, Liling, Zheng, Liu, Jianhua, & Balasubramanian, Mohan. 2004. The N-degron approach to create temperature-sensitive mutants in Schizosaccharomyces pombe. *Methods (San Diego, Calif.)*, **33**(3), 206–12.
- Raju, Gollapalli Naga, Karumudi, Bhavya Sai, & Rao, N. Rama. 2015. Benzothiazole - Versatile heterocyclic nucleus in medicinal chemistry: A review. *International Journal of Pharmaceutical Chemistry*, **5**(4), 104–114.
- Ranaweera, Ruchira S., & Yang, Xiaolu. 2013. Auto-ubiquitination of Mdm2 enhances its substrate ubiquitin ligase activity. *Journal of Biological Chemistry*, **288**(26), 18939–18946.
- Rao, H, Uhlmann, F, Nasmyth, K, & Varshavsky, a. 2001. Degradation of a cohesin subunit by the N-end rule pathway is essential for chromosome stability. *Nature*, **410**(6831), 955–9.
- Redden, Heidi, & Alper, Hal S. 2015. The development and characterization of synthetic minimal yeast promoters. *Nature Communications*, **6**, 7810.
- Reiss, Yuval, Kaim, David, & Hershko, Avram. 1988. Specificity of Binding of NHa-terminal Residue of Proteins to Ubiquitin-Protein Ligase. *Journal of Biological Chemistry*, **414**(10).
- Reitter, Julie N., Cousin, Christopher E., Nicastrì, Michael C., Jaramillo, Mario V., & Mills, Kenneth V. 2016. Salt-Dependent Conditional Protein Splicing of an Intein from Halobacterium salinarum. *Biochemistry*, **55**(9), 1279–1282.
- Remington, S. James. 2011. Green fluorescent protein: A perspective. *Protein Science*, **20**(9), 1509–1519.
- Renicke, Christian, Schuster, Daniel, Usherenko, Svetlana, Essen, Lars-Oliver, & Taxis, Christof. 2013a. A LOV2 domain-based optogenetic tool to control protein degradation and cellular function. *Chemistry & biology*, **20**(4), 619–26.



- Renicke, Christian, Spadaccini, Roberta, & Taxis, Christof. 2013b. A tobacco etch virus protease with increased substrate tolerance at the P1' position. *PLoS ONE*, **8**(6), e67915.
- Rerie, W G, Feldmann, K A, & Marks, M D. 1994. The GLABRA2 gene encodes a homeodomain protein required for normal trichome development in Arabidopsis. *Genes Dev.*, **8**, 1388–1399.
- Riechmann, J L, Ito, T, & Meyerowitz, E M. 1999. Non-AUG initiation of AGAMOUS mRNA translation in Arabidopsis thaliana. *Molecular and cellular biology*, **19**(12), 8505–8512.
- Riechmann, Josie Luis, Krizek, Beth Allyn, & Meyerowitz, Elliot M. 1996. Dimerization specificity of Arabidopsis MADS domain homeotic proteins APETALA1, APETALA3, PISTILLATA, and AGAMOUS. *Proceedings of the National Academy of Sciences of the United States of America*, **93**(May), 4793–4798.
- Rodriguez, Susana, & Wolfgang, Michael J. 2012. Targeted chemical-genetic regulation of protein stability in vivo. *Chemistry and Biology*, **19**(3), 391–398.
- Román-Hernández, Giselle, Grant, Robert A, Sauer, Robert T, & Baker, Tania A. 2009. Molecular basis of substrate selection by the N-end rule adaptor protein ClpS. *Proceedings of the National Academy of Sciences of the United States of America*, **106**(22), 8888–8893.
- Román-Hernández, Giselle, Hou, Jennifer Y., Grant, Robert A., Sauer, Robert T., & Baker, Tania A. 2011. The ClpS Adaptor Mediates Staged Delivery of N-End Rule Substrates to the AAA+ ClpAP Protease. *Molecular Cell*, **43**(2), 217–228.
- Rottmann, William H., Meilan, Richard, Sheppard, Lorraine A., Brunner, Amy M., Skinner, Jeffrey S., Ma, Caiping, Cheng, Shuping, Jouanin, Lise, Pilate, Gilles, & Strauss, Steven H. 2000. Diverse effects of overexpression of LEAFY and PTLF, a poplar (*Populus*) homolog of LEAFY/FLORICAULA, in transgenic poplar and Arabidopsis. *The Plant Journal*, **22**(3), 235–245.
- Rudolph, M J, Wuebbens, M M, Rajagopalan, K V, & Schindelin, H. 2001. Crystal structure of molybdopterine synthase and its evolutionary relationship to ubiquitin activation. *Nature structural biology*, **8**(1), 42–46.
- Ruggiano, Annamaria, Foresti, Ombretta, & Carvalho, Pedro. 2014. ER-associated degradation: Protein quality control and beyond. *Journal of Cell Biology*, **204**(6), 869–879.
- Ruschak, Amy M., Religa, Tomasz L., Breuer, Sarah, Witt, Susanne, & Kay, Lewis E. 2010. The proteasome antechamber maintains substrates in an unfolded state. *Nature*, **467**(7317), 868–871.
- Sablowski, Robert W. M., & Meyerowitz, Elliot M. 1998. Temperature-Sensitive Splicing in the Floral Homeotic Mutant *apetala3-1*. *The Plant Cell*, **10**(9), 1453–1464.
- Saez, E, No, D, West, a, & Evans, R M. 1997. Inducible gene expression in mammalian cells and transgenic mice. *Current opinion in biotechnology*, **8**(5), 608–616.
- Saito, M, Iwakaki, T, Taya, C, Yonekawa, H, Noda, M, Inui, Y, Mekada, E, Kimata, Y, Tsuru, a, & Kohno, K. 2001a. Diphtheria toxin receptor-mediated conditional and targeted cell ablation in transgenic mice. *Nature biotechnology*, **19**(8), 746–750.
- Saito, M, Iwakaki, T, Taya, C, Yonekawa, H, Noda, M, Inui, Y, Mekada, E, Kimata, Y, Tsuru, a, & Kohno, K. 2001b. Diphtheria toxin receptor-mediated conditional and targeted cell ablation in transgenic mice. *Nature biotechnology*, **19**(8), 746–750.
- Savage, M, Soffle, RL, & Leibowitz, MJ. 1983. A mutant of *Saccharomyces cerevisiae* defective in arginyl-tRNA-protein transferase. *Current Genetics*, **7**(4), 285–288.
- Sayou, Camille, Monniaux, Marie, Nanao, Max H, Moyroud, Edwige, Brockington, Samuel F, Thévenon, Emmanuel, Chahtane, Hicham, Warthmann, Norman, Melkonian, Michael, Zhang, Yong, Wong, Gane Ka-Shu, Weigel, Detlef, Parcy, François, & Dumas, Renaud. 2014. A Promiscuous Intermediate Underlies the Evolution of LEAFY DNA Binding Specificity. *Science*, **343**(6171), 645–648.
- Sayou, Camille, Nanao, Max H, Jamin, Marc, Posé, Daniel, Thévenon, Emmanuel, Grégoire, Laura, Tichtinsky, Gabrielle, Denay, Grégoire, Ott, Felix, Lobet, Marta Peirats, Schmid, Markus, Dumas, Renaud, & Parcy, François. 2016. A SAM oligomerization domain shapes the genomic binding landscape of the LEAFY transcription factor. *Nature communications*, **7**.
- Scaglione, K Matthew, Bansal, Parmil K, Deffenbaugh, Andrew E, Kiss, Alexi, Moore, Johnnie M, Korolev, Sergey, Cocklin, Ross, Goebel, Mark, Kitagawa, Katsumi, & Skowrya, Dorota. 2007. SCF E3-mediated autoubiquitination negatively regulates activity of Cdc34 E2 but plays a nonessential role in the catalytic cycle in vitro and in vivo. *Molecular and cellular biology*, **27**(16), 5860–70.

- Schauber, C, Chen, L, Tongaonkar, P, Vega, I, Lambertson, D, Potts, W, & Madura, K. 1998. Rad23 links DNA repair to the ubiquitin/proteasome pathway. *Nature*, **391**(6668), 715–718.
- Schlesinger, David H, & Goldstein, Gideon. 1975. Molecular conservation of 74 amino acid sequence of ubiquitin between cattle and man. *Nature*, **255**(5507), 423–424.
- Schmid, Markus, Davison, Timothy S, Henz, Stefan R, Pape, Utz J, Demar, Monika, Vingron, Martin, Schölkopf, Bernhard, Weigel, Detlef, & Lohmann, Jan U. 2005. A gene expression map of Arabidopsis thaliana development. *Nature genetics*, **37**(5), 501–6.
- Schmidt, Ronny, Zahn, Regina, Bukau, Bernd, & Mogk, Axel. 2009. ClpS is the recognition component for Escherichia coli substrates of the N-end rule degradation pathway. *Molecular Microbiology*, **72**(2), 506–517.
- Schmitz, Jürgen, Prüfer, Dirk, Rohde, Wolfgang, & Tacke, Eckhard. 1996. Non-canonical translation mechanisms in plants: Efficient in vitro and in planta initiation at AUU codons of the tobacco mosaic virus enhancer sequence. *Nucleic Acids Research*, **24**(2), 257–263.
- Schnittger, a, Jürgens, G, & Hülskamp, M. 1998. Tissue layer and organ specificity of trichome formation are regulated by GLABRA1 and TRIPTYCHON in Arabidopsis. *Development (Cambridge, England)*, **125**(12), 2283–2289.
- Schreiner, Patrick, Chen, Xiang, Husnjak, Koraljka, Randles, Leah, Zhang, Naixia, Elsasser, Suzanne, Finley, Daniel, Dikic, Ivan, Walters, Kylie J., & Groll, Michael. 2008. Ubiquitin docking at the proteasome through a novel pleckstrin-homology domain interaction. *Nature*, **453**(7194), 548–552.
- Schuenemann, Verena J, Kralik, Stephanie M, Albrecht, Reinhard, Spall, Sukhdeep K, Truscott, Kaye N, Dougan, David A, & Zeth, Kornelius. 2009. Structural basis of N-end rule substrate recognition in Escherichia coli by the ClpAP adaptor protein ClpS. *EMBO reports*, **10**(5), 508–14.
- Schulman, Brenda a, & Harper, J Wade. 2009. Ubiquitin-like protein activation by E1 enzymes: the apex for downstream signalling pathways. *Nat Rev Mol Cell Biol*, **10**(5), 319–331.
- Schultz, Ea, & Haughn, Gw. 1991. LEAFY, a Homeotic Gene That Regulates Inflorescence Development in Arabidopsis. *The Plant Cell*, **3**(8), 771–781.
- Schwab, B, Folkers, U, Ilgenfritz, H, & Hülskamp, M. 2000. Trichome morphogenesis in Arabidopsis. *Philosophical transactions of the Royal Society of London. Series B, Biological sciences*, **355**(1399), 879–883.
- Schwartz, Alan L, & Ciechanover, Aaron. 2009. Targeting proteins for destruction by the ubiquitin system: implications for human pathobiology. *Annual review of pharmacology and toxicology*, **49**, 73–96.
- Sen, Nandini, Sen, Adrish, & Mackow, Erich R. 2007. Degrons at the C terminus of the pathogenic but not the nonpathogenic hantavirus G1 tail direct proteasomal degradation. *Journal of virology*, **81**(8), 4323–30.
- Sheard, Laura B, Tan, Xu, Mao, Haibin, Withers, John, Ben-Nissan, Gili, Hinds, Thomas R, Kobayashi, Yuichi, Hsu, Fong-Fu, Sharon, Michal, Browse, John, He, Sheng Yang, Rizo, Josep, Howe, Gregg a, & Zheng, Ning. 2010. Jasmonate perception by inositol-phosphate-potentiated COI1-JAZ co-receptor. *Nature*, **468**(7322), 400–405.
- Sheff, Mark A., & Thorn, Kurt S. 2004. Optimized cassettes for fluorescent protein tagging in Saccharomyces cerevisiae. *Yeast*, **21**(8), 661–670.
- Sheikh, Arsheed H, Eschen-Lippold, Lennart, Pecher, Pascal, Hoehenwarter, Wolfgang, Sinha, Alok K, Scheel, Dierk, & Lee, Justin. 2016. Regulation of WRKY46 Transcription Factor Function by Mitogen-Activated Protein Kinases in Arabidopsis thaliana. *Frontiers in Plant Science*, **7**.
- Shemorry, Anna, Hwang, Cheol Sang, & Varshavsky, Alexander. 2013. Control of Protein Quality and Stoichiometries by N-Terminal Acetylation and the N-End Rule Pathway. *Molecular Cell*, **50**(4), 540–551.
- Shibata, Yuri, Tokunaga, Fuminori, Goto, Eiji, Komatsu, Ginga, Gohda, Jin, Saeki, Yasushi, Tanaka, Keiji, Takahashi, Hirotaka, Sawasaki, Tatsuya, Inoue, Satoshi, Oshiumi, Hiroyuki, Seya, Tsukasa, Nakano, Hiroyasu, Tanaka, Yuetsu, Iwai, Kazuhiro, & Inoue, Jun-ichiro. 2017. HTLV-1 Tax Induces Formation of the Active Macromolecular IKK Complex by Generating Lys63- and Met1-Linked Hybrid Polyubiquitin Chains. *PLOS Pathogens*, **13**(1), e1006162.
- Shih, Yan-Ping, Wu, Hui-Chung, Hu, Su-Ming, Wang, Ting-Fang, & Wang, Andrew H-J. 2005. Self-cleavage of fusion protein in vivo using TEV protease to yield native protein. *Protein Science*, **14**(4), 936–41.
- Shortle, D, Novick, P, & Botstein, D. 1984. Construction and genetic characterization of temperature-sensitive mutant alleles of the yeast actin gene. *Proceedings of the National Academy of Sciences of the United States of America*, **81**(15), 4889–4893.

- Shrader, Thomas E, Tobias, John W, & Varshavsky, Alexander. 1993. The N-end rule in Escherichia coli: cloning and analysis of the leucyl , phenylalanyl-tRNA-Protein transferase gene *aat*. *Journal of Bacteriology*, **175**(14), 4364–4374.
- Simpson, Gordon G, Laurie, Rebecca E, Dijkwel, Paul P, Quesada, Victor, Stockwell, Peter a, Dean, Caroline, & Macknight, Richard C. 2010. Noncanonical translation initiation of the Arabidopsis flowering time and alternative polyadenylation regulator FCA. *The Plant Cell*, **22**(11), 3764–77.
- Siriwardana, Nirodhini S., & Lamb, Rebecca S. 2012. A conserved domain in the N-terminus is important for LEAFY dimerization and function in Arabidopsis thaliana. *The Plant Journal*, **71**(5), 736–749.
- Sirkis, Roy, Gerst, Jeffrey E., & Fass, Deborah. 2006. Ddi1, a Eukaryotic Protein With the Retroviral Protease Fold. *Journal of Molecular Biology*, **364**(3), 376–387.
- Speese, SD, Trotta, Nick, & Rodesch, CK. 2003. The ubiquitin proteasome system acutely regulates presynaptic protein turnover and synaptic efficacy. *Current Biology*, **13**, 899–910.
- Spratt, Donald E, Walden, Helen, & Shaw, Gary S. 2014. RBR E3 ubiquitin ligases: new structures, new insights, new questions. *The Biochemical journal*, **458**(3), 421–37.
- Sriram, S M, Kim, B Y, & Kwon, Y T. 2011. The N-end rule pathway: emerging functions and molecular principles of substrate recognition. *Nat Rev Mol Cell Biol*, **12**(11), 735–747.
- Sriram, Shashi, Lee, Jung Hoon, Mai, Binh Khanh, Jiang, Yanxialei, Kim, Yongho, Yoo, Young Dong, Banerjee, Rajkumar, Lee, Seung Han, & Lee, Min Jae. 2013. Development and characterization of monomeric N-end rule inhibitors through in vitro model substrates. *Journal of Medicinal Chemistry*, **56**(6), 2540–2546.
- Staes, An, Van Damme, Petra, Helsens, Kenny, Demol, Hans, Vandekerckhove, Joel, & Gevaert, Kris. 2008. Improved recovery of proteome-informative, protein N-terminal peptides by combined fractional diagonal chromatography (COFRADIC). *Proteomics*, **8**(7), 1362–1370.
- Stary, Susanne, Yin, Xiao-jun, Potuschak, Thomas, Schlo, Peter, Nizhynska, Victoria, & Bachmair, Andreas. 2003. PRT1 of Arabidopsis Is a Ubiquitin Protein Ligase of the Plant N-End Rule Pathway with Specificity for Aromatic Amino-Terminal Residues 1. *Plant Physiology*, **133**(November), 1360–1366.
- Stebbins, M J, Urlinger, S, Byrne, G, Bello, B, Hillen, W, & Yin, J C. 2001. Tetracycline-inducible systems for Drosophila. *Proceedings of the National Academy of Sciences of the United States of America*, **98**(19), 10775–10780.
- Steele-Mortimer, Olivia. 2011. Exploitation of the Ubiquitin System by Invading Bacteria. *Traffic*, **12**(2), 162–169.
- Stein, Benjamin J., Grant, Robert A., Sauer, Robert T., & Baker, Tania A. 2016. Structural Basis of an N-Degron Adaptor with More Stringent Specificity. *Structure*, **24**(2), 232–242.
- Stieglitz, Benjamin, Morris-Davies, Aylin C, Koliopoulos, Marios G, Christodoulou, Evangelos, & Rittinger, Katrin. 2012. LUBAC synthesizes linear ubiquitin chains via a thioester intermediate. *EMBO reports*, **13**(9), 840–6.
- Strittmatter, Günter, Janssens, Jan, Opsomer, Chris, & Botterman, Johan. 1995. Inhibition of Fungal Disease Development in Plants by Engineering Controlled Cell Death. *Nature Biotechnology*, **13**, 565–576.
- Strober, Warren. 2015. Trypan Blue Exclusion Test of Cell Viability. *Pages 1–3 of: John E. Coligan (ed), Current protocols in immunology*, vol. 111.
- Sturm, Arnd, & Lienhard, Susanne. 1998. Two isoforms of plant RAD23 complement a UV-sensitive RAD23 mutant in yeast. *Plant Journal*, **13**(6), 815–821.
- Su, Xinyi, Bernal, Juan a, & Venkitaraman, Ashok R. 2008. Cell-cycle coordination between DNA replication and recombination revealed by a vertebrate N-end rule degron-Rad51. *Nature structural & molecular biology*, **15**(10), 1049–58.
- Summers, Matthew K., Pan, Borlan, Mukhyala, Kiran, & Jackson, Peter K. 2008. The Unique N Terminus of the UbcH10 E2 Enzyme Controls the Threshold for APC Activation and Enhances Checkpoint Regulation of the APC. *Molecular Cell*, **31**(4), 544–556.
- Suzuki, Tetsuro, & Varshavsky, Alexander. 1999. Degradation signals in the lysine-asparagine sequence space. *The EMBO journal*, **18**(21), 6017–6026.
- Szymanski, D B, Jilk, R a, Pollock, S M, & Marks, M D. 1998. Control of GL2 expression in Arabidopsis leaves and trichomes. *Development (Cambridge, England)*, **125**(7), 1161–71.

- Takeuchi, Junko, Chen, Hui, & Coffino, Philip. 2007. Proteasome substrate degradation requires association plus extended peptide. *The EMBO journal*, **26**(1), 123–31.
- Tan, Guihong, Chen, Ming, Foote, Christopher, & Tan, Change. 2009. Temperature-sensitive mutations made easy: Generating conditional mutations by using temperature-sensitive inteins that function within different temperature ranges. *Genetics*, **183**(1), 13–22.
- Tanaka, Seiji, Miyazawa-Onami, Mayumi, Iida, Tetsushi, & Araki, Hiroyuki. 2015. iAID: an improved auxin-inducible degron system for the construction of a 'tight' conditional mutant in the budding yeast *Saccharomyces cerevisiae*. *Yeast*, **32**, 567–581.
- Tasaki, Takafumi, & Kwon, Yong Tae. 2007. The mammalian N-end rule pathway: new insights into its components and physiological roles. *Trends in Biochemical Sciences*, **32**(11), 520–528.
- Tasaki, Takafumi, Mulder, Lubbertus C F, Iwamatsu, Akihiro, Lee, Min Jae, Davydov, Ilia V, Varshavsky, Alexander, Muesing, Mark, & Kwon, Yong Tae. 2005. A Family of Mammalian E3 Ubiquitin Ligases That Contain the UBR Box Motif and Recognize N-Degrans. *Molecular and cellular biology*, **25**(16), 7120–7136.
- Tasaki, Takafumi, Sriram, Shashikanth M., Park, Kyong Soo, & Kwon, Yong Tae. 2012. The N-End Rule Pathway. *Annual Review of Biochemistry*, **81**(1), 261–289.
- Taxis, Christof, Stier, Gunter, Spadaccini, Roberta, & Knop, Michael. 2009. Efficient protein depletion by genetically controlled deprotection of a dormant N-degron. *Molecular systems biology*, **5**(267), 267.
- Thines, Bryan, Katsir, Leron, Melotto, Maeli, Niu, Yajie, Mandaokar, Ajin, Liu, Guanghui, Nomura, Kinya, He, Sheng Yang, Howe, Gregg A, & Browse, John. 2007. JAZ repressor proteins are targets of the SCF(COI1) complex during jasmonate signalling. *Nature*, **448**(7154), 661–665.
- Thompson, C J, Movva, N R, Tizard, R, Cramer, R, Davies, J E, Lauwereys, M, & Botterman, J. 1987. Characterization of the herbicide-resistance gene bar from *Streptomyces hygroscopicus*. *The EMBO journal*, **6**(9), 2519–23.
- Thorsness, M. K., Kandasamy, M. K., Nasrallah, M. E., & Nasrallah, J. B. 1993. Genetic Ablation of Floral Cells in Arabidopsis. *The Plant Cell*, **5**(3), 253–261.
- Thrower, J S, Hoffman, L, Rechsteiner, M, & Pickart, C M. 2000. Recognition of the polyubiquitin proteolytic signal. *The EMBO journal*, **19**(1), 94–102.
- Tian, Yong-Sheng, Xu, Jing, Zhao, Wei, Xing, Xiao-Juan, Fu, Xiao-Yan, Peng, Ri-He, & Yao, Quan-Hong. 2015. Identification of a phosphinothricin-resistant mutant of rice glutamine synthetase using DNA shuffling. *Scientific reports*, **5**(October), 15495.
- Trott, Maria, Weiß, Svenja, Antoni, Sascha, Koch, Joachim, Von Briesen, Hagen, Hust, Michael, & Dietrich, Ursula. 2014. Functional characterization of two scFv-Fc antibodies from an HIV controller selected on soluble HIV-1 Env complexes: A neutralizing V3- and a trimer-specific gp41 antibody. *PLoS ONE*, **9**(5).
- Tsugeki, R, & Fedoroff, N V. 1999. Genetic ablation of root cap cells in Arabidopsis. *Proceedings of the National Academy of Sciences of the United States of America*, **96**(22), 12941–12946.
- Twell, D. 1995. Diphtheria toxin-mediated cell ablation in developing pollen: Vegetative cell ablation blocks generative cell migration. *Protoplasma*, **187**(1-4), 144–154.
- Urakubo, Yoshiaki, Ikura, Teikichi, & Ito, Nobutoshi. 2008. Crystal structural analysis of protein-protein interactions drastically destabilized by a single mutation. *Protein science : a publication of the Protein Society*, **17**(6), 1055–65.
- Urbanus, Susan L, de Folter, Stefan, Shchennikova, Anna V, Kaufmann, Kerstin, Immink, Richard G H, & Angenent, Gerco C. 2009. In planta localisation patterns of MADS domain proteins during floral development in Arabidopsis thaliana. *BMC Plant Biology*, **9**(5).
- Usherenko, Svetlana, Stibbe, Hilke, Muscò, Massimiliano, Essen, Lars-Oliver, Kostina, Ekaterina a, & Taxis, Christof. 2014. Photo-sensitive degron variants for tuning protein stability by light. *BMC systems biology*, **8**(1), 128.
- Varfolomeev, Eugene, Blankenship, John W., Wayson, Sarah M., Fedorova, Anna V., Kayagaki, Nobuhiko, Garg, Parie, Zobel, Kerry, Dynek, Jasmin N., Elliott, Linda O., Wallweber, H. J A, Flygare, John A., Fairbrother, Wayne J., Deshayes, Kurt, Dixit, Vishva M., & Vucic, Domagoj. 2007. IAP Antagonists Induce Autoubiquitination of c-IAPs, NF- $\kappa$ B Activation, and TNF $\alpha$ -Dependent Apoptosis. *Cell*, **131**(4), 669–681.
- Varshavsky, Alexander. 1991. Naming a targeting signal. *Cell*, **64**(1), 13–15.

- Varshavsky, Alexander. 2003. The N-end rule and regulation of apoptosis. *Nature cell biology*, **5**(5), 373–6.
- Varshavsky, Alexander. 2005. Ubiquitin fusion technique and related methods. *Chap. 51, pages 777–99 of: Shukla, Arun K. (ed), Methods in enzymology*, vol. 399. Elsevier.
- Varshavsky, Alexander. 2011. The N-end rule pathway and regulation by proteolysis. *Protein science : a publication of the Protein Society*, **20**(jun), 1298–1345.
- Venne, A Saskia, Solari, Fiorella A, Faden, Frederik, Paretto, Tomasso, Dissmeyer, Nico, & Zahedi, René P. 2015. An improved workflow for quantitative N-terminal charge-based fractional diagonal chromatography (ChaFRADIC) to study proteolytic events in *Arabidopsis thaliana*. *Proteomics*, **15**(14), 2458–69.
- Verhoef, Lisette G G C, Heinen, Christian, Selivanova, Alexandra, Halff, Els F, Salomons, Florian A, & Dantuma, Nico P. 2009. Minimal length requirement for proteasomal degradation of ubiquitin-dependent substrates. *FASEB journal : official publication of the Federation of American Societies for Experimental Biology*, **23**(1), 123–33.
- Vidali, Luis, Augustine, Robert C, Fay, Scotty N, Franco, Paula, Pattavina, Kelli A, & Bezanilla, Magdalena. 2009. Rapid screening for temperature-sensitive alleles in plants. *Plant physiology*, **151**(2), 506–514.
- Vierstra, Richard D. 2009. The ubiquitin-26S proteasome system at the nexus of plant biology. *Nature reviews. Molecular cell biology*, **10**(6), 385–97.
- Wada, Masato, Cao, Qiu Fen, Kotoda, Nobuhiro, Soejima, Jun Ichi, & Masuda, Tetsuo. 2002. Apple has two orthologues of FLORICAULA/LEAFY involved in flowering. *Plant Molecular Biology*, **49**(6), 567–577.
- Wagner, D, Sablowski, R W, & Meyerowitz, E M. 1999. Transcriptional activation of APETALA1 by LEAFY. *Science*, **285**(5427), 582–584.
- Walczak, Henning, Iwai, Kazuhiro, & Dikic, Ivan. 2012. Generation and physiological roles of linear ubiquitin chains. *BMC Biology*, **10**(1), 23.
- Wallace, Bret D, Wang, Hongwei, Lane, Kimberly T, Scott, John E, Orans, Jillian, Koo, Seol, Venkatesh, Madhukumar, Jobin, Christian, Yeh, Li-an, Mani, Sridhar, & Redinbo, Matthew R. 2010. Alleviating Cancer Drug Toxicity by Inhibiting a Bacterial Enzyme. *Science*, **330**(6005), 831–835.
- Wallace, Bret D., Roberts, Adam B., Pollet, Rebecca M., Ingle, James D., Biernat, Kristen A., Pellock, Samuel J., Venkatesh, Madhu Kumar, Guthrie, Leah, O’Neal, Sara K., Robinson, Sara J., Dollinger, Makani, Figueroa, Esteban, McShane, Sarah R., Cohen, Rachel D., Jin, Jian, Frye, Stephen V., Zamboni, William C., Pepe-Ranney, Charles, Mani, Sridhar, Kelly, Libusha, & Redinbo, Matthew R. 2015. Structure and Inhibition of Microbiome  $\beta$ -Glucuronidases Essential to the Alleviation of Cancer Drug Toxicity. *Chemistry and Biology*, **22**(9), 1238–1249.
- Walsh, Charlotte Kirsten, & Sadanandom, Ari. 2014. Ubiquitin chain topology in plant cell signaling: a new facet to an evergreen story. *Plant Genetics and Genomics*, **5**(April), 122.
- Wang, C, Xi, J, Begley, T P, & Nicholson, L K. 2001. Solution structure of ThiS and implications for the evolutionary roots of ubiquitin. *Nature structural biology*, **8**(1), 47–51.
- Wang, Feng, Zhu, Danmeng, Huang, Xi, Li, Shuang, Gong, Yinan, Yao, Qinfang, Fu, Xiangdong, Fan, Liu-Min, & Deng, Xing Wang. 2009. Biochemical insights on degradation of *Arabidopsis* DELLA proteins gained from a cell-free assay system. *The Plant Cell*, **21**(8), 2378–2390.
- Wang, Qinghua, Goh, Amanda M., Howley, Peter M., & Walters, Kylie J. 2003. Ubiquitin Recognition by the DNA Repair Protein hHR23a. *Biochemistry*, **42**(46), 13529–13535.
- Waugh, David S. 2011. An overview of enzymatic reagents for the removal of affinity tags. *Protein Expression and Purification*, **80**(2), 283–293.
- Wehrmann, Axel, Vliet, Adri Van, Opsomer, Chris, Botterman, Johan, & Schulz, Arno. 1996. The similarities of bar and pat gene products make them equally applicable for plant engineers. *Nature biotechnology*, **14**(10), 1274–1278.
- Weigel, Detlef, & Meyerowitz, Elliot M. 1994. The ABCs of floral homeotic genes. *Cell*, **78**(2), 203–209.
- Weigel, Detlef, & Nilsson, Ove. 1995. A developmental switch sufficient for flower initiation in diverse plants. *Nature*, **377**(12), 495–500.
- Weigel, Detlef, Alvarez, John, Smyth, David R., Yanofsky, Martin F., & Meyerowitz, Elliot M. 1992. LEAFY controls floral meristem identity in *Arabidopsis*. *Cell*, **69**(5), 843–859.
- Weigel, Martin, Varotto, Claudio, Pesaresi, Paolo, Finazzi, Giovanni, Rappaport, Fabrice, Salamini, Francesco,

- & Leister, Dario. 2003. Plastocyanin is indispensable for photosynthetic electron flow in *Arabidopsis thaliana*. *Journal of Biological Chemistry*, **278**(33), 31286–31289.
- Weijers, D, VanHamburg, J P, VanRijn, E, Hooykaas, P J J, & Offringa, R. 2003. Diphtheria toxin-mediated interregional communication seed development. *Plant Physiology*, **133**(4), 1882–1892.
- Weinhandl, Katrin, Winkler, Margit, Glieder, Anton, & Camattari, Andrea. 2014. Carbon source dependent promoters in yeasts. *Microbial cell factories*, **13**, 5.
- Weiss, Gregory A., Watanabe, Colin K., Zhong, Alan, Goddard, Audrey, & Sidhu, Sachdev S. 2000. Rapid mapping of protein functional epitopes by combinatorial alanine scanning. *Proceedings of the National Academy of Sciences of the United States of America*, **97**(16), 8950–8954.
- Weits, Daan A, Giuntoli, Beatrice, Kosmacz, Monika, Parlanti, Sandro, Hubberten, Hans-michael, Riegler, Heike, Hoefgen, Rainer, Perata, Pierdomenico, van Dongen, Joost T., & Licausi, Francesco. 2014. Plant cysteine oxidases control the oxygen-dependent branch of the N-end-rule pathway. *Nature communications*, **5**, 3425.
- Wendler, Christine, Barniske, Manuela, & Wild, Aloysius. 1990. Effect of phosphinothricin (glufosinate) on photosynthesis and photorespiration of C3 and C4 plants. *Photosynthesis Research*, **24**(1), 55–61.
- White, Mark D, Klecker, Maria, Hopkinson, Richard J, Weits, Daan, & Mueller, Carolin. 2017. Plant Cysteine Oxidases are Dioxygenases that Directly Enable Arginyl Transferase-Catalyzed Arginylation of N-End Rule Targets. *Nature communications (in press)*.
- Whittington, a T, Vugrek, O, Wei, K J, Hasenbein, N G, Sugimoto, K, Rashbrooke, M C, & Wasteneys, G O. 2001. MOR1 is essential for organizing cortical microtubules in plants. *Nature*, **411**(6837), 610–3.
- Wilkinson, K. D., Urban, M. K., & Haas, A. L. 1980. Ubiquitin is the ATP-dependent proteolysis factor I of rabbit reticulocytes. *Journal of Biological Chemistry*, **255**(16), 7529–7532.
- Winter, Debbie, Vinegar, Ben, Nahal, Hardeep, Ammar, Ron, Wilson, Greg V., & Provart, Nicholas J. 2007. An "electronic fluorescent pictograph" Browser for exploring and analyzing large-scale biological data sets. *PLoS ONE*, **2**(8).
- Wohlleben, W., Arnold, W., Broer, I., Hillemann, D., Strauch, E., & Punier, A. 1988. Nucleotide sequence of the phosphinothricin N-acetyltransferase gene from *Streptomyces viridochromogenes* Tü494 and its expression in *Nicotiana tabacum*. *Gene*, **70**(1), 25–37.
- Wollmann, Heike, Mica, Erica, Todesco, Marco, Long, Jeff a, & Weigel, Detlef. 2010. On reconciling the interactions between APETALA2, miR172 and AGAMOUS with the ABC model of flower development. *Development (Cambridge, England)*, **137**(21), 3633–42.
- Wong, Stanley, Mosabbir, Abdullah A., & Truong, Kevin. 2015. An engineered split intein for photoactivated protein trans-splicing. *PLoS ONE*, **10**(8), 1–16.
- Worley, Cathy Kingdon, Ling, Richard, & Callis, Judy. 1998. Engineering in vivo instability of firefly luciferase and *Escherichia coli*  $\beta$ -glucuronidase in higher plants using recognition elements from the ubiquitin pathway. *Plant Molecular Biology*, **37**(2), 337–347.
- Wu, Fu-Hui, Shen, Shu-Chen, Lee, Lan-Ying, Lee, Shu-Hong, Chan, Ming-Tsar, & Lin, Choun-Sea. 2009. Tape-*Arabidopsis* Sandwich - a simpler *Arabidopsis* protoplast isolation method. *Plant methods*, **5**(jan), 16.
- Wu, Xiuli, Yen, Lily, Irwin, Lisa, Sweeney, Colleen, Iii, L Carraway, & Iii, Kermit L Carraway. 2004. Stabilization of the E3 Ubiquitin Ligase Nrdp1 by the Deubiquitinating Enzyme USP8. *Molecular and Cellular Biology*, **24**(17), 7748–7757.
- Xia, Zanzian, Turner, Glenn C., Hwang, Cheol Sang, Byrd, Christopher, & Varshavsky, Alexander. 2008a. Amino acids induce peptide uptake via accelerated degradation of CUP9, the transcriptional repressor of the PTR2 peptide transporter. *Journal of Biological Chemistry*, **283**(43), 28958–28968.
- Xia, Zanzian, Webster, Ailsa, Du, Fangyong, Piatkov, Konstantin, Ghislain, Michel, & Varshavsky, Alexander. 2008b. Substrate-binding sites of UBR1, the ubiquitin ligase of the N-end rule pathway. *Journal of Biological Chemistry*, **283**(35), 24011–24028.
- Xia, Zanzian, Webster, Ailsa, Du, Fangyong, Piatkov, Konstantin, Ghislain, Michel, & Varshavsky, Alexander. 2008c. Substrate-binding sites of UBR1, the ubiquitin ligase of the N-end rule pathway. *The Journal of biological chemistry*, **283**(35), 24011–28.
- Xu, Ping, Duong, Duc M., Seyfried, Nicholas T., Cheng, Dongmei, Xie, Yang, Robert, Jessica, Rush, John,

- Hochstrasser, Mark, Finley, Daniel, & Peng, Junmin. 2009. Quantitative Proteomics Reveals the Function of Unconventional Ubiquitin Chains in Proteasomal Degradation. *Cell*, **137**(1), 133–145.
- Yamaguchi, Nobutoshi, Jeong, Cheol Woong, Nole-Wilson, Staci, Krizek, Beth A., & Wagner, Doris. 2015. AINTEGUMENTA and AINTEGUMENTA-LIKE6/PLETHORA3 induce LEAFY expression in response to auxin to promote the onset of flower formation in Arabidopsis. *Plant Physiology*, **170**(January), 283–293.
- Yamaizumi, Masaru, Mekada, Eisuke, Uchida, Tsuyoshi, & Okada, Yoshio. 1978. One molecule of diphtheria toxin fragment a introduced into a cell can kill the cell. *Cell*, **15**(1), 245–250.
- Yanofsky, M F, Ma, H, Bowman, J L, Drews, G N, Feldmann, K a, & Meyerowitz, E M. 1990. The protein encoded by the Arabidopsis homeotic gene agamous resembles transcription factors. *Nature*, **346**(6279), 35–39.
- Yoshida, Satoko, Ito, Masaki, Callis, Judy, Nishida, Ikuo, & Watanabe, Akira. 2002. A delayed leaf senescence mutant is defective in arginyl-tRNA : protein arginyltransferase , a component of the N-end rule pathway in Arabidopsis. *The Plant Journal*, **32**, 129–137.
- Yu, Houqing, Kago, Grace, Yellman, Christopher M, & Matouschek, Andreas. 2016. Ubiquitin-like domains can target to the proteasome but proteolysis requires a disordered region. *The EMBO journal*, 1–15.
- Zattas, Dimitrios, & Hochstrasser, Mark. 2015. Ubiquitin-dependent protein degradation at the yeast endoplasmic reticulum and nuclear envelope. *Critical Reviews in Biochemistry and Molecular Biology*, **50**(1), 1–17.
- Zeidler, Martin P, Tan, Change, Bellaiche, Yohanns, Cherry, Sara, Häder, Sabine, Gayko, Urte, & Perrimon, Norbert. 2004. Temperature-sensitive control of protein activity by conditionally splicing inteins. *Nature biotechnology*, **22**(7), 871–876.
- Zenker, Martin, Mayerle, Julia, Lerch, Markus M, Tagariello, Andreas, Zerres, Klaus, Durie, Peter R, Beier, Matthias, Hulskamp, Georg, Guzman, Celina, Rehder, Helga, Beemer, Frits A, Hamel, Ben, Vanlieferinghen, Philippe, Gershoni-Baruch, Ruth, Vieira, Marta W, Domic, Miroslav, Auslender, Ron, Gil-da Silva-Lopes, Vera L, Steinlicht, Simone, Rauh, Manfred, Shalev, Stavit A, Thiel, Christian, Winterpacht, Andreas, Kwon, Yong Tae, Varshavsky, Alexander, & Reis, Andre. 2005. Deficiency of UBR1, a ubiquitin ligase of the N-end rule pathway, causes pancreatic dysfunction, malformations and mental retardation (Johanson-Blizzard syndrome). *Nat Genet*, **37**(12), 1345–1350.
- Zeth, Kornelius, Ravelli, Raimond B, Paal, Klaus, Cusack, Stephen, Bukau, Bernd, & Dougan, David a. 2002. Structural analysis of the adaptor protein ClpS in complex with the N-terminal domain of ClpA. *Nature structural biology*, **9**(12), 906–11.
- Zhang, Daoning, Chen, Tony, Ziv, Inbal, Rosenzweig, Rina, Matiuhin, Yulia, Bronner, Vered, Glickman, Michael H., & Fushman, David. 2009. Together, Rpn10 and Dsk2 Can Serve as a Polyubiquitin Chain-Length Sensor. *Molecular Cell*, **36**(6), 1018–1033.
- Zhang, Liangyu, Ward, Jordan D, Cheng, Ze, & Dernburg, Abby F. 2015. The auxin-inducible degradation (AID) system enables versatile conditional protein depletion in *C. elegans*. *Development*, **142**(24), 4374–4384.
- Zhou, Jie, Zhang, Yan, Qi, Jingxia, Chi, Yingjin, Fan, Baofang, Yu, Jing Quan, & Chen, Zhixiang. 2014. E3 Ubiquitin Ligase CHIP and NBR1-Mediated Selective Autophagy Protect Additively against Proteotoxicity in Plant Stress Responses. *PLoS Genetics*, **10**(1).





## 7 Acknowledgments

Für die Möglichkeit diese Arbeit am IPB in Halle anzufertigen möchte ich als erstes Dr. Nico Dissmeyer und Prof. Dierk Scheel danken, die mir dies ermöglichten. Desweiteren möchte ich mich bei den Gutachtern dieser Arbeit besonders bedanken.

Obwohl das letztendliche Thema meiner Arbeit nicht genau dem Entsprach, was ursprünglich geplant war (aber bei wem tut es das schon?), so hatte ich doch alle Möglichkeiten viele verschiedene Herangehensweisen auszuprobieren und zu erlernen. Für diese Möglichkeit bin ich Dr. Dissmeyer sehr dankbar, der mich bei diesen Dingen immer unterstützt hat.

Mein ganz besonders großer Dank gilt meiner Kollegin Christin Neumann, die mit mir zusammen dieses Labor "eröffnet" hat. Es hat immer viel Spaß gemacht zusammen zu arbeiten und man konnte sich immer aufeinander verlassen.

Außerdem möchte ich mich bei allen anderen Mitgliedern meiner Arbeitsgruppe, Maria Klecker und Pavel Reichmann für die gute Arbeitsatmosphäre, die guten und fruchtbaren Diskussionen sowie des immer funktionierenden Austausch von Protokollen, Materialeien und Ergebnissen bedanken. Dies gilt auch für die Nachbararbeitsgruppe von Dr. Marco Trujillo, deren Hilfe sowie vor allem die Teilnahme an ihrem Literaturseminar mir sehr geholfen haben. Ein besondere Dank gilt hier Maria Klecker, die die SPOT-Versuche in unserem Labor eingeführt hat und die ihr Wissen und ihre Plasmide immer großzügig mit mir geteilt hat.

Bedanken möchte ich mich auch bei den verschiedenen Studenten, die ich im Laufe der Jahre als Praktikanten, Bachelor- oder Masterstudenten betreut haben und die viele Seitenprojekte mitbearbeitet haben für die ich alleine keine Zeit gehabt hätte.

Bedanken möchte ich mich auch bei den sonstigen Angestellten des IPB, sei es bei technischen Assistenten, wissenschaftlichen Mitarbeiter oder der Verwaltung, die mir bei verschiedensten Dingen geholfen und so diese Arbeit erst ermöglicht haben. Besonders hervorheben möchte ich hier die Gärtner, die mehr als einen meinen Versuche in dieser Form erst möglich gemacht haben und die immer freundlich, hilfsbereit und geduldig waren wenn ich mal wieder 1000 Pflanzen pikiert haben wollte oder vergessen hatte meine Pflanzen zeitgerecht in den entsprechenden Datenbanken einzutragen.

Danke auch an meine Freunde und besonders meine Familie, die mich immer unterstützt haben und ohne die ich heute vielleicht diese Zeilen nicht schreiben würde. Mein letzter Dank gilt meiner Verlobten, die mich immer unterstützt hat und mir immer zur Seite stand.



# 8 Personal data and information on education / Angaben zur Person und zum Bildungsgang

## 8.1 Personal data / Angaben zur Person

- Name: Frederik Faden
- Place of birth / Geburtsort: Siegburg, Germany
- Date of birth / Geburtstag: 15.07.1986
- OrchidID: [orcid.org/0000-0002-8588-3142](https://orcid.org/0000-0002-8588-3142)

## 8.2 Information on education / Angaben zum Bildungsgang

- 01.08.2011 - 13.02.2017 (submission of thesis / Abgabe der Arbeit) - Ph.D. candidate at the Martin-Luther-University and the Leibniz Institute of Plant Biochemistry (IPB), Halle (execution of the thesis at the IPB) / Doktorand an der Martin-Luther-Universität und dem Leibniz-Institut für Pflanzenbiochemie (IPB), Halle (Ausführung der Arbeit am IPB)
- 01.10.2006 - 31.03.2011 - Studies in biology at the University of Bonn; Degree: Diploma / Studium der Biologie an der Universität Bonn; Abschluss: Diplom
- 1996 - 2005 - Secondary school Collegium Josephinum Bonn; Degree: Abitur / Besuch des Gymnasiums Collegium Josephinum Bonn; Abschluss: Abitur

### 8.3 Publications

- Mot, Augustin C., Prell, Erik, Klecker, Maria, Naumann, Christin, **Faden, Frederik**, Westermann, B. & Dissmeyer, Nico. 2017. Real-time detection of PRT1-mediated ubiquitination via fluo- rescently labeled substrate probes. *New Phytologist*
- **Faden, Frederik**, Ramezani, Thomas, Mielke, Stefan, Almudi, Isabel, Nairz, Knud, Froehlich, Marcell S., Höckendorf, Jörg, Brandt, Wolfgang, Höhenwarter, Wolfgang, Dohmen, R. Jürgen, Schnittger, Arp & Dissmeyer, Nico. 2016. Phenotypes on demand via switchable target protein degradation in multicellular organisms. *Nature communications*
- **Faden, Frederik**, Eschen-Lippold, Lennart & Dissmeyer, Nico. 2016. Normalized Quantitative Western Blotting Based on Standardized Fluorescent Labeling. *Plant Proteostasis: Methods and Protocols*
- Venne, a. Saskia, Solari, Fiorella A., **Faden, Frederik**, Paretto, Tomaso, Dissmeyer, Nico & Zahedi, René P. 2015. An improved workflow for quantitative N-terminal charge-based fractional diagonal chromatography (ChaFRADIC) to study proteolytic events in *Arabidopsis thaliana*. *Proteomics*
- **Faden, Frederik**, Mielke, Stefan, Lange, Dieter & Dissmeyer, Nico. 2014. Generic tools for conditionally altering protein abundance and phenotypes on demand. *Biological chemistry*

## 9 Statement / Eidesstattliche Erklärung

Ich habe diese Arbeit selbständig und ohne fremde Hilfe verfasst, andere als die von mir angegebenen Quellen und Hilfsmittel nicht benutzt und die den benutzten Werken wörtlich oder inhaltlich entnommenen Stellen als solche kenntlich gemacht.

Außerdem versichere ich hiermit, dass ich mich bis jetzt noch nicht um einen Doktorgrad beworben habe.

Halle (13.02.2017)

---

(Frederik Faden)